Development of a stratum corneum substitute for in vitro percutaneous penetration studies : a skin barrier model comprising synthetic stratum corneum lipids

Jager, Miranda Wilhelmina de

Development of a stratum corneum substitute for in vitro percutaneous penetration studies

a skin barrier model comprising synthetic stratum corneum lipids

The investigations described in this thesis were performed at the Division of Drug Delivery Technology of the Leiden/Amsterdam Center for Drug Research, Leiden University, Leiden, The Netherlands.

Cover photo: Marius Bennenk

Development of a stratum corneum substitute for in vitro percutaneous penetration studies

a skin barrier model comprising synthetic stratum corneum lipids

Proefschrift

ter verkrijging van
de graad van Doctor aan de Universiteit Leiden,
op gezag van de Rector Magnificus Dr. D.D. Breimer,
hoogleraar in de faculteit der Wiskunde en
Natuurwetenschappen en die der Geneeskunde,
volgens besluit van het College voor Promoties
te verdedigen op donderdag 27 april 2006
klokke 15.15 uur

door

Miranda Wilhelmina de Jager
geboren te Hardinxveld-Giessendam in 1977

Promotiecommissie

Promotor:	Prof. dr. J.A. Bouwstra
Co-promotor:	Dr. M. Ponec
Referent:	Dr. T.M. Callaghan (proDERM, Duitsland)
Overige leden:	Prof. dr. J.A. Killian (Universiteit Utrecht)
	Prof. dr. J.P. Abrahams
	Prof. dr. T.J.C. van Berkel
	Prof. dr. M. Danhof

Publication of this thesis was financially supported by N.V. Organon.

Table of contents

Chapter 1

General introduction

1. INTRODUCTION

The skin of an average adult body covers a surface area of approximately 2 m^2 and weighs more than 10% of the total body mass [1]. The skin separates the vital organs from the external environment and acts as a barrier against desiccation and various environmental influences. It plays a crucial role in the regulation of the body temperature and serves as a sensory organ transmitting external environmental information, such as pain and heat [2, 3].

Microscopically, the skin is a multilayered organ composed of many histological layers. It is generally subdivided into three layers: The epidermis, the dermis and the hypodermis [4]. The uppermost nonviable layer of the epidermis, the stratum corneum, has been demonstrated to constitute the principal barrier to percutaneous penetration [5, 6]. The excellent barrier properties of the stratum corneum can be ascribed to its unique structure and composition. The viable epidermis is situated beneath the stratum corneum and is responsible for generation of the stratum corneum. The dermis is directly adjacent to the epidermis and is composed of a matrix of connective tissue, which renders the skin its elasticity and resistance to deformation. The blood vessels that are present in the dermis provide the skin with nutrients and oxygen [4]. The hypodermis or subcutaneous fat tissue is the lowermost layer of the skin. It supports the dermis and epidermis and provides thermal isolation and mechanical protection of the body.

The outer layer of the skin forms an effective barrier to retain water within the body and keep exogenous compounds out of the body. As a result, the major problem in dermal and transdermal drug delivery is the low penetration of drug compounds through the stratum corneum. Dermal drug delivery comprises the topical application of drugs for the local treatment of skin diseases. It requires the permeation of a drug through the outer skin layers to reach its site of action within the skin, with little or no systemic uptake. The application of drugs to the skin for systemic therapy is referred to as transdermal drug delivery. Hence, it is required that a pharmacologically potent drug reaches the dermis where it can be taken up by the systemic blood circulation. In either case, the drug has to cross the outermost layer of the skin, the stratum corneum.

In the first part of this chapter, the formation and structure of the stratum corneum will be discussed. The second part describes the composition and organisation of the intercellular stratum corneum lipids in vivo and in vitro. In the third part of this chapter

some diffusion characteristics and penetration models, which are currently used to predict the in vitro and in vivo penetration of drugs through the skin, will be discussed. Finally, the objective and outline of this thesis will be presented.

2. KERATINOCYTE TERMINAL DIFFERENTIATION

2.1 The viable epidermis

The epidermis is approximately 100 to 150 µm thick and consists of various layers, characterised by different stages of differentiation. Figure 1 shows a schematic representation of the four layers present in the epidermis: stratum basale (or basal layer), stratum spinosum (or spinous layer), stratum granulosum (or granular layer), and stratum corneum (or cornified layer). The main cell type in the viable epidermis is the keratinocyte, which contains keratin filaments and constitutes for approximately 90% of the tissue [7]. Other more sparingly distributed cells in the viable epidermis are melanocytes for pigment formation, Merkell cells for sensory reception and the antigen-presenting Langerhans cells.

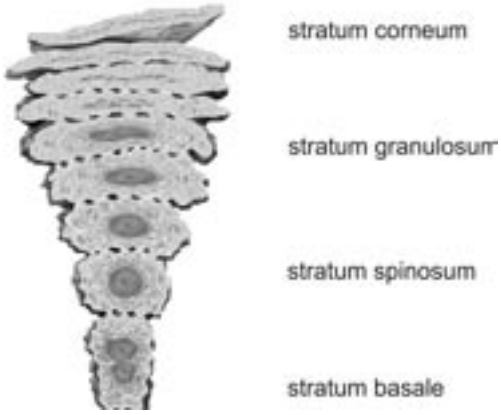

Figure 1 - Schematic overview of the different cell layers in the epidermis.

The innermost layer of the epidermis, the stratum basale, consists of a single layer of columnar-shaped, undifferentiated stem cells. Mitosis of these cells constantly renews the epidermis and this proliferation compensates the loss of dead stratum corneum cells (corneocytes) from the skin surface. As the cells produced by the basal layer move upwards, they alter morphologically as well as histochemically to form the outermost layer the stratum corneum. Over a 4 to 5 week period the entire epidermis is renewed [8].

At the spinous layer, the cells appear to be nearly round in shape. They still contain a nucleus and organelles, but contain more keratin filament bundles and are connected by more desmosomes than the basal cells. Desmosomes are specialised structures that are involved in intercellular adhesion between adjacent keratinocytes. They create a transcellular network of keratin filaments and are therefore crucial for tissue integrity [9, 10]. From the basal side of the stratum spinosum to the stratum granulosum, the keratinocytes flatten and some cell organelles disappear. In the upper spinous regions, two types of intracellular granules are formed: keratohyalin granules and membrane-bound granules. Keratohyalin granules are electron dense, irregularly shaped granules, which are predominantly composed of profilaggrin, loricrin and keratin [11, 12]. Membrane-bound granules, often referred to as lamellar bodies or membrane-coated granules, are round to ovoid in shape, measure about 0.2 μm and contain flattened lamellar disks. They were first observed by Selby in the late 1950s [13] and were later described in detail by others [14-16]. Lipid analysis of isolated lamellar bodies revealed that these organelles are mainly enriched in polar lipids, including glucosylsphingolipids, phospholipids, free sterols and cholesterol sulphate, which are present as lipid stacks. Furthermore, they contain catabolic enzymes, like acid hydrolases, sphingomyelinase and phospholipase A_2 [17-19].

The stratum granulosum is the last cell layer of the viable epidermis and contains highly differentiated keratinocytes. The lamellar bodies, which have been formed in the stratum spinosum, migrate to the apical periphery of the uppermost granular cells and eventually fuse with the membrane of the keratinocyte. Via exocytosis their content is extruded into the intercellular space at the stratum granulosum-stratum corneum interface. The lipids derived from the lamellar bodies are essential for the formation of the stratum corneum barrier.

2.2 The stratum corneum

The outermost layer of the skin, the cornified layer or stratum corneum, has been identified as the principal diffusion barrier for substances, including water [5, 6]. It is approximately 10 to 15 μm thick when dry, but swells to several times this thickness when fully hydrated [20]. It contains 10 to 25 layers of parallel to the skin surface lying nonviable cells, the corneocytes, which are surrounded by a cell envelope and are embedded in a lipid matrix. This architecture is often modelled as a wall-like structure, with the corneocytes as protein "bricks" embedded in a lipid "mortar" [21]. Similarly as the viable epidermis, desmosomes (corneodesmosomes) contribute to the cell

cohesion.

During the transition of the mature keratinocyte into the corneocyte, profilaggrin that is released from the keratohyalin granules is dephosphorylated and proteolytically processed to filaggrin monomers. Filaggrin is responsible for the formation of extensive disulphide bonds between keratin fibres. This aggregation results in a macrostructure of keratin fibres, which ultimately fill the interior of the corneocytes. Subsequently, filaggrin is degraded into free amino acids and their derivatives, which contribute to the hydration of the stratum corneum [reviewed in 22].

The corneocytes are entirely enveloped in a uniform 12 nm thick proteinaceous layered structure. This cornified envelope is formed via a complex, but well-organised process during terminal differentiation. Several precursor proteins, including involucrin, loricrin and cornifine [23, 24], are cross-linked by the action of calcium dependent transglutaminases, resulting in a very rigid and stable structure. The protein envelope has a lipoidal exterior formed by a monolayer of lipids. These lipids are covalently bound to the cornified envelope proteins, most abundantly to involucrin, and mainly consist of long chain (C30-C34) ω-hydroxy fatty acids, linked to sphingosine and 6-hydroxysphingosine, respectively [25, 26]. A number of possible roles for the covalently bound lipids have been hypothesised [27]: (i) The covalently bound lipids are assumed to play an important role in the organisation of the intercellular lipids by acting as a substrate that facilitates the orientation of the lamellae parallel to the corneocyte surface. (ii) The covalently bound lipids may facilitate the interaction of the hydrophilic interior of corneocytes with the intercellular lipid domain. (iii) The covalently bound lipids may stabilise the stratum corneum structure and the cohesiveness with the intercellular lipids. (iv) The covalently bound lipids may provide a permeability barrier around each corneocyte to impede diffusion of substances across the envelope.

The cornified envelope has an unusual high resistance to proteolytic enzymes and organic solvents. Lipid extraction causes collapse of the intercellular spaces, but does not result in disintegration of the cells. Instead, the covalently bound lipids interdigitate to close the intercellular space and hold together the cell layers [25-27]. Abnormalities in the process of envelope formation strongly influence the structural and functional integrity of the cornified envelope. For instance, in lamellar ichthyosis a genetic deficiency of transglutaminase 1 activity is observed [28, 29]. Transglutaminase 1 is not only involved in the cross-linking process of the precursor proteins, but is the only transglutaminase that is capable to covalently attach the lipids onto the proteins. Hence, mutations in transglutaminase 1 result in severe defects in the formation of

the skin barrier. The amount of protein-bound ω-hydroxyceramides is also significantly reduced in atopic dermatitis [30].

Just prior to the formation of the cornified envelope, the content of the lamellar bodies is discharged into the intercellular space. After extrusion, the polar glucosylceramides are enzymatically converted into ceramides, whereas the phospholipids are catabolised into saturated fatty acids. The stacks of disks rearrange parallel to the corneocytes and join edge-to-edge to form multiple, continuous intercellular lipid sheets or lamellae [27]. These lamellae have been visualised by electron microscopy using ruthenium post-fixation and have a unique structure of alternating broad-narrow-broad sequences of electron lucent bands. The lipids from which the intercellular lamellae are composed are highly unusual. The major lipid classes present are ceramides, cholesterol and free fatty acids. In addition, minor amounts of cholesterol sulphate are present. The composition and molecular organisation of the intercellular lipids will be discussed in more detail in the next section.

2.3 Desquamation

The thickness of the stratum corneum is fairly constant at a given body site. This implies that a fraction of the most superficial parts of the stratum corneum must be continuously shed at a rate that balances the production of cells at the stratum granulosum-stratum corneum interface. Although the process that allows cell shedding is not yet fully understood, proteolytic degradation of corneodesmosomes in the upper layers of the stratum corneum is a prerequisite for desquamation [31]. Glycosidases and trypsin- and chymotrypsin-like proteases are implicated to be involved in corneodesmosomal degradation [reviewed in 22]. However, the definitive identification of the proteolytic enzymes involved remains a challenge.

The hydration state of the stratum corneum is crucial for the activity of the desquamatory enzymes, as it has been demonstrated that corneodesmosomal degradation is inhibited at low environmental humidity [32]. Another known major factor that influences desquamation is the level of cholesterol sulphate in the superficial layers of the stratum corneum. Although the exact mechanism by which excess cholesterol sulphate inhibits desquamation and its hydrolysis promotes desquamation is still under investigation, it has been demonstrated that cholesterol sulphate inhibits some of the activity of proteases that are involved in corneodesmosome breakdown [33]. In addition, cholesterol sulphate affects the organisation of the lipid lamellae [34, 35]. As the activity of desquamatory enzymes may be affected by the physical

properties of the lamellar lipids, the desquamation process may also be indirectly influenced by cholesterol sulphate.

A normal desquamation is very important to maintain a normal stratum corneum function and skin appearance. Disturbances in the desquamation process, due to a decreased rate of cell shedding, result in the accumulation of scales on the skin surface and a consequent thickening of the stratum corneum. A clinical example of a disturbed desquamation process is the skin disorder recessive X-linked ichthyosis, in which a thickening of the stratum corneum is observed due to a cholesterol sulphatase deficiency [35, 36].

3. STRATUM CORNEUM BARRIER LIPIDS

3.1 Penetration pathways through the stratum corneum

A compound may use two diffusional routes to penetrate normal intact human skin: the transappendageal route and the transepidermal route. The transappendageal route involves transport via the sweat glands or the pilosebaceous units (hair follicles with their associated sebaceous glands). This route circumvents penetration through the stratum corneum and is therefore known as shunt route. The transappendageal route is considered to be less important than the transepidermal route because of its relatively small area, approximately 0.1% of the total skin area [3]. However, recent studies have demonstrated the possibility of specifically targeting certain compounds to the pilosebaceous structures [37, 38]. The rate of success largely depends on the lipophilicity of the permeant and the composition of the vehicle. The appendageal route is further of importance during electrically enhanced transport, such as iontophoresis [39].

Compounds that penetrate the stratum corneum via the transepidermal route may follow a transcellular (or intracellular) or intercellular pathway (see Fig. 2). Because of the highly impermeable character of the cornified envelope (see previous section), the tortuous intercellular pathway has been suggested to be the route of preference for most drug molecules [40]. This is confirmed by several microscopic transport studies, in which compounds have been visualised in the intercellular space of the stratum corneum [41-43]. Moreover, it has been demonstrated that drug permeation across stratum corneum increases many folds after lipid extraction [44]. Hence, knowledge of the structure and physical properties of the intercellular lipids is crucial to increase our insight in the skin barrier function.

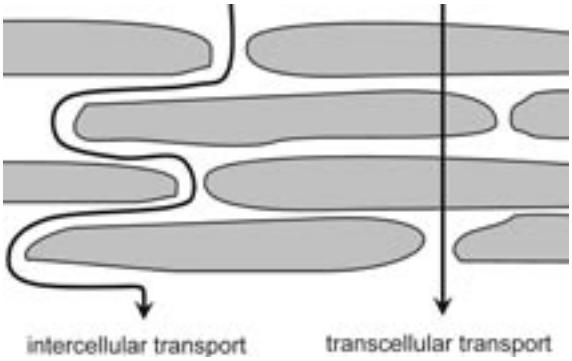

Figure 2 - Two possible transepidermal penetration pathways. The intercellular route only involves transport along the lipid lamellae, whereas the transcellular route crosses the corneocytes and intervening lipids.

3.2 Composition of the intercellular lipids in the stratum corneum

The lipid composition changes considerably during terminal differentiation. After extrusion from the lamellar bodies, the polar lipid precursors are enzymatically converted into more hydrophobic lipids. As a result, phospholipids are almost absent in the stratum corneum. The lipid lamellae, which surround the corneocytes, are predominantly composed of ceramides, cholesterol and free fatty acids. It is generally assumed that these lipids are present in nearly equimolar ratios. However, inspection of literature data shows that there is a high inter-individual variability in the lipid composition [45].

Figure 3 illustrates the various classes of ceramides present in human and pig stratum corneum. Ceramides are structurally heterogeneous and consist of two long saturated hydrocarbon chains and a small polar head group with several functional groups. Each of the 9 ceramides (CER1-CER9) identified in human stratum corneum [46-49] contains a sphingoid base and a fatty acid, which are linked by an amide bond between the carboxyl group of the fatty acid and the amino group of the base. The sphingoid moiety can be sphingosine (S), phytosphingosine (P) or 6-hydroxysphingosine (H), whereas the fatty acid moiety is non-hydroxylated (N) or α-hydroxylated (A) with chain lengths of predominantly 24 to 26 hydrocarbon atoms. The most remarkable ceramides are the acylceramides (CER1, CER4 and CER9). These ceramides consist of an unusual long ω-hydroxy fatty acid of 30 to 34 hydrocarbon atoms to which unsaturated linoleic acid is ester-linked (EO). As an essential fatty acid, linoleate has to be derived from our diet, but it may also be recycled within the epidermis [50, 51].

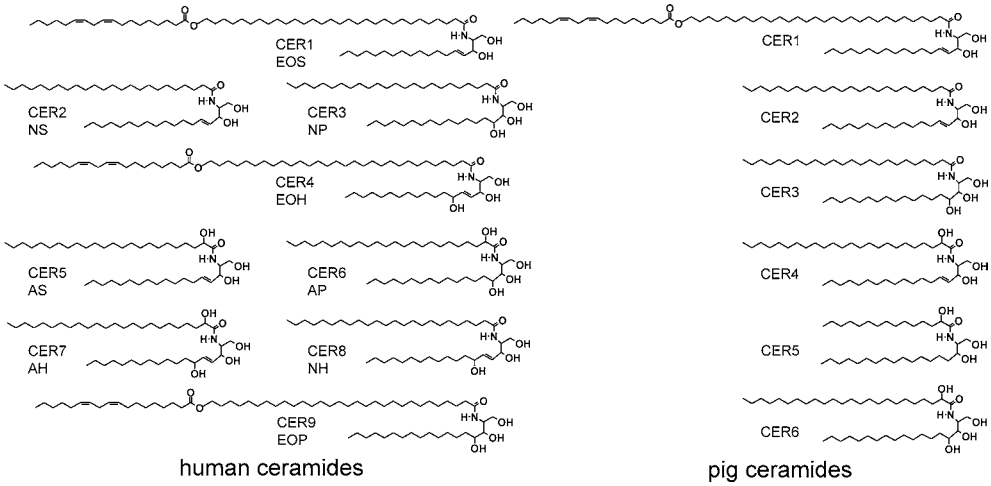

Figure 3 - Molecular structures of the ceramides (CER) present in human stratum corneum and pig stratum corneum.

The composition of the free fatty acids is also unique. In both human and pig stratum corneum, the free fatty acids fraction mainly consists of long and saturated hydrocarbon chains [52, 53]. Oleic and linoleic acid are the only unsaturated free fatty acids detected in the stratum corneum. There are various sterols present in human stratum corneum, of which cholesterol predominates. Cholesterol is the only major lipid class that is present in both plasma membranes and the intercellular lipid lamellae. Cholesterol is synthesised in the epidermis and this synthesis is independent of the hepatic one. A minor fraction is sulphated to form cholesterol sulphate. Although it is present in only small amounts (typically 2-5% w/w), cholesterol sulphate is considered to play an important role in the desquamation process of the stratum corneum (see section 2.2 of this chapter).

3.3 Lipid organisation

3.3.1 In vivo

The intercellular lipid lamellae were first visualised in the early 1970s using freeze fracture electron microscopy [54]. However, they could not be visualised in transmission electron microscopy. It is now well recognised that the saturated nature of the stratum corneum lipids does not permit a chemical reaction with the osmium tetroxide that is routinely used in the preparation of specimens for transmission electron microscopy. However, the use of ruthenium tetroxide as a post-fixation agent made it possible to

visualise the unique lamellar arrangement of the intercellular lipids [55, 56]: multiple lamellae, consisting of a broad-narrow-broad sequence of electron lucent bands, exist throughout the depth in the stratum corneum. Measurements of the broad-narrow-broad sequence of electron lucent bands reveal the presence of a 13 nm phase.

This periodicity could be confirmed by small-angle X-ray diffraction studies on human, pig and mouse stratum corneum [57-61]. However, besides a 13 nm lamellar phase, indicated as the long periodicity phase, a second lamellar phase could be demonstrated. The periodicity of this phase is approximately 6 nm and this phase is therefore indicated as the short periodicity phase. In contrast to the short periodicity phase, the long periodicity phase is only identified in the stratum corneum and not in other biological membranes. Due to its characteristic periodicity, it is generally suggested that this phase plays an important role in the skin barrier function.

Besides the lamellar organisation, the crystallinity of the intercellular lipids is also of crucial importance for the barrier function of human skin. The packing density decreases in the order orthorhombic>hexagonal>liquid. As a result, the orthorhombic packing is the least permeable structure, whereas the liquid phase is highly permeable. Wide-angle X-ray diffraction studies reveal that the lipids in human stratum corneum are predominantly packed in an orthorhombic lattice, although the presence of a coexisting hexagonal packing could not be excluded [62]. In addition, it could not be concluded whether a liquid phase coexists, as its broad reflection in the diffraction pattern was overlapped by the reflections attributed to keratin, which is present in the corneocytes. Electron diffraction and fourier transformed infrared studies on tape-stripped stratum corneum have confirmed that the bulk of the stratum corneum lipids forms an orthorhombic phase. However, near the skin surface an increased fraction of lipids is in a hexagonal state [63, 64]. It is suggested that this transition from an orthorhombic to a hexagonal packing is caused by interaction of the intercellular lipids with sebum. Sebum is excreted by the sebaceous glands and forms a protective layer, which covers the skin surface. It consists of neutral, polar lipids that contain primarily tri-glycerides, short-chain free fatty acids, wax esters, and squalene, as well as small amounts of cholesterol and cholesteryl esters [65].

3.3.2 In vitro

To further increase our insight in the stratum corneum barrier function, stratum corneum lipid models have been developed. The main advantage of these lipid models is that the composition of the mixtures can be systematically altered, which allows

studying the individual role of the various lipid classes in the stratum corneum lipid organisation. Furthermore, proteins (keratin) are absent. This considerably facilitates the interpretation of the results. Equimolar mixtures of the commercially available bovine brain ceramide type III (structurally similar to CER2, but with shorter fatty acid chain lengths [66]), cholesterol and palmitic acid have been extensively studied. Using NMR, it has been demonstrated that the majority of these lipids forms an orthorhombic phase, whereas a small portion forms a more mobile phase [67, 68]. FTIR studies on similar stratum corneum lipid models, containing bovine brain ceramide type IV, synthetic CER2 or synthetic CER5, confirm the presence of orthorhombic lattices [69-71]. However, small-angle X-ray diffraction studies reveal that mixtures prepared with these (semi-)synthetic ceramides do not form the characteristic long periodicity phase [72]. This can most likely be ascribed to the structure of the ceramides and the chain length of the fatty acid, which both do not mimic the in vivo situation.

In contrast to mixtures prepared with synthetic ceramides, hydrated mixtures of cholesterol and purified ceramides isolated from human or pig stratum corneum do resemble the characteristic stratum corneum lipid organisation. Over a wide molar range (0.4 to 2), two lamellar phases with periodicities of 5.2 and 12.2 nm are formed in mixtures prepared with cholesterol and pig ceramides [73]. Addition of long-chain free fatty acids increases the packing density and induces a hexagonal to an orthorhombic transition. In addition, free fatty acids slightly increase the periodicity of the long periodicity phase to 13 nm. Additional studies revealed that the lipid organisation in equimolar mixtures of cholesterol and pig ceramides is insensitive to the composition of the ceramides [74]. The only exception is CER1, as the formation of the long periodicity phase is dramatically decreased in the absence of CER1 [75-77]. This demonstrates that CER1 is of crucial importance for proper lipid organisation in stratum corneum. The role of the fatty acid, which is linked to the ω-hydroxy fatty acid of CER1, on the lipid phase behaviour was elucidated in an additional study [78]. This was performed with equimolar mixtures of cholesterol, free fatty acids and isolated human ceramides, in which native CER1 was replaced by synthetic CER1 linoleate, CER1 oleate or CER1 stearate. The results show that the degree of saturation of the fatty acid chain of CER1 highly affects the lamellar and lateral lipid organisation. The long periodicity phase is predominantly present in mixtures prepared with CER1 linoleate, to a lesser extent in mixtures prepared with CER1 oleate and absent in mixtures prepared with CER1 stearate. Concerning the lateral packing, besides the hexagonal and orthorhombic packing, a small fraction of lipids forms a fluid phase. The formation of this fluid phase

decreases in the order CER1 oleate>CER1 linoleate>CER1 stearate, indicating that the formation of the long periodicity phase correlates with the presence of a fluid phase and that for the formation of the 13 nm phase a certain optimal amount of lipids should be present in a fluid phase [78].

Cholesterol sulphate is another intercellular lipid. Addition of low levels of cholesterol sulphate, as observed in normal healthy stratum corneum, to lipid mixtures has little effect on the phase behaviour at room temperature. However, addition of high levels of cholesterol sulphate, as observed in the skin disease recessive X-linked ichthyosis, promotes the formation of the long periodicity phase, induces the formation of a fluid phase and increases the solubility of cholesterol in the lamellar phases [79, 80].

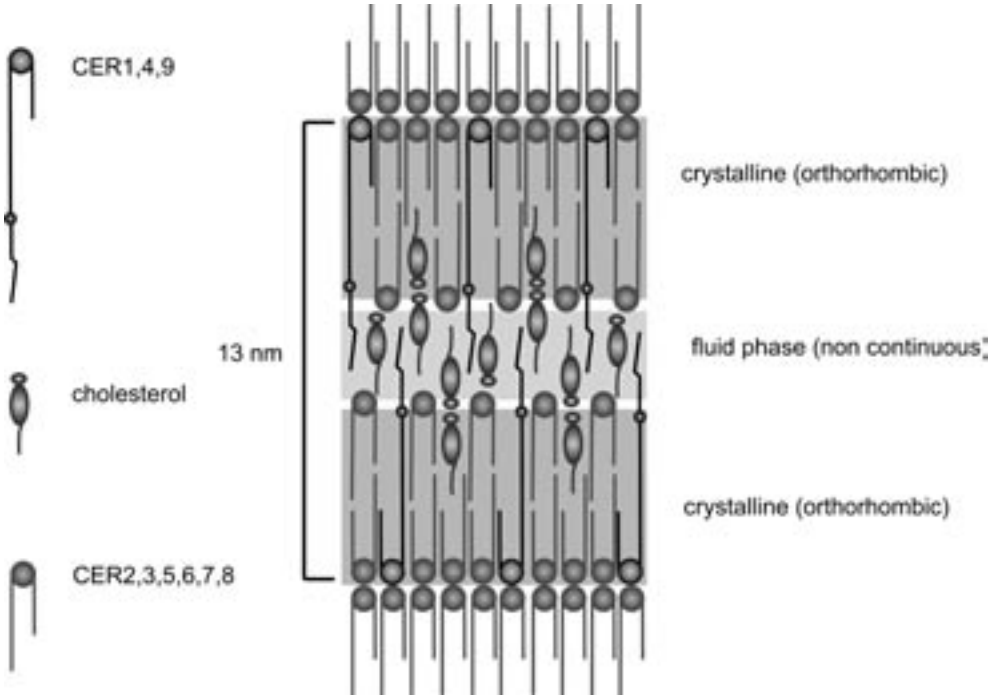

Figure 4 - Lipid organisation in the 13 nm lamellar phase according to the sandwich model.

Various models have been proposed to describe the molecular organisation of intercellular stratum corneum lipids, such as the stacked monolayer model [81], the domain mosaic model [82], the single gel phase model [83] and the sandwich model [78, 84]. According to the sandwich model (see Fig. 4) the lipids within the long periodicity phase are organised in a tri-layer structure: two broad layers with a crystalline (orthorhombic) structure are separated by a narrow central lipid layer with

fluid domains. This broad-narrow-broad pattern of hydrocarbon chains corresponds to the images obtained with electron microscopy of the stratum corneum intercellular lamellae. Cholesterol and the linoleic acid moiety of the acylceramides CER1, CER4 and CER9 are proposed to be located in the central narrow layer, whereas crystalline packed ceramides are present on both sides of this central layer [78]. Due to their unusual long structure, the acylceramides are able to span a layer and extend into another layer. The acylceramides are therefore thought to contribute to the stability of the 13 nm phase. The central, non-continuous fluid phase may be of importance for proper elasticity of the lamellae and for the enzyme activity in the stratum corneum, as enzymes are unlikely to be active in crystalline phases.

3.4 Altered lipid composition and organisation in diseased and dry skin

There are several genetic skin diseases with known defects in the lipid metabolism. Atopic dermatitis, lamellar ichthyosis and psoriasis have been the most widely studied with respect to epidermal barrier function and alterations in the lipid profile. Deviations in the lipid profile have been linked with an impaired stratum corneum barrier function. Atopic dermatitis is characterised by inflammatory, dry and easily irritable skin and overall reduced levels of ceramides in the stratum corneum [85-87]. In particular a significant decrease in the CER1, level is observed, whereas the levels of oleate, which is esterified to CER1 are elevated [86]. Both aberrations may be responsible for the reduced order of the lamellar phases as observed with freeze fracture electron microscopy [88]. It has further been established that, in comparison to healthy stratum corneum, the fraction of lipids that forms a hexagonal packing is increased [88]. A recent study reveals that the level of free fatty acids with more than 24 carbon atoms is remarkably reduced in both lesion and nonlesion parts of atopic skin as compared to healthy skin [30]. Previous X-ray diffraction studies on mixtures prepared with isolated ceramides reveal that long-chain fatty acids are required for the formation of the orthorhombic packing. In addition, it was demonstrated that the fraction of lipids that forms a hexagonal packing is increased at reduced CER1 levels [73, 76]. Both observations may explain the decreased packing density of the lipids in atopic dermatitis.

Lamellar ichthyosis is a rare skin disorder that is characterised by thick plate-like scales, skin dryness and variable redness. Characteristics of this skin disorder are significantly reduced levels of free fatty acids and an altered overall ceramide profile, without significant changes in the CER1 content [89]. These changes in lipid profile likely

explain the altered lamellar organisation in lamellar ichthyosis, as observed by X-ray diffraction [89]. Transmission electron microscopy studies using ruthenium tetroxide as a post-fixation agent further showed that in the intercellular space irregularly distributed lipid lamellae are present with areas containing excessive numbers of lamellae [90]. Concerning the lateral lipid organisation, it has been established that the lateral packing is predominantly hexagonal rather than orthorhombic [88]. This latter observation can be associated with reduced levels of free fatty acids.

Psoriasis is a chronic skin disorder, in which an abnormally fast transition of basal cells into corneocytes results in a thickening of the stratum corneum. Transmission electron microscopy studies show an aberrant stratum corneum lipid ultrastructure in psoriatic skin [91], which is expected to be related to abnormalities in the lipid profile. Particularly, a significant reduction in CER1 and a predominance of sphingosine ceramides at the expense of phytosphingosine ceramides are reported in psoriatic stratum corneum [92, 93].

In recessive X-linked ichthyosis, the amount of cholesterol sulphate in the stratum corneum is increased due to a deficiency in cholesterol sulphatase deficiency [35, 36]. Lipid analysis of scales reveals a nearly 10-fold increase in the cholesterol sulphate to free cholesterol ratio as compared to healthy stratum corneum [94]. Previous X-ray diffraction studies on isolated ceramide mixtures revealed that increased cholesterol sulphate levels induce the formation of a fluid phase, which is likely to reduce the skin barrier function [80].

Abnormalities in the lipid composition and organisation have also been established in dry skin. Interestingly, pronounced seasonal changes in the stratum corneum lipid profile have been reported. During the winter months, decreased levels of all major lipid species are observed [95]. In addition, the CER1 linoleate to CER1 oleate ratio considerably drops from 1.74 in summer to 0.51 in winter. These changes may explain the disorganised lipid lamellae, which are observed in winter xerosis [96]. Similarly as psoriatic skin, dry skin contains reduced levels of phytosphingosine ceramides and increased levels of sphingosine ceramides [97]. One of the suggested pathways for the phytosphingosine biosynthesis involves the addition of water to the corresponding sphingosine double bond. The observed changes in the sphingosine to phytosphingosine ceramide ratio may therefore be caused by disturbed water availability, associated with dry skin [92].

All the aforementioned changes in lipid composition and organisation in diseased and dry skin likely contribute to an impaired stratum corneum barrier function and

increased susceptibility to dry skin. However, as previously indicated, abnormalities in the process of envelope formation may also influence the stratum corneum barrier integrity. Therefore, more information is required to elucidate the precise mechanisms by which stratum corneum structure and function are altered.

4. DRUG TRANSPORT THROUGH THE SKIN

4.1 Diffusion characteristics

Skin permeation is a complex multistep process. Initially, a drug must be released from the vehicle and partition into the stratum corneum before it can diffuse through the stratum corneum. Subsequently, the drug needs to partition from the lipophilic stratum corneum environment into the more hydrophilic viable tissue, where the drug is eventually taken up by the blood circulation. As described in the previous section, the stratum corneum represents the main barrier to diffusion of drugs through the skin. The passive diffusion process of a drug through the stratum corneum can most simply be described by Fick's law [6, 98]:

$$J = (K*D*C_d)/h$$

In this equation, J represents the flux of the permeant through the stratum corneum ($\mu g/cm^2/s$), K the partition coefficient of the permeant between the stratum corneum and the vehicle, D the diffusion coefficient of the permeant in the stratum corneum (cm^2/s), C_d the concentration of the permeant in the vehicle ($\mu g/cm^3$) and h the length of the pathway through the stratum corneum (cm). The equation will only hold for steady state conditions, assuming that the stratum corneum is a homogeneous barrier and the concentration of the drug in the acceptor phase is negligible.

Permeation data of drugs such as steady state flux, lag time and diffusion coefficient are often obtained from in vitro permeation experiments. When the dose delivered to the skin is "infinite", there will first be a lag period in which the concentration gradient across the stratum corneum is established. After this lag time, the flux will become constant, provided that there is no permeability change in the stratum corneum and the drug concentration in the donor compartment is constant. The constant flux is referred to as the steady state flux. A typical profile of the cumulative amount of penetrated drug versus time is illustrated in Figure 5. The steady state flux can be determined from the linear part of the plot. Together with the pharmacokinetic parameters of a

drug, it determines whether or not therapeutic plasma levels will be achieved in vivo. The lag time, indicative for the time required before the steady state flux is reached, can be determined by extrapolation of this curve to the intercept with the time axis.

Diffusion is a process of mass transfer of individual molecules due to a concentration gradient and random molecular motion [99]. The concentration gradient in the stratum corneum provides the driving force for diffusion. To obtain a high initial concentration in the first layers of the stratum corneum, a drug should have a high tendency to leave the vehicle and migrate into the stratum corneum. The relative affinity of a drug compound for the stratum corneum and the vehicle is expressed in the value of the partition coefficient, K. As the stratum corneum acts as a lipophilic diffusional barrier, a high lipid solubility ($logP_{oct/water}$ of about 1-3 [100]) and a low but sufficient solubility in the vehicle are necessary for a maximal input of the drug into the stratum corneum. However, it should be noted that once the drug has crossed the stratum corneum, it must partition into and pass the underlying viable epidermis, dermis and circulatory system. As these tissues are more hydrophilic than the stratum corneum, they should be taken into consideration as part of the barrier for extremely lipophilic drugs [2]. It is generally considered that the wash out by the blood circulation is sufficiently fast as not to be a rate-limiting factor in the absorption of drugs.

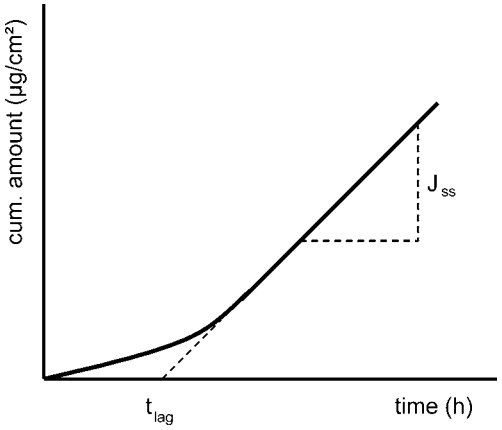

Figure 5 –Typical permeation profile of a drug diffusing through the skin

The diffusion coefficient or diffusivity, D, is a rough measure of the ease with which a molecule can move through a medium, in this case the stratum corneum [99]. It is dependent on the properties of the drug (e.g. size, shape, polarity) and the degree of interaction between the permeant and the stratum corneum. K, D and h are often

expressed in the permeability coefficient P:

$$P = (K*D)/h$$

Thus, when the donor concentration and the flux of the drug are known, the permeability coefficient can be determined. It is this parameter that is widely used to characterise the percutaneous absorption of many drug compounds under steady state conditions.

4.2 In vitro penetration studies

In vitro transport studies are often used to predict the penetration of possible drug candidates through the skin in vivo. Diffusion cells generally comprise a donor compartment and an acceptor compartment, separated by a piece of epidermis or stratum corneum, isolated from excised skin. Static and flow-through diffusion cells are both acceptable to obtain permeation data. However, the in vivo situation is more closely resembled using a flow-through cell, as the acceptor solution is continuously replaced (see Fig. 6). This prevents accumulation of the permeating compound in the acceptor compartment, which would decrease the concentration gradient and hence the flux through the skin [101, 102].

The composition, viscosity and pH of the donor solution may have significant effects on the drug permeation. Moreover, penetration enhancers can be incorporated into the donor solution, which enhance drug transport across the stratum corneum. An ideal penetration enhancer locally and reversibly reduces the barrier resistance of the stratum corneum, without irritating or damaging the skin.

The acceptor solution used in diffusion cells should not only act as an acceptor for permeating drugs but should also provide the environment for the skin membrane to function at physiological temperature, pH and osmotic strength. To maintain sink conditions, the concentration of the drug in the acceptor solution should always be less than 10% of its saturated concentration. The appropriate total volume of the acceptor fluid depends on the solubility and analytical detectability of the permeant. For lipophilic compounds, serum albumin or other solubility enhancing components may be added to the acceptor solution. However, their effects on the skin and stratum corneum integrity should be considered.

Ideally, one would like to use epidermis or stratum corneum, isolated from excised human skin to evaluate penetration properties of drug candidates. However, this approach has a number of limitations. Human skin is only available in limited quantities

from surgical or post-mortem sources. In various countries the use of excised human skin is even prohibited. Furthermore, the age, race, body site and skin condition of the donor cannot be controlled, which results in considerable permeability variations within and between individuals [103]. As it is rather difficult to obtain human skin on a regular basis, various published papers used skin that was stored in the freezer prior to the diffusion studies. However, large ice crystals and osmotic pressure differences, which are induced during freezing and subsequent thawing of the skin, damage the skin structure and decrease its barrier integrity [104].

4.3 Models for human skin

4.3.1 Animal skin

The quest to circumvent the aforementioned problems has prompted an extensive search for reliable in vitro penetration models. Many studies have been performed to investigate the suitability of animal skin as a model for human skin. Various animal species have been studied, such as the mouse, rabbit, guinea pig, rat, pig and snake. The available information in literature on comparative penetration studies using human and animal skin is sometimes contradictory. The permeability coefficients for some compounds are almost similar to those across human skin, whereas others differ greatly [105]. Rodent skin is usually much more permeable than human skin [105, 106]. As a result, the skin permeability can be considerably overestimated when data is directly extrapolated to humans. Differences in the barrier integrity between human and rodent skin can be explained by significant morphological differences. In particular the presence of many hair follicles and sebaceous glands, altered composition and organisation of the intercellular stratum corneum lipids and altered stratum corneum thickness may account for the increased permeability of rodent skin. Another problem with rodent skin, in particular hairless mouse, is its susceptibility to hydration effects. After prolonged exposure to an aqueous donor and acceptor solution, the barrier integrity of rodent skin decreases many folds [107, 108]. Rodent skin should therefore be used with caution as a predictive in vitro model for human skin. Nevertheless, many patents are issued based on data collected using rodent skin. The utility of these patents for the clinical practice may therefore be limited.

Another alternative to human skin is shed snake skin. In contrast to rodent skin, shed snake skin tends to underestimate the permeability coefficients, in particular of ionised compounds and during iontophoresis [109-112]. Snake skin lacks appendages such as hair follicles, which may account for the observed differences in barrier function

between human and snake skin.

Pig skin has been postulated as the most suitable predictive in vitro animal model for human skin. The epidermal thickness, morphology and the stratum corneum lipid composition and organisation have been reported to be similar to human skin [61, 113]. The flux values of various permeants through pig skin are of the same order of magnitude as through human skin, with differences of at most 3-fold [105, 114-117]. Therefore, severe overestimation or underestimation of the permeability of human skin appears unlikely.

4.3.2 Reconstructed epidermis

Another alternative for human skin is reconstructed human skin, which is generated in vitro by growing differentiated keratinocytes cultures on a dermal substrate at the air-liquid interface. Marked progress in the culture techniques [118-121] has led to various skin reconstructs of which the morphological features closely resemble those of native epidermis. Examination of these reconstructed skin models showed the presence of all strata, including the stratum corneum. Ultrastructural analysis of the cornified envelope proteins and covalently bound lipids further reveal great compositional similarities between native and reconstructed skin. Furthermore, all major lipid classes are synthesised under in vitro conditions and the lipids organise parallel to the corneocyte surface according to a broad-narrow-broad sequence of electron lucent bands [reviewed in 122].

Despite the high degree of similarity between native and reconstructed epidermis, some differences in the lipid composition and organisation have been observed. In reconstructed epidermis, the amount of free fatty acids is reduced and the major acyl chain lengths are shorter than in native stratum corneum [49, 123]. In addition, the content of linoleic acid in CER1 is lower and the total ceramide profile deviates from that of native stratum corneum. Investigation of reconstructed epidermis with small-angle X-ray diffraction revealed the presence of a lamellar phase with a long periodicity of 12 nm. However, in contrast to native stratum corneum, the short periodicity phase is missing [119, 123, 124]. Furthermore, the lateral packing in reconstructed skin is predominantly hexagonal instead of orthorhombic [124, 125].

All these differences may explain the increased permeability of reconstructed epidermis in comparison to human skin. Penetration studies performed with various substances typically show 5 to 20-fold higher fluxes through cultured skin than through human skin [105, 126-130]. However, differences up to 50-fold have been

reported. This indicates that the permeability of cultured skin is equivalent, although sometimes even inferior, to that of mouse, rat or guinea pig skin. Taking into account the excellent reproducibility of skin culture models [131], reconstructed epidermis may be a promising percutaneous penetration model when the culture conditions are further improved to minimise differences in the lipid composition and organisation as compared to native skin.

4.3.3 Synthetic membranes

Synthetic polymeric membranes such as Silastic® (polydimethylsiloxane), Carbosil (polydimethylsiloxane-polycarbonate block copolymer), pHEMA (poly(2-hydroxyethyl methacrylate), or cellulose acetate have also been used as an alternative permeability model for human skin [132-134]. However, inspection of literature reveals that their predictability is rather limited. Although interesting correlations have been reported for silicone membranes and excised human epidermis, the former appears to be 10 to 100 times more permeable [134, 135]. Cellulose acetate and pHEMA membranes show permeability profiles that are not representative for transport across excised stratum corneum [134]. The fact that permeability coefficients cannot be predicted adequately when using artificial polymeric membranes is likely due to their simplicity and non-resemblance with the stratum corneum structure.

Another attempt has been to reconstitute stratum corneum lipids on a porous membrane. As the major transport route of substances is through the intercellular lipid matrix of the stratum corneum, it is reasonable to suggest that a membrane containing these lipids would be a relevant model for permeation studies. The use of synthetic lipids is a prerequisite, as the isolation and separation of lipids from the stratum corneum is a time-consuming and laborious procedure. Various papers report the use of model membranes prepared with the commercially available bovine brain ceramide type III or IV [136-141]. However, as discussed in section 3.3 of this chapter, those lipid membranes bear little resemblance to human stratum corneum, as the characteristic long periodicity phase is not formed in mixtures composed of cholesterol, free fatty acids and bovine brain ceramides [72, 138]. Furthermore, no data on the orientation of the lamellae have been reported. Although the available information in literature about their use as percutaneous penetration model is somewhat limited, these lipid membranes are reported to have similar permeability properties as guinea pig skin [140, 141]. However, as stated previously, rodent skin is usually much more permeable than human skin.

5. THIS THESIS

5.1 Objectives of this thesis

In vitro transport studies are frequently used to predict the drug transport through the skin in vivo. However, this approach is hampered by the low availability of excised human skin, large inter- and intra-individual variations and the lack of alternative skin models that closely mimic the barrier properties of native human skin. The intercellular lipids in the stratum corneum have been demonstrated to represent the major barrier to the diffusion of substances through the skin. As described in this chapter, diseased and dry skin often show a defective barrier function at the diseased state, which is at least partially due to deviations in the lipid profile and organisation. Although a number of topical products are specially designed for these skin types, reproducible in vitro models are currently lacking.

The present thesis will outline the development of a skin barrier model, consisting of synthetic stratum corneum lipids on a porous substrate, which can be used in diffusion studies to predict drug transport through the skin (see Fig. 6). The skin lipid membrane can be used for large-scale screening of formulations, will circumvent problems related to stratum corneum sheets isolated from human or animal skin and may allow studying the effects of temperature or different agents on permeability and membrane organisation. Another advantage of this so-called stratum corneum substitute is that its lipid composition can be accurately chosen and modified. In this way the lipid organisation in diseased and dry skin may also be imitated, which provides unique possibilities to more adequately predict the permeability of diseased and dry skin to drug candidates.

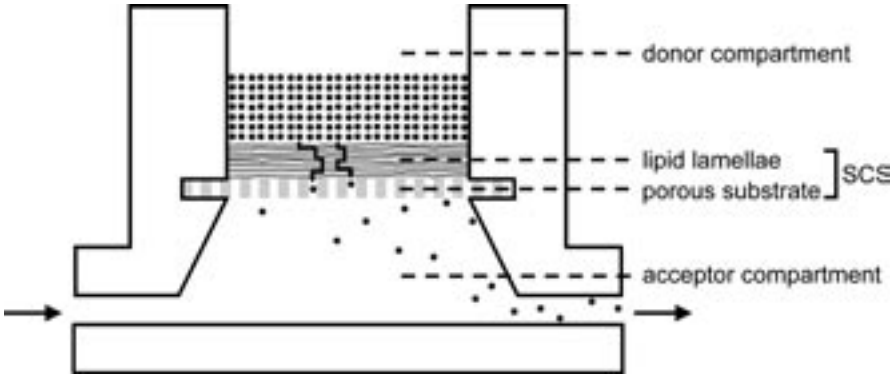

Figure 6 – Schematic representation of the stratum corneum substitute (SCS) in a diffusion cell.

The objectives of this thesis are:

(i) Selection of a synthetic ceramide mixture that mimics the phase behaviour of the intercellular lipids in human stratum corneum.

(ii) Preparation of a homogeneous stratum corneum substitute in terms of lipid composition, organisation, orientation and layer thickness.

(iii) Evaluation of the permeability barrier of the stratum corneum substitute.

5.2 Outline of this thesis

In the first part of this thesis the lamellar and lateral organisation in various synthetic lipid mixtures were studied with small-angle and wide-angle X-ray diffraction, whereas the second part describes the preparation and characterisation of the stratum corneum substitute.

Chapter 2 describes the phase behaviour of four (semi)-synthetic ceramides, either single or in a mixture with cholesterol, or cholesterol and free fatty acids. The effects of compositional changes on the phase behaviour of the lipid mixtures were systematically examined. Chapter 3 and 4 are follow-ups of the study described in chapter 2. In these chapters the importance of the equilibration temperature during sample preparation, the ratio between the individual ceramides and the presence of free fatty acids in the lipid mixture for the formation of the 13 and 6 nm lamellar phases are reported. The importance of acylceramide type and relative content for proper lipid organisation in this lipid mixture is demonstrated in chapter 5. Furthermore, a ceramide mixture that mimics the composition of the ceramides in pig stratum corneum has been studied, of which the results are reported in chapter 6. Special focus in this chapter is addressed to the role of free fatty acids on the lipid organisation and the sensitivity of the lipid organisation towards exclusion or replacement of certain ceramide classes.

In Chapter 7 the application method, which was selected and constructed to spray the lipids onto a porous substrate, is introduced. The stratum corneum substitute is subsequently characterised in terms of lipid distribution, uniformity of the lipid layer and organisation and orientation of the lipid lamellae. The barrier integrity of the stratum corneum substitute is reported in chapter 8. Passive diffusion studies are performed with three structurally related substances, using isolated human stratum corneum as a control sample. The influences of lipid layer thickness, permeant lipophilicity and altered lipid composition on the diffusion characteristics are investigated.

6. REFERENCES

1. Moore L., Chien Y.W. Transdermal drug delivery: A review of pharmaceutics, pharmacokinetics, and pharmacodynamics. *Crit. Rev. Ther. Drug Carrier Syst.* **4** (1988) 285-349.

2. Williams A.C., Barry B.W. Skin absorption enhancers. *Crit. Rev. Ther. Drug Carrier Syst.* **9** (1992) 305-353.

3. Barry B.W. Structure, function, diseases, and topical treatment of human skin. In: Dermatological Formulations: Percutaneous absorption. Marcel Dekker Inc., New York, 1983, pp 1-48.

4. Schaefer H., Redelmeier T.E. Skin barrier. Principles of percutaneous absorption. Karger, Basel, 1996.

5. Blank I.H. Transport across the stratum corneum. *Toxicol. Appl. Pharmacol. Suppl.* **3** (1969) 23-29.

6. Scheuplein R.J., Blank I.H. Permeability of the skin. *Physiol. Rev.* **51** (1971) 702 -747.

7. Eckert R.L. Structure, function, and differentiation of the keratinocyte. *Physiol. Rev.* **69** (1989) 1316-1346.

8. Baker H., Kligman A.M. Technique for estimating turnover time of human stratum corneum. *Arch. Dermatol.* **95** (1967) 408-411.

9. Burdett I.D. Aspects of the structure and assembly of desmosomes. *Micron.* **29** (1998) 309-328.

10. Fuchs E., Raghavan S. Getting under the skin of epidermal morphogenesis. *Nat. Rev. Genet.* **3** (2002) 199-209.

11. Harding C.R., Scott I.R. Histidine-rich proteins (filaggrins): structural and functional heterogeneity during epidermal differentiation. *J. Mol. Biol.* **170** (1983) 651-673.

12. Steven A.C., Bisher M.E., Roop D.R., Steinert P.M. Biosynthetic pathways of filaggrin filaggrin and loricrin - two major proteins expressed by terminally differentiated epidermal keratinocytes. *J. Struct. Biol.* **104** (1990) 150-162.

13. Selby C.C. An electron microscope study of thin sections of human skin. II. Superficial layers of footpad epidermis. *J. Invest. Dermatol.* **29** (1957) 131-149.

14. Odland G.F. A submicroscopic granular component in human epidermis. *J. Invest. Dermatol.* **34** (1960) 11-15.

15. Elias P.M, McNutt N.S., Friend D.S. Membrane alterations during cornification of mammalian squamous epithelia: A freeze-fracture, tracer and thin-section study. *Anat. Rec.* **189** (1977) 577-594.

16. Landmann L. Lamellar granules in mammalian, avian, and reptilian epidermis. *J. Ultrastr. Res.* **72** (1980) 245-263.

17. Freinkel R.K., Traczyk T.N. Lipid composition and acid hydrolase content of lamellar granules of fetal rat epidermis. *J. Invest. Dermatol.* **85** (1985) 295-298.

18. Wertz P.W., Downing D.T., Freinkel R.K., Traczyk T.N. Sphingolipids of the stratum corneum and lamellar granules of fetal rat epidermis. *J. Invest. Dermatol.* **83** (1984) 193-195.

19. Wertz P.W. Epidermal lipids. *Semin. Dermatol.* **11** (1992) 106-113.

20. Bouwstra J.A., de Graaff A., Gooris G.S., Nijsse J., Wiechers J.W., van Aelst A.C. Water distribution and related morphology in human stratum corneum at different hydration levels. *J. Invest. Dermatol.* **120** (2003) 750-758.

21. Elias P.M. Epidermal lipids, barrier function, and desquamation. *J. Invest. Dermatol.* **80** (1983) 44s-49s.

22. Harding C.R., Watkinson A., Rawlings A.V. Dry skin, moisturization and corneodesmolysis. *Int. J. Cosm. Sci.* **22** (2000) 21-52.

23. Harding C.R., Long S., Richardson J., Rogers J., Zhang Z., Bush A., Rawlings A.V. The cornified cell envelope: An important marker of stratum corneum maturation in healthy and dry skin. *Int. J. Cosm. Sci.* **25** (2003) 157-167.

24. Hirao T. Involvement of transglutaminase in ex vivo maturation of cornified envelopes in the stratum corneum. *Int. J. Cosm. Sci.* **25** (2003) 245-257.

25. Swartzendruber D.C., Wertz P.W., Madison K.C., Downing D.T. Evidence that the corneocyte has a chemically bound lipid envelope. *J. Invest. Dermatol.* **88** (1987) 709-713.

26. Wertz P.W., Madison K.C., Downing D.T. Covalently bound lipids of human stratum corneum. *J. Invest. Dermatol.* **92** (1989) 109-111.

27. Wertz P.W., Downing D.T. Stratum corneum: biological and biochemical considerations. In: Hadgraft J., Guy R.H. Transdermal drug delivery: developmental issues and research initiatives. Marcel Dekker Inc., New York, 1989, pp 1-22.

28. Huber M., Rettler I., Bernasconi K., Frenk E., Lavrijsen S.P., Ponec M., Bon A., Lautenschlager S., Schorderet D.F., Hohl D. Mutations of keratinocyte transglutaminase in lamellar ichthyosis. *Science* **267** (1995) 525-528.

29. Hohl D., Huber M., Frenk E. Analysis of the cornified cell envelope in lamellar ichthyosis. *Arch. Dermatol.* **129** (1993) 618-624.

30. Macheleidt O., Kaiser H.W., Sandhoff K. Deficiency of epidermal protein-bound omega-hydroxyceramides in atopic dermatitis. *J. Invest. Dermatol.* **119** (2002) 166-173.

31. Rawlings A.V. Trends in stratum corneum research and the management of dry skin conditions. *Int. J. Cosm. Sci.* **25** (2003) 63-95.

32. Rawlings A.V., Harding C.R., Watkinson A., Banks J., Ackerman C., Sabin R. The effect of glycerol and humidity on desmosome degradation in stratum corneum. *Arch. Dermatol. Res.* **287** (1995) 457-464.

33. Sato J., Denda M., Nakanishi J., Nomura J., Koyama J. Cholesterol sulfate inhibits proteases that are involved in desquamation of stratum corneum. *J. Invest. Dermatol.* **111** (1998) 189-193.

34. Bouwstra J.A., Gooris G.S., Dubbelaar F.E., Ponec M. Cholesterol sulfate and calcium affect stratum corneum lipid organization over a wide temperature range. *J. Lipid Res.* **40** (1999) 2303-2312.

35. Zettersten E., Man M.Q., Sato J., Denda M., Farrell A., Ghadially R., Williams M.L., Feingold K.R., Elias P.M. Recessive x-linked ichthyosis: role of cholesterol-sulfate accumulation in the barrier abnormality. *J. Invest. Dermatol.* **111** (1998) 784-790.

36. Rehfeld S.J., Plachy W.Z., Williams M.L., Elias P.M. Calorimetric and electron spin resonance examination of lipid phase transitions in human stratum corneum: molecular basis for normal cohesion and abnormal desquamation in recessive X-linked ichthyosis. *J. Invest. Dermatol.* **91** (1988) 499-505.

37. Rolland A., Wagner N., Chatelus A., Shroot B., Schaefer H. Site-specific drug delivery to pilosebaceous structures using polymeric microspheres. *Pharm. Res.* **10** (1993) 1738-1744.

38. Grams Y.Y., Alaruikka S., Lashley L., Caussin J., Whitehead L., Bouwstra J.A. Permeant lipophilicity and vehicle composition influence accumulation of dyes in hair follicles of human skin. *Eur. J. Pharm. Sci.* **18** (2003) 329-336.

39. Cullander C., Guy R.H. Visualization of iontophoretic pathways with confocal microscopy and the vibrating probe electrode. *Solid State Ionics* **53-56** (1992) 197-206.

40. Williams M.L., Elias P.M. The extracellular matrix of stratum corneum: role of lipids in normal and pathological function. *Crit. Rev. Ther. Drug Carrier Syst.* **3** (1987) 95-122.

41. Boddé H.E., van den Brink I., Koerten H.K., de Haan F.H.N. Visualization of in vitro percutaneous penetration of mercuric chloride transport through intercellular space versus cellular uptake through desmosomes. *J. Control. Release* **15** (1991) 227-236.

42. Johnson M.E., Blankschtein D., Langer R. Evaluation of solute permeation through the stratum corneum: lateral bilayer diffusion as the primary transport mechanism. *J. Pharm. Sci.* **86** (1997) 1162-1172.

43. Meuwissen M.E.M.J., Janssen J., Cullander C., Junginger H.E., Bouwstra J.A. A cross-section device to improve visualization of fluorescent probe penetration into the skin by confocal laser scanning microscopy. *Pharm. Res.* **15** (1998) 352-356.

44. Rastogi S.M., Singh J. Lipid extraction and transport of hydrophilic solutes through porcine epidermis. *Int. J. Pharm.* **225** (2001) 75-82.

45. Weerheim A., Ponec M. Determination of stratum corneum lipid profile by tape stripping in combination with high-performance thin-layer chromatography. *Arch. Dermatol. Res.* **293** (2001) 191-199.

46. Wertz P.W., Miethke M.C., Long S.A., Strauss J.S., Downing D.T. The composition of the ceramides from human stratum corneum and from comedones. *J. Invest. Dermatol.* **84** (1985) 410-412.

47. Robson K.J., Stewart M.E., Michelsen S., Lazo N.D., Downing D.T. 6-Hydroxy-4-sphingenine in human epidermal ceramides. *J. Lipid Res.* **35** (1994) 2060-2068.

48. Stewart M.E., Downing D.T. A new 6-hydroxy-4-sphingenine-containing ceramide in human skin. *J. Lipid Res.* **4** (1999) 1434-1439.

49. Ponec M., Weerheim A., Lankhorst P., Wertz P. New acylceramide in native and reconstructed epidermis. *J. Invest. Dermatol.* **120** (2003) 581-588.

50. Madison K.C., Swartzendruber D.C., Wertz P.W., Downing D.T. Murine keratinocyte cultures grown at the air/medium interface synthesize stratum corneum lipids and "recycle" linoleate during differentiation. *J. Invest. Dermatol.* **93** (1989) 10-17.

51. Wertz P.W., Downing D.T. Metabolism of linoleic acid in porcine epidermis. *J. Lipid Res.* **31** (1990) 1839-1844.

52. Wertz P.W., Downing D.T.: In: Goldsmith LA, ed. Physiology, Biochemistry and Molecular Biology of the Skin, 2nd edn. Oxford University Press, Oxford, 1991, pp 205-235.

53. Ponec M., Gibbs S., Pilgram G., Boelsma E., Koerten H., Bouwstra J., Mommaas M. Barrier function in reconstructed epidermis and its resemblance to native human skin. *Skin Pharmacol. Appl. Skin Physiol.* **14** Suppl. 1 (2001) 63-71.

54. Breathnach A.S., Goodman T., Stolinski C., Gross M. Freeze fracture replication of cells of stratum corneum of human epidermis. *J. Anat.* **114** (1973) 65-81.

55. Madison K.C., Schwartzendruber D.C., Wertz P.W., Downing D.T. Presence of intact intercellular lipid lamellae in the upper layers of the stratum corneum. *J. Invest. Dermatol.* **88** (1987) 714-718.

56. Hou S.Y., Mitra A.K., White S.H., Menon G.K., Ghadially R., Elias P.M. Membrane structures in normal and essential fatty acid-deficient stratum corneum: characterization by ruthenium tetroxide staining and x-ray diffraction. *J. Invest. Dermatol.* **96** (1991) 215-223.

57. White S.H., Mirejovsky D., King G.I. Structure of lamellar lipid domains and corneocyte envelopes in murine stratum corneum: An X-ray diffraction study. *Biochemistry* **27** (1988) 3725-3732.

58. Bouwstra J.A., Gooris G.S., van der Spek J.A., Bras W. The structure of human stratum corneum as determined by small angle X-ray scattering. *J. Invest. Dermatol.* **96** (1991) 1006-1014.

59. Bouwstra J.A., Gooris G.S., van der Spek J.A., Bras W. Structural investigations of human stratum corneum by small angle X-ray scattering. *J. Invest. Dermatol.* **97** (1991) 1005-1012.

60. Bouwstra J.A., Gooris G.S., van der Spek J.A., Lavrijsen S., Bras W. The lipid and protein structure of mouse stratum corneum: a wide and small angle diffraction study. *Biochim. Biophys. Acta.* **1212** (1994) 183-192.

61. Bouwstra J.A., Gooris G.S., Bras W., Downing D.T. Lipid organization in pig stratum corneum. *J. Lipid Res.* **36** (1995) 685-695.

62. Bouwstra J.A., Gooris G.S., Salomons-de Vries M.A., van der Spek J.A., Bras W. Structure of human stratum corneum as a function of temperature and hydration: A wide-angle X-ray diffraction study. *Int. J. Pharm.* **84** (1992) 205-216.

63. Pilgram G.S.K., Engelsma-van Pelt A.M., Bouwstra J.A., Koerten H.K. Electron diffraction provides new information on human stratum corneum lipid organization studied in relation to depth and temperature. *J. Invest. Dermatol.* **113** (1999) 403-409.

64. Bommannan D., Potts R.O., Guy R.H. Examination of stratum corneum barrier function in vivo by infrared spectroscopy. *J. Invest. Dermatol.* **95** (1990) 403-408.

65. Stewart M.E., Downing D.T. Chemistry and function of mammalian sebaceous lipids. *Adv. Lipid Res.* **24** (1991) 263-301.

66. ten Grotenhuis E., Demel R.A., Ponec M., Boer D.R., van Miltenburg J.C., Bouwstra J.A. Phase-behavior of stratum corneum lipids in mixed langmuir-blodgett monolayers. *Biophys. J.* **71** (1996) 1389-1399.

67. Fenske D.B., Thewalt J.L., Bloom M., Kitson N. Models of stratum corneum intercellular membranes: ^{2}H NMR of microscopically oriented multilayers. *Biophys. J.* **67** (1994) 1562-1573.

68. Kitson N., Thewalt J., Lafleur M., Bloom M. A model membrane approach to the epidermal permeability barrier. *Biochemistry* **33** (1994) 6707-6715.

69. Moore D.J., Rerek M.E., Mendelsohn R. Lipid domains and orthorhombic phases in model stratum corneum: evidence from fourier transform infrared spectroscopy studies. *Biochem. Biophys. Res. Commun.* **231** (1997) 797-801.

70. Lafleur M. Phase behaviour of model stratum corneum lipid mixtures: an infrared spectroscopy investigation. *Can. J. Chem.* **76** (1998) 1500-1511.

71. Moore D.J., Rerek M.E. Insights into the molecular organisation of lipids in the skin barrier from infrared spectroscopy studies of stratum corneum lipid models. *Acta Derm. Venereol. Suppl. (Stockh.)* **208** (2000) 16-22.

72. Bouwstra J.A., Thewalt J., Gooris G.S., Kitson N. A model membrane approach to the epidermal permeability barrier: an X-ray diffraction study. *Biochemistry* 36 (1997) 7717-7725.

73. Bouwstra J.A., Gooris G.S., Cheng K., Weerheim A., Bras W., Ponec M. Phase behavior of isolated skin lipids. *J. Lipid Res.* **37** (1996) 999-1011.

74. Bouwstra J.A., Dubbelaar F.E.R., Gooris G.S., Weerheim A.M., Ponec M. The role of ceramide composition in the lipid organisation of the skin barrier. *Biochim. Biophys. Acta* **1419** (1999) 127-136.

75. McIntosh T.J., Stewart M.E., Downing D.T., 1996. X-ray diffraction analysis of isolated skin lipids: reconstitution of intercellular lipid domains. *Biochemistry* **35** (1996) 3649-3653.

76. Bouwstra J.A., Gooris G.S., Dubbelaar F.E.R., Weerheim A.M., IJzerman A.P., Ponec M. Role of ceramide 1 in the molecular organization of the stratum corneum lipids. *J. Lipid Res.* **39** (1998) 186-196.

77. Bouwstra J.A., Gooris G.S., Dubbelaar F.E.R., Ponec M. Phase behavior of lipid mixtures based on human ceramides: coexistence of crystalline and liquid phases. *J. Lipid Res.* **42** (2001) 1759-1770.

78. Bouwstra J.A., Gooris G.S., Dubbelaar F.E.R., Ponec M. Phase behavior of stratum corneum lipid mixtures based on human ceramides: the role of natural and synthetic ceramide 1. *J. Invest. Dermatol.* **118** (2002) 606-617.

79. Bouwstra J.A., Dubbelaar F.E.R., Gooris G.S., Weerheim A.W., Ponec M. pH, cholesterol sulfate, and fatty acids affect the stratum corneum lipid organization. *J. Invest. Dermatol. Symp. Proc.* **3** (1998) 69-73.

80. Bouwstra J.A., Gooris G.S., Dubbelaar F.E.R., Ponec M. Cholesterol sulfate and calcium affect stratum corrneum lipid organization over a wide temperature range. *J. Lipid Res.* **40** (1999) 2303-2312.

81. Swartzendruber D.C., Wertz P.W., Kitko D.J., Madison K.C., Downing D.T. Molecular models of the intercellular lipid lamellae in mammalian stratum corneum. *J. Invest. Dermatol.* **92** (1989) 251-257.

82. Forslind B. A domain mosaic model of the skin barrier. Acta Derm. Venereol. **74** (1994) 1-6.

83. Norlen L. Skin barrier structure and function: the single gel phase model. *J. Invest. Dermatol.* **117** (2001) 830-836.

84. Bouwstra J.A., Dubbelaar F.E.R., Gooris G.S., Ponec M. The lipid organisation in the skin barrier. *Acta Derm. Venereol. Suppl. (Stockh).* **208** (2000) 23-30.

85. Imokawa G., Abe A., Jin K., Higaki Y., Kawashima M., Hidano A. Decreased level of ceramides in stratum corneum of atopic dermatitis: an etiologic factor in atopic dry skin? *J. Invest. Dermatol.* **96** (1991) 523-526.

86. Yamamoto A., Serizaka S., Ito M., Sato Y.. Stratum corneum lipid abnormalities in atopic dermatitis. *Arch. Dermatol. Res.* **283** (1991) 219-223.

87. Di Nardo A., Wertz P., Giannetti A., Seidenari S. Ceramide and cholesterol composition of the skin of patients with atopic dermatitis. *Acta Derm. Venereol.* **78** (1998) 27-30.

88. Pilgram G.S.K., Vissers D.C.J., van der Meulen H., Pavel S, Lavrijsen S.P.M., Bouwstra J.A., Koerten H.K. Aberrant lipid organization in stratum corneum of patients with atopic dermatitis and lamellar ichthyosis. *J. Invest.Dermatol.* **117** (2001) 710-717.

89. Lavrijsen A.P.M., Bouwstra J.A., Gooris G.S., Weerheim A., Bodde H.E., Ponec M. Reduced skin barrier function parallels abnormal stratum corneum lipid organization in patients with lamellar ichthyosis. *J. Invest. Dermatol.* **105** (1995) 619-624.

90. Fartasch M. Epidermal barrier in disorders of the skin. Microsc. Res. Tech. **38** (1997) 361 -372.

91. Ghadially R., Reed J.T., Elias P.M. Stratum corneum structure and function correlates with phenotype in psoriasis. *J. Invest. Dermatol.* **107** (1996) 558-564.

92. Motta S., Monti M., Sesana S., Caputo R., Carelli S., Ghidoni R. Ceramide composition of the psoriatic scale. *Biochim Biophys Acta.* **1182** (1993) 147-151.

93. Motta S., Monti M., Sesana S., Mellesi L., Ghidoni R., Caputo R. Abnormality of water barrier function in psoriasis. *Arch. Dermatol.* **130** (1994) 452-456.

94. Williams M.L., Elias P.M. Stratum corneum lipids in disorders of cornification: increased cholesterol sulphate content of stratum corneum in recessive x-linked ichthyosis. *J. Clin. Invest.* **68** (1981) 1404-1410.

95. Rogers J., Harding C., Mayo A., Banks J., Rawlings A. Stratum corneum lipids: the effect of ageing and the seasons. *Arch. Dermatol. Res.* **288** (1996) 765-770.

96. Rawlings A.V., Watkinson A., Rogers J. Mayo A.M., Hopes J., Scott I.R. Abnormalities in stratum corneum structure, lipid composition, and desmosome degradation in soap-induced winter xerosis. *J. Soc. Cosmet. Chem.* **45** (1994) 203-220.

97. Fulmer A.W., Kramer G.J. Stratum corneum lipid abnormalities in surfactant-induced dry scaly skin. *J. Invest. Dermatol.* **86** (1986) 598-602.

98. Higuchi T. Physical chemical analysis of percutaneous absorption process from creams and ointment. *J. Soc. Cosm. Chem.* **11** (1960) 85-97.

99. Martin A. Physical pharmacy: physical chemical principles in the pharmaceutical sciences. 4th edition. Lea & Febiger, Malvern, 1993.

100. Hadgraft J. Skin deep. *Eur. J. Pharm. Biopharm.* **58** (2004) 291-299.

101. Squier C.A., Kremer M., Wertz P.W. Continuous flow mucosal cells for measuring the in-vitro permeability of small tissue samples. *J. Pharm. Sci.* **86** (1997) 82-84.

102. Friend D.R. In vitro skin permeation techniques. *J. Control. Release* **18** (1992) 235-248.

103. Southwell D., Barry B.W., Woodford R. Variations in permeability of human skin within and between specimens. *Int. J. Pharm.* **18** (1984) 299-309.

104. Swarbrick J., Lee G., Brom J. Drug permeation through the skin: I. Effect of storage conditions of skin. *J. Invest. Dermatol.* **78** (1982) 63-66.

105. Schmook F.P., Meingassner J.G., Billich A. Comparison of human skin or epidermis models with human and animal skin in in-vitro percutaneous absorption. *Int. J. Pharm.* **215** (2001) 51-56.

106. Catz P., Friend D.R. Transdermal delivery of levonorgestrel. VII. Effect of enhancers on rat skin, hairless mouse skin, hairless guinea pig skin, and human skin. *Int. J. Pharm.* **58** (1990) 93-102.

107. Rigg P.C., Barry B.W. Shed snake skin and hairless mouse skin as model membranes for human skin during permeation studies. J*. Invest. Dermatol.* **94** (1990) 235-240.

108. Behl C.R., Flynn G.L., Kurihara T., Smith W., Higuchi W.I., Ho N.F.W., Pierson C.L. Hydration and percutaneous absorption: I. Influence of hydration on alcohol permeation through hairless mouse skin. *J. Invest. Dermatol.* **75** (1980) 346-352.

109. Itoh T., Xia J., Magavi R., Nishihata T., Rytting J.H. Use of shed snake skin as a model membrane for in vitro percutaneous penetration studies: Comparison with human skin. *Pharm. Res.* **7** (1990) 1042-1047.

110. Craane-van Hinsberg W.H.M., Verhoef J.C., Bax L.J., Junginger H.E., Bodde H.E. Role of appendages in skin resistance and iontophoretic peptide flux: human versus snake skin. *Pharm. Res.* **12** (1995) 1506-1512.

111. Takahashi K., Sakano H., Rytting J.H., Numata N., Kuroda S., Mizuno N. Influence of pH on the permeability of p-toluidine and aminopyrine through shed snake skin as a model membrane. *Drug Dev. Ind. Pharm.* **27** (2001) 159-164.

112. Li G.L., van der Geest R., Chanet L., van Zanten E., Danhof M., Bouwstra J.A. In vitro iontophoresis of R-apomorphine across human stratum corneum. Structure-transport relationship of penetration enhancement. *J. Control. Release* **84** (2002) 49-57.

113. Montagna W., Yun J.S. The skin of the domestic pig. *J. Invest. Dermatol.* **42** (1964) 11-21.

114. Hawkins G.S., Reifenrath W.G. Influence of skin source, penetration cell fluid, and partition coefficient on in vitro skin penetration. *J. Pharm. Sci.* **75** (1986) 378-381.

115. Sato K., Sugibayashi K., Morimoto Y. Species differences in percutaneous absorption of nicorandil. *J. Pharm. Sci.* **80** (1991) 104 -107.

116. Chambin O., Bevan B., Teillaud E. Pig skin as an animal model for in-vitro percutaneous absorption studies. In: Brain KR, James V.J., Walters K.A., editors. Prediction of percutaneous penetration Vol 3B, 1993 Cardiff, UK: STS Publishing pp.111-116.

117. Sekkat N., Kalia Y.N., Guy R.H. Biophysical Study of porcine ear skin in vitro and its comparison to human skin in vivo. *J. Pharm. Sci.* **91** (2002) 2376-2381.

118. Prunieras M., Regnier M., Woodley D. Methods for cultivation of keratinocytes with an air-liquid interface. *J. Invest. Dermatol.* **81** Suppl. 1 (1983) 28s-33s.

119. Ponec M., Weerheim A., Kempenaar J., Mulder A., Gooris G.S., Bouwstra J., Mommaas A.M. The formation of competent barrier lipids in reconstructed human epidermis requires the presence of vitamin C. *J. Invest. Dermatol.* **109** (1997) 348-355.

120. Gibbs S., Vicanova J., Bouwstra J., Valstar D., Kempenaar J., Ponec M. Culture of reconstructed epidermis in a defined medium at 33 degrees C shows a delayed epidermal maturation, prolonged lifespan and improved stratum corneum. *Arch. Dermatol. Res.* **289** (1997) 585-595.

121. Vicanova J., Boelsma E., Mommaas A.M., Kempenaar J.A., Forslind B., Pallon J., Egelrud T., Koerten H.K., Ponec M. Normalization of epidermal calcium distribution profile in reconstructed human epidermis is related to improvement of terminal differentiation and stratum corneum barrier formation. *J. Invest. Dermatol.* **111** (1998) 97-106.

122. Ponec M. Skin constructs for replacement of skin tissues for in vitro testing. *Adv. Drug Deliv. Rev.* **54** (2002) S19 -S30.

123. Ponec M., Boelsma E., Weerheim A., Mulder A., Bouwstra J., Mommaas M. Lipid and ultrastructural characterization of reconstructed skin models. *Int. J. Pharm.* **203** (2000) 211-225.

124. Bouwstra J.A., Gooris G.S., Weerheim A., Kempenaar J., Ponec M. Characterization of stratum corneum structure in reconstructed epidermis by X-ray diffraction. *J. Lipid Res.* **36** (1995) 496-504.

125. Pilgram G.S.K., Gibbs S., Ponec M., Koerten H.K., Bouwstra J.A. The lateral lipid organization in stratum corneum of a human skin equivalent is predominantly hexagonal. In: A close look at the stratum corneum organization by cryo-electron diffraction, PhD thesis, Leiden University, 2000, pp 95-102.

126. Roy S.D., Fujiki J., Fleitman J.S. Permeabilities of alkyl p-aminobenzoates through living skin equivalent and cadaver skin. *J. Pharm. Sci.* **82** (1993) 1266 -1268.

127. Robert M., Dusser I., Muriel M.P., Noel-Hudson M.S., Aubery M., Wepierre J. Barrier function of reconstructed epidermis at the air-liquid interface: influence of dermal cells and extracellular components. *Skin Pharmacol.* **10** (1997) 247-260.

128. Wagner H., Kosta K.H., Lehr K.M., Schaefer U.F. Interrelation of permeation and penetration parameters obtained from in vitro experiments with human skin and skin equivalents *J. Control. Release* **75** (2001) 283-295.

129. Zghoul N., Fuchs R., Lehr C.M., Schaefer U.F. Reconstructed skin equivalents for assessing percutaneous drug absorption from pharmaceutical formulations. *ALTEX* **18** (2001) 103-106.

130. Garcia N., Doucet O., Bayer M., Fouchard D., Zastrow L., Marty J.P. Characterization of the barrier function in a reconstituted human epidermis cultivated in chemically defined medium. *Int. J. Cosm. Sci.* **24** (2002) 25-34.

131. Lotte C., Patouillet C., Zanini M., Messager A., Roguet R. Permeation and skin absorption: reproducibility of various industrial reconstrucuted human skin models. *Skin Pharmacol. Appl. Skin Physiol.* **15** Suppl. 1 (2002) 18-30.

132. Hatanaka T., Inuma M., Sugibayashi K., Morimoto Y. Prediction of skin permeability of drugs. I. Comparison with artificial membrane. *Chem. Pharm. Bull.* **38** (1990) 3452-3459.

133. Yamaguchi Y., Usami T., Natsume H., Aoyagi T., Nagase Y., Sugibayashi K., Morimoto Y. Evaluation of skin permeability of drugs by newly prepared polymer membranes. *Chem. Pharm. Bull.* **45** (1997) 537-541.

134. Houk J., Guy R.H. Membrane models for skin penetration studies. *Chem. Rev.* **88** (1988) 455-471.

135. Feldstein M.M., Raigorodskii I.M., Iordanskii A.L., Hadgraft J. Modeling of percutaneous drug transport in vitro using skin-imitating Carbosil membrane. *J. Control. Release* **52** (1998) 25-40.

136. Abraham W., Downing D.T. Preparation of model membranes for skin permeability studies using stratum corneum lipids. *J. Invest. Dermatol.* **93** (1989) 809-813.

137. Friberg S.E., Kayali I.. Water evaporation rates from a model of stratum corneum lipids. *J. Pharm. Sci.* **78** (1989) 639-643.

138. Lieckfeldt R., Villalain J., Gomez-Fernandez J.C., Lee G. Diffusivity and structural polymorphism in some model stratum corneum lipid systems. *Biochim. Biophys. Acta* **1151** (1993) 182-188.

139. Kittayanond D., Dowton S.M., Ramachandran C., Flynn G.L., Weiner N. Development of a model of the lipid constituent phase of the stratum corneum: II. Preparation of artificial membranes from synthetic lipids and assessment of permeability properties using in vitro diffusion experiments. J. *Soc. Cosmet. Chem.* **43** (1992) 237-249.

140. Matsuzaki K., Imaoka T., Asano M., Miyajima K. Development of a model membrane system using stratum corneum lipids for estimation of drug skin permeability. *Chem. Pharm. Bull.* **41** (1993) 575-579.

141. Miyajima K., Tanikawa S., Asano M., Matsuzaki K. Effects of absorption enhancers and lipid composition on drug permeability through the model membrane using stratum corneum lipids. *Chem. Pharm. Bull.* **42** (1994) 1345-1347.

Part I

Selection of a synthetic stratum corneum lipid mixture

Chapter 2

The phase behaviour of skin lipid mixtures based on synthetic ceramides

M.W. de Jager,* G.S. Gooris,* I.P. Dolbnya,# W. Bras,# M. Ponec,§ and J.A. Bouwstra*

* Leiden/Amsterdam Center for Drug Research, Department of Drug Delivery Technology, University of Leiden, P.O. Box 9502, 2300 RA Leiden, The Netherlands.
# Netherlands Organisation for Scientific Research, DUBBLE CRG/ESRF, Grenoble, France.
§ Department of Dermatology, Leiden University Medical Center, Leiden, The Netherlands.

(adapted from *Chem. Phys. Lipids* **124** (2003) 123-134)

ABSTRACT

The lipid lamellae present in the outermost layer of the skin, the stratum corneum, form the main barrier for diffusion of molecules across the skin. The main lipid classes in stratum corneum are cholesterol, free fatty acids and at least 9 classes of ceramides, referred to as CER1 to CER9. In the present study the phase behaviour of four synthetic ceramides, either single or mixed with cholesterol or cholesterol and free fatty acids, has been studied using small-angle and wide-angle X-ray diffraction. The lipid mixtures show complex phase behaviour with coexistence of several phases. The results further reveal that the presence of synthetic CER1 as well as a proper composition of the other ceramides in the mixture are crucial for the formation of a phase with a long periodicity, characteristic for the stratum corneum lipid phase behaviour. Only a mixture containing synthetic CER1, CER3, cholesterol and free fatty acids shows similar phase behaviour to that of stratum corneum.

1. INTRODUCTION

For the majority of chemicals, the barrier function of the skin is unquestionably attributed to its superficial layer, the stratum corneum. Stratum corneum consists of keratin-filled corneocytes, organised in a matrix of highly ordered multi-lamellar lipid sheets. This is often referred to as a brick wall-like structure, with the corneocytes forming the bricks and the intercellular lipids representing the mortar [1]. Several microscopic transport studies have demonstrated that the lipid matrix is the major rate-limiting pathway by which most drugs traverse the stratum corneum [2-4]. For this reason, the structure and physical properties of the stratum corneum lipids are considered to play an essential role in the skin barrier function.

The lipid composition in stratum corneum is unique. Unlike biological membranes, it is almost devoid of phospholipids and the major constituents are ceramides, cholesterol and long-chain free fatty acids. At least 9 different classes of ceramides have been identified in human stratum corneum [5-8], which are referred to as CER1 to CER9. The ceramides are composed of a sphingosine, a phytosphingosine or a 6-hydroxysphingosine base to which nonhydroxy or α-hydroxy fatty acid is linked. These fatty acids have a chain length distribution with 24 (C24) and 26 (C26) carbon atoms being the most abundantly present. CER1, CER4 and CER9 are unique in structure since these acylceramides contain linoleic acid bound to an ω-hydroxy fatty acid with a chain length of 30 to 32 carbon atoms.

X-ray diffraction studies on stratum corneum have demonstrated that the stratum corneum lipids are structured in two coexisting crystalline lamellar phases with periodicities of approximately 6 nm (referred to as the short periodicity phase: SPP) and 13 nm (referred to as the long periodicity phase: LPP), respectively [9-11]. The presence of the 13 nm lamellar phase and the crystalline nature of the lipid packing are believed to be critical for an adequate skin barrier function.

Several studies have been performed in order to attempt reproduction of the stratum corneum lipid organisation, using a model system prepared with isolated pig or human ceramides, cholesterol and free fatty acids. It was found that the phase behaviour of isolated ceramides mixed with cholesterol in a wide range of molar ratios was similar to that of native stratum corneum [12-14]. Mixtures prepared with isolated pig ceramides showed the presence of two lamellar phases with periodicities of 5.2 and 12.2 nm, whereas the repeat distances of both phases were 5.4 and 12.8 nm in mixtures containing human ceramides. The lamellar organisation in lipid mixtures

prepared with cholesterol, ceramides and free fatty acids resembled that of stratum corneum even closer. Addition of free fatty acids to equimolar mixtures of cholesterol and ceramides induced a phase transition from a hexagonal to an orthorhombic packing [15]. In addition, the presence of CER1 was shown to be crucial for the formation of the LPP.

Other studies have described the phase behaviour of stratum corneum lipid models based on synthetic ceramides. The majority of those studies focused on equimolar mixtures containing cholesterol, palmitic acid and the commercially available bovine brain ceramide type III (ΣCERIII, see Fig. 1), which is structurally similar to the most abundant CER2 in stratum corneum. Using nuclear magnetic resonance, it was found that at physiological temperatures the lipids predominantly form crystalline phases [16, 17]. In addition, several fourier transform infrared spectroscopy measurements showed that both ceramides and palmitic acid phase-separate into crystalline domains with an orthorhombic chain packing [18-20]. Similarly, domains enriched in cholesterol, ceramides, or palmitic acid were detected with Raman microscopy [21]. In mixtures consisting of cholesterol, hexadecanoic acid and either synthetic CER2 or CER5 it was also observed that the lipids were not properly mixed in one orthorhombic lattice, but coexisted in various phases [22]. The lipid composition of those models differs from that of the intact stratum corneum with respect to the molecular structure of the individual ceramides and the chain length of the free fatty acids. Stratum corneum mainly contains long-chain free fatty acids [23], while palmitic acid is only present in very small amounts. However, despite the simplicity of those model mixtures, some features of the stratum corneum lateral organisation appeared to be reproduced. Concerning the lamellar organisation, small-angle X-ray diffraction studies revealed that the characteristic LPP is not present in mixtures consisting of bovine brain ceramide type III, cholesterol and palmitic acid [12, 24]. In one paper the observed formation of a 10.4 nm lamellar phase in a mixture of bovine brain ceramide type III and cholesterol was attributed to the formation of a double-bilayer structure [25]. It is a matter of debate to consider this phase as representative for stratum corneum, since its repeat distance noticeably differs from that of the LPP in stratum corneum. Moreover, the LPP is most likely not a double-bilayer structure, but a tri-layer structure [14].

The main objective of the present study was to prepare a lipid mixture with synthetic ceramides that would mimic the stratum corneum lipid phase behaviour with respect to the lamellar and lateral arrangement. The phase behaviour of four synthetic ceramides (see Fig. 1), either single or in a mixture with cholesterol (CHOL:CER) or

cholesterol and free fatty acids (CHOL:CER:FFA) were therefore investigated using small-angle X-ray diffraction (SAXD) and wide-angle X-ray diffraction (WAXD). The effects of compositional changes, including the addition of synthetic CER1, on the phase behaviour of the lipid mixtures were systematically examined.

2. MATERIALS AND METHODS

2.1 Materials

Palmitic acid, stearic acid, arachidic acid, behenic acid, tricosanoic acid, lignoceric acid, cerotic acid, cholesterol and ceramides modified from bovine brain sphingomyelin (type III and IV) were purchased from Sigma-Aldrich Chemie GmbH (Schnelldorf, Germany). N-(30-Linoleoyloxy-triacontanoyl)-sphingosine (synthetic ceramide1(C30)-linoleate) was a gift from Beiersdorf AG (Hamburg, Germany). N-Tetracosanoyl-phytosphingosine (synthetic ceramide 3(C24)) and N-Stearoyl-phytosphingosine (synthetic ceramide 3(C16)) were generously provided by Cosmoferm B.V. (Delft, the Netherlands). All organic solvents used were of analytical grade and manufactured by Labscan Ltd (Dublin, Ireland).

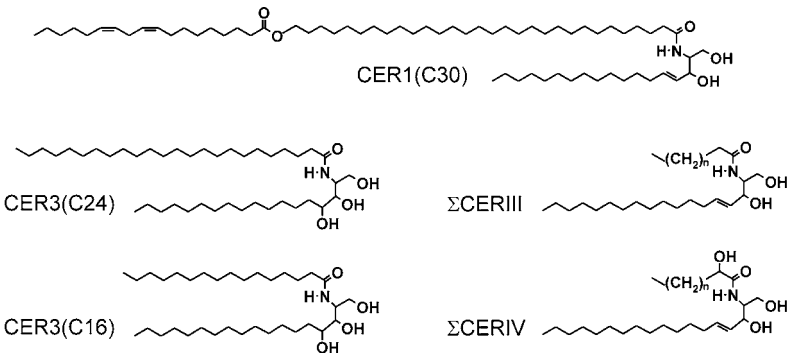

Figure 1 - The molecular structures of the ceramides used in the study. The acyl chain lengths of CER1(C30), CER3(C16) and CER3(C24) are well-defined, whereas bovine brain ceramide type III and IV (ΣCERIII and ΣCERIV) show a chain length distribution with C18 and C24 as the most abundantly present.

2.2 Methods

2.2.1 Preparation of lipid mixtures

For the preparation of the three component mixtures (CHOL:CER:FFA), the following free fatty acid mixture was used: C16:0, C18:0, C20:0, C22:0, C23:0, C24:0 and C26:0

at molar ratios of respectively 1.3, 3.3, 6.7, 41.7, 5.4, 36.8 and 4.7, respectively. Appropriate amounts of individual lipids dissolved in chloroform:methanol 2:1 (v/v) were combined to yield lipid mixtures of approximately 1.5 mg total dry weight at the desired composition at a total lipid concentration of 7 mg/ml. A Camag Linomat IV was used to apply the lipid mixtures onto mica. This was done at a rate of 4.3 µl/min under a continuous nitrogen flow. The samples were equilibrated for 10 minutes at 60°C and subsequently hydrated with an acetate buffer of pH 5.0. Finally, the samples were homogenised by 10 successive freeze-thawing cycles between –20°C and room temperature, during which the samples were stored under gaseous nitrogen.

2.2.2 Small-angle X-ray diffraction analysis

All measurements were performed at the European Synchrotron Radiation Facility (ESRF, Grenoble), using the Dutch-Belgian beamline (BM26B). A more detailed description of this beamline has been given elsewhere [26]. The X-ray wavelength and the sample-to-detector distance were 1.24Å and 1.7m, respectively. Diffraction data were collected on a two-dimensional multiwire gas-filled area detector. The spatial calibration of this detector was performed using silver behenate. The samples were mounted in a specially designed sample holder with mica windows. All measurements were recorded at room temperature for a period of 10 minutes.

SAXD provides information about the larger structural units in the sample, such as the repeat distance of a lamellar phase. The scattering intensity I (in arbitrary units) was measured as a function of the scattering vector q (in reciprocal nm). The latter is defined as $q=(4\pi\sin\theta)/\lambda$, in which θ is the scattering angle and λ is the wavelength. From the positions of a series of equidistant peaks (q_n), the periodicity, or d-spacing, of a lamellar phase was calculated using the equation $q_n=2n\pi/d$, n being the order number of the diffraction peak.

2.2.3 Wide-angle X-ray diffraction analysis

WAXD provides information about the smaller structural units, like the lateral packing of the lipids within the lamellae. Diffraction data were collected on a microstrip gas chamber detector with an opening angle of 60° [27]. The sample-to-detector distance was 36 cm and the X-ray wavelength was 1.24Å. The spatial calibration of the detector was performed with a mixture of silicium and cholesterol.

The SAXD and WAXD data were collected simultaneously.

3. RESULTS

3.1 Lamellar ordering of single CER, CHOL:CER mixtures and CHOL:CER:FFA mixtures

The spacings derived from the diffraction data and the corresponding phases of the lipid mixtures studied are summarised in Table 1. One phase with a periodicity of 5.26 nm, of which the first, second and third order diffraction peaks were located at q = 1.19, 2.40 and 3.61 nm^{-1} is present in bovine brain ceramide type III (ΣCERIII). In the equimolar CHOL:ΣCERIII mixture, the periodicity of this phase slightly shifts to 5.15 nm. In addition, phase-separated cholesterol is present, which can be deduced from the peaks located at 1.87 and 3.74 nm^{-1}. The latter peak is not symmetric, but exhibits a shoulder at the left-hand side, which can be ascribed to the third order peak of the 5.15 nm phase. From Figure 2, in which the diffraction patterns of the equimolar mixtures CHOL:ΣCERIII and CHOL:ΣCERIII:FFA are plotted, it can be observed that addition of an equimolar amount of free fatty acids to the binary mixture does not significantly change the positions or intensities of the diffraction peaks. However, in the ternary mixture an additional reflection is observed at q = 3.26 nm^{-1}, which is closely located to the third order diffraction peak of pure free fatty acids (data not shown).

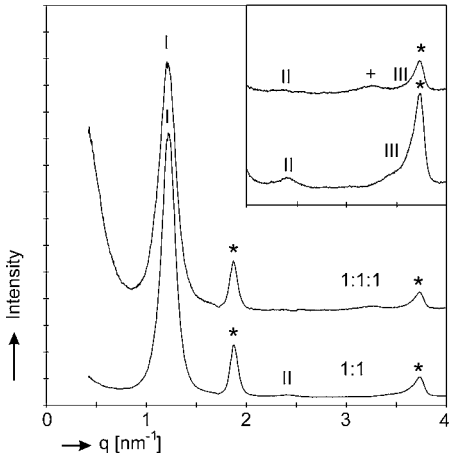

Figure 2 - Diffraction patterns of the equimolar CHOL:ΣCERIII and CHOL:ΣCERIII:FFA mixtures. The inset is a magnification of the reflections in the q-range between 2 and 4 nm^{-1}. The reflections indicated by Roman numbers are attributed to the first, second and third order reflections of a SPP (repeat distance of 5.15 and 5.18 nm for the binary and ternary mixture, respectively), whereas the asterisk (*) denotes the two reflections attributed to crystalline cholesterol. The plus sign refers to the additional peak present in the ternary mixture at a spacing of 1.92 nm (q = 3.26 nm^{-1}), likely due to phase-separated free fatty acids.

Similar results were obtained with mixtures prepared with ΣCERIV (compare conditions 1-3 with 4-6 in Table 1). Again, no LPP can be detected. The diffraction pattern of single ΣCERIV shows three reflections that can be ascribed to a 5.44 nm phase. The periodicity of this phase slightly reduces to 5.33 nm in the equimolar CHOL:ΣCERIV mixture and to 5.38 nm in the equimolar CHOL:ΣCERIV:FFA mixture. In

Table 1 - The reflections and corresponding phases in the lipid mixtures examined

lipid mixture		small-angle reflections (nm)
1	ΣCERIII	d_l = **5.26** [5.26(1), 2.62(2), 1.74(3)]
2	CHOL:ΣCERIII 1:1	d_l = **5.15** [5.15(1), 2.59(2), 1.78*(3)] ; d = **3.35** [3.35(1), 1.68(2)]
3	CHOL:ΣCERIII:FFA 1:1:1	d = **5.76**? [1.92*(3)] ; d_l = **5.18** [5.18(1), 2.59(2), 1.74*(3)] ; d = **3.35** [3.35(1), 1.68(2)]
4	ΣCERIV	d_l = **5.44** [5.44(1), 2.72(2), 1.82(3)]
5	CHOL:ΣCERIV 1:1	d_l = **5.33** [5.33(1), 2.67(2), 1.80(3)] ; d = **3.35** [3.35(1), 1.68(2)]
6	CHOL:ΣCERIV:FFA 1:1:1	d = **5.82**? [1.94*(3)] ; d_l = **5.38** [5.38(1), 2.69(2), 1.80(3)] ; d = **3.35** [3.35(1), 1.68(2)]
7	CER3(C16)	d = **4.03** [4.03(1), 2.02(2)] ; d = **3.59** [3.59(1), 1.80(2)]
8	CHOL:CER3(C16) 0.5:1	d = **4.03** [4.03(1), 2.02(2)] ; d = **3.59** [3.59(1), 1.80(2)] ; d = **3.44** [1.72*(2)] ; d = **3.35** [3.35(1), 1.68(2)]
9	CHOL:CER3(C16) 1:1	d = **3.59** [3.59(1), 1.80(2)] ; d = **3.43** [3.43*(1), 1.72(2)] ; d = **3.35** [1.68*(2)]
10	CHOL:CER3(C16):FFA 1:1:1	d_l = **5.89** [5.89(1), 1.97(3)] ; d = **5.73**? [1.91*(3)] ; d = **3.58** [3.58(1), 1.79(2)] ; d = **3.35** [3.35(1), 1.68(2)]
11	CER3(C24)	d = **4.26** [4.26(1), 2.14(2)] ; d = **3.71** [3.71(1), 1.85(2)]
12	CHOL:CER3(C24) 0.5:1	d = **3.70** [3.70(1), 1.85(2)] ; d = **3.44** [3.44(1), 1.72(2)]
13	CHOL:CER3(C24) 1:1	d = **3.71** [3.71(1), 1.85(2)] ; d = **3.44** [3.44(1), 1.72(2)] ; d = **3.35** [1.68*(2)]
14	CHOL:CER3(C24):FFA 1:1:1	d_l = **5.28** [5.28(1), 2.65(2)] ; d = **3.81** [3.81(1), 1.90(2)] ; d = **3.71**? [1.86(2)] ; d = **3.35** [3.35(1), 1.68(2)]
15	CHOL:[CER1:ΣCERIII] 1:[0.1:0.9]	d_l = **5.41** [5.41(1), 2.72(2), 1.82(3)] ; d = **3.35** [3.35(1), 1.68(2)]
16	CHOL:[CER1:ΣCERIII]:FFA 1:[0.1:0.9]:1	d = **5.70**? [1.90(3)] ; d_l = **5.40** [5.40(1), 2.71(2)] ; d = **3.35** [3.35(1), 1.68(2)]
17	CHOL:[CER1:ΣCERIV] 1:[0.1:0.9]	d = **5.70**? [1.90(3)] ; d_l = **5.40** [5.40(1), 2.71(2)] ; d = **3.35** [3.35(1), 1.68(2)]
18	CHOL:[CER1:ΣCERIV]:FFA 1:[0.1:0.9]:1	d = **5.76**? [1.92(3)] ; d_l = **5.42** [5.42(1), 2.72(2), 1.81(3)] ; d = **3.35** [3.35(1), 1.68(2)]
19	CHOL:[CER1:CER3(C24)] 1:[0.1:0.9]	d = **3.78** [3.78(1), 1.84(2)] ; d = **3.43** [3.43(1), 1.72(2)] ; d = **3.35** [1.68*(2)]
20	CHOL:[CER1:CER3(C24)]:FFA 1:[0.1:0.9]:1	d_l = **11.6** [11.6(1), 3.92(3)] ; d_l = **5.42** [5.42(1), 2.72(2), 1.79(3)] ; d = **3.35** [3.35(1), 1.68(2)]

d = 5.26 [5.26(1), 2.62(2), 1.74(3)] means that the periodicity of the phase present is 5.26 nm, based on the presence of the first, second and third order reflections, located at a spacing of 5.26 nm (q = 1.19 nm^{-1}), 2.62 nm (q = 2.40 nm^{-1}) and 1.74 nm (q = 3.61 nm^{-1}). The real spacings (nm) were calculated from the q values (nm^{-1}) using the equation $q = 2n\pi/d$. The presence of a lamellar phase is indicated with d_l. Diffraction peaks present as a shoulder are denoted with an asterisk. A question mark indicates that the interpretation of this phase is uncertain.

addition, in the binary and ternary mixtures the two reflections of crystalline cholesterol are present. Again a small additional peak (at q = 3.24 nm^{-1}) can be observed in the presence of free fatty acids.

CER3(C16) shows more complex phase behaviour than ΣCER. In the diffraction pattern of single CER3(C16), two phases can be observed with periodicities of 4.03 and 3.59 nm, respectively. The intensities of the two reflections attributed to the 4.03 nm phase are considerably smaller than the two strong reflections of the 3.59 nm phase. Addition of cholesterol to CER3(C16), achieving a molar ratio of CHOL:CER3(C16) 0.5:1 results in a similar diffraction pattern (Fig. 3A). However, besides the 4.03 and 3.59 nm phases, crystalline cholesterol can be detected. A weak shoulder at the left-hand side of the peak at q = 3.74 nm^{-1} indicates the presence of another phase with a periodicity of about 3.44 nm (Fig. 3A; for explanation see below). In the equimolar CHOL:CER3(C16) mixture, two interesting features are observed. Crystalline CER3(C16) is still present, as indicated by the strong peak located at 1.75 nm^{-1}. However, the phase with a repeat distance of 4.03 nm completely disappeared. Additionally, the presence of the phase with a periodicity of about 3.44 nm can clearly be derived from the asymmetry of the reflection located at q = 1.75 nm^{-1} and the presence of a strong second order peak at q = 3.66 nm^{-1}. The shoulder present at the right-hand side of the reflection at q = 3.66 nm^{-1} indicates that phase-separated cholesterol is also present.

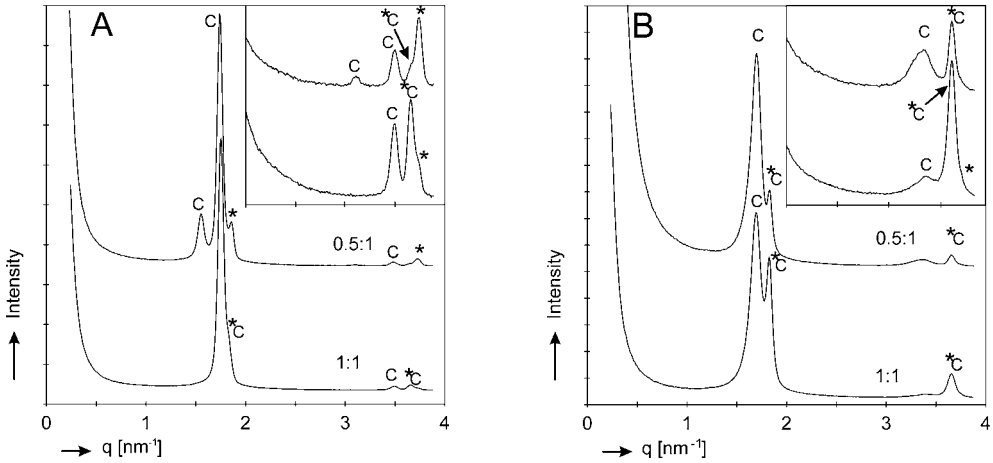

Figure 3 - Diffraction patterns of the CHOL:CER3 mixtures (A) CHOL:CER3(C16) at a molar ratio of 0.5:1 and 1:1, (B) CHOL:CER3(C24) at a molar ratio of 0.5:1 and 1:1. The inset is a magnification of the reflections in the q-range between 2 and 4 nm^{-1}. The diffraction peaks indicated by the letter C are attributed to the first and second order reflections of two crystalline phases of CER3. The asterisk indicates the reflections of crystalline cholesterol, whereas *C denotes the diffraction peaks of the 3.44 nm phase.

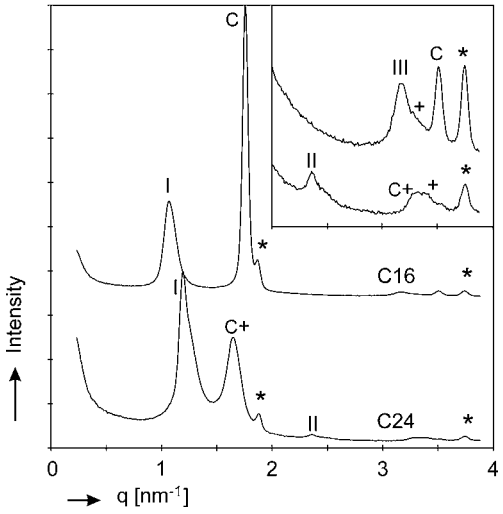

Figure 4 - Diffraction patterns of the equimolar CHOL:CER3(C16):FFA and CHOL:CER3(C24):FFA mixtures. The peaks indicated by Roman numbers are attributed to the reflections of the SPP (repeat distance of 5.89 nm and 5.28 nm in the mixture prepared with CER3(C16) and CER3(C24), respectively). The peaks indicated by the letter C are attributed to phase-separated CER3. C+ refers to the diffraction peaks of the 3.82 nm phase, whereas the asterisk indicates the reflections of crystalline cholesterol. The plus sign refers to the additional peak present in the ternary mixture prepared with CER3(C16), likely due to phase-separated free fatty acids.

Figure 4 shows the diffraction pattern of the equimolar CHOL:CER3(C16):FFA mixture. Addition of free fatty acids to the CHOL:CER3(C16) mixture induces the formation of a 5.89 nm lamellar phase, of which the first and third order peaks are apparent. In addition, crystalline CER3(C16) and crystalline cholesterol are present. In contrast to the CHOL:CER3(C16) mixtures, the phase with a spacing of about 3.44 nm is not present in the ternary mixture. Similarly as the observations made with ΣCER, addition of free fatty acids to the binary mixture results in the formation of a very weak shoulder at q = 3.29 nm^{-1}, which might be ascribed to the third order diffraction peak of pure free fatty acids.

In certain aspects the phase behaviour of CER3(C24) resembles that of CER3(C16). Single CER3(C24) also shows the presence of two phases. However, the periodicities are slightly increased as compared to those of CER3(C16). The reflections attributed to a 4.26 nm phase are weaker than the diffraction peaks of the phase with a repeat distance of 3.71 nm. Figure 3B shows the diffraction patterns of the CHOL:CER3(C24) mixture at a molar ratio of 0.5:1 and 1:1. In both mixtures, the 4.26 nm phase is not present, whereas the intensities of the reflections attributed to the 3.71 nm phase hardly change compared to single CER3(C24). In addition, the phase with a repeat distance of 3.44 nm is present in both mixtures. The intensities of the two reflections attributed to this phase increase with an increasing cholesterol fraction, which is similar to the observations made with CHOL:CER3(C16) mixtures. A weak shoulder at the right-hand side of the reflection at q = 3.66 nm^{-1} indicates that a small fraction of phase-separated

cholesterol might be present in the equimolar CHOL:CER3(C24) mixture. In Figure 4 the diffraction pattern of the equimolar CHOL:CER3(C24):FFA mixture is depicted. In the presence of free fatty acids a phase with a periodicity of 5.28 nm is formed, of which the first and second order diffraction peaks are clearly visible. Furthermore, a phase with a repeating unit of 3.81 nm and crystalline cholesterol are present. In contrast to the CHOL:CER3(C24) mixtures, the phase with a repeat distance of 3.44 nm is not present in the equimolar CHOL:CER3(C24):FFA mixture. The same trend was observed with the mixtures prepared with CER3(C16).

3.2 Effect of addition of CER1 on the lamellar ordering

The influence of synthetic CER1 on the phase behaviour was investigated by mixing CER1 with either ΣCERIII, ΣCERIV or CER3(C24) at a molar ratio of 0.1:0.9. As the acyl chain lengths in native ceramides are mainly C24 and C26, CER3(C16) was excluded from this part of the study. The ceramides were mixed either with cholesterol (CHOL:CER) or cholesterol and free fatty acids (CHOL:CER:FFA) at an equimolar ratio. The spacings derived from the diffraction data and the corresponding phases of the lipid mixtures studied are summarised in Table 1.

The diffraction patterns obtained with ΣCERIII and ΣCERIV are very similar and almost identical to those obtained in the absence of CER1 (e.g. compare condition 3 with 16 and condition 16 with 18 in Table 1). In all samples a phase with a periodicity of about 5.4 nm and phase-separated cholesterol are present and addition of free fatty acids results in the formation of an additional peak. The diffraction curves do not show any indication for the presence of a LPP.

The diffraction pattern of the CHOL:[CER1:CER3] mixture also resembles the one obtained in the absence of CER1 (compare conditions 13 and 19 in Table 1). Both the 3.78 nm phase and the 3.43 nm phase are indicated by the presence of the first and second order diffraction peaks. The shoulder at the right-hand side of the reflection at 3.66 nm^{-1} suggests that phase-separated cholesterol is also present in the mixture. In Figure 5, the diffraction curve of the CHOL:[CER1:CER3]:FFA mixture is shown. Addition of free fatty acids to the binary mixture induced the formation of a phase with a repeat distance of 11.6 nm, indicated by peaks located at q = 0.54 nm^{-1} (first order) and 1.62 nm^{-1} (third order). Furthermore, three reflections indicate the presence of a 5.42 nm phase (SPP) and two reflections that of crystalline cholesterol.

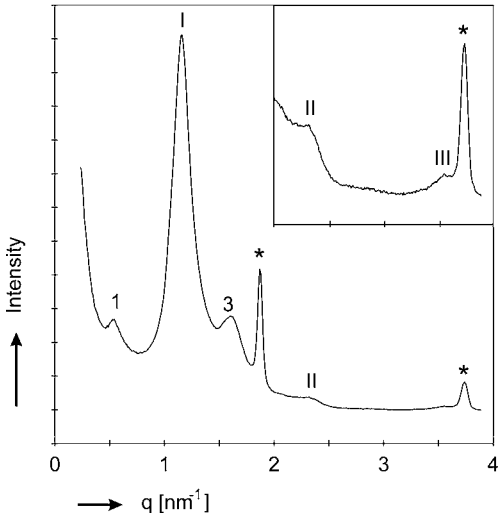

Figure 5 - Diffraction pattern of the mixture CHOL:[CER1:CER3(C24)]:FFA at a molar ratio of 1:[0.1:0.9]:1. The inset is a magnification of the reflections in the q-range between 2 and 4 nm^{-1}. The peaks indicated by Arabic numbers are attributed to the first and third order reflections of a lamellar phase with a repeat distance of 11.6 nm. The first, second and third order reflections of the SPP (periodicity of 5.42 nm) are indicated by Roman numbers. The asterisk denotes the reflections of crystalline cholesterol.

3.3 Lateral arrangement of CHOL:[CER1:CER3]:FFA mixture

Figure 6 shows the WAXD pattern of the CHOL:[CER1:CER3]:FFA mixture. Two strong 0.41 and 0.37 nm reflections indicate an orthorhombic lateral packing. The presence of a coexisting hexagonal or liquid phase cannot be deduced from these data. The lateral packing of the mixture in the absence of CER1 was also measured. The presence of the same reflections again suggests an orthorhombic chain packing (see Fig. 6).

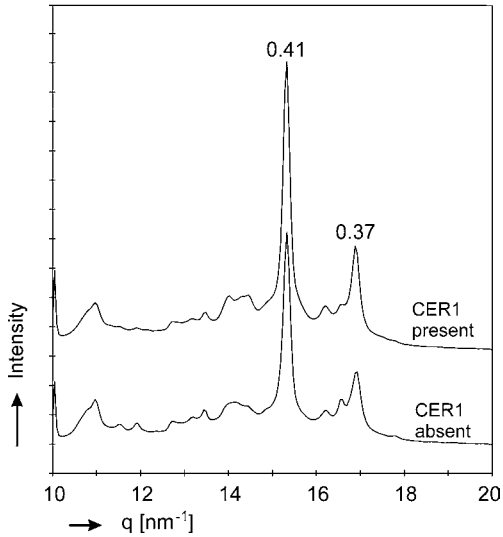

Figure 6 - The lateral packing of the CHOL:[CER1:CER3(C24)]:FFA and CHOL:CER3(C24):FFA mixtures.

4. DISCUSSION

The aim of this study was to prepare a lipid mixture with commercially available ceramides, which can be used as a model for studies on the stratum corneum lipid organisation. In this respect, the present study can be considered as a first link between the phase behaviour of well-defined synthetic ceramides mixtures and the more complex ceramide mixtures isolated from native stratum corneum.

A widely used model to investigate the phase behaviour of the stratum corneum lipids is the equimolar mixture of cholesterol, ΣCERIII and palmitic acid. As previously mentioned, the formation of heterogeneous phase-separated domains in this mixture has frequently been reported [18-21]. Previous SAXD measurements performed with this mixture revealed the presence of several coexisting phases in the lipid mixture, among others phase-separated palmitic acid [24]. The results obtained in the present study show that in the equimolar CHOL:ΣCERIII:FFA mixture a diffraction peak is present that might be ascribed to phase-separated free fatty acids (the peak at q = 3.26 nm^{-1} is at the same position as the third order reflection of the free fatty acids mixture). However, the peak intensity is rather weak and the first and second order reflections cannot be detected. From these observations it can be concluded that, in contrast to palmitic acid, a mixture of free fatty acids with varying hydrocarbon chain lengths promotes almost complete mixing of ceramides, cholesterol and free fatty acids. Moreover, free fatty acids with varying chain lengths more closely represent the composition of the free fatty acids in native stratum corneum [23].

In the present study it was further observed that mixtures containing CER3 show complex phase behaviour. In CER3(C16) and CER3(C24) the coexistence of two phases was observed. This polymorphism has previously been reported by Dahlen and Pascher [28]. According to those authors, synthetic CER3(C24) can crystallise in six solid phases, depending on the thermal history of the samples. In five of the configurations, the ceramide molecules form a V-shaped structure, due to strong intermolecular headgroup hydrogen bonding. As a result, phytosphingosine and fatty acid chains form separate matrices. Within this structure, CER3(C24) organises into a tilted arrangement of the hydrocarbon chains. The differences in periodicities between the five phases depend on the tilt angles. The two phases found in the present study for CER3(C24) (repeat distances of 3.71 and 4.26 nm) can be explained by the presence of two of the aforementioned V-shaped crystal structures, as previously described by Dahlen and Pascher (periodicities of 3.73 and 4.30 nm). Under the experimental conditions used

in the present study, the more dense 3.7 nm packing of CER3(C24) was favoured, although a small fraction of CER3(C24) formed a 4.3 nm phase (less effective chain packing). Apparently, the free energy required for the formation of the 3.7 nm phase is very similar to the free energy required for the formation of the 4.3 nm phase. Hence a small difference in the experimental conditions (e.g. lipid composition, equilibration temperature) may result in increased formation of one phase at the expense of the other phase. This is most likely the reason why the 4.3 nm phase could not be detected in the binary or ternary samples. Similarly as described above, the presence of one or two phases in CER3(C16) can be explained.

Addition of cholesterol to either CER3(C16) or CER3(C24) resulted in the formation of three phases, namely crystalline CER3, crystalline cholesterol and a phase with a periodicity close to that of cholesterol (3.44 nm). In a recent atomic force microscopy study on lipid monolayers it was demonstrated that small amounts of synthetic CER3(C16) and CER3(C24) were miscible in a cholesterol-rich phase [29]. The 3.44 nm phase might therefore represent a cholesterol-rich phase with a small fraction of CER3.

The equimolar ternary mixture prepared with CER3(C16) showed the formation of a lamellar phase with a repeating unit of 5.89 nm. The components of this phase cannot be precisely defined, but most likely comprise free fatty acids and a small fraction of CER3(C16) and cholesterol. This is based on the following observations: (i) The weak shoulder at $q = 3.29\ nm^{-1}$ is the only reflection that might be attributed to crystalline free fatty acids, indicating that only a very small fraction of free fatty acids might be present as a separate phase. (ii) In the absence of free fatty acids the 5.89 nm phase is not formed. (iii) The 3.44 nm phase has disappeared, which indicates that these lipids are then present in another phase. However, a major fraction of CER3(C16) is still present as a crystalline phase, as can be deduced from the presence of two strong reflections at $q = 1.76$ and $3.50\ nm^{-1}$ (first and second order diffraction peaks of the 3.58 nm phase). Similar phase behaviour was observed for the equimolar CHOL: CER3(C24):FFA mixture, although no strong reflections of phase-separated CER3(C24) phase could be detected. Instead, slightly broader and less intense diffraction peaks at $q = 1.65$ and $3.30\ nm^{-1}$ were present, attributed to a phase with a periodicity of 3.81 nm. This phase most likely consists of CER3(C24) and free fatty acids. As the chain lengths of the free fatty acids mixture are mainly C22 and C24, it is likely that the free fatty acids are at least partially miscible with CER3(C24) and consequently can form a separate phase with CER3(C24). However, the presence of cholesterol in this phase

cannot be excluded.

It appears that for the formation of the LPP appropriate molar ratios of individual lipids are required. In particular, ceramides by themselves or mixtures of single ceramides with cholesterol (and free fatty acids) do not produce the characteristic LPP as detected in stratum corneum. The presence of CER1 seems to be crucial. These observations are in line with results obtained with ceramides isolated from native stratum corneum [12, 14, 30], where it was demonstrated that in the absence of CER1 the LPP was hardly formed.

The results further show that, even in the presence of CER1, bovine brain ceramides (ΣCERIII or ΣCERIV) do not form the characteristic LPP when mixed with cholesterol or cholesterol and free fatty acids. This indicates that not only the presence of CER1, but also a proper composition of the other ceramides is important for LPP formation. In the lipid mixtures studied so far, only the CHOL:[CER1:CER3(C24)]:FFA mixture revealed the formation of the LPP. However, the intensities of the reflections attributed to this phase are relatively weak, indicating that only a small fraction of lipids is involved in the formation of this phase. The presence of a strong reflection at $q = 1.16\ nm^{-1}$ (first order reflection of 5.42 nm phase) indeed confirms that most lipids are present in another phase.

Concerning the lateral arrangement of the lipids, the results show a crystalline packing for the CHOL:[CER1:CER3(C24)]:FFA mixture. Since WAXD only provides information on the bulk of the lipids, however, no discrimination can be made between the lateral packing of the different phases. Furthermore, the peaks of the orthorhombic phase overlap the peak of the 0.406 nm hexagonal phase. Therefore, the presence of lipids forming a hexagonal phase cannot be excluded. Previous fourier transformed infrared spectroscopy measurements performed with several synthetic ceramide mixtures [18, 19, 22] revealed that the lipids form phase-separated crystalline domains with an orthorhombic chain packing. This is in agreement with the results of the present study, in which the mixture lacking CER1 also revealed the coexistence of several phases (SAXD) and a crystalline lateral packing (WAXD).

In conclusion, from the results it is evident that the LPP, characteristic for stratum corneum lipid phase behaviour, is not formed in mixtures prepared with bovine brain ceramides (ΣCERIII or ΣCERIV). Even in the presence of CER1, only a lamellar phase with a short periodicity is present. Mixtures composed of cholesterol, ΣCERIII and palmitic acid, which are the subject of several phase behaviour studies, therefore cannot be considered as representative for the stratum corneum lipid phase behaviour.

It is possible to mimic the lipid organisation in native stratum corneum to a certain extent with a synthetic ceramide mixture, consisting of CER1 and CER3(C24). However, the periodicity of 11.6 nm differs from that obtained with ceramides isolated from native stratum corneum. Moreover, the intensities of the diffraction peaks attributed to the 11.6 nm phase are considerably weaker than observed for isolated ceramides. To increase the repeat distance and the fraction of lipids forming the LPP one may consider to optimise the preparation method of the lipid mixtures as well as the lipid composition of the mixture. For the preparation of the synthetic lipid mixtures the same method was used as for mixtures based on isolated ceramides. Due to differences between synthetic and isolated ceramides, however, the equilibration temperature used might not be optimal for appropriate mixing of individual synthetic lipids and for the formation of the LPP. The influence of equilibration temperature modulation and ceramide composition will therefore be the subject of future studies.

Acknowledgements

This work was supported by a grant from the Technology Foundation STW (LGN.4654). The Netherlands Organisation for Scientific Research (NWO) is acknowledged for the provision of the beamtime. We would like to thank the companies Cosmoferm and Beiersdorf for the provision of the synthetic ceramides.

REFERENCES

1. Elias, P.M. Epidermal lipids, barrier function, and desquamation. *J. Invest. Dermatol.* **80** (1983) 44s-49s.

2. Boddé, H.E., van den Brink, I., Koerten, H.K., de Haan, F.H.N. Visualization of in vitro percutaneous penetration of mercuric chloride transport through intercellular space versus cellular uptake through desmosomes. *J. Control. Release* **15** (1991) 227-236.

3. Meuwissen, M.E.M.J., Janssen, J., Cullander, C., Junginger, H.E., Bouwstra, J.A. A cross-section device to improve visualization of fluorescent probe penetration into the skin by confocal laser scanning microscopy. *Pharm. Res.* **15** (1998) 352-356.

4. Talreja, P.S., Kasting, G.B., Kleene N.K., Pickens W.L., Wang T.F. Visualization of the lipid barrier and measurement of lipid pathlength in human stratum corneum. *AAPS Pharm. Sci.* **3** (2001) E13.

5. Wertz, P.W., Miethke, M.C., Long, S.A., Strauss, J.S., Downing, D.T. The composition of the ceramides from human stratum corneum and from comedones. *J. Invest. Dermatol.* **84** (1985) 410-412.

6. Robson, K.J., Stewart, M.E., Michelsen, S., Lazo, N.D., Downing, D.T. 6-Hydroxy-4-sphingenine in human epidermal ceramides. *J. Lipid Res.* **35** (1994) 2060-2068.

7. Stewart, M.E., Downing, D.T. A new 6-hydroxy-4-sphingenine-containing ceramide in human skin. *J. Lipid Res.* **4** (1999) 1434-1439.

8. Ponec, M., Weerheim, A., Lankhorst, P., Wertz, P. New acylceramide in native and reconstructed epidermis, *J. Invest. Dermatol.* **120** (2003) 581-588.

9. Bouwstra, J.A., Gooris, G.S., van der Spek, J.A., Bras, W. The structure of human stratum corneum as determined by small angle X-ray scattering. J*. Invest. Dermatol.* **96** (1991) 1006-1014.

10. Bouwstra, J.A., Gooris, G.S., van der Spek, J.A., Bras, W. Structural investigations of human stratum corneum by small angle X-ray scattering. *J. Invest. Dermatol.* **97** (1991) 1005-1012.

11. Bouwstra, J.A., Gooris, G.S., Bras, W., Downing, D.T. Lipid organization in pig stratum corneum. *J. Lipid Res.* **36** (1995) 685-695.

12. McIntosh, T.J., Stewart, M.E., Downing, D.T. X-ray diffraction analysis of isolated skin lipids: reconstitution of intercellular lipid domains. *Biochemistry* **35** (1996) 3649-3653.

13. Bouwstra, J.A., Gooris, G.S., Cheng, K., Weerheim, A., Bras, W., Ponec, M. Phase behavior of isolated skin lipids. *J. Lipid Res.* **37** (1996) 999-1011.

14. Bouwstra, J.A., Gooris, G.S., Dubbelaar, F.E.R., Ponec, M. Phase behavior of stratum corneum lipid mixtures based on human ceramides: the role of natural and synthetic ceramide 1. *J. Invest. Dermatol.* **118** (2002) 606-617.

15. Bouwstra, J.A., Gooris, G.S., Dubbelaar, F.E.R., Weerheim, A.M., Ponec, M. pH, cholesterol sulfate, and fatty acids affect the stratum corneum lipid organization. *J. Invest. Dermatol.* **3** (1998) 69-73.

16. Fenske, D.B., Thewalt, J.L., Bloom, M., Kitson, N. Models of stratum corneum intercellular membranes: ^{2}H NMR of microscopically oriented multilayers. *Biophys. J.* **67** (1994) 1562-1573.

17. Kitson, N., Thewalt, J., Lafleur, M., Bloom, M. A model membrane approach to the epidermal permeability barrier. *Biochemistry* **33** (1994) 6707-6715.

18. Moore, D.J., Rerek, M.E., Mendelsohn, R. Lipid domains and FTIR spectroscopy studies of the conformational order and phase behavior of ceramides. *J. Phys. Chem. B* **101** (1997) 8933-8940.

19. Moore, D.J., Rerek, M.E., Mendelsohn, R. Lipid domains and orthorhombic phases in model stratum corneum: evidence from fourier transform infrared spectroscopy studies. *Biochem. Biophys. Res. Commun.* **231** (1997) 797 -801.

20. Lafleur, M. Phase behaviour of model stratum corneum lipid mixtures: an infrared spectroscopy investigation. *Can. J. Chem.* **76** (1998) 1500-1511.

21. Percot, A., Lafleur, M. Direct observations of domains in model stratum corneum lipid mixtures by Raman microspectroscopy. *Biophys. J.* **81** (2001) 2144-2153.

22. Moore, D.J., Rerek, M.E. Insights into the molecular organisation of lipids in the skin barrier from infrared spectroscopy studies of stratum corneum lipid models. *Acta Derm. Venereol. Suppl. (Stockh.)* **208** (2000) 16-22.

23. Wertz, P.W., Downing, D.T., 1991. Epidermal lipids. In: Physiology, Biochemistry and Molecular Biology of the Skin, L.A. Goldsmith (ed), Oxford University Press, Oxford, pp. 205-235.

24. Bouwstra, J.A., Thewalt, J., Gooris, G.S., Kitson, N. A model membrane approach to the epidermal permeability barrier: an X-ray diffraction study. *Biochemistry* **36** (1997) 7717-7725.

25. Parrott, D.T., Turner, J.E. Mesophase formation by ceramides and cholesterol: a model for stratum corneum lipid packing? *Biochim. Biophys. Acta* **1147** (1993) 273-276.

26. Bras, W. A SAXS/WAXS beamline at the ESRF and future experiments. *J. Macromol. Sci. Phys. B* **37** (1998) 557-566.

27. Dolbnya, I.P., Alberda, H., Hartjes, F.G., Udo, F., Bakker, R.E., Konijnenburg, M., Homan, E., Cerjak, I., Goedtkindt, P., Bras, W. A fast position sensitive MSGC detector at high count rate operation. *Rev. Sci. Instrum.* **73** (2002) 3754-3758.

28. Dahlen, B., Pascher, I. Molecular arrangements in sphingolipids. Thermotropic phase behaviour of tetracosanoylphytosphingosine. *Chem. Phys. Lipids* **24** (1979) 119-133.

29. Sparr, E., Eriksson, L., Bouwstra, J.A., Ekelund, K. AFM Study of lipid monolayers: III. Phase behavior of ceramides, cholesterol and fatty acids. *Langmuir* **17** (2001) 164-172.

30. Bouwstra, J.A., Gooris, G.S., Dubbelaar, F.E.R., Weerheim, A.M., Ijzerman, A.P., Ponec, M. Role of ceramide 1 in the molecular organization of the stratum corneum lipids. *J. Lipid Res.* **39** (1998) 186-196.

Chapter 3

Novel lipid mixtures based on synthetic ceramides reproduce the unique stratum corneum lipid organisation

M.W. de Jager,* G.S. Gooris,* I.P. Dolbnya,# W. Bras,# M. Ponec,§ and J.A. Bouwstra*

*Leiden/Amsterdam Center for Drug Research, Department of Drug Delivery Technology, University of Leiden, P.O. Box 9502, 2300 RA Leiden, The Netherlands.
#Netherlands Organisation for Scientific Research, DUBBLE CRG/ESRF, Grenoble, France.
§Department of Dermatology, Leiden University Medical Center, Leiden, The Netherlands.

(adapted from *J. Lipid Res.* **45** (2004) 923-932)

ABSTRACT

Lipid lamellae present in the outermost layer of the skin protect the body from uncontrolled water loss. In human stratum corneum two crystalline lamellar phases are present, which contain mostly cholesterol, free fatty acids and 9 types of free ceramides. Previous studies have demonstrated that the stratum corneum lipid organisation can be mimicked with model mixtures based on isolated stratum corneum lipids. However, those studies are hampered by low availability and high inter-individual variability of the native tissue. To elucidate the role of each lipid class in the formation of a competent skin barrier, the use of synthetic lipids would offer an alternative. The small-angle and wide-angle X-ray diffraction results of the present study show for the first time that synthetic lipid mixtures, containing only three synthetic ceramides, reflect to a high extent the stratum corneum lipid organisation. Both an appropriately chosen preparation method and lipid composition promote the formation of two characteristic lamellar phases with repeat distances similar to those found in native stratum corneum. From all synthetic lipid mixtures examined, equimolar mixtures of cholesterol, ceramides, and free fatty acids equilibrated at 80°C resemble to the highest extent the lamellar and lateral stratum corneum lipid organisation, both at room and elevated temperatures.

1. INTRODUCTION

One of the most important functions of the skin is to serve as a barrier to protect the body against uncontrolled water loss and to prevent the penetration of harmful agents. The protective function of the skin is provided primarily by the stratum corneum, the outermost layer of the skin. Stratum corneum has a unique morphology, where keratin-filled corneocytes are surrounded by multi-lamellar lipid regions [1]. The highly ordered intercellular lipid matrix is considered to play a crucial role in the maintenance of the barrier properties of the skin. Knowledge of the composition and the organisation of the stratum corneum lipids is therefore essential to increase our insight in the skin barrier function.

The composition of the stratum corneum lipids differs from that of biological membranes, since phospholipids are nearly absent. Ceramides (CER) belong to the major lipid species of the stratum corneum. Together with cholesterol (CHOL) and long-chain free fatty acids (FFA) they form the highly ordered intercellular lipid lamellae. At least 9 different types of free ceramides have been identified in human stratum corneum [2-5], which are classified as CER1 to CER9. The ceramides are composed of a sphingosine (S), a phytosphingosine (P) or a 6-hydroxysphingosine (H) base, to which a nonhydroxy (N) or α-hydroxy (A) fatty acid is chemically linked. CER1, CER4 and CER9 have a unique molecular structure as they contain linoleic acid bound to an ω-hydroxy fatty acid (EO) with a chain length of approximately 30 to 32 carbon atoms. The molecular structures of the ceramides are illustrated in Figure 1.

The lipids in stratum corneum are organised in two coexisting crystalline lamellar phases: the short periodicity phase (SPP) with a repeat distance of approximately 6 nm and the long periodicity phase (LPP) with a periodicity of around 13 nm [6-8]. Both the molecular organisation of the LPP and the predominantly crystalline nature of the lipid packing in the presence of substantial amounts of cholesterol are unique and are therefore suggested to be crucial for the barrier function of the skin.

In order to elucidate the role of each lipid class in the formation of a competent skin barrier, the phase behaviour of the stratum corneum lipids has been studied extensively. Using small-angle and wide-angle X-ray diffraction it has been demonstrated that mixtures of cholesterol, free fatty acids and ceramides isolated from either pig or human stratum corneum (natCER), closely mimic the lipid organisation in stratum corneum. The results further reveal that in particular cholesterol and ceramides play a key role in the formation of the LPP, whereas free fatty acids are required to induce the

orthorhombic packing of the lipids [9-11].

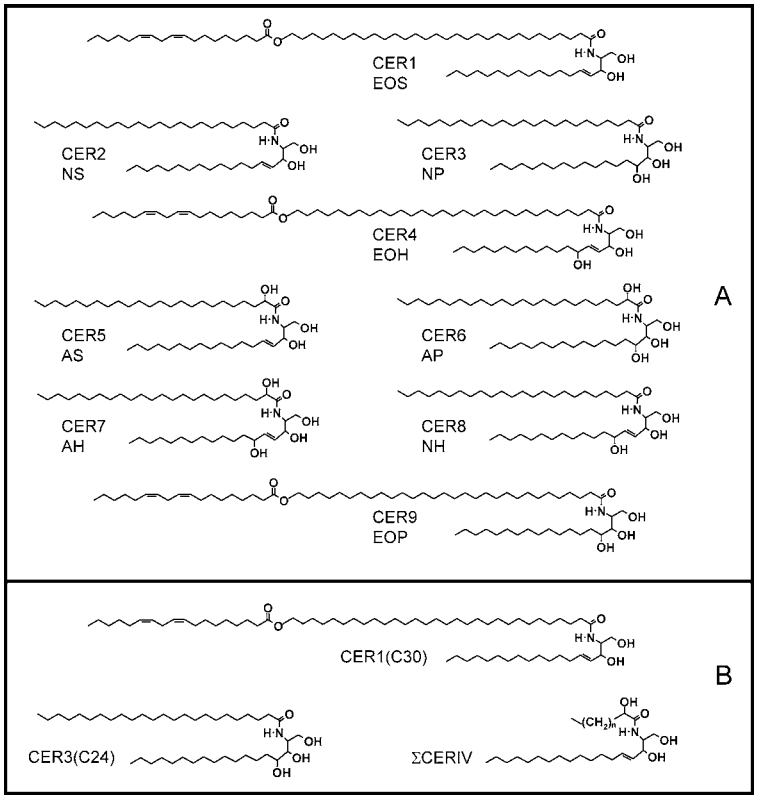

Figure 1 - (A) The molecular structures of the ceramides present in human stratum corneum, indicated according to the numbering system (based on chromatographic migration) and according to the structure. (B) The molecular structures of the synthetic ceramides used in the study. The acyl chain lengths of CER1(C30) and CER3(C24) are well-defined, whereas bovine brain ceramide type IV (ΣCERIV) shows a distribution in chain lengths, with C18 and C24 as the most abundantly present.

Extensive studies with lipids isolated from stratum corneum are hampered by the low availability and high inter-individual variability of the native tissue. In addition, the isolation and separation of the ceramides from the stratum corneum is very labour-intensive and expensive. The use of synthetic ceramides (synthCER) may therefore offer an attractive alternative. Moreover, each subclass of natCER shows a variation in acyl chain length [2], whereas synthCER have a well-defined acyl chain length. Therefore, synthCER also enable studying in detail the influence of the acyl chain length on the SC lipid phase behaviour.

In recent years, several studies have been performed with model mixtures based on synthCER. The most frequently studied mixtures contain cholesterol and/or palmitic acid and the commercially available bovine brain ceramide type III or type IV [12-17]. Other studies focused on mixtures prepared with for instance synthetic CER2, CER3 or CER5 [18-22]. Using a variety of techniques, it has been elucidated that the packing of the lipids is mainly orthorhombic. However, the results demonstrate that the lipids are not properly mixed in one lattice, but coexist in various phases, enriched in one of the components of the lipid mixture. Moreover, small-angle X-ray diffraction studies reveal that the characteristic LPP is not present in mixtures consisting of bovine brain ceramide type III, cholesterol and palmitic acid [23, 24].

In a recent study we have demonstrated that lamellar phases are formed in mixtures prepared with bovine brain ceramide type III or type IV. However, no LPP could be detected [25]. Moreover, the phase behaviour of mixtures prepared with synthetic CER3, having an acyl chain length of 24 or 16 carbon atoms, was studied. Mixtures prepared with CER3 revealed the presence of several coexisting phases, among others crystalline V-shaped CER3 structures. These V-shaped structures are not observed in stratum corneum and can therefore not be considered as representative for the stratum corneum lipid phase behaviour. The effect of synthetic CER1 on the phase behaviour of synthetic skin lipid mixtures was also studied. From all mixtures examined, only one mixture containing synthetic CER1, CER3, cholesterol and free fatty acids showed similar phase behaviour to that of stratum corneum. However, the repeat distance of the LPP was shorter than that observed in stratum corneum. The LPP was not formed in the absence of CER1, which is similar to previous observations made with mixtures containing natCER [11, 24, 26].

The objective of the present study is to generate a lipid mixture with synthCER, which closely mimics the natural stratum corneum lipid phase behaviour. In a previous study performed with natCER, it became evident that a certain degree of fluidity of the lipid mixture is required for the formation of the LPP [11]. As synthCER have uniform chain lengths and form highly crystalline phases, it is reasonable to assume that increased lipid mobility and thus a possible enhancement of the formation of the LPP can be achieved by introducing variations in either acyl chain length or head group architecture. Therefore, in the present study bovine brain ceramide type IV was included in the lipid mixture. Bovine brain ceramide type IV consists of a sphingosine base linked to an α-hydroxy fatty acid with varying acyl chain lengths (see Fig. 1B), in which C18 and C24 are the most abundantly present [chapter 4]. In addition, the

preparation method was optimised to increase the degree of fluidity of the lipids in order to accomplish LPP formation.

The present study shows that both a proper choice of the lipid composition as well as an optimal equilibration temperature during sample preparation are crucial for the formation of the LPP in mixtures based on synthCER.

2. MATERIALS AND METHODS

2.1 Materials

Palmitic acid, stearic acid, arachidic acid, behenic acid, tricosanoic acid, lignoceric acid, cerotic acid, cholesterol and bovine brain ceramide type IV were purchased from Sigma-Aldrich Chemie GmbH (Schnelldorf, Germany). N-(30-Linoleoyloxy-triacontanoyl)-sphingosine (synthetic ceramide 1(C30)-linoleate) was a gift from Beiersdorf AG (Hamburg, Germany). N-Tetracosanoyl-phytosphingosine (synthetic ceramide 3(C24)) was generously provided by Cosmoferm B.V. (Delft, the Netherlands). Figure 1B shows the ceramides used in this study. All organic solvents used were of analytical grade and manufactured by Labscan Ltd (Dublin, Ireland).

2.2 Preparation of the lipid mixtures

All samples were prepared with a synthCER mixture, consisting of CER1, CER3 and bovine brain ceramide type IV (further referred to as ΣCERIV) at a molar ratio of 1:7:2. The synthCER mixture was mixed with cholesterol an in equimolar ratio. For the preparation of the CHOL:synthCER:FFA mixtures, the fatty acids C16:0, C18:0, C20:0, C22:0, C23:0, C24:0 and C26:0 were mixed at molar ratios of respectively 1.3, 3.3, 6.7, 41.7, 5.4, 36.8 and 4.7. This ratio is similar to that found in the native SC. Appropriate amounts of individual lipids dissolved in chloroform:methanol (2:1) were combined to yield mixtures of approximately 1.5 mg total dry weight at the desired composition at a total lipid concentration of 7 mg/ml. A Camag Linomat IV was used to apply the lipid mixtures onto mica. This was done at a rate of 4.3 µl/min under a continuous nitrogen stream. The samples were equilibrated for 10 minutes at the appropriate temperature that varied between 60 and 100°C and subsequently hydrated with an acetate buffer of pH 5.0. Finally, the samples were homogenised by 10 successive freeze-thawing cycles between –20°C and room temperature, during which the samples were stored under gaseous argon.

2.3 Small-angle X-ray diffraction (SAXD)

All measurements were performed at the European Synchrotron Radiation Facility (ESRF, Grenoble), using station BM26B [27]. The X-ray wavelength and the sample-to-detector distance were 1.24Å and 1.7m, respectively. Diffraction data were collected on a two-dimensional multiwire gas-filled area detector. The spatial calibration of this detector was performed using silver behenate. The samples were mounted in a temperature-controlled sample holder with mica windows. Static diffraction patterns of the lipid mixtures were obtained at room temperature for a period of 10 minutes. The temperature-induced phase changes were investigated by collecting diffraction patterns, while raising the temperature of the sample from 25 to 95°C at a rate of 2°C/min. Each successive diffraction curve was collected for a period of one minute. All measurements were performed at least in duplicate.

SAXD provides information about the larger structural units in the sample, such as the repeat distance of a lamellar phase. The scattering intensity I (in arbitrary units) was measured as a function of the scattering vector q (in reciprocal nm). The latter is defined as $q=(4\pi\sin\theta)/\lambda$, in which θ is the scattering angle and λ is the wavelength. From the positions of a series of equidistant peaks (q_n), the periodicity, or d-spacing, of a lamellar phase was calculated using the equation $q_n=2n\pi/d$, n being the order number of the diffraction peak.

2.4 Wide-angle X-ray diffraction (WAXD)

Wide-angle X-ray diffraction provides information about the lateral packing of the lipids within the lamellae. Wide-angle X-ray diffraction data were collected on a microstrip gas chamber detector with an opening angle of 60° [28]. The sample-to-detector distance was 36 cm and the X-ray wavelength was 1.24Å. The spatial calibration of the detector was performed with a mixture of silicium and cholesterol. The SAXD and WAXD data were collected simultaneously.

3. RESULTS

3.1 Effect of the equilibration temperature during the sample preparation

Mixtures consisting of CHOL:[CER1:CER3:ΣCERIV] at a molar ratio of 1:[0.1:0.7:0.2] were equilibrated at different temperatures ranging from 60°C to 100°C. The effect of the equilibration temperature on the lipid phase behaviour is summarised in Table 1. The corresponding diffraction patterns are described below.

Table 1 - The effect of the equilibration temperature on the formation of the phases in equimolar CHOL: synthCER mixtures

Temp (°C)	LPP	SPP	CER3		CHOL
60	--	5.7 (1, 2)	3.7 (1, 2)		3.35 (1, 2)
70	12.8 (2)	5.7 (1)	3.7 (1, 2)		3.35 (1, 2)
80	12.5 (1, 2, 3) #	5.7 (1)	3.7 (1, 2)	4.3 (1)	3.35 (1, 2)
90	12.6 (1, 2, 3*)	5.5 (1*, 3*)	3.7 (1, 2)	4.3 (1, 2)	3.35 (1, 2)
95	12.3 (1, 2, 3*, 4, 7)	5.3 (1, 2)	3.7 (1, 2)	4.3 (1, 2)	3.35 (1, 2)
100	12.2 (1, 2, 3*, 4, 6, 7)	5.3 (1, 3)		4.3 (1, 2)	3.35 (1, 2)

12.5 (1, 2, 3) means the periodicity of the phase is 12.5 nm, and interpretation is based on the first, second and third order reflections. An asterisk (*) indicates that the peak is present as a shoulder.

Figure 2A shows the diffraction pattern of a lipid mixture equilibrated at 100°C. A lamellar structure with a repeat distance of 12.2 nm (LPP) is indicated by the presence of 6 diffraction peaks (q = 0.52, 1.03, 1.54, 2.06, 3.08 and 3.58 nm^{-1}). The reflections at q = 1.17 and 3.51 nm^{-1} correspond to the first and third order maxima of a lamellar phase with a periodicity of 5.3 nm (SPP). The two sharp peaks at 1.46 and 2.91 nm^{-1} indicate the presence of a 4.3 nm phase, ascribed to crystalline CER3 in a V-shaped structure [19, 22, 25]. The presence of crystalline cholesterol in separate domains can be deduced from the reflections at 1.87 and 3.74 nm^{-1}.

A reduction in equilibration temperature from 100 to 95°C does not affect the formation of the LPP and SPP (data not shown). However, X-ray diffraction patterns of lipid mixtures equilibrated at 95°C reveal the presence of a new structure with a repeat distance of 3.7 nm, suggested by two reflections at respectively 1.69 and 3.40 nm^{-1}. This phase can be assigned to another crystalline V-shaped structure of CER3 [19, 22, 25]. The intensities of the peaks attributed to the 4.3 nm phase are slightly reduced compared to those observed in the samples that were equilibrated at 100°C.

The repeat distance of the LPP increases to 12.6 nm when an equilibration temperature of 90°C is used during sample preparation (see Fig. 2A). However, only three reflections can be observed that attribute to this phase. The periodicity of the SPP has slightly increased to 5.5 nm, as deduced from the first and third order reflections. Both reflections show partial overlap with other peaks in the diffraction pattern. Crystalline cholesterol and the two coexisting crystalline CER3 phases are also present in the lipid mixture.

The diffraction pattern of the lipid mixture prepared using an equilibration temperature of 80°C is illustrated in Figure 2B. It is evident that lowering the equilibration temperature reduces the intensities of the three equidistant LPP reflections compared to

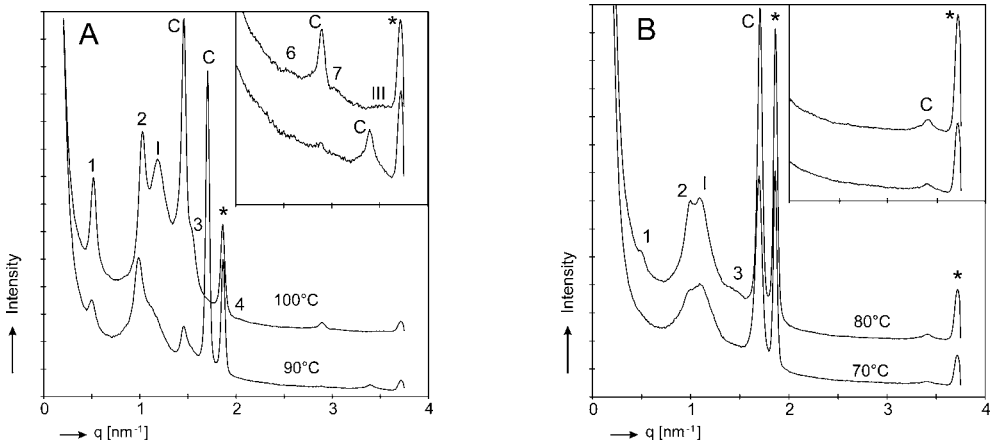

Figure 2 - The effect of the equilibration temperature on the phase behaviour of equimolar CHOL: synthCER mixtures. The inset is a magnification of the reflections in the q-range between 2 and 4 nm^{-1}. The Arabic and Roman numbers indicate the diffraction orders of the LPP and SPP, respectively. The letter C refers to the two crystalline phases of CER3. The asterisk (*) indicates the reflections of crystalline cholesterol located at 1.87 and 3.74 nm^{-1}. (A) Diffraction patterns of mixtures equilibrated at 100°C and 90°C. The various orders of the LPP are located at q = 0.52 nm^{-1} (1) , 1.03 nm^{-1} (2), 1.54 nm^{-1} (3) , 2.06 nm^{-1} (4) , 3.08 nm^{-1} (6) and 3.58 nm^{-1} (7). The various orders of the SPP are located at q = 1.17 nm^{-1} (I) and 3.51 nm^{-1} (III). The reflections at 1.46 and 2.91 nm^{-1} are attributed to crystalline CER3 (4.3 nm phase). (B) Diffraction patterns of mixtures equilibrated at 80°C and 70°C. The various orders of the LPP are located at q = 0.49 nm^{-1} (1) , 0.99 nm^{-1} (2) and 1.48 nm^{-1} (3). The only reflection attributed to the SPP is located at q = 1.09 nm^{-1} (I). The reflection at 1.46 nm^{-1} is attributed to crystalline CER3 (4.3 nm phase) and the reflections at 1.71 and 3.41 nm^{-1} are attributed to crystalline CER3 (3.7 nm phase).

the intensities of the peaks attributed to the SPP (and crystalline CER3 and cholesterol). The repeat distance of the SPP has slightly increased to 5.7 nm. Additionally, crystalline cholesterol and crystalline CER3 are present in the lipid mixture. The latter forms predominantly a 3.7 nm phase, although a weak reflection at q = 1.46 nm^{-1} indicates that a small fraction of CER3 might still be present as a 4.3 nm phase. A further reduction in the equilibration temperature to 70°C (see Fig. 2B) results in a diffraction pattern in which the diffraction peaks attributed to the LPP have almost disappeared. Only a weak reflection at q = 0.99 nm^{-1} (second order) reveals that a small fraction of lipids might form a LPP with a periodicity of about 12.8 nm. Compared to the diffraction pattern of the lipid mixture equilibrated at 80°C, no significant shift is observed in the positions of the reflections attributed to the SPP and crystalline cholesterol. All phase-separated CER3 forms a 3.7 nm phase, as the only two additional reflections observed in the diffraction pattern are located at 1.69 and 3.40 nm^{-1}. Equilibration of the lipid mixture at 60°C (data not shown) does not result in the formation of the LPP. Instead,

broad reflections indicate the presence of a SPP with a repeat distance of 5.7 nm. In addition, crystalline cholesterol and crystalline CER3 (3.7 nm phase) can be detected.

3.2 The effect of addition of free fatty acids

To investigate the influence of free fatty acids on the formation of the lamellar phases, free fatty acids were added to the above-mentioned CHOL:[CER1:CER3:ΣCERIV] mixture prepared at a molar ratio of 1:[0.1:0.7:0.2]. Based on the results obtained with the CHOL:synthCER mixtures, the initially chosen equilibration temperature was 95°C. However, equilibration of an equimolar CHOL:synthCER:FFA mixture at 95°C did not result in the formation of the LPP, but in melting of the lipids (data not shown). Therefore, the equilibration temperature was reduced to 80°C. The effect of free fatty acids on the phase behaviour was examined with CHOL:synthCER:FFA mixtures, in which the amount of free fatty acids was gradually increased to achieve molar ratios ranging from 1:1:0 to 1:1:1.8. The results are summarised in Table 2.

The corresponding diffraction patterns are described below. Firstly, the diffraction curve of the CHOL:synthCER:FFA mixture at a molar ratio of 1:1:1 will be described (see Fig. 3A). Subsequently, the effect of decreased and increased free fatty acids levels on the lipid phase behaviour will be presented. The equimolar CHOL:synthCER:FFA mixture shows the presence of a LPP with a repeat distance of 12.2 nm, of which the first five reflections can be detected. The SPP with a periodicity of 5.5 nm is characterised by the presence of the first three diffraction peaks. Crystalline cholesterol and the two coexisting crystalline phases of CER3 with periodicities of 3.7 and 4.3 nm can also be detected in the lipid mixture.

Table 2 - The effect of free fatty acids on the formation of the phases in the lipid mixtures

CHOL:CER:FFA	LPP	SPP	CER3(C24)		CHOL
1:1:0	12.5 (1*, 2, 3)	5.5 (1*)	3.7 (1, 2)		3.35 (1, 2)
1:1:0.25	12.5 (1*, 2, 3)	5.5 (1*)	3.7 (1, 2)		3.35 (1, 2)
1:1:0.5	12.5 (1, 2, 4) #	5.5 (1*, 2)	3.7 (1, 2)	4.3 (1, 2)	3.35 (1, 2)
1:1:0.75	12.3 (1, 2 , 3*, 4)	5.5 (1, 2, 3)	3.7 (1, 2)	4.3 (1, 2)	3.35 (1, 2)
1:1:1	12.2 (1, 2, 3*, 4, 5)	5.5 (1, 2, 3)	3.7 (1, 2)	4.3 (1, 2)	3.35 (1, 2)
1:1:1.4	12.0 (1, 2, 3*, 4)	5.4 (1, 2)	3.7 (1, 2)	4.3 (1, 2)	3.35 (1, 2)
1:1:1.8	12.0 (1*, 2, 4)	5.6 (1, 2)	3.7 (1, 2)	4.3 (1, 2)	3.35 (1, 2)

12.5 (1, 2, 4) means the periodicity of the phase is 12.5 nm, and interpretation is based on the first, second and fourth order reflections. An asterisk (*) indicates that the peak is present as a shoulder.

The diffraction pattern of the 1:1:0.75 CHOL:synthCER:FFA mixture is depicted in Figure 3A. Compared to the equimolar lipid mixture, a slight decrease in the intensities

of the reflections attributed to the LPP compared to the intensities of the peaks attributed to the SPP is observed. Furthermore, the peak intensities of the 3.7 nm phase are markedly increased compared to the reflections attributed to the 4.3 nm phase. Additionally, crystalline cholesterol can be detected.

A further decrease in free fatty acids content to a molar ratio of 1:1:0.5 resulted in the diffraction pattern illustrated in Figure 3B. Compared to the diffraction patterns obtained at higher free fatty acids content (1:1:0.75 and 1:1:1), the peak intensities of both LPP and SPP are considerably reduced. Only three orders of the LPP can be detected. Although a small fraction of CER3 forms the 4.3 nm phase, the first order reflection of the 3.7 nm phase is the most prominent peak in the diffraction pattern ($q = 1.69\ nm^{-1}$).

At a CHOL:synthCER:FFA molar ratio of 1:1:0.25 (data not shown) the intensities of the three reflections attributed to the LPP further decreases at the expense of the peak intensities of the 3.7 nm phase. Of the SPP only the first order reflection can be detected, which partially overlaps with the second order of the LPP. At this molar ratio, a very small fraction of crystalline CER3 is present as a 4.3 nm phase, since the two reflections attributed to this phase are only weakly present. Crystalline cholesterol is again present, derived from the presence of its two reflections. The diffraction pattern of the CHOL:synthCER:FFA mixture at a molar ratio of 1:1:0 (Fig. 3B) closely resembles that of the 1:1:0.25 mixture: a small fraction of lipids forms the LPP and SPP, whereas the peaks of the 3.7 nm phase dominate the diffraction pattern.

Figure 3C illustrates the effect of increasing the free fatty acids content to levels above equimolar ones. At a molar ratio of 1:1:1.4, four diffraction peaks are attributed to the LLP with a periodicity of 12.0 nm. Furthermore, the SPP (repeat distance 5.3 nm) is present in the lipid mixture. Compared to Figure 3A, in which the diffraction pattern of the equimolar lipid mixture is plotted, a slight decrease in the intensities of the reflections attributed to the LPP compared to those attributed to the SPP is observed, similarly as observed for the 1:1:0.75 mixture. Both the 3.7 nm and 4.3 nm phases are present. However, the peak intensities of the 4.3 nm phase are markedly decreased compared to the equimolar mixture. Additionally, crystalline cholesterol can be detected.

The diffraction pattern of the 1:1:1.8 mixture is plotted in Figure 3C. A very broad peak is observed at $1.12\ nm^{-1}$, caused by an overlap of the second order reflection of the LPP and the first order peak of the SPP. A further reduction in the intensities of the LPP reflections compared to the SPP reflections is observed. A weak reflection at

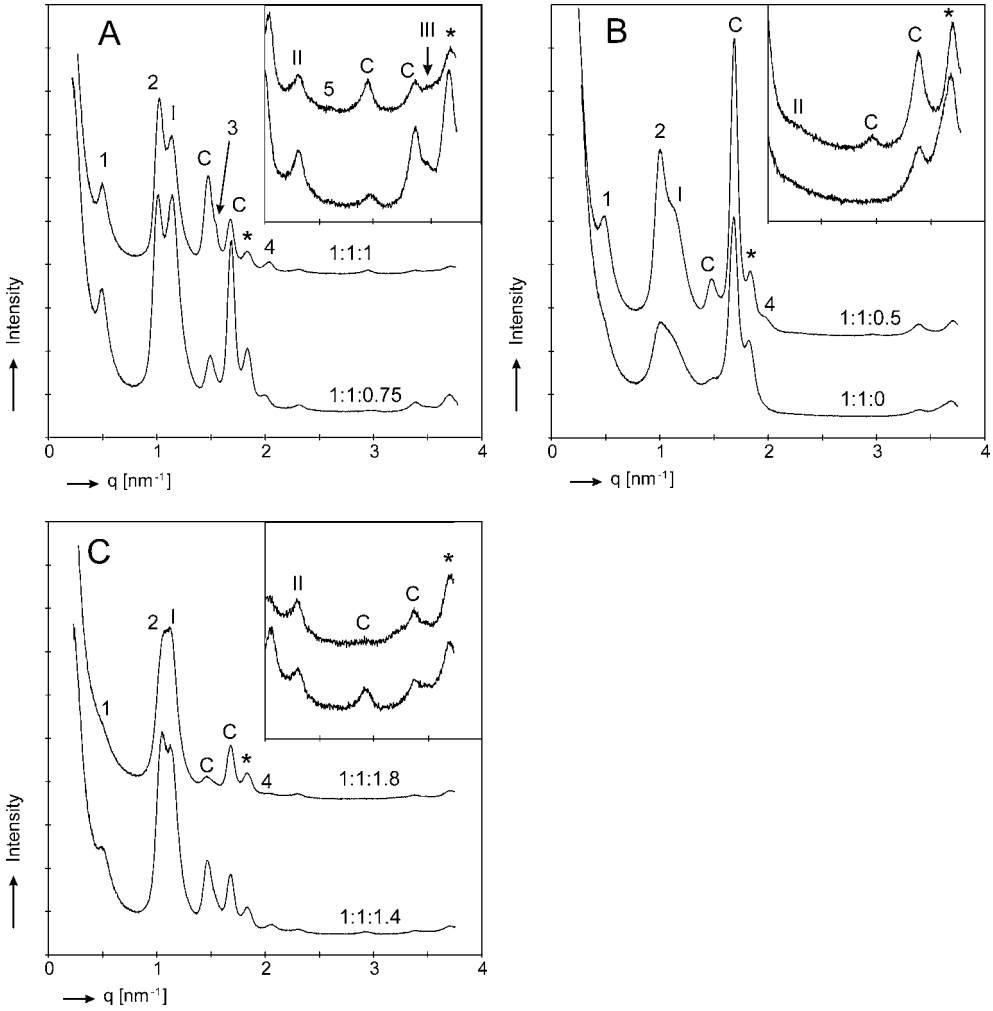

Figure 3 - The effect of the free fatty acids content on the phase behaviour of CHOL:synthCER:FFA mixtures. The inset shows a magnification of the reflections in the q-range between 2 and 4 nm^{-1}. The Arabic and Roman numbers indicate the diffraction orders of the LPP and SPP, respectively. The letter C refers to the two crystalline phases of CER3. The reflections at 1.46 and 2.91 nm^{-1} are attributed to crystalline CER3 (4.3 nm phase) and the reflections at 1.71 and 3.41 nm^{-1} are attributed to crystalline CER3 (3.7 nm phase). The asterisk (*) indicates the reflections of crystalline cholesterol located at 1.87 and 3.74 nm^{-1}. (A) Diffraction patterns of mixtures at a molar ratio of 1:1:1 and 1:1:0.75. The various orders of the LPP are located at q = 0.51 nm^{-1} (1), 1.02 nm^{-1} (2), 1.53 nm^{-1} (3), 2.04 nm^{-1} (4) and 2.56 nm^{-1} (5). The various orders of the SPP are located at q = 1.14 nm^{-1} (I), 2.31 nm^{-1} (II) and 3.47 nm^{-1} (III). (B) Diffraction patterns of mixtures at a molar ratio of 1:1:0.5 and 1:1:0. The various orders of the LPP are located at q = 0.50 nm^{-1} (1), 1.00 nm^{-1} (2) and 2.00 nm^{-1} (4). The various orders of the SPP are located at q = 1.12 nm^{-1} (I) and 2.23 nm^{-1} (II). (C) Diffraction patterns of mixtures at a molar ratio of 1:1:1.4 and 1:1:1.8. The various orders of the LPP are located at q = 0.52 nm^{-1} (1), 1.05 nm^{-1} (2) and 2.07 nm^{-1} (4). The various orders of the SPP are located at q = 1.12 nm^{-1} (I) and 2.24 nm^{-1} (II).

1.46 nm^{-1} reveals that only a very small amount CER3 phase separates into a 4.3 nm phase. Furthermore, crystalline cholesterol and the 3.7 nm phase are present in the lipid mixture.

3.3 The phase transitions as a function of temperature

The lipid phase behaviour of the equimolar CHOL:synthCER and CHOL:synthCER: FFA mixtures (equilibrated at 95 and 80°C, respectively) has been examined in the temperature range from 25 to 95°C. In Figure 4A and B sequential diffraction curves as a function of temperature are presented. Each curve represents the lipid organisation during a temperature shift of 2°C. The diffraction pattern of the equimolar CHOL: synthCER mixture at 25°C (see Fig. 4A) reveals a number of diffraction peaks that can be assigned to the presence of a LPP and SPP with periodicities of respectively 12.6 and 5.4 nm, similarly as described for Figure 2A. The reflections attributed to the SPP disappear at around 43°C. In the same temperature region the reflections (first and second order) of the LPP start to reduce in intensity and disappear at 55°C. Striking is the appearance of a new phase with a repeat distance of around 9.9 nm between 59°C and 73°C. This phase might be formed by CER1 that crystallises into separate domains. In the same temperature region the reflections of the 3.7 and 4.3 nm phases, both attributed to crystalline CER3 slightly shift to lower q-values, corresponding to spacings of 4.0 and 4.5 nm, respectively. The intensities of the peaks attributed to the latter phase markedly increase with increasing temperature, whereas the intensity of the former hardly increases. Both phases are still present at 95°C. The cholesterol reflections disappear at a temperature of approximately 57°C.

The equimolar CHOL:synthCER:FFA mixture shows the presence of two lamellar phases with periodicities of 12.0 and 5.4 nm (see Fig. 4B). The intensities of the diffraction peaks attributed to the LPP and SPP hardly change between 25°C and 49°C. A further increase in temperature gradually decreases the intensities of the reflections of the SPP, resulting in a disappearance of this phase at around 59°C. The reflections of the LPP start to decrease in intensity at approximately 59°C and disappear at 65°C. Similarly as observed for the CHOL:synthCER mixture, the peaks attributed to the 3.7 and 4.3 nm phase formed by CER3 shift to lower q-values. However, the shift of the reflections of the 3.7 nm phase is abrupt at 43°C, whereas the reflection of the 4.3 nm phase gradually shifts over a wide temperature range to a spacing of 4.6 nm at 63°C. At around 45°C a new phase is formed, of which only one reflection can be detected ($q = 1.37\ nm^{-1}$). The reflection considerably increases in intensity, being the

most prominent peak in the diffraction pattern at elevated temperatures. A maximal intensity is reached at around 71°C. A further increase in temperature reduces the peak intensity. The reflections at 1.37 and 1.57 nm^{-1} both disappear between 81°C and 85°C. In this temperature range a broad peak at q = 1.90 nm^{-1} is formed, which is still present at 95°C.

3.4 Lateral packing of the lipids

A hexagonal lateral packing is characterised by a strong 0.41 nm reflection in the WAXD pattern, whereas the diffraction pattern of an orthorhombic packing is characterised by two strong 0.41 and 0.37 nm reflections. All lipid mixtures measured during this study are characterised by a large number of strong and weak reflections in the WAXD pattern. In the CHOL:synthCER mixtures a reflection at 0.41 nm is present, although its intensity is rather weak compared to the various strong neighbouring reflections attributed to either crystalline cholesterol or CER3 (data not shown). Therefore, it cannot be deduced with certainty whether a hexagonal lateral packing is present in the CHOL:synthCER mixtures.

In the equimolar CHOL:synthCER:FFA mixture two strong 0.408 and 0.367 nm reflections indicate an orthorhombic lateral packing (data not shown). This is already observed at low free fatty acids content, such as in the mixture at a molar ratio of CHOL:CER:FFA 1:1:0.25. A further increase in free fatty acids content in the CHOL:CER:FFA mixture to 1:1:1.8 does not affect the lateral packing, but drastically changes the diffraction pattern by weakening the intensities of the numerous cholesterol and CER3 reflections. Both SAXD and WAXD data obviously show that an increased free fatty acids content results in reduced intensities of the cholesterol and CER3 reflections, indicating an increased solubility of both components in the lamellar phases.

The diffraction patterns of the equimolar CHOL:synthCER:FFA mixture monitored as a function of temperature are plotted in Figure 4C. The 0.408 and 0.367 nm peaks indicate an orthorhombic lateral packing. Between 35 and 37°C, the 0.367 nm reflection disappears, indicating an orthorhombic-hexagonal phase transition. The intensity of the 0.408 nm reflection initially decreases. However, a further temperature rise increases the intensity of the 0.408 nm reflection slightly, indicating a metastable to stable phase change. Similar results were obtained with stratum corneum [Bouwstra J.A., Gooris G.S., unpublished results]. A disappearance of this peak is observed at 65°C, which is at the same temperature at which the LPP disappears in the SAXD pattern.

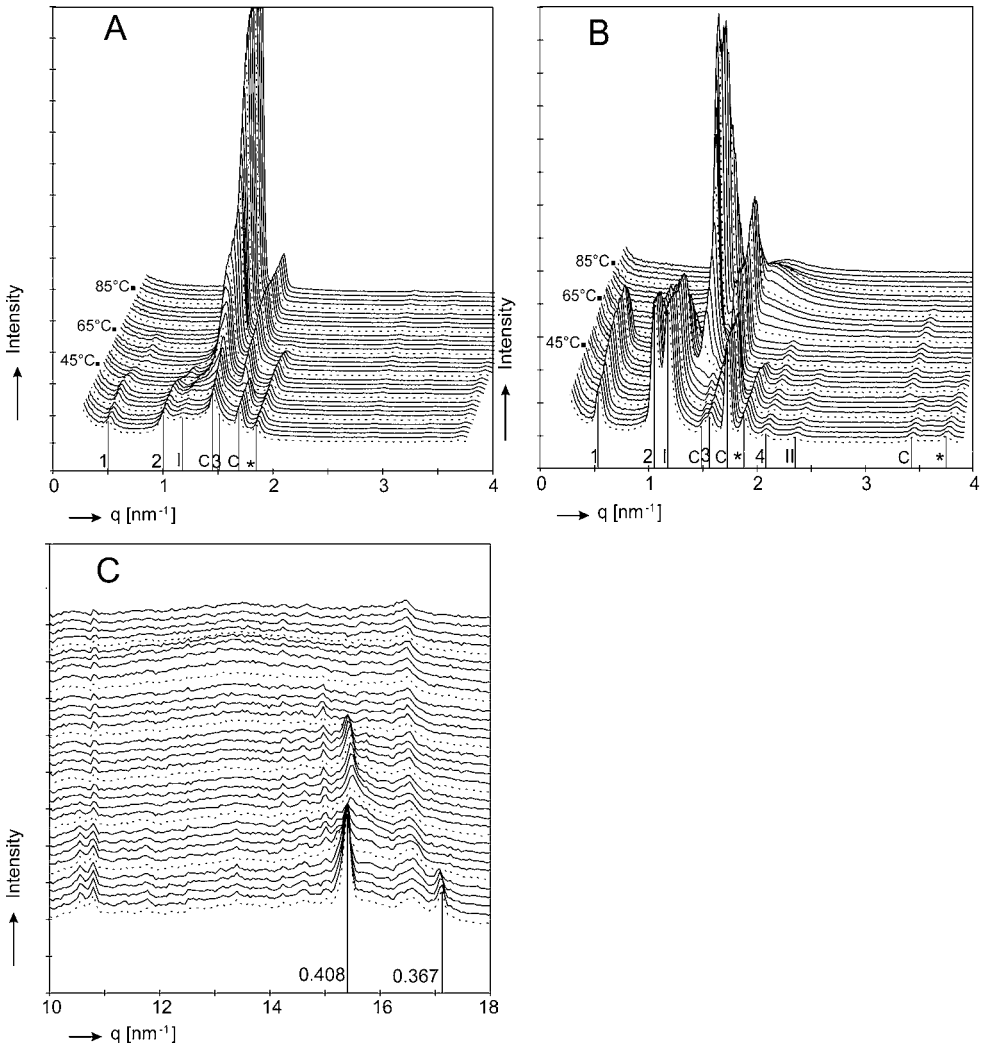

Figure 4 - Changes in the lipid phase behaviour as a function of temperature. (A) The lamellar organisation of equimolar CHOL:synthCER mixtures. (B) The lamellar organisation of equimolar CHOL:synthCER:FFA mixtures. (C) The lateral packing of CHOL:synthCER:FFA mixtures. The Arabic and Roman numbers indicate the diffraction orders of the LPP and SPP, respectively. The letter C refers to the two crystalline phases of CER3. The asterisk (*) indicates the reflections of crystalline cholesterol. The dashed line represents the diffraction curves at 25, 35, 45, 55, 65, 75 and 85°C.

4. DISCUSSION

For detailed studies on the effect of molecular structure of individual ceramides on the stratum corneum lipid organisation the use of synthCER offers an attractive approach, as both the head group and acyl chain composition can be systematically modified. One should, however, be aware that the prerequisite to replace natCER by synthCER is that their phase behaviour reflects that of the stratum corneum. The major difference between natCER and synthCER is great variation in acyl chain length in natCER versus well-defined acyl chain length in synthCER. Previous studies with mixtures prepared with ceramides isolated from native stratum corneum revealed that the stratum corneum phase behaviour can be mimicked with simplified mixtures, provided that CER1 is present [29]. In the present study a synthCER mixture was studied consisting of CER1, CER3 and bovine brain CER type IV mixed in a 1:7:2 ratio. The results clearly demonstrate that the lipid composition as well as the temperature at which the samples are equilibrated play an important role in the formation of the LPP.

4.1 Influence of equilibration temperature on phase behaviour

The formation of the LPP in equimolar CHOL:synthCER mixtures is enhanced when an increased equilibration temperature is used during the sample preparation. The mechanism behind this phenomenon is, however, not yet known, but will be subject of future studies. It is likely to assume that at elevated temperatures the formation of the LPP is promoted up to a certain optimal fluidity or mobility of the hydrocarbon chains. For example, for CHOL:synthCER mixtures equilibrated at 95°C or 100°C, the diffraction patterns are very similar and show a dominant formation of the LPP, indicating that the optimum has most likely been achieved. A further increase to 105°C or 110°C results in melting of the lipids and in a decreased formation of the LPP.

4.2 Influence of free fatty acids on phase behaviour

Addition of free fatty acids to the equimolar CHOL:synthCER mixture obviously increases the fluidity of the lipids at elevated temperatures, as equilibration at 95°C resulted in melting of the lipids. This can most likely be ascribed to the chain length variation in free fatty acids, ranging from 16 to 26 carbon atoms. It further becomes evident that for the formation of the LPP, an optimal amount of free fatty acids is required. Systematic increase in free fatty acids content to achieve an equimolar CHOL: synthCER:FFA mixture promotes the formation of the LPP. However, when the relative

amount of free fatty acids further increases, the formation of the LPP is reduced and the SPP dominates. A lower equilibration temperature would probably shift the optimal amount of free fatty acids for the formation of the LPP to higher values, whereas the opposite is true for a higher equilibration temperature. From these observations we can conclude that for each lipid composition an optimal equilibration temperature is required.

Free fatty acids seem to play an important role in the lipid phase behaviour. This conclusion is drawn from the following observations made with CHOL:synthCER:FFA mixtures: (i) cholesterol is better incorporated (dissolved), as reflected by weaker intensities of the cholesterol reflections than seen in the absence of free fatty acids. The same trend is observed with natCER [9, 11]. (ii) The intensities of the peaks attributed to crystalline CER3 are also weaker than those observed in the CHOL: synthCER mixtures, indicating better incorporation of CER3 in the presence of free fatty acids. (iii) A better ordering of the lamellar structures, because in the presence of free fatty acids, more higher order diffraction peaks can be observed for both LPP and SPP than in the absence of free fatty acids. (iv) Free fatty acids have a profound effect on the lateral packing, since only in their presence the packing is orthorhombic, similarly as observed for lipid mixtures based on isolated pig or human ceramides [10, 11] and in human stratum corneum [30].

4.3 Comparison between synthCER and natCER

The potential use of synthCER instead of natCER to study the stratum corneum lipid organisation is supported by the observations made at elevated temperatures. Many similarities can be observed in the lipid phase behaviour between CHOL:CER:FFA mixtures containing synthCER or natCER. Firstly, the LPP disappears at approximately 65°C. This temperature is close to 63°C and 67°C found for mixtures prepared with pig natCER and human natCER, respectively [9, 31]. Furthermore, the SPP and the reflections of phase-separated cholesterol disappear in the same temperature range as observed for mixtures prepared with natCER. Moreover, a new phase with a repeat distance of 4.6 nm is formed at elevated temperatures. The formation of a similar phase is observed in lipid mixture containing natCER, although the periodicity of 4.3 nm slightly differs from the 4.6 nm found in the mixtures based on synthCER.

Concerning the changes in lateral packing at elevated temperatures, at around 35°C there is a phase transition from an orthorhombic to a hexagonal lateral packing in the CHOL:synthCER:FFA mixture. As described above, no changes in lamellar

organisation have been noticed at this temperature, suggesting that the transition does not affect the lamellar lipid phase behaviour. The hexagonal lateral packing disappears at around 65°C, which is the same temperature at which the LPP disappears. This suggests that either an orthorhombic or a hexagonal lateral packing is a prerequisite for LPP formation. This confirms the findings with natCER, which revealed that when the fraction of lipids in a liquid phase is too high the formation of the SPP is increased at the expense of the LPP [11].

In spite of many similarities, also some differences are observed between mixtures prepared with synthetic and natural lipids. The main difference is that in mixtures prepared with synthCER two additional phases are present with repeat distances of 3.7 and 4.3 nm, respectively. These phases, which are attributed to crystalline CER3, have never been observed in the mixtures containing ceramides isolated from pig or human stratum corneum. From the present study it is evident that an increase in equilibration temperature from 60°C to 100°C or an increase in free fatty acids content in CHOL:synthCER:FFA mixtures from 1:1:0 to 1:1:1 increases the intensities of the peaks attributed to 4.3 nm phase at the expense of the 3.7 nm phase. A further rise in the free fatty acids content leads to a marked reduction of the peak intensities of the 4.3 nm phase. However, under these conditions the fraction of lipids forming the characteristic LPP is also diminished.

Another difference between the phase behaviour of CHOL:CER:FFA mixtures prepared with synthCER or natCER is the repeat distance of the LPP. In the absence of free fatty acids, the periodicity of the LPP in CHOL:synthCER mixtures equilibrated at 95°C or 100°C is about 12.3 nm. The periodicity of the LPP in mixtures prepared with isolated human or pig ceramides is very similar, being 12.8 and 12.2 nm, respectively. When free fatty acids are included to reach an equimolar CHOL:natCER:FFA mixture, the repeat distance of the LPP slightly increases to 13.0 nm (human) and 13.3 nm (pig). These values are similar to that reported for native stratum corneum. However, this behaviour is not observed for mixtures prepared with synthCER. There, a rise in the free fatty acid level or equilibration temperature led to a slight decrease in the LPP repeat distance to approximately 12.2 nm (see Table 1 and Table 2).

The relative intensities of the various diffraction orders provide information on the relative electron density distribution in the LPP. Therefore, we determined the relative intensities of the various reflections of the LPP in six equimolar CHOL:synthCER:FFA mixtures, measured during four different X-ray diffraction sessions, and compared the values with those obtained with equimolar CHOL:pigCER:FFA mixtures. The results

given in Table 3 show that the relative intensities of the peaks attributed to the LPP show the same trend in all samples. However, in the synthCER mixtures the relative intensities of some LPP reflections differ from those found in the CHOL:pigCER:FFA mixtures. This indicates that the localisation of the lipids within the LPP in mixtures prepared with synthCER might differ slightly.

Table 3 - Relative intensities of the diffraction peaks of the LPP in equimolar CHOL:synthCER:FFA mixtures and equimolar CHOL:pigCER mixtures

order	12 nm phase CHOL:synthCER:FFA	13 nm phase CHOL:pigCER:FFA *
1	1.0	1.0
2	2.94 ± 0.36	2.55 ± 0.28
3	0.37 ± 0.06	0.81 ± 0.10
4	0.15 ± 0.02	0.09 ± 0.01
7	0.04 ± 0.03	0.08 ± 0.03

For scaling, the intensity of the first order diffraction peak of the LPP was set equal to 1. The values are presented as the average (n=6) ± the standard deviation. * de Jager et al., unpublished results

In conclusion, the results of the present study demonstrate for the first time that one can generate lipid mixtures, containing synthCER, which closely mimic the phase behaviour observed in native stratum corneum. Prerequisite is that the experimental conditions are appropriately chosen, as the composition of the lipid mixtures and the temperature at which the lipid mixtures are equilibrated play a crucial role for the formation of the characteristic LPP. From all lipid mixtures tested, the phase behaviour of the equimolar CHOL:[CER1:CER3:ΣCERIV]:FFA mixtures resemble to the highest extent the lamellar and lateral stratum corneum lipid organisation, both at room and elevated temperatures.

Acknowledgements

This work was supported by a grant from the Technology Foundation STW (LGN4654). The Netherlands Organisation for Scientific Research (NWO) is acknowledged for the provision of the beamtime. We would like to thank the companies Cosmoferm and Beiersdorf for the provision of the synthetic ceramides.

REFERENCES

1. Elias P.M. Epidermal lipids, barrier function, and desquamation. *J. Invest. Dermatol.* **80** (1983) 44s-49s.

2. Ponec M., Weerheim A., Lankhorst P., Wertz P. New acylceramide in native and reconstructed epidermis. *J. Invest. Dermatol.* **120** (2003) 581-588.

3. Robson K.J., Stewart M.E., Michelsen S., Lazo N.D., Downing D.T. 6-Hydroxy-4-sphingenine in human epidermal ceramides. *J. Lipid Res.* **35** (1994) 2060-2068.

4. Stewart M.E., Downing D.T. A new 6-hydroxy-4-sphingenine-containing ceramide in human skin. *J. Lipid Res.* **4** (1999) 1434-1439.

5. Wertz P.W., Miethke M.C., Long S.A., Strauss J.S., Downing D.T. The composition of the ceramides from human stratum corneum and from comedones*. J. Invest. Dermatol.* **84** (1985) 410-412.

6. Bouwstra J.A., Gooris G.S., van der Spek J.A., Bras W. The structure of human stratum corneum as determined by small angle X-ray scattering. *J. Invest. Dermatol.* **96** (1991) 1006-1014.

7. Bouwstra J.A., Gooris G.S., van der Spek J.A., Bras W. Structural investigations of human stratum corneum by small angle X-ray scattering*. J. Invest. Dermatol.* **97** (1991) 1005-1012.

8. Bouwstra J.A., Gooris G.S., Bras W., Downing D.T. Lipid organization in pig stratum corneum. *J. Lipid Res.* **36** (1995) 685-695.

9. Bouwstra J.A., Gooris G.S., Cheng K., Weerheim A., Bras W., Ponec M. Phase behavior of isolated skin lipids. *J. Lipid Res.* **37** (1996) 999-1011.

10. Bouwstra J.A., Gooris G.S., Dubbelaar F.E.R., Weerheim A.M., Ponec M. pH, cholesterol sulfate, and fatty acids affect the stratum corneum lipid organization. *J. Invest. Dermatol.* **3** (1998) 69-73.

11. Bouwstra J.A., Gooris G.S., Dubbelaar F.E.R., Ponec M. Phase behavior of stratum corneum lipid mixtures based on human ceramides: the role of natural and synthetic ceramide 1. *J. Invest. Dermatol.* **118** (2002) 606-617.

12. Fenske D.B., Thewalt J.L., Bloom M., Kitson N. Models of stratum corneum intercellular membranes: ^{2}H NMR of microscopically oriented multilayers. *Biophys. J.* **67** (1994) 1562-1573.

13. Kitson N., Thewalt J., Lafleur M., Bloom M. A model membrane approach to the epidermal permeability barrier. *Biochemistry* **33** (1994) 6707-6715.

14. Moore, D.J., Rerek M.E., Mendelsohn R. Lipid domains and orthorhombic phases in model stratum corneum: evidence from fourier transform infrared spectroscopy studies. *Biochem. Biophys. Res. Commun.* **231** (1997) 797-801.

15. Neubert R., Rettig W., Wartewig S., Wegener M., Wienhold A. Structure of stratum corneum lipids characterized by FT-Raman spectrospcopy and DSC. II. Mixtures of ceramides and saturated fatty acids. *Chem. Phys. Lipids* **89** (1997) 3-14.

16. Percot A., Lafleur M. Direct observations of domains in model stratum corneum lipid mixtures by Raman microspectroscopy. *Biophys. J.* **81** (2001) 2144-2153.

17. Wegener M., Neubert R., Rettig W., Wartewig S. Structure of stratum corneum lipids characterized by FT-Raman spectrospcopy and DSC. III. Mixtures of ceramides and cholesterol. *Chem. Phys. Lipids* **88** (1997) 73-82.

18. Chen H., Mendelsohn R., Rerek M.E., Moore D.J. Fourier transform infrared spectroscopy and differential scanning calorimetry studies of fatty acid homogeneous ceramide 2. *Biochim. Biophys. Acta.* **1468** (2000) 293-303.

19. Dahlen B., Pascher I. Molecular arrangements in sphingolipids. Thermotropic phase behaviour of tetracosanoylphytosphingosine. *Chem. Phys. Lipids* **24** (1979) 119-133.

20. Moore D.J., Rerek M.E. Insights into the molecular organization of lipids in the skin barrier from infrared spectroscopy studies of stratum corneum lipid models. *Acta Derm. Venereol. Suppl. (Stockh.)* **208** (2000) 16-22.

21. Ohta N., Hatta I. Interaction among molecules in mixtures of ceramide/stearic acid, ceramide./cholesterol and ceramide/stearic acid/ cholesterol. *Chem. Phys. Lipids* **115** (2002) 93-105.

22. Raudenkolb S., Hübner W., Rettig W., Wartewig S., Neubert R.H.H. Polymorphism of ceramide 3. Part 1: an investigation focused on the head group of N-octadecanoylphytosphingosine. *Chem. Phys. Lipids* **123** (2003) 9-17.

23. Bouwstra J.A., Thewalt J., Gooris G.S., Kitson N. A model membrane approach to the epidermal permeability barrier: an X-ray diffraction study. *Biochemistry* **36** (1997) 7717-7725.

24. McIntosh T.J., Stewart M.E., Downing D.T. X-ray diffraction analysis of isolated skin lipids: reconstitution of intercellular lipid domains. *Biochemistry* **35** (1996) 3649-3653.

25. de Jager M.W., Gooris G.S., Dolbnya I.P., Bras W., Ponec M., Bouwstra J.A. The phase behaviour of lipid mixtures based on synthetic ceramides. *Chem. Phys. Lipids* **124** (2003) 123-134.

26. Bouwstra J.A., Gooris G.S., Dubbelaar F.E.R., Weerheim A.M., IJzerman A.P., Ponec M. Role of ceramide 1 in the molecular organization of the stratum corneum lipids. *J. Lipid Res.* **39** (1998) 186-196.

27. Bras W. A SAXS/WAXS beamline at the ESRF and future experiments. *J. Macromol. Sci. Phys. B* **37** (1998) 557-566.

28. Dolbnya I.P., Alberda H., Hartjes F.G., Udo F., Bakker R.E., Konijnenburg M., Homan E., Cerjak I., Goedtkindt P., Bras W. A fast position sensitive MSGC detector at high count rate operation. *Rev. Sci. Instrum.* **73** (2002) 3754-3758.

29. Bouwstra J.A., Gooris G.S., Dubbelaar F.E.R., Ponec M. The lipid organisation in the skin barrier. *Acta Derm. Venereol. Supp. (Stockh.)* **208** (2000) 23-30.

30. Bouwstra J.A., Gooris G.S., Salomons-de Vries M.A., van der Spek J.A., Bras W. Structure of human stratum corneum as a function of temperature and hydration: a wide-angle X-ray diffraction study. *Int. J. Pharm.* **84** (1992) 205-216.

31. Bouwstra J.A., Gooris G.S., Dubbelaar F.E.R., Ponec M. Phase behavior of lipid mixtures based on human ceramides: coexistence of crystalline and liquid phases. *J. Lipid Res.* **42** (2001) 1759-1770.

Chapter 4

Modelling the stratum corneum lipid organisation with synthetic lipid mixtures: the importance of synthetic ceramide composition

M.W. de Jager,* G.S. Gooris,* I.P. Dolbnya,# M. Ponec,§ and J.A. Bouwstra*

*Leiden/Amsterdam Center for Drug Research, Department of Drug Delivery Technology, University of Leiden, P.O. Box 9502, 2300 RA Leiden, The Netherlands.
#Netherlands Organisation for Scientific Research, DUBBLE CRG/ESRF, Grenoble, France.
§Department of Dermatology, Leiden University Medical Center, Leiden, The Netherlands.

(adapted from *Biochim. Biophys. Acta* **1684** (2004) 132-140)

ABSTRACT

Cholesterol, free fatty acids and 9 classes of ceramides (CER1-CER9) form the main components of the intercellular lipid lamellae in stratum corneum, which are responsible for the skin barrier function. Both the presence of a unique 13 nm lamellar phase, of which the formation depends on the presence of CER1, and the dense lateral lipid packing are characteristic for the stratum corneum lipid organisation. The present study focuses on the organisation in mixtures prepared with cholesterol, free fatty acids and a limited number of synthetic ceramides, namely CER1, CER3 and bovine brain ceramide type IV (ΣCERIV). The main objective is to determine the optimal molar ratio between CER3 and ΣCERIV for the formation of the 13 nm lamellar phase. CER3 contains a uniform acyl chain length, whereas ΣCERIV contains fatty acids with varying chain lengths. Using small-angle X-ray diffraction, it is demonstrated that the CER3: ΣCERIV molar ratio affects the formation of the 13 nm lamellar phase and that the optimal ratio depends on the presence of free fatty acids. Furthermore, the formation of the 13 nm lamellar phase is not very sensitive to variations in the total ceramide level, which is similar to the in vivo situation.

1. INTRODUCTION

The barrier properties of mammalian skin can be ascribed to the unique composition and structure of its most apical layer, the stratum corneum. The stratum corneum consists of flat corneocytes, embedded in an intercellular matrix of lipids. Since these lipid domains form the only continuous structure in the stratum corneum, they are considered to play a crucial role in the maintenance of the skin barrier. Therefore, detailed information on the structure and organisation of the stratum corneum lipids is essential for a better understanding of the skin barrier function.

The main constituents of the intercellular lipid matrix are ceramides (CER), cholesterol (CHOL) and long-chain free fatty acids (FFA). Nine different extractable ceramides have been detected in human stratum corneum [1-4], which are classified as CER1 to CER9. The ceramides can be subdivided into three main groups, based on the nature of their head group architecture (sphingosine (S), phytosphingosine (P) or 6-hydroxysphingosine (H)). Through an amide bonding, long-chain nonhydroxy (N) or α-hydroxy (A) fatty acids with varying acyl chain lengths are chemically linked to the sphingosine bases. CER1 (EOS), CER4 (EOH) and CER9 (EOP) are unique in structure as they contain linoleic acid linked to an ω-hydroxy fatty acid (EO) with a chain length of 30 to 32 carbon atoms. The molecular structures of the ceramides are illustrated in Figure 1A.

X-ray diffraction studies on native stratum corneum have demonstrated that the stratum corneum lipids are organised in two coexisting crystalline lamellar phases: the short periodicity phase (SPP) with a periodicity of approximately 6 nm and the long periodicity phase (LPP) with a periodicity of approximately 13 nm [5-7]. The 13 nm lamellar phase and the predominantly orthorhombic lipid packing are considered to be crucial for the skin barrier function. X-ray diffraction studies on lipid mixtures prepared with isolated pig or human ceramides, cholesterol and free fatty acids revealed that the lipid organisation in these mixtures is similar to that observed in native stratum corneum. The main advantage of these stratum corneum lipid models is the possibility to selectively exclude particular lipid classes from the mixtures, which is not possible with stratum corneum. Therefore, these studies greatly contributed to our present knowledge on the role of individual lipid classes in the lipid organisation. Interestingly, the formation of the characteristic LPP depends on the presence of cholesterol and specific ceramides, in particular CER1, whereas free fatty acids are required for the crystalline (orthorhombic) character of the lateral lipid packing [8-11].

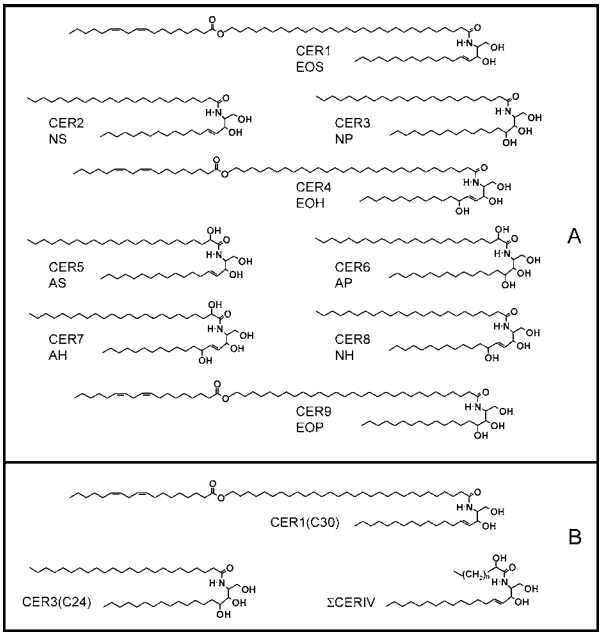

Figure 1 – (A) The molecular structures of the ceramides present in human SC. (B) The molecular structures of the synthetic CER used in the study. The acyl chain lengths of CER1(C30) and CER3(C24) are well-defined, whereas bovine brain CER type IV (ΣCERIV) shows a distribution in chain lengths with C18 and C24 as the most abundantly present.

The use of synthetic lipids can overcome problems related to isolated stratum corneum lipids, such as variability of the native tissue and the laborious isolation and separation of the stratum corneum lipids. In a previous study it was shown for the first time that the stratum corneum lipid phase behaviour can already be reproduced to a high extent with a synthetic lipid mixture consisting of only three synthetic ceramides [12]. In that study a fixed ceramide composition was used, namely CER1, CER3 and bovine brain ceramide type IV (referred to as ΣCERIV) at a molar ratio of 1:7:2. In synthetic CER1 and CER3 a fatty acid with a well-defined acyl chain length is bound to the sphingoid backbone, whereas in ΣCERIV fatty acids with varying acyl chain lengths are present (see Fig. 1 and Table 1). Both an appropriately chosen equilibration temperature during the sample preparation and the presence of free fatty acids in the mixture are crucial to achieve a similar lipid organisation as found in native stratum corneum [12]. In spite of great similarities in lipid phase behaviour between mixtures prepared with natural ceramides (natCER) and synthetic ceramides (synthCER), some differences have also been disclosed. The main difference is the presence of either one

or two additional phases in mixtures prepared with synthetic lipids. These additional phases, with repeat distances of respectively 3.7 and 4.3 nm, can be ascribed to crystalline CER3 in a V-shaped structure [13-15].

In the study presented in this paper, we further optimised the composition of the synthetic lipid mixtures to accomplish higher resemblance to the stratum corneum lipid organisation. To diminish the formation of the additional crystalline phases, which are not present in native stratum corneum, the amount of CER3 in the mixture was gradually reduced in favour of ΣCERIV. The main objective of the present study was to establish the optimal molar ratio of CER3 to ΣCERIV for the formation of the characteristic LPP and to determine the sensitivity of the lipid organisation to this ratio. In addition, the sensitivity of the lipid organisation to changes in the total synthCER level was studied. This was performed by varying the composition of the CHOL:synthCER:FFA mixture over a wide range of molar ratios, thereby maintaining a constant CHOL:FFA ratio.

2. MATERIALS AND METHODS

2.1 Synthetic lipids used in the study

Palmitic acid, stearic acid, arachidic acid, behenic acid, tricosanoic acid, lignoceric acid, cerotic acid, cholesterol and bovine brain ceramide type IV were purchased from Sigma-Aldrich Chemie GmbH (Schnelldorf, Germany). N-(30-Linoleoyloxy-triacontanoyl)-sphingosine (synthetic ceramide 1(C30)-linoleate) was a gift from Beiersdorf AG (Hamburg, Germany). N-Tetracosanoyl-phytosphingosine (synthetic ceramide 3(C24)) was generously provided by Cosmoferm B.V. (Delft, the Netherlands). Figure 1B shows the ceramides used in this study. All organic solvents used were of analytical grade and manufactured by Labscan Ltd (Dublin, Ireland).

2.2 Preparation and analysis of fatty acid methyl esters (FAMEs)

To establish the fatty acid profile in ΣCERIV, the lipid was dissolved in 100 µl toluene and transmethylated in 1 ml boron trichloride in methanol (10%) using microwave irradiation, which was carried out at the lowest power setting (85W) for 4 hours. FAMEs dissolved in hexane and purified on a silica gel column were separated and analysed on a Vega GC 6000 gas chromatograph (Carlo Erba Instruments, Italy) using capillary column CP Wax 52 (Chrompack, The Netherlands). An initial temperature of 80°C was increased to 160°C with a rate of 40°C/min followed by a 4°C/min increase to 250°C that was maintained until all peaks had eluted. The peaks were identified by

comparison with FAME standards (Sigma-Aldrich Chemie GmbH, Germany). Integration of peak areas and calculation of relative percentages were performed by Baseline 810 integrator. Heptadecanoic acid was used as an internal standard.

2.3 Preparation of the lipid mixtures

For the preparation of all CHOL:synthCER and CHOL:synthCER:FFA mixtures, a synthetic ceramide mixture was used that consisted of CER1, CER3 and ΣCERIV at a molar ratio ranging from 1:1:8 to 1:8:1. For the preparation of the CHOL:synthCER:FFA mixtures, the following fatty acid mixture was used: C16:0, C18:0, C20:0, C22:0, C23:0, C24:0 and C26:0 at molar ratios of 1.3, 3.3, 6.7, 41.7, 5.4, 36.8 and 4.7, respectively. This ratio is similar to that found in native stratum corneum [16]. Appropriate amounts of individual lipids dissolved in chloroform:methanol (2:1) were combined to yield lipid mixtures of approximately 1.5 mg dry weight at the desired composition at a total lipid concentration of 7 mg/ml. A Camag Linomat IV was used to apply the lipid mixtures onto mica. This was done at a rate of 4.3 µl/min under a continuous nitrogen flow. The samples were equilibrated for 10 minutes at the appropriate elevated temperature that varied from 70 to 90°C and subsequently hydrated with an acetate buffer of pH 5.0. Finally, the samples were homogenised by 10 successive freeze-thawing cycles between -20°C and room temperature, during which the samples were stored under gaseous argon.

2.4 Small-angle X-ray diffraction (SAXD)

All measurements were performed at the European Synchrotron Radiation Facility (ESRF, Grenoble), using station BM26B. A more detailed description of this beamline has been given elsewhere [17]. The X-ray wavelength and the sample-to-detector distance were 1.24Å and 1.7m, respectively. Diffraction data were collected on a two-dimensional multiwire gas-filled area detector. The spatial calibration of this detector was performed using silver behenate. The samples were mounted in a specially designed sample holder with mica windows. All measurements were recorded at room temperature for a period of 10 minutes.

SAXD provides information about the larger structural units in the sample, such as the repeat distance of a lamellar phase. The scattering intensity I (in arbitrary units) was measured as a function of the scattering vector q (in reciprocal nm). The latter is defined as $q=(4\pi\sin\theta)/\lambda$, in which θ is the scattering angle and λ is the wavelength. From the positions of a series of equidistant peaks (q_n), the periodicity, or d-spacing,

of a lamellar phase was calculated using the equation $q_n=2n\pi/d$, n being the order number of the diffraction peak.

3. RESULTS

3.1 Fatty acid profile in ΣCERIV

To assess the fatty acid profile in ΣCERIV, two batches of ΣCERIV were subjected to transmethylation with boron trichloride in methanol followed by purification of the FAME by column chromatography. In this way, fractions containing methyl esters of α-hydroxy fatty acids were collected and subsequently analysed by gas chromatography. The results of the FAME analysis summarised in Table 1 show low batch-to-batch variation in the composition and the relative amounts of the various α-hydroxy fatty acids. All lipid mixtures used in our studies were prepared with batch 2. There, the most abundantly fatty acids were C18 (22%) and C24 (42%).

Table 1 - α-hydroxy acyl profile in two batches of ΣCERIV given as percentages of total α-hydroxy acids

acyl chain length α-hydroxy fatty acid	batch 1 (%)	batch 2 (%)
C18	18.0	22.2
C20	1.7	0.5
C22	8.0	7.9
C23	11.1	10.6
C24	44.0	41.8
C25	11.3	11.5
C26	5.9	5.5

3.2 Mixtures prepared with equimolar ratios of cholesterol and synthetic ceramides

The main objective of these studies is to determine the optimal molar ratio between CER3 and ΣCERIV for the formation of the LPP. All synthetic ceramide mixtures contained the same relative amount of CER1 (10%mol/mol), as earlier studies revealed that this amount is sufficient for the formation of the LPP. The relative content of CER3 and ΣCERIV in CER1:CER3:ΣCERIV mixtures was varied between a molar ratio of 1:1:8 and 1:8:1. During preparation, the dry lipid mixtures were equilibrated at either 80°C or 90°C. These temperatures were chosen, as use of a higher temperature results in melting of the CER1:CER3:ΣCERIV mixture with molar ratio of 1:1:8, while use of a lower equilibration temperature results in reduced LPP formation [12]. As no clear differences in the formation of the lamellar phases were observed between the lipid mixtures prepared at 80°C or 90°C, only the results of the mixtures equilibrated at

90°C will be presented.

The diffraction pattern of the equimolar CHOL:synthCER mixture in which the CER fraction was prepared by mixing CER1:CER3:ΣCERIV to achieve a molar ratio of 1:1:8 is shown in Figure 2A. A lamellar phase with a repeat distance of 5.5 nm (SPP) is indicated by the presence of a strong reflection at q = 1.14 nm^{-1} and two weak reflections at 2.29 and 3.43 nm^{-1}. The diffraction pattern further depicts three weak diffraction peaks at 0.48, 0.97 and 1.45 nm^{-1}, respectively. Taking into account the diffraction patterns depicted in Figure 2 and 3 (see below), it is conceivable to ascribe these reflections to the 1st, 2nd and 3rd order maxima of the LPP with a repeat distance of approximately 13 nm. In addition, crystalline cholesterol in separate domains is present, deduced from the sharp peaks at 1.87 and 3.74 nm^{-1}.

A rise in the CER3 content at the expense of ΣCERIV to reach a CER1:CER3:ΣCERIV molar ratio of 1:3:6 was accompanied by a slight increase in peak width (Fig. 2A). This results in a partial overlap of the peaks located at 0.98 and 1.16 nm^{-1}. In addition, a new structure with a repeat distance of 3.7 nm is present in the mixture, suggested by two reflections at 1.69 and 3.40 nm^{-1}, respectively. This phase can be ascribed to crystalline CER3 in a V-shaped structure [13-15].

Figure 2B shows the diffraction pattern of the CHOL:synthCER mixture prepared at a 1:5:4 ratio of CER1, CER3 and ΣCERIV. Compared to the diffraction patterns obtained at lower CER3 content (1:1:8 and 1:3:6), the peak intensities of the LPP are considerably increased compared to the reflections attributed to the SPP, indicating that the formation of the LPP is promoted at increased CER3 content. Similarly as in the 1:3:6 mixture, only one reflection of the SPP can be detected. In addition, crystalline CER3 and crystalline cholesterol are present. A further rise in CER3 content to a CER1: CER3:ΣCERIV ratio of 1:7:2 results in the diffraction pattern illustrated in Figure 2C. Obviously, the reflection at q = 1.71 nm^{-1} is the most prominent peak in the diffraction pattern. This suggests that a considerable amount of crystalline CER3 phase separates into a 3.7 nm phase. The LPP and SPP are still present in the mixture, but their peak intensities are weaker than the those of cholesterol and CER3.

At a CER1:CER3:ΣCERIV ratio of 1:8:1, a marked reduction of LPP formation is observed. Only a small lipid fraction forms a lamellar phase with a periodicity of 12.4 nm, whereas substantial amounts of crystalline CER3 are present in separate domains.

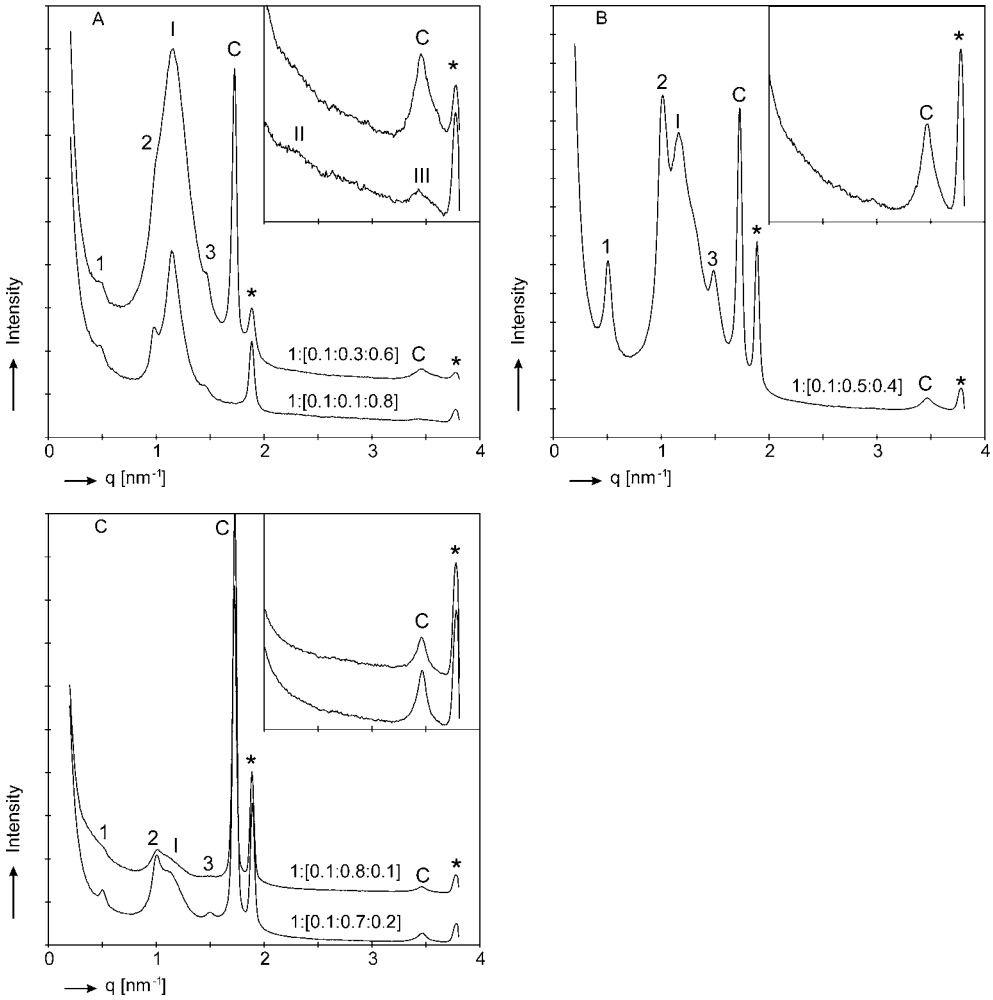

Figure 2 - The effect of the CER3 to ΣCERIV molar ratio on the phase behaviour of equimolar CHOL: synthCER mixtures. The inset shows a magnification of the reflections in the q-range between 2 and 4 nm^{-1}. The Arabic and Roman numbers indicate the diffraction orders of the LPP and SPP, respectively. The letter C refers to the reflections of crystalline phase of CER3 at 1.71 and 3.42 nm^{-1}. The asterisk (*) indicates the reflections of crystalline CHOL located at 1.87 and 3.74 nm^{-1}. (A) Diffraction patterns of CHOL:[CER1:CER3:ΣCERIV] mixtures at a molar ratio of 1:[0.1:0.1:0.8] and 1:[0.1:0.3:0.6]. The various orders of the LPP are located at q = 0.48 nm^{-1} (1), 0.97 nm^{-1} (2) and 1.45 nm^{-1} (3). The various orders of the SPP are located at q = 1.14 nm^{-1} (I), 2.29 nm^{-1} (II) and 3.43 nm^{-1} (III). (B) Diffraction pattern of 1:[0.1:0.5:0.4] mixture. The various orders of the LPP are located at q = 0.50 nm^{-1} (1), 1.01 nm^{-1} (2) and 1.49 nm^{-1} (3). The only reflection attributed to the SPP is located at q = 1.16 nm^{-1} (1). (C) Diffraction patterns of 1:[0.1:0.7:0.2] and 1:[0.1:0.8:0.1] mixtures. The various orders of the LPP are located at q = 0.50 nm^{-1} (1), 1.01 nm^{-1} (2) and 1.49 nm^{-1} (3). The only reflection attributed to the SPP is located at q = 1.14 nm^{-1} (I).

3.3 Mixtures prepared with equimolar ratios of cholesterol, synthetic ceramides and free fatty acids

The lipid organisation of mixtures containing free fatty acids has also been examined, as free fatty acids represent the third major lipid species in the stratum corneum. In a previous study it was observed that CHOL:synthCER:FFA mixtures melted at a lower equilibration temperature than CHOL:synthCER mixtures [11]. The lipid mixtures in the present study were therefore equilibrated at slightly lower temperatures, namely at 70°C or 80°C. As no obvious differences could be observed in the formation of the lamellar phases between mixtures equilibrated at 70° or 80°C, only the results obtained at an equilibration temperature of 80°C will be reported.

The phase behaviour of the CHOL:[CER1:CER3:ΣCERIV]:FFA mixture prepared at a molar ratio of 1:[0.1:0.1:0.8]:1 is depicted in Figure 3A. The diffraction pattern reveals the presence of a strong reflection at q = 1.05 nm^{-1} and two weak reflections at 2.09 and 3.15 nm^{-1}. These peaks are located at positions at which the 2^{nd}, 4^{th} and 6^{th} order diffraction peaks of the LPP should be expected. However, as no 1^{st} and 3^{rd} order reflections of the LPP are present, the reflections may also be related to another phase with a periodicity of 6.0 nm. In addition, the SPP with a periodicity of 5.4 nm is present, deduced from the presence of a shoulder at the right-hand side of the strong peak (1^{st} order) and a weak reflection at 3.50 nm^{-1} (3^{rd} order). A small fraction of cholesterol phase separates into crystalline domains, indicated by one weak reflection at 1.87 nm^{-1}.

A rise in CER3 content to reach a CER1:CER3:ΣCERIV ratio of 1:3:6 results in a clear appearance of the reflections attributed to the LPP. At this increased CER3 level, crystalline CER3 is present in separate domains as indicated by the two peaks at 1.71 and 3.43 nm^{-1}. In addition, the SPP and small amounts of crystalline cholesterol are present in the lipid mixture.

The diffraction pattern of the mixture at a CER1:CER3:ΣCERIV molar ratio of 1:5:4 is presented in Figure 3B. A rise in the CER3 level obviously increases the intensities of the peaks attributed to the LPP compared to those attributed to the SPP. Five diffraction peaks of the LPP with a periodicity of 12.0 are present and two reflections of a 5.4 nm phase (SPP) can be detected. Crystalline CER3 and crystalline cholesterol can also be detected in the mixture.

A further rise in the CER3 content to a molar ratio of 1:7.2 promotes the formation of the LPP even more. The presence of the LPP, with a slightly decreased repeat distance of 11.9 nm, is indicated by six reflections, whereas the SPP is indicated by

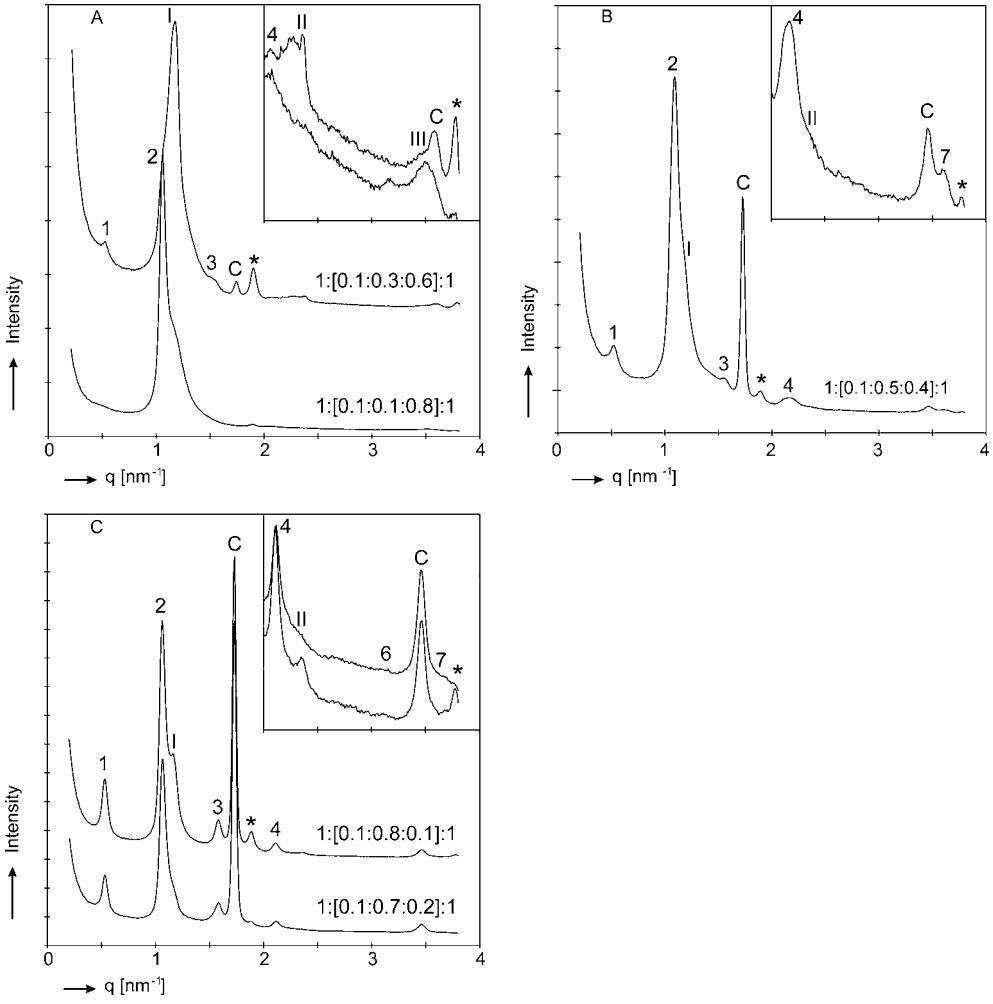

Figure 3 - The effect of the CER3 to ΣCERIV molar ratio on the phase behaviour of equimolar CHOL: synthCER:FFA mixtures. The inset shows a magnification of the reflections in the q-range between 2 and 4 nm^{-1}. The Arabic and Roman numbers indicate the diffraction orders of the LPP and SPP, respectively. The letter C refers to the reflections of crystalline phase of CER3 at 1.71 and 3.42 nm^{-1}. The asterisk (*) indicates the reflections of crystalline CHOL located at 1.87 and 3.74 nm^{-1}. (A) Diffraction patterns of CHOL:[CER1:CER3:ΣCERIV]:FFA mixtures at a molar ratio of 1:[0.1:0.1:0.8]:1 and 1:[0.1:0.3:0.6]:1. The various orders of the LPP in the latter mixture are located at q = 0.52 nm^{-1} (1), 1.03 nm^{-1} (2), 1.52 nm^{-1} (3), and 2.06 nm^{-1} (4). The various orders of the SPP are located at q = 1.16 nm^{-1} (I), 2.31 nm^{-1} (II), and 3.48 nm^{-1} (III). (B) Diffraction pattern of 1:[0.1:0.5:0.4]:1 mixture. The various orders of the LPP are located at q = 0.52 nm^{-1} (1), 1.05 nm^{-1} (2), 1.56 nm^{-1} (3), 2.11 nm^{-1} (4), and 3.64 nm^{-1} (7). The various reflections attributed to the SPP are located at q = 1.16 nm^{-1} (I) and 2.33 nm^{-1} (II). (C) Diffraction patterns of 1:[0.1:0.7:0.2]:1 and 1:[0.1:0.8:0.1]:1 mixture. The various orders of the LPP are located at q = 0.52 nm^{-1} (1) , 1.05 nm^{-1} (2), 1.58 nm^{-1} (3) , 2.11 nm^{-1} (4) , 3.12 nm^{-1} (6), and 3.65 nm^{-1} (7). The various orders of the SPP are located at q = 1.17 nm^{-1} (I) and 2.34 nm^{-1} (II).

two reflections. Weak reflections designate small amounts of crystalline cholesterol, whereas strong reflections at 1.71 and 3.43 nm^{-1} indicate that a substantial amount of CER3 phase separates in a crystalline phase.

The diffraction pattern of the lipid mixture prepared with a 1:8:1 composition of CER1:CER3:ΣCERIV is plotted in Figure 3C. Compared to the diffraction pattern of the 1:7:2 mixture, the relative intensities of the reflections of both LPP and SPP have not changed significantly. However, the number of higher order reflections, which can be detected for both LPP and SPP, are reduced.

3.4 CHOL:synthCER:FFA mixtures with a variation in synthetic ceramide content

To determine the sensitivity of the lipid organisation towards changes in the total content of synthetic ceramides, the composition of the CHOL:synthCER:FFA mixture was varied over a wide synthetic ceramide level, thereby maintaining an equimolar cholesterol to free fatty acids ratio.

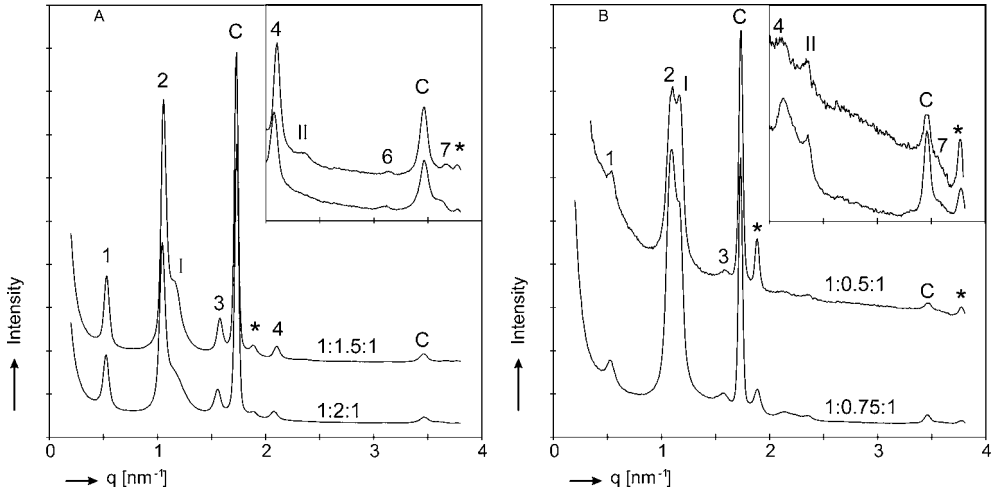

Figure 4 - Effect of changing the ceramide molar ratio, thereby maintaining an equimolar cholesterol to free fatty acids ratio. The inset shows a magnification of the reflections in the q-range between 2 and 4 nm^{-1}. The Arabic and Roman numbers indicate the diffraction orders of the LPP and SPP, respectively. The letter C refers to the reflections of crystalline phase of CER3 at 1.71 and 3.42 nm^{-1}. The asterisk (*) indicates the reflections of crystalline CHOL located at 1.87 and 3.74 nm^{-1}. (A) Diffraction patterns of CHOL:synthCER:FFA mixtures at a molar ratio of 1:2:1 and 1:1.5:1. The various orders of the LPP are located at q = 0.52 nm^{-1} (1), 1.03 nm^{-1} (2), 1.56 nm^{-1} (3), 2.08 nm^{-1} (4) , 3.09 nm^{-1} (6) and 3.60 nm^{-1} (7). The various orders of the SPP are located at q = 1.16 nm^{-1} (I) and 2.32 nm^{-1} (II). (B) Diffraction patterns of 1:0.75:1 and 1:0.5:1 mixtures. The various orders of the LPP are located at q = 0.49 nm^{-1} (1), 0.99 nm^{-1} (2), 1.48 nm^{-1} (3), 1.99 nm^{-1} (4) and 3.49 nm^{-1} (7). The various reflections attributed to the SPP are located at q = 1.17 nm^{-1} (I) and 2.34 nm^{-1} (II).

The synthetic ceramide fraction was prepared with a 1:7:2 molar ratio of CER1, CER3 and ΣCERIV, as this appeared to be optimal for the formation of the LPP in the presence of free fatty acids. At a CHOL:synthCER:FFA molar ratio of 1:2:1 and 1:1.5:1, the majority of the lipids forms the LPP with a repeat distance of 12.0 nm (Fig. 4A). Reducing the synthetic ceramide content to a CHOL:synthCER:FFA ratio of 1:0.75:1 does not considerably affect the formation of the LPP or SPP. A further decrease in the synthetic ceramide content to 1:0.5:1 is accompanied by a slight reduction in the fraction of lipids forming the LPP (Fig. 4B). These findings indicate that the formation of the lamellar phases is not extremely sensitive towards changes in the relative synthetic ceramide content.

Concerning phase-separated cholesterol, we observe that an increased relative amount of cholesterol results in increased intensities of the reflections attributed to phase-separated cholesterol, whereas almost no phase-separated choleseterol is present at a CHOL:synthCER:FFA ratio of 1:2:1. This is in agreement with the findings of McIntosh et al. [11, 18], who do not observe phase separation of cholesterol at a CHOL:CER:FFA ratio of 1:2:1.

4. DISCUSSION

Previous studies revealed that mixtures prepared with cholesterol, free fatty acids and ceramides isolated from pig or human stratum corneum closely mimic the stratum corneum lipid phase behaviour [8-10]. These observations offered an attractive opportunity to study the role of these lipids in the stratum corneum lipid organisation. Furthermore, due to its lipophilic nature, CER1 could be separated from the remaining ceramides and isolated in sufficient large quantities. This offered the possibility to examine in detail the role CER1 plays in stratum corneum lipid organisation. As each subclass of natural ceramides consists of ceramides with varying acyl chain lengths [4], the study on the effect of the variation in acyl chain length on the stratum corneum lipid phase behaviour is difficult to perform with natural ceramides. Therefore, the use of synthetic ceramides with a well-defined acyl chain length and head group architecture may overcome this problem. In a previous study, a first step has been made to investigate this by selecting a synthetic ceramide mixture consisting of CER1 and either synthetic CER3 with a uniform acyl chain length of 24 carbon atoms or semi-synthetic ΣCERIV containing fatty acids with varying acyl chain lengths. We demonstrated that equimolar CHOL:synthCER mixtures prepared with CER1 and ΣCERIV do not form the

LPP, whereas in mixtures prepared with synthetic CER1 and CER3 a small lipid fraction forms a 11.6 nm lamellar phase [13].

In a very recent study, we studied the phase behaviour of CHOL:synthCER and CHOL:synthCER:FFA mixtures prepared with a 1:7:2 molar ratio of CER1, CER3 and ΣCERIV [12]. The results of that study reveal that the LPP is formed in the lipid mixtures, provided that an optimal equilibration temperature is used during the preparation procedure. The phase behaviour of equimolar CHOL:synthCER:FFA mixtures equilibrated at 80°C resembled to a high extent the lamellar and lateral lipid organisation found in native human or pig stratum corneum. However, the presence of one or two additional crystalline phases was noticed, which are not present in stratum corneum and can be ascribed to crystalline CER3. Furthermore, the relative intensities of the various LPP reflections slightly differed from those observed with mixtures prepared with isolated ceramides.

In the present study, the CER3 to ΣCERIV ratio was varied to enhance the formation of the LPP and to reduce the formation of additional crystalline phases. The results clearly demonstrate that in the absence of free fatty acids, a CER1:CER3:ΣCERIV molar ratio of 1:5:4 is optimal for the formation of the LPP. In the presence of free fatty acids, the optimal synthetic ceramide composition shifts to a CER1:CER3:ΣCERIV molar ratio of 1:7:2. Furthermore, the peak width at half maximum of a number of reflections is much smaller in the diffraction patterns of the mixtures prepared with free fatty acids compared to those of the CHOL:synthCER mixtures. This indicates that free fatty acids increase the ordering of the lipid organisation. This has also been observed in our previous study [12]. Although the optimal synthetic ceramide compositions could be selected for the formation of the LPP, it is obvious from our data that the lipid organisation is not extremely sensitive towards variations in relative amounts of CER3 and ΣCERIV in the lipid mixture. This is similar to the observations made with equimolar CHOL:natCER mixtures, which were remarkably insensitive towards changes in the natural ceramide composition [19]. Only a strong reduction in the level of natCER1 decreased the formation of the LPP.

In equimolar CHOL:synthCER:FFA mixtures, the intensities of the reflections attributed to crystalline cholesterol are much weaker than in the CHOL:synthCER mixtures. This indicates that free fatty acids increase the solubility of cholesterol into the lamellar phases, which is consistent with observations made with mixtures based on natural ceramides [8-10, 18]. Furthermore, the diffraction patterns of the synthetic ceramides mixtures do not show reflections ascribed to free fatty acids in a separate

phase (Fig. 3 and 4). This suggests that free fatty acids are completely intercalated in the lamellar phases and their presence is required for the formation of an orthorhombic sublattice within the lipid lamellae [8, 10, 12].

The synthetic lipid mixtures also contain an additional 3.7 nm phase, which is not present in native stratum corneum and can be ascribed to crystalline CER3. A rise in ΣCERIV content at the expense of CER3 increases the acyl chain length variation in the synthCER mixture (Table 1) and reduces the formation of phase-separated crystalline CER3. For a complete elimination of the 3.7 nm phase, the relative CER3 level should be below 3 (CER1:CER3:ΣCERIV molar ratio of 1:3:6). However, this increased ΣCERIV level is accompanied by a reduction in LPP formation, as is clearly demonstrated by the results of the present study. Partial replacement of CER3 by CER4 with known acyl chain lengths (e.g. C18 and C24 at a ratio of 1:2, mimicking the distribution in the ΣCERIV batch used in the present study) might offer a possibility to reduce the amount of phase-separated CER3.

The present study further demonstrates that a reduction in LPP formation is only observed when the total synthetic ceramide content is reduced to a CHOL: synthCER:FFA molar ratio of 1:0.5:1. This low sensitivity towards changes in the CHOL:synthCER:FFA molar ratio is in agreement with previous studies performed with mixtures prepared with natural ceramides [8, 10]. When extrapolating these findings to the in vivo situation, one can state that small variations in the molar ratios of the stratum corneum lipids will not lead to a substantial change in lipid organisation. Most phase behaviour studies performed with either isolated or synthetic lipids have been carried out with equimolar lipid mixtures. A recent study on tape-stripped stratum corneum shows that cholesterol, ceramides and free fatty acids are present at a molar ratio of approximately 1:1.5:1 [20], rather than the generally assumed equimolar ratio. However, inspection of literature data shows that there is a high inter-individual variability in stratum corneum lipid composition. This high variability together with the finding that the LPP has been detected in all stratum corneum samples studied so far can be ascribed to the fact that the LPP is formed in CHOL:CER:FFA mixtures even when the composition varies over a wide molar range.

In conclusion, the results of the present study and previous studies demonstrate that one can generate lipid mixtures with limited number of synthetic ceramides that mimic closely the lipid phase behaviour of native stratum corneum. The presence of free fatty acids, the temperature used for equilibrating the mixtures and the CER3 to ΣCERIV ratio are important parameters for proper lipid organisation.

Acknowledgements

This work was supported by a grant from the Technology Foundation STW (LGN4654). The Netherlands Organisation for Scientific Research (NWO) is acknowledged for the provision of the beamtime. We would like to thank A.M. Weerheim for providing the FAME data shown in Table 1 and the companies Cosmoferm and Beiersdorf for the provision of the synthetic ceramides.

REFERENCES

1. Wertz P.W., Miethke M.C., Long S.A., Strauss J.S., Downing D.T. The composition of the ceramides from human stratum corneum and from comedones. *J. Invest. Dermatol.* **84** (1985) 410-412.

2. Robson K.J., Stewart M.E., Michelsen S., Lazo N.D., Downing D.T. 6-Hydroxy-4-sphingenine in human epidermal ceramides. *J. Lipid Res.* **35** (1994) 2060-2068.

3. Stewart M.E., Downing D.T. A new 6-hydroxy-4-sphingenine-containing ceramide in human skin. J. Lipid Res. **4** (1999) 1434-1439.

4. Ponec M., Weerheim A., Lankhorst P., Wertz P. New acylceramide in native and reconstructed epidermis. *J. Invest. Dermatol.* **120** (2003) 581-588.

5. Bouwstra J.A., Gooris G.S., van der Spek J.A., Bras W. The structure of human stratum corneum as determined by small angle X-ray scattering. *J. Invest. Dermatol.* **96** (1991) 1006-1014.

6. Bouwstra J.A., Gooris G.S., van der Spek J.A., Bras W. Structural investigations of human stratum corneum by small angle X-ray scattering. *J. Invest. Dermatol.* **97** (1991) 1005-1012.

7. Bouwstra J.A., Gooris G.S., Bras W., Downing D.T. Lipid organization in pig stratum corneum. *J. Lipid Res.* **36** (1995) 685-695.

8. Bouwstra J.A., Gooris G.S., Cheng K., Weerheim A., Bras W., Ponec M. Phase behavior of isolated skin lipids. *J. Lipid Res*. **37** (1996) 999-1011.

9. Bouwstra J.A., Gooris G.S., Dubbelaar F.E.R., Weerheim A.M., Ponec M. pH, cholesterol sulfate, and fatty acids affect the stratum corneum lipid organization. *J. Invest. Dermatol.* **3** (1998) 69-73.

10. Bouwstra J.A., Gooris G.S., Dubbelaar F.E.R., Ponec M. Phase behavior of stratum corneum lipid mixtures based on human ceramides: the role of natural and synthetic ceramide 1. *J. Invest. Dermatol.* **118** (2002) 606-617.

11. McIntosh T.J., Stewart M.E., Downing D.T. X-ray diffraction analysis of isolated skin lipids: reconstruction of intercellular lipid domains. *Biochemistry* **35** (1996) 3649-3653.

12. de Jager M.W., Gooris G.S., Dolbnya I.P., Bras W., Ponec M., Bouwstra J.A. Novel lipid mixtures based on synthetic ceramides reproduce the unique stratum corneum lipid organization. *J. Lipid Res.* **45** (2004) 923-932.

13. de Jager M.W., Gooris G.S., Dolbnya I.P., Bras W., Ponec M., Bouwstra J.A. The phase behaviour of skin lipid mixtures based on synthetic ceramides. *Chem. Phys. Lipids* **124** (2003) 123-134.

14. Dahlen B., Pascher I. Molecular arrangements in sphingolipids. Thermotropic phase behaviour of tetracosanoylphytosphingosine. *Chem. Phys. Lipids* **24** (1979) 119-133.

15. Raudenkolb S., Hubner W., Rettig W., Wartewig S., Neubert R.H. Polymorphism of ceramide 3. Part 1: an investigation focused on the head group of N-octadecanoylphytos phingosine. *Chem. Phys. Lipids* **123** (2003) 9-17.

16. Wertz P.W., Downing D.T. Epidermal lipids, in: L.A. Goldsmith (Eds.), Physiology, Biochemistry and Molecular Biology of the Skin, 2nd edition, Oxford University Press, Oxford, 1991, pp 205-235.

17. Bras W. A SAXS/WAXS beamline at the ESRF and future experiments. *J. Macromol. Sci. Phys. B* **37** (1998) 557-566.

18. McIntosh T.J. Organization of skin stratum corneum extracellular lamellae: diffraction evidence for asymmetric distribution of cholesterol, *Biophys. J.* **85** (2003) 1675-1681.

19. Bouwstra J.A., Dubbelaar F.E.R., Gooris G.S., Weerheim A.M., Ponec M. The role of ceramide composition in the lipid organisation of the skin barrier. *Biochim. Biophys. Acta* **1419** (1999) 127-136.

20. Weerheim A., Ponec M. Determination of stratum corneum lipid profile by tape stripping in combination with high-performance thin-layer chromatography. *Arch. Dermatol. Res.* **293** (2001) 191-199.

Chapter 5

Acylceramide head group architecture affects lipid organisation in synthetic ceramide mixtures

M.W. de Jager,* G.S. Gooris,* M. Ponec,§ and J.A. Bouwstra*

*Leiden/Amsterdam Center for Drug Research, Department of Drug Delivery Technology, University of Leiden, P.O. Box 9502, 2300 RA Leiden, The Netherlands.
§Department of Dermatology, Leiden University Medical Center, Leiden, The Netherlands.

(adapted from *J. Invest. Dermatol.* **123** (2004) 911-916)

ABSTRACT

The lipid organisation in the upper layer of the skin, the stratum corneum, is important for the skin barrier function. This lipid organisation, including the characteristic 13 nm lamellar phase, can be reproduced in vitro with mixtures based on cholesterol, free fatty acids and natural as well as synthetic ceramides. In human stratum corneum, nine ceramide classes have been identified (CER1-CER9). Detailed studies on the effect of molecular structure of individual ceramides on the stratum corneum lipid organisation are only possible with synthetic lipid mixtures, as their composition can be accurately chosen and systematically modified. In the present study, small-angle X-ray diffraction was used to examine the organisation in synthetic lipid mixtures of which the synthetic ceramide fraction was prepared with sphingosine based CER1 or phytosphingosine based CER9. The latter acylceramide contains an additional hydroxyl group at the sphingoid backbone. The results show that a gradual increase in CER1 level consistently promotes the formation of the 13 nm lamellar phase and that partial replacement of CER1 by CER9 does not affect the phase behaviour. Interestingly, complete substitution of CER1 with CER9 reduces the formation of the long periodicity phase and results in phase separation of CER9.

1. INTRODUCTION

Ceramides (CER), cholesterol (CHOL) and long-chain free fatty acids (FFA) are the most abundant lipid species present in the stratum corneum and are responsible for proper function of the skin barrier. Human stratum corneum contains at least 9 extractable ceramide types [1-4], classified as CER1 to CER9. The ceramides can be subdivided into three main groups, based on the nature of their backbone (sphingosine (S), phytosphingosine (P) and 6-hydroxysphingosine (H)). Through an amide bonding, long-chain nonhydroxy (N) or α-hydroxy (A) fatty acids with varying acyl chain lengths are chemically linked to the sphingosine bases. The acylceramides CER1 (EOS), CER4 (EOH) and the recently identified CER9 (EOP) are unique in structure as they contain linoleic acid linked to an ω-hydroxy fatty acid (EO) with a chain length of 30 to 32 carbon atoms.

X-ray diffraction studies demonstrated the presence of two coexisting lamellar phases in human stratum corneum: the short periodicity phase (SPP) with a repeat distance of approximately 6 nm and the long periodicity phase (LPP) with a repeat distance of approximately 13 nm [5-7]. The molecular organisation of the LPP together with the predominantly orthorhombic lipid packing in the presence of substantial amounts of cholesterol are exceptional and are therefore considered to play an important role in the skin barrier function [8].

X-ray diffraction studies on lipid mixtures prepared with cholesterol, free fatty acids and ceramides isolated from human or pig stratum corneum revealed that the lipid organisation in these mixtures closely mimics that observed in native stratum corneum. Those studies have markedly contributed to our present knowledge on the stratum corneum lipid organisation and the role the main lipid classes play in the stratum corneum lipid organisation [9-11]. However, the role of the head group architecture or acyl chain length on the lipid phase behaviour cannot be studied using natural ceramides, as it is impossible to isolate the individual ceramide subclasses in large quantities. For this reason, we decided to investigate the lipid organisation in mixtures prepared with synthetic ceramides (synthCER), which offers the possibility to substitute one single ceramide subclass for another one. However, a first prerequisite for the possibility to use synthetic ceramides is that their phase behaviour reflects that observed in stratum corneum. In previous studies we have demonstrated that the stratum corneum lipid organisation can be reproduced to a high extent with equimolar mixtures of cholesterol, free fatty acids and a limited number of synthetic ceramides,

namely CER1, CER3 and bovine brain ceramide type IV (referred to as ΣCERIV) mixed in a 1:7:2 molar ratio [12, 13]. In synthetic CER1 and CER3 non-hydroxy fatty acids of a uniform acyl chain length are linked to the (phyto)sphingoid backbone, whereas the sphingosine based ΣCERIV contains α-hydoxy fatty acids with varying acyl chain lengths, with C18 (22%) and C24 (42%) as the most abundantly present [13]. For achievement of a similar lipid organisation as observed in the stratum corneum, the presence of free fatty acids and an optimal ratio of CER3 and ΣCERIV are crucial [13].

The present study focuses on the role the head group architecture of the acylceramides plays on the phase behaviour of synthetic lipid mixtures. In human stratum corneum, approximately 8.3% of the total ceramide fraction comprises CER1 (sphingosine base), whereas CER9 (phytosphingosine base) accounts for 6.4% [4]. For this reason, we studied synthetic ceramide mixtures containing only one acylceramide (CER1 or CER9) as well as mixtures in which both acylceramides are present, by partially substituting CER1 with CER9. The use of CER9 with an ω-hydroxy fatty acid chain length of either 30 or 27 carbon atoms also allowed us to study the role of the acyl chain length on the lipid organisation. The major finding of the present study is that partial replacement of CER1 by CER9 does not affect the lipid organisation, whereas complete substitution of CER1 with CER9 inhibits the formation of the LPP and results in phase separation of CER9.

2. MATERIALS AND METHODS

2.1 Materials

Palmitic acid, stearic acid, arachidic acid, behenic acid, tricosanoic acid, lignoceric acid, cerotic acid, cholesterol and bovine brain ceramide type IV were purchased from Sigma-Aldrich Chemie GmbH (Schnelldorf, Germany). N-(30-Linoleoyloxy-triacontanoyl)-sphingosine (synthetic ceramide 1(C30)-linoleate), N-(30-Linoleoyloxy-triacontanoyl)-phytosphingosine (synthetic ceramide 9(C30)-linoleate), N-(27-Linoleyl-heptacosanoyl)-phytosphingosine (synthetic ceramide 9(C27)-linoleate) and N-Tetracosanoyl-phytosphingosine (synthetic ceramide 3(C24)) were generously provided by Cosmoferm B.V. (Delft, the Netherlands). All organic solvents used were of analytical grade and manufactured by Labscan Ltd (Dublin, Ireland).

2.2 Preparation of the lipid mixtures

For the preparation of the CHOL:synthCER:FFA mixtures, the following fatty acid mixture was used: C16:0, C18:0, C20:0, C22:0, C23:0, C24:0 and C26:0 at molar ratios of 1.3, 3.3, 6.7, 41.7, 5.4, 36.8 and 4.7, respectively. This is similar to the free fatty acids ratio found in stratum corneum [14]. Appropriate amounts of individual lipids dissolved in chloroform:methanol (2:1) were combined to yield mixtures of approximately 1.5 mg dry weight at the desired composition at a total lipid concentration of 7 mg/ml. A Camag Linomat IV was used to spray the lipid mixtures onto mica. This was done at a rate of 4.3 µl/min under a continuous nitrogen stream. The samples were equilibrated for 10 minutes at 80°C (CHOL:synthCER:FFA) or 95°C (CHOL:synthCER) and subsequently hydrated with an acetate buffer of pH 5.0. Finally, the samples were homogenised by 10 successive freeze-thawing cycles between –20°C and room temperature, during which the samples were stored under gaseous argon.

2.3 Small-angle X-ray diffraction (SAXD)

All measurements were performed at the European Synchrotron Radiation Facility (ESRF, Grenoble), using station BM26B [15]. The X-ray wavelength and the sample-to-detector distance were 1.24Å and 1.7m, respectively. Diffraction data were collected on a two-dimensional multiwire gas-filled area detector. The spatial calibration of this detector was performed using silver behenate. The samples were mounted in a sample holder with mica windows. Diffraction patterns of the lipid mixtures were obtained at room temperature for a period of 5 minutes. All measurements were performed at least in duplicate during two different sessions.

SAXD provides information about the larger structural units in the sample, such as the repeat distance of a lamellar phase. The scattering intensity I (in arbitrary units) was measured as a function of the scattering vector q (in reciprocal nm). The latter is defined as $q=(4\pi\sin\theta)/\lambda$, in which θ is the scattering angle and λ is the wavelength. From the positions of a series of equidistant peaks (q_n), the periodicity, or d-spacing, of a lamellar phase was calculated using the equation $q_n=2n\pi/d$, n being the order number of the diffraction peak.

3. RESULTS

3.1 LPP is formed in equimolar CHOL:synthCER:FFA mixtures prepared with CER1 or CER9

The diffraction pattern of a CHOL:[CER1:CER3:ΣCERIV]:FFA mixture prepared at a molar ratio of 1:[0.1:0.7:0.2] is shown in Figure 1A. The LPP with a repeat distance of 12.2 nm is indicated by the presence of six reflections (q = 0.52, 1.03, 1.54, 2.06, 3.08 and 3.59 nm^{-1}). The reflections at q = 1.16 and 2.33 nm^{-1} correspond to the first and second order diffraction peaks of a lamellar phase with a periodicity of 5.4 nm (SPP). The two strong reflections at 1.71 and 3.43 nm^{-1} reveal the presence of a phase with a periodicity of 3.7 nm, ascribed to crystalline CER3 in a V-shaped structure [16-18]. The presence of crystalline cholesterol in separate domains can be deduced from the peaks at 1.87 and 3.74 nm^{-1}.

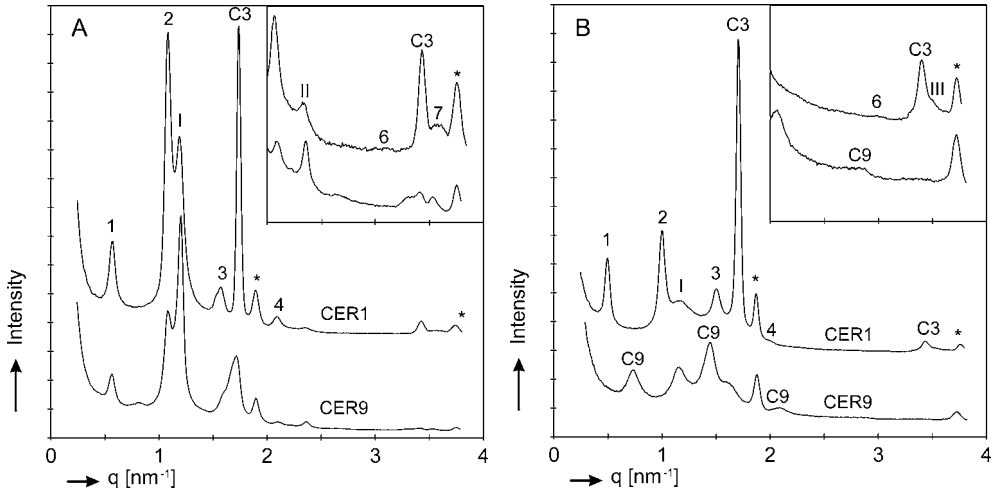

Figure 1 - FFA promote LPP formation in mixtures containing 10% CER1 or 10% CER9. The inset shows a magnification of the reflections in the q-range between 2 and 4 nm^{-1}. The Arabic and Roman numbers indicate the diffraction orders of the LPP and SPP, respectively. C3 refers to the reflections of crystalline CER3 located at 1.71 and 3.42 nm^{-1}, whereas C9 refers to the reflections of crystalline CER9 located at 0.70, 1.41, 2.10 and 2.79 nm^{-1}. The asterisk (*) indicates the reflections of crystalline cholesterol located at 1.87 and 3.74 nm^{-1}. (A) Diffraction patterns of CHOL:synthCER:FFA mixtures prepared with CER1 or CER9. The various orders of the LPP are located at q = 0.52 nm^{-1} (1), 1.03 nm^{-1} (2), 1.56 nm^{-1} (3), 2.08 nm^{-1} (4), 3.09 nm^{-1} (6) and 3.56 nm^{-1} (7). The various orders of the SPP are located at q = 1.17 nm^{-1} (I) and 2.34 nm^{-1} (II). (B) Diffraction patterns of CHOL:synthCER mixtures prepared with CER1 or CER9. The various orders of the LPP are located at q = 0.52 nm^{-1} (1), 1.03 nm^{-1} (2), 1.56 nm^{-1} (3), 2.08 nm^{-1} (4) and 3.09 nm^{-1} (6). The various orders of the SPP are located at q = 1.17 nm^{-1} (I) and 3.51 nm^{-1} (III).

Complete substitution of CER1 with CER9(C30) results in the diffraction pattern depicted in Figure 1A. Obviously, the LPP with a repeat distance of 12.1 nm is also formed in the presence of CER9(C30), although the intensities of its reflections in comparison to the SPP reflections are weaker than observed for the CER1 containing mixture. A weak reflection at 0.70 nm^{-1} suggests that a small fraction of CER9(C30) phase separates (see next section for a more detailed description of this phase). In addition, crystalline cholesterol and CER3 in a V-shaped formation are present in the lipid mixture.

Replacement of CER9(C30) with CER9(C27) in the mixture results in a marked reduction of LPP formation (data not shown). In addition, the repeat distance of this phase shifts to 11.7 nm. The formation of the other above-mentioned phases is not affected by the reduced ω-hydroxy fatty acid chain length of CER9(C27).

3.2 LPP is not formed in mixtures prepared with CER9 in the absence of free fatty acids

Figure 1B shows the diffraction pattern of the equimolar CHOL:synthCER mixture, prepared at a 1:7:2 ratio of CER1, CER3 and ΣCERIV. Five equidistant peaks suggest the presence of the LPP (12.2 nm), whereas the SPP (5.3 nm) is indicated by two reflections. In addition, phase-separated CER3 and cholesterol can be detected. Compared to the diffraction curve of the equimolar CHOL:synthCER:FFA mixture prepared with CER1, the intensities of the reflections attributed to the LPP and SPP decreased as compared to those of crystalline CER3 and cholesterol.

Complete substitution of CER1 with CER9(C30) results in the diffraction pattern depicted in Figure 1B. Three major changes are observed in the presence of CER9(C30): (i) No reflections can be detected that might be ascribed to the LPP, indicating that no LPP is formed. (ii) Four reflections at 0.70, 1.41, 2.10 and 2.79 nm^{-1} indicate the presence of a phase with a repeat distance of 9.0 nm. This periodicity well corresponds to the length of two opposing CER9(C30) molecules in a hairpin formation and is similar to the repeat distance found for hydrated pig CER1 [9]. Taking into account the diffraction patterns depicted in Figure 2B (see below), it is conceivable to assign this phase to crystalline CER9(C30) in separate domains. (iii) The 3.7 nm phase, attributed to crystalline CER3, is not present. Instead, a shoulder at 1.57 nm^{-1} might designate the presence of a new phase with a periodicity of 4.0 nm. However, no higher order reflections can be detected. The exact composition and nature of this phase is not known.

The diffraction pattern of the mixture containing CER9(C27) is almost identical to the one obtained with CER9(C30) (data not shown). No LPP is present in the mixture and several reflections indicate the presence of a phase with a repeat distance of 8.7 nm, ascribed to phase-separated CER9. The slightly shorter periodicity of this phase can be explained by the shorter ω-hydroxy fatty acid chain length of CER9(C27).

3.3 LPP formation in equimolar CHOL:synthCER:FFA mixtures depends on acylceramide content

To assess the effect of the relative acylceramide content on the lipid organisation in equimolar mixtures of cholesterol, synthetic ceramides and free fatty acids, the amount of CER1 or CER9 in the synthetic ceramide fraction was gradually increased from 0 to 20% mol/mol, thereby maintaining the ratio between CER3 and ΣCERIV constant. As CER9(C27) is less effective in promoting the formation of the LPP, these experiments were only performed with CER1 and CER9(C30). Below, the changes in lipid organisation as a function of acylceramide type and relative amount are presented.

In the absence of CER1 and CER9, the characteristic LPP is not present (data not shown). Instead, three strong reflections indicate the presence of a 5.4 nm lamellar phase (SPP). In addition, crystalline CER3 and cholesterol are present in the mixture, both indicated by two reflections.

In the equimolar CHOL:synthCER:FFA mixture in which the synthetic ceramide fraction contains 5% CER1, only a small fraction of lipids forms the LPP, as deduced from the presence of four weak reflections in the diffraction pattern (see Fig. 2A). The diffraction curve of the mixture prepared with 10% CER1 is illustrated in Figure 1A (see previous section for a more detailed description of the phases present). Evidently, the fraction of lipids that forms the LPP increased. A rise in CER1 content to 15 or 20% results in diffraction patterns in which the intensities of the LPP reflections further increase as compared to the peak intensities of the SPP, CER3 and cholesterol. Even in the presence of 20% CER1 (see Fig. 2A), no peaks can be detected that might be ascribed to crystalline CER1 in separate domains.

The diffraction pattern of the equimolar CHOL:synthCER:FFA mixture of which the synthetic ceramide fraction contains 5% CER9 (see Fig. 2B) is similar to the one obtained with 5% CER1. The majority of lipids forms the SPP, although weak reflections indicate that a minute fraction of lipids forms a phase with a periodicity of 12.0 nm. In addition, crystalline CER3 and cholesterol are present in the mixture. The diffraction curve of the mixture prepared with 10% CER9 (see Fig. 1A) has already been explained

in the previous section. At this relative amount, the LPP is clearly present and a small fraction of CER9 phase separates. When the amount of CER9 in the synthetic ceramide fraction is further raised to 15 or 20% (see Fig. 2B), some striking changes in the lipid organisation are observed: (i) The reflections attributed to the LPP markedly reduce in intensity as compared to the peak intensities of the other phases. Moreover, only the first three order diffraction peaks of the LPP can be detected. This indicates that at increased CER9 content, the formation of the LPP is inhibited. (ii) An increased amount of CER9 phase separates into separate domains, indicated by strong reflections at q = 0.70, 1.40, 2.10 and 2.80 nm^{-1}, which reveal the presence of a 9.0 nm phase. (iii) The reflections ascribed to phase-separated CER3, which is present at a CER9 level of 5 and 10%, completely disappear when the amount of CER9 in the mixture is increased.

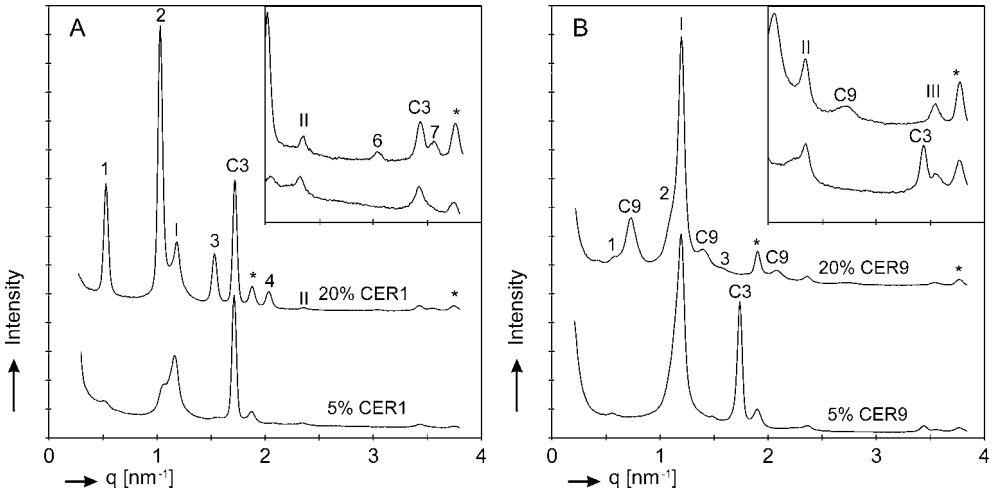

Figure 2 - LPP formation in equimolar CHOL:synthCER:FFA mixtures depends on acylceramide content. The inset shows a magnification of the reflections in the q-range between 2 and 4 nm^{-1}. The Arabic and Roman numbers indicate the diffraction orders of the LPP and SPP, respectively. C3 refers to the reflections of crystalline CER3 located at 1.71 and 3.42 nm^{-1}, whereas C9 refers to the reflections of crystalline CER9 located at 0.70, 1.40, 2.10 and 2.80 nm^{-1}. The asterisk (*) indicates the reflections of crystalline cholesterol located at 1.87 and 3.74 nm^{-1}. (A) Diffraction patterns of CHOL:synthCER:FFA mixtures prepared with 5 and 20% CER1. The various orders of the LPP are located at q = 0.52 nm^{-1} (1), 1.03 nm^{-1} (2), 1.56 nm^{-1} (3) , 2.08 nm^{-1} (4), 3.09 nm^{-1} (6) and 3.56 nm^{-1} (7). The various orders of the SPP are located at q = 1.17 nm^{-1} (I) and 2.34 nm^{-1} (II). (B) Diffraction patterns of CHOL:synthCER:FFA mixtures prepared with 5 and 20% CER9. The various orders of the LPP are located at q = 0.52 nm^{-1} (1), 1.03 nm^{-1} (2) and 1.56 nm^{-1} (3). The various orders of the SPP are located at q = 1.17 nm^{-1} (I), 2.34 nm^{-1} (II) and 3.51 nm^{-1} (III).

3.4 No change in LPP formation upon partial substitution of CER1 with CER9 in equimolar CHOL:synthCER:FFA mixtures.

As native stratum corneum contains both CER1 (8.3%) and CER9 (6.4%), we also prepared lipid mixtures in which both acylceramides were present in ratios similar to that found in human stratum corneum. The mixtures were prepared with a synthetic ceramide fraction that contained 5% CER1 and 10% CER9 and vice versa, thereby maintaining the ratio between CER3 and ΣCERIV constant. In both mixtures, six diffraction peaks clearly indicate the presence of the LPP, whereas the SPP is identified by two diffraction peaks (see Fig. 3). In addition, crystalline CER3 and cholesterol are present. The relative intensities of the reflections attributed to the various phases in both diffraction patterns are similar. Moreover, the diffraction patterns resemble closely the one obtained with the mixture prepared with 15% CER1.

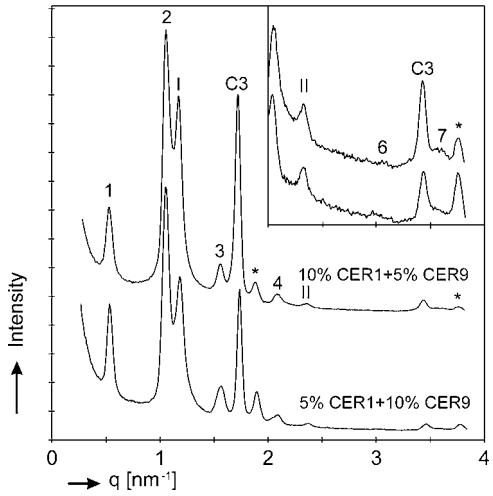

Figure 3 - No substantial change in lipid organisation in CHOL:synthCER:FFA mixtures in which CER1 is partially substituted with CER9. The inset shows a magnification of the reflections in the q-range between 2 and 4 nm^{-1}. The Arabic and Roman numbers indicate the diffraction orders of the LPP and SPP, respectively. C3 refers to the reflections of crystalline CER3 located at 1.71 and 3.42 nm^{-1}. The asterisk (*) indicates the reflections of crystalline cholesterol located at 1.87 and 3.74 nm^{-1}. The various orders of the LPP are located at q = 0.52 nm^{-1} (1), 1.03 nm^{-1} (2), 1.56 nm^{-1} (3) , 2.08 nm^{-1} (4), 3.09 nm^{-1} (6) and 3.56 nm^{-1} (7). The various orders of the SPP are located at q = 1.17 nm^{-1} (I) and 2.34 nm^{-1} (II).

4. DISCUSSION

In human stratum corneum, approximately 8.3% of the total ceramide fraction comprises CER1, whereas CER4 and CER9 account for 5.0 and 6.4%, respectively [4]. From studies performed with mixtures based on natural ceramides, we know that CER1 plays a prominent role in the formation of the LPP, characteristic for the stratum corneum lipid phase behaviour. After exclusion of CER1 from mixtures prepared with ceramides isolated from human stratum corneum, still a small fraction of lipids forms the LPP [11]. This indicates that CER4 or CER9 or both contribute to a certain extent to

the formation of the LPP. However, until now the role CER4 and CER9 play in the lipid organisation could not be studied, as it is impossible to isolate these acylceramides in sufficient quantities from human stratum corneum. As we now have available synthetic CER9, this is the first study in which the role of CER9 and CER9 in combination with CER1 on the lipid organisation could be systematically studied. Several important features were noticed:

(i) CER1 promotes the formation of the LPP to a higher extent than CER9.

(ii) The maximum solubility of CER9 in the lipid lamellar phases is lower than that of CER1.

(iii) CER1 promotes incorporation of CER9 into the lamellar phases.

What can we learn from these observations?

The presence of an additional hydroxyl group and simultaneous loss of a double bond at the sphingoid base of acylceramides impedes the formation of the LPP. This is specially observed in equimolar CHOL:synthCER mixtures in which CER9 is not able to induce the formation of the LPP. Instead, strong reflections in the diffraction pattern reveal the presence of crystalline CER9 in separate domains. A possible explanation for this finding is that the larger and more hydrophilic head group of CER9 inhibits the formation of the LPP. The situation changes when free fatty acids were added to the CHOL:synthCER mixtures: phase separation of CER9 is reduced and the LPP is formed. Unlike the synthetic ceramides, the free fatty acids fraction shows a high variation in acyl chain lengths. This may suggest that incorporation of CER9 into the lamellar phases in synthetic lipid mixtures requires the presence of acyl chains with varying lengths. However, additional studies with mixtures prepared with free fatty acids of a uniform chain length should be performed to elucidate this. Furthermore, it needs to be emphasised that, due to limited variability in head group architecture and acyl chain length in the synthetic ceramide fraction, the simplified synthetic lipid mixtures used might be more sensitive to phase separation than natural ceramides in native stratum corneum.

Interestingly, the chain length of the ω-hydroxy acid in CER9 seems to have a major influence on the lamellar ordering of the lipids, as CER9(C27) is less effective in promoting the formation of the LPP than CER9(C30). Possibly, the shorter ω-hydroxy acid in CER9(C27) less efficiently spans the two broad lipid layers within the suggested tri-layer unit of the LPP [19]. This may result in a reduced stability of the LPP and a shift of the repeat distance to lower values (11.7 nm).

Another difference observed between CER1 and CER9 is the dependence of the formation of the LPP on the acylceramide level. Whereas a rise in CER1 content from 0 to 20% leads to a consistent enhancement of the LPP formation, a more complex phase behaviour is observed in mixtures prepared with CER9. There, a rise in CER9 content up to 10% promotes the formation of the LPP. A further rise in the CER9 content reduces the formation of the LPP and results in the formation of crystalline CER9 in separate domains. Phase separation of CER9 is already observed in mixtures in which the synthetic ceramide fraction is prepared with 10% CER9. This means that even in the presence of free fatty acids, the amount of CER9 that can be incorporated into the LPP is limited.

The findings that only a minute fraction of lipids organises into the LPP when the synthetic ceramide fraction contains 5% CER9 and that no LPP is present in the absence of CER1 and CER9 confirm and extend previous results obtained with mixtures prepared with natural ceramides [11]. Based on the results of the present study, we may speculate that CER9 is indeed able to promote the formation the LPP in natural ceramide mixtures, which are excluded from CER1. However, from our results we cannot deduce whether the relative amount of CER9 present in the stratum corneum is insufficient to effectively promote the formation of the LPP or that its larger and more hydrophilic head group hampers the formation of the LPP. Although the differences in phase behaviour between CER1 and CER9 in synthetic ceramide mixtures are much more pronounced at increased acylceramide levels, CER1 always more effectively promotes the formation of the LPP than CER9, even at a relative amount of 5%. The question whether CER4, which contains a 6-hydroxysphingosine head group that is even larger than the phytosphingosine head group of CER9, is also able to promote the formation of the LPP remains unanswered.

In spite of the finding that CER9 is less efficient in enhancing the formation of the LPP than CER1, partial substitution of CER1 with CER9 does not significantly affect the lipid organisation. When extrapolating these findings to the in vivo situation, it is expected that small variations in the relative content of individual acylceramides will not substantially change the stratum corneum lipid organisation. However, in vivo the situation is usually more complex. In lamellar ichthyosis and atopic dermatitis, a marked reduction in CER1 in the lesion parts of the stratum corneum is observed [20-23]. In addition, in various skin disorders simultaneous changes in composition and content of various lipid classes are observed [24]. All these changes may explain the reduced LPP formation in these skin disorders.

In conclusion, lipid mixtures prepared with synthetic ceramides offer an attractive tool to unravel the importance of molecular structure of individual ceramides on the stratum corneum lipid organisation. The primary finding of the present study is that the head group architecture of acylceramides considerably affects the lipid organisation. Compared to CER1, containing a sphingosine base, CER9 with its phytosphingosine base is less efficient in promoting the formation of the characteristic LPP and the level CER9 in the LPP is limited.

Acknowledgements

This work was supported by a grant from the Technology Foundation STW (LGN4654). The Netherlands Organisation for Scientific Research (NWO) is acknowledged for the provision of the beamtime. We would like to thank Igor Dolbnya and Wim Bras for technical assistance at the ESRF. The company Cosmoferm is acknowledged for the provision of the synthetic ceramides.

REFERENCES

1. Wertz P.W., Miethke M.C., Long S.A., Strauss J.S., Downing D.T. The composition of the ceramides from human stratum corneum and from comedones. *J. Invest. Dermatol.* **84** (1985) 410-412.

2. Robson K.J., Stewart M.E., Michelsen S., Lazo N.D., Downing D.T. 6-Hydroxy-4-sphingenine in human epidermal ceramides. *J. Lipid Res.* **35** (1994) 2060-2068.

3. Stewart M.E., Downing D.T. A new 6-hydroxy-4-sphingenine-containing ceramide in human skin. *J. Lipid Res.* **4** (1999) 1434-1439.

4. Ponec M., Weerheim A., Lankhorst P., Wertz P. New acylceramide in native and reconstructed epidermis. *J. Invest. Dermatol.* **120** (2003) 581-588.

5. Bouwstra J.A., Gooris G.S., van der Spek J.A., Bras W. The structure of human stratum corneum as determined by small angle X-ray scattering. *J. Invest. Dermatol.* **96** (1991) 1006-1014.

6. Bouwstra J.A., Gooris G.S., van der Spek J.A., Bras W. Structural investigations of human stratum corneum by small angle X-ray scattering. *J. Invest. Dermatol.* **97** (1991) 1005-1012.

7. Bouwstra J.A., Gooris G.S., Bras W., Downing D.T. Lipid organization in pig stratum corneum. *J. Lipid Res.* **36** (1995) 685-695.

8. Bouwstra J.A., Gooris G.S., Dubbelaar F.E.R., Ponec M. Phase behavior of stratum corneum lipid mixtures based on human ceramides: the role of natural and synthetic ceramide 1. *J. Invest. Dermatol.* **118** (2002) 606-617.

9. McIntosh T.J., Stewart M.E., Downing D.T. X-ray diffraction analysis of isolated skin lipids: reconstruction of intercellular lipid domains. *Biochemistry* **35** (1996) 3649-3653.

10. Bouwstra J.A., Gooris G.S., Cheng K., Weerheim A., Bras W., Ponec M. Phase behavior of isolated skin lipids. *J. Lipid Res*. **37** (1996) 999-1011.

11. Bouwstra J.A., Gooris G.S., Dubbelaar F.E.R., Ponec M. Phase behaviour of lipid mixtures based on human ceramides. *J. Lipid Res.* **42** (2001) 1759-1770.

12. de Jager M.W., Gooris G.S., Dolbnya I.P., Bras W., Ponec M., Bouwstra J.A. Novel lipid mixtures based on synthetic ceramides reproduce the unique stratum corneum lipid organization. *J. Lipid Res.* **45** (2004) 923-932.

13. de Jager M.W., Gooris G.S., Dolbnya I.P., Ponec M., Bouwstra J.A. Modelling the stratum corneum lipid organisation with synthetic lipid mixtures: The importance of ceramide composition. *Biochim. Biophysic. Acta* **1684** (2004) 132-140.

14. Wertz P.W., Downing D.T. Epidermal lipids, in: L.A. Goldsmith (Eds.), Physiology, Biochemistry and Molecular Biology of the Skin, 2nd edition, Oxford University Press, Oxford, 1991, pp 205-235.

15. Bras W. A SAXS/WAXS beamline at the ESRF and future experiments. *J. Macromol. Sci. Phys. B* **37** (1998) 557-566.

16. de Jager M.W., Gooris G.S., Dolbnya I.P., Bras W., Ponec M., Bouwstra J.A. The phase behaviour of skin lipid mixtures based on synthetic ceramides. *Chem. Phys. Lipids* **124** (2003) 123-134.

17. Dahlen B., Pascher I. Molecular arrangements in sphingolipids. Thermotropic phase behaviour of tetracosanoylphyto-sphingosine. *Chem. Phys. Lipids* **24** (1979) 119-133.

18. Raudenkolb S., Hubner W., Rettig W., Wartewig S., Neubert R.H. Polymorphism of ceramide 3. Part 1: an investigation focused on the head group of N-octadecanoylphytosphingosine. *Chem. Phys. Lipids* **123** (2003) 9-17.

19. Bouwstra J.A., Gooris G.S., Cheng K., Weerheim A.M., IJzerman A.P., Ponec M. Role of ceramide 1 in the molecular organization of the stratum corneum. *J. Lipid Res.* **39** (1998) 186-196.

20. Yamamoto A., Serizaka S., Ito M., Sato Y. Stratum corneum lipid abnormalities in atopic dermatitis. *Arch. Dermatol. Res.* **283** (1991) 219-223.

21. Lavrijsen A.P.M., Bouwstra J.A., Gooris G.S., Boddé H.E., Ponec M. Reduced skin barrier function parallels abnormal stratum corneum lipid organisation in patients with lamellar ichthyosis. *J. Invest. Dermatol.* **105** (1995) 619-624.

22. Di Nardo A., Wertz P., Giannetti A., Seidenari S. Ceramide and cholesterol composition in the skin in patients with atopic dermatitis. *Acta Derm. Venereol. (Stockh.)* **78** (1998) 27-30.

23. Bleck O., Abeck D., Ring J., Hoppe U., Vietzke J.P., Wolber R., Brandt O., Schreiner V. Two ceramide subfractions detectable in CER(AS) position by HPTLC in skin surface lipids of non-lesional skin of atopic eczema. *J. Invest. Dermatol.* **113** (1999) 894-900.

24. Motta S.M., Monti M., Sesana S., Caputo R., Carelli S., Ghidoni R. Ceramide composition of psoriatic scale. *Biochim. Biophysic. Acta* **1182** (1993) 147-151.

Chapter 6

Lipid mixtures prepared with well-defined synthetic ceramides closely mimic the unique stratum corneum lipid phase behaviour

M.W. de Jager,* G.S. Gooris,* M. Ponec,§ and J.A. Bouwstra*

*Leiden/Amsterdam Center for Drug Research, Department of Drug Delivery Technology, University of Leiden, P.O. Box 9502, 2300 RA Leiden, The Netherlands.
§Department of Dermatology, Leiden University Medical Center, Leiden, The Netherlands.

(adapted from *J. Lipid. Res.* **46** (2005) 2649-2656)

ABSTRACT

Lipid lamellae present in the outermost layer of the skin, the stratum corneum, form the main barrier for diffusion of molecules through the skin. The presence of a unique 13 nm lamellar phase and the high crystallinity are characteristic for the stratum corneum lipid phase behaviour. In the present study, small-angle and wide-angle X-ray diffraction were used to examine the organisation in lipid mixtures prepared with a unique set of well-defined synthetic ceramides, varying from each other in head group architecture and acyl chain length. The results show that equimolar mixtures of cholesterol, free fatty acids and synthetic ceramides (resembling the composition of pig ceramides) closely resemble the lamellar and lateral stratum corneum lipid organisation, both at room and elevated temperatures. Exclusion of several ceramide classes from the mixture does not affect the lipid organisation. However, complete substitution of ceramide 1 (acylceramide with a sphingosine base) with ceramide 9 (acylceramide with a phytosphingosine base) reduces the formation of the long periodicity lamellar phase. This indicates that the head group architecture of acylceramides affects the lipid organisation. In conclusion, lipid mixtures prepared with well-defined synthetic ceramides offer an attractive tool to unravel the importance of molecular structure of individual ceramides for proper lipid organisation.

1. INTRODUCTION

The barrier function of the skin is predominantly attributed to its outermost layer, the stratum corneum, which efficiently protects the body from desiccation and percutaneous penetration of compounds. The stratum corneum consists of several layers of overlapping corneocytes, embedded in a matrix of lipids. It has generally been accepted that the intercorneocyte lipids, with a very specific composition and organisation, play an important role in the skin barrier function. Unlike biological membranes, phospholipids are nearly absent in the stratum corneum and the major constituents are ceramides (CER), cholesterol (CHOL) and long-chain free fatty acids (FFA). Ceramides are structurally heterogeneous and together with cholesterol and free fatty acids they exhibit quite different phase behaviour than phospholipids and other more widely studied biological membrane lipids.

Ceramides are composed of a long-chain sphingosine (S), phytosphingosine (P) or 6-hydroxysphingosine (H) base with variations in position and number of hydroxyl groups and double bonds [1-4]. Through an amide bonding, long-chain nonhydroxy (N) or α-hydroxy fatty acids (A) with varying acyl chain lengths (predominantly 24 and 26 carbon atoms) are linked to the sphingoid bases. In pig stratum corneum, the exceptions are CER1 (EOS) and CER5 (AS). The former contains an ω-hydroxy fatty acid with a chain length of 30 to 32 carbon atoms to which linoleic acid is linked (EO), whereas CER5 (AS) contains a fatty acid with a chain length of only 16 to 18 carbon atoms. In human stratum corneum, three ceramides (CER1 (EOS), CER4 (EOH) and CER9 (EOP)) have an exceptional long molecular structure, whereas CER5 (AS) has a fatty acid chain length of approximately 24 carbon atoms.

Several studies have been performed to provide insight into the complex lipid architecture underlying the skin barrier function. Electron microscopy studies demonstrated that the intercellular lipids in the stratum corneum have a lamellar organisation with a repeating pattern of approximately 13 nm, consisting of a broad-narrow-broad sequence of electron lucent bands [5, 6]. X-ray diffraction studies demonstrated the presence of two coexisting lamellar phases in human stratum corneum: the short periodicity phase (SPP) with a repeat distance of around 6 nm and the long periodicity phase (LPP) with a repeat distance of approximately 13 nm [7-9]. The molecular organisation of the LPP together with the predominantly orthorhombic lipid packing in the presence of substantial amounts of cholesterol are exceptional and are therefore considered to play an important role for the maintenance of a competent

skin barrier.

Mixtures prepared with cholesterol, free fatty acids and ceramides isolated from human or pig stratum corneum closely mimic the lipid organisation found in the SC [10-12]. It has been demonstrated that in particular cholesterol and ceramides are important for the formation of the LPP, whereas free fatty acids are required for the crystalline (orthorhombic) character of the lateral lipid packing. As natural ceramides contain various subclasses of ceramides with varying acyl chain lengths, it is practically impossible to selectively remove individual ceramides in quantities. Detailed studies on the effect of molecular structure of individual ceramides on the stratum corneum lipid organisation are therefore only possible with mixtures based on synthetic ceramides, as their composition can be accurately chosen and systematically modified. The prerequisite to replace natural ceramides (natCER) by synthetic ones (synthCER) is that their phase behaviour reflects that of the stratum corneum. In previous studies we have demonstrated that equimolar mixtures of cholesterol, free fatty acids and a limited number of synthetic ceramides, namely CER1, CER3 and bovine brain ceramide type IV (referred to as ΣCERIV) mixed in a 1:7:2 ratio, closely resemble the lamellar and lateral stratum corneum lipid organisation, both at room and elevated temperatures [13, 14]. CER1 (EOS) and CER3 (NP) contain fatty acids of a uniform acyl chain length, whereas ΣCERIV (AS) contains fatty acids with varying acyl chain lengths, with C18 and C24 as the most abundantly present [14]. Mixtures prepared with CER1, CER3 and ΣCERIV are denoted as synthCER I mixtures. It has been demonstrated that proper lipid organisation in synthCER I mixtures can only be achieved with an optimal CER3: ΣCERIV ratio in the presence of CER1 [14, 15].

In spite of many similarities, also some differences are observed between mixtures prepared with natCER or synthCER I. The main difference is the presence of one or two additional phases with repeat distances of 3.7 and 4.3 nm, respectively. These phases have never been observed in mixtures containing natCER and can be ascribed to crystalline CER3, present in separate domains. Another difference is the repeat distance of the LPP, which is slightly shorter in synthCER mixtures (~12 nm) than in natCER mixtures (~13 nm). In addition, the relative intensities of the reflections attributed to the LPP in mixtures prepared with synthCER slightly differ from those observed in mixtures prepared with natCER [13]. This indicates that the localisation of the lipids within the LPP in mixtures prepared with synthCER might differ slightly.

Currently, we have at our disposal a unique set of synthesised ceramides, which closely mimic the ceramides composition of pig stratum corneum (see Fig. 1). In

addition, we have synthetic CER9 (EOP), which is present in human stratum corneum, but not in pig stratum corneum. CER9 is structurally similar to CER1, but contains an additional hydroxyl group at the sphingoid backbone. Each of the synthetic ceramides has a well-defined head group architecture and acyl chain length. Mixtures prepared with the well-defined synthetic ceramides are referred to as synthCER II. As the synthetic counterpart of CER5 (AS) (acyl chain length 16 carbon atoms) is not available, all synthCER II mixtures were prepared with CER3 (NP) with an acyl chain of 16 carbon atoms (CER3(C16)).

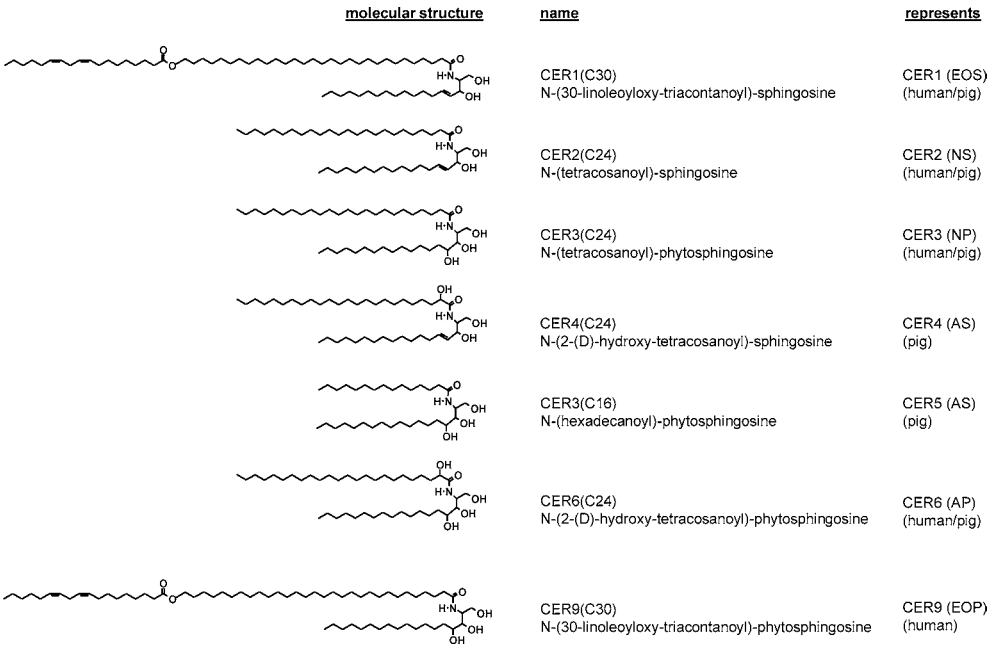

Figure 1 - The molecular structures of the synthetic ceramides used in the present study.

The aim of the present study is three-fold and can be summarised in the following questions:

(i) Is it possible to mimic the stratum corneum lipid phase behaviour with mixtures prepared with well-defined synthetic ceramides at room and elevated temperatures? We will particularly focus on the role of free fatty acids, the presence of additional phases and the intensity distribution of the diffraction peaks of the LPP.

(ii) Is the formation of the LPP also enhanced when CER1 is gradually substituted with CER9?

(iii) Is it possible to reduce the number of synthetic ceramides classes in the mixture, without affecting the formation of the lamellar phases?

In order to answer the aforementioned questions, the phase behaviour of various equimolar CHOL:synthCER II:FFA mixtures was studied. Firstly, a mixture was studied that closely mimics the composition of the ceramides in pig stratum corneum [10, 16]. Subsequently, the synthCER II composition was gradually changed (see Table 1) to elucidate the role various synthetic ceramides play in the formation of the LPP.

Table 1 - The composition of the synthetic ceramides fractions used in this study (in molar ratios).

mixture	CER1	CER2	CER3(C24)	CER4	CER3(C16)	CER6	CER9
synthCER II_1	0.15	0.51	0.16	0.04	0.09	0.05	-
synthCER II_2	0.10	0.51	0.16	0.04	0.09	0.05	0.05
synthCER II_3	0.05	0.51	0.16	0.04	0.09	0.05	0.10
synthCER II_4	-	0.51	0.16	0.04	0.09	0.05	0.15
synthCER II_5	-	0.60	0.19	0.04	0.11	0.06	-
synthCER II_6	0.15	0.53	0.17	-	0.10	0.05	-
synthCER II_7	0.15	0.54	0.17	0.04	0.10	-	-
synthCER II_8	0.15	0.57	0.18	-	0.10	-	-
synthCER II_9	0.15	0.25	0.29	0.06	0.16	0.09	-

2. MATERIALS AND METHODS

2.1 Materials

Palmitic acid, stearic acid, arachidic acid, behenic acid, tricosanoic acid, lignoceric acid, cerotic acid and cholesterol were purchased from Sigma-Aldrich Chemie GmbH (Schnelldorf, Germany). CER1(C30)-linoleate, CER2(C24), CER3(C24), CER3(C16), CER4(C24), CER6(C24) and CER9(C30)-linoleate were generously provided by Cosmoferm B.V. (Delft, the Netherlands). All organic solvents used were of analytical grade and manufactured by Labscan Ltd (Dublin, Ireland).

2.2 Preparation of the lipid mixtures

For the preparation of the CHOL:synthCER:FFA mixtures, the following free fatty acid mixture was used: C16:0, C18:0, C20:0, C22:0, C23:0, C24:0 and C26:0 at molar ratios of 1.3, 3.3, 6.7, 41.7, 5.4, 36.8 and 4.7, respectively. This is similar to the composition of the free fatty acids in native stratum corneum [17]. Appropriate

amounts of individual lipids dissolved in chloroform:methanol (2:1) were combined to yield mixtures of approximately 1.5 mg dry weight at the desired composition at a total lipid concentration of 7 mg/ml. A Camag Linomat IV was used to spray the lipid mixtures onto mica. This was done at a rate of 4.3 µl/min under a continuous nitrogen stream. Subsequently, the samples were equilibrated for 10 minutes at the optimal temperature, being 70°C for equimolar CHOL:synthCER:FFA mixtures and 85°C for equimolar CHOL:synthCER mixtures and hydrated with an acetate buffer of pH 5.0. Finally, the samples were homogenised by 10 successive freeze-thawing cycles between –20°C and room temperature, during which the samples were stored under gaseous argon.

2.3 Small-angle X-ray diffraction

All measurements were performed at the European Synchrotron Radiation Facility (ESRF, Grenoble), using station BM26B [18]. The X-ray wavelength and the sample-to-detector distance were 1.24Å and 1.7m, respectively. Diffraction data were collected on a two-dimensional multiwire gas-filled area detector. The spatial calibration of this detector was performed using silver behenate. The samples were mounted in a sample holder with mica windows. Static diffraction patterns of the lipid mixtures were obtained at room temperature for a period of 5 minutes. The temperature-induced phase changes were investigated by collecting diffraction patterns, during which the temperature of the sample was increased from 25 to 95°C at a rate of 2°C/min. Each successive diffraction curve was collected for a period of one minute.

Small-angle X-ray diffraction provides information about the larger structural units in the sample, such as the repeat distance of a lamellar phase. The scattering intensity I (in arbitrary units) was measured as a function of the scattering vector q (in reciprocal nm). The latter is defined as $q=(4\pi\sin\theta)/\lambda$, in which θ is the scattering angle and λ is the wavelength. From the positions of a series of equidistant peaks (q_n), the periodicity, or d-spacing, of a lamellar phase was calculated using the equation $q_n=2n\pi/d$, n being the order number of the diffraction peak.

2.4 Wide-angle X-ray diffraction

Wide-angle X-ray diffraction provides information about the lateral packing of the lipids within the lamellae. Wide-angle X-ray diffraction data were collected on a microstrip gas chamber detector with an opening angle of 60° [19]. The sample-to-detector distance was 36 cm and the X-ray wavelength was 1.24Å. The spatial

calibration of the detector was performed with a mixture of silicium and cholesterol.

The small-angle and wide-angle X-ray diffraction data were collected simultaneously.

3. RESULTS

3.1 Importance of free fatty acids for proper lamellar organisation

The role of free fatty acids for the formation of the lamellar phases was investigated using a synthetic ceramide mixture that closely mimics the composition of the ceramides in pig stratum corneum (synthCER II_1; see Table 1 for detailed composition). The corresponding diffraction patterns are illustrated in Figure 2. The diffraction pattern of the equimolar CHOL:synthCER II_1:FFA mixture reveals the presence of five reflections (q = 0.52, 1.03, 1.56, 2.08 and 3.09 nm^{-1}) that can be ascribed to a 12.2 nm phase (LPP). The reflections at q = 1.18 and 2.36 nm^{-1} correspond to the first and second order diffraction peaks of a lamellar phase with a periodicity of 5.3 nm (SPP). The two reflections at 1.87 and 3.74 nm^{-1} reveal the presence of crystalline cholesterol in separate domains.

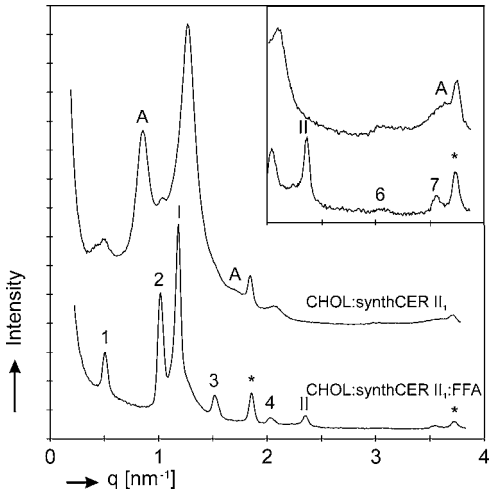

Figure 2 - Free fatty acids promote the formation of the LPP in CHOL:synthCER II_1 mixtures. The inset shows a magnification of the reflections in the q-range between 2 and 4 nm^{-1}. The Arabic and Roman numbers indicate the diffraction orders of the LPP and SPP, respectively. The asterisk (*) indicates the reflections of crystalline cholesterol located at 1.87 and 3.74 nm^{-1}. The letter A refers to the reflections of the additional phase with a repeat distance of 7.1 nm present in the absence of free fatty acids (q = 0.89, 1.77 and 3.57 nm^{-1}). The various orders of the LPP are located at q = 0.52 nm^{-1} (1), 1.03 nm^{-1} (2), 1.56 nm^{-1} (3), 2.08 nm^{-1} (4) and 3.09 nm^{-1} (6). The various orders of the SPP are located at q = 1.18 nm^{-1} (I) and 2.36 (II).

In the absence of free fatty acids, three major changes are observed in the diffraction pattern: (i) The reflections attributed to the LPP markedly reduce in intensity. In addition, an increased peak width is observed, indicating a reduced ordering of the lipids within the LPP. (ii) Three reflections at 0.89, 1.77 and 3.57 nm^{-1} reveal the presence of a phase with a repeat distance of 7.1 nm. The exact composition and

nature of this phase is not known. (iii) The broad reflection at 1.30 nm^{-1} might be ascribed to the SPP with a reduced periodicity of 4.8 nm. However, no higher order reflections can be detected, which makes the interpretation uncertain.

3.2 Substitution of CER1 with CER9 in equimolar CHOL:synthCER II:FFA mixtures

To investigate whether an additional hydroxyl group at the sphingoid head group of CER1 influences the formation of the LPP, mixtures were prepared in which CER1 was gradually substituted with CER9, thereby maintaining the molar ratio between the remaining synthetic ceramides constant. The lipid organisation in mixtures prepared with 10% CER1 and 5% CER9 (synthCER II_2) and vice versa (synthCER II_3) closely resembles that obtained with the mixture prepared with 15% CER1 only (synthCER II_1). Five diffraction peaks indicate the presence of the LPP, whereas the SPP is identified by three equidistant peaks.

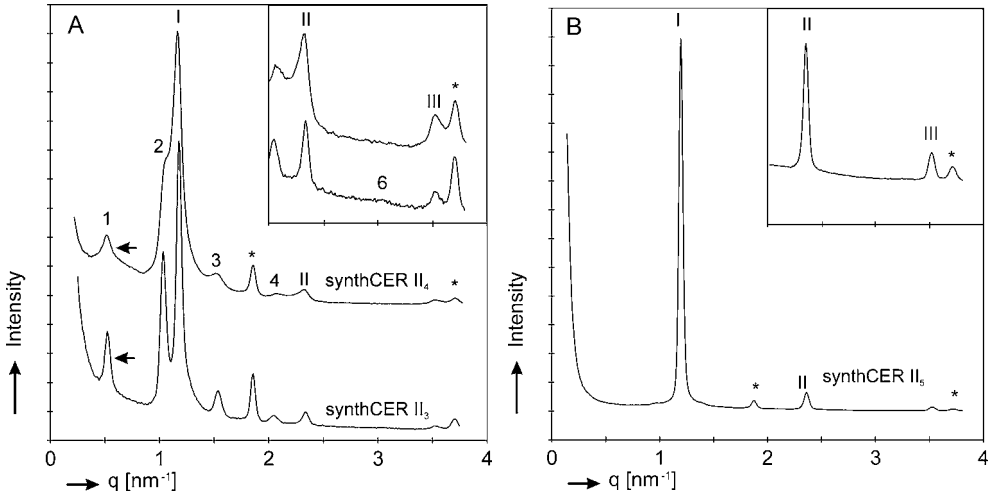

Figure 3 - Influence of acylceramide type on the lamellar lipid organisation. (A) Partial substitution of CER1 with CER9 does not affect the lipid organisation in equimolar CHOL:synthCER:FFA mixtures, whereas complete substitution inhibits the formation of the LPP. The arrow indicates the increased peak width at half maximum. (B) LPP is only present in acylceramide containing mixtures. The inset shows a magnification of the reflections in the q-range between 2 and 4 nm^{-1}. The Arabic and Roman numbers indicate the diffraction orders of the LPP and SPP, respectively. The asterisk (*) indicates the reflections of crystalline cholesterol located at 1.87 and 3.74 nm^{-1}. The various orders of the LPP are located at q = 0.52 nm^{-1} (1), 1.03 nm^{-1} (2), 1.56 nm^{-1} (3) , 2.08 nm^{-1} (4) and 3.09 nm^{-1} (6). The various orders of the SPP are located at q = 1.16 nm^{-1} (I), 2.36 (II) and 3.51 nm^{-1} (III).

In addition, two reflections indicate the presence of crystalline CHOL. The diffraction pattern of the mixture prepared with 5% CER1) and 10% CER9 (synthCER II_3) is illustrated in Figure 3A.

Complete substitution of CER1 with CER9 (synthCER II_4) results in decreased relative intensities of the reflections attributed to the LPP as compared to those of the SPP (see Fig. 3A). In addition, a slightly increased peak width at half maximum of the LPP reflections is observed, which indicates a reduced ordering of the lipids. No reflections can be detected that might be ascribed to crystalline CER9 in separate domains [15]. As observed in previous studies [15, 20], the characteristic LPP is not present in mixtures prepared in the absence of any acylceramide (synthCER II_5). Instead, three strong reflections indicate the presence of a 5.4 nm lamellar phase (SPP). In addition, crystalline cholesterol is present in the mixture (Fig. 3B).

3.3 Effect of reducing the number of individual synthetic ceramides in equimolar CHOL:synthCER II:FFA mixtures

Mixtures prepared in the absence of CER4, CER6 or both (synthCER $II_{6\text{-}8}$) were studied to elucidate the sensitivity of the lipid phase behaviour towards a reduction in the number of synthetic ceramide classes. The choice to exclude CER4 and CER6 from the mixture is based on the low relative amounts of these synthetic ceramides in the synthCER II mixture. In addition, one mixture was examined in which the amount of CER2 in the synthetic ceramide fraction was decreased to 50% of its original amount (synthCER II_9).

Exclusion of CER4, CER6 or both from the synthetic ceramide mixtures does not affect the phase behaviour of the lipid mixtures (see Fig. 4; only the curve of the lipid mixture prepared with synthCER II_8 is presented). Five equidistant peaks suggest the presence of the LPP (12.2 nm), whereas the SPP (5.4 nm) is indicated by three reflections. In addition, phase-separated cholesterol can be detected. The intensities of the reflections attributed to the LPP and SPP show high similarity to those observed in the equimolar CHOL:synthCER II_1:FFA mixture.

The diffraction pattern of the equimolar CHOL:synthCER II_9:FFA mixture is also shown in Figure 4. A reduction in CER2 content to 25% does not affect the formation of the LPP and SPP. However, it results in the appearance of a weak reflection at q = 1.45 nm^{-1}. Although no higher order reflections can be detected, this reflection can most likely be attributed to a phase with a repeat distance of 4.3 nm, ascribed to crystalline CER3(C24) in separate domains [13, 20].

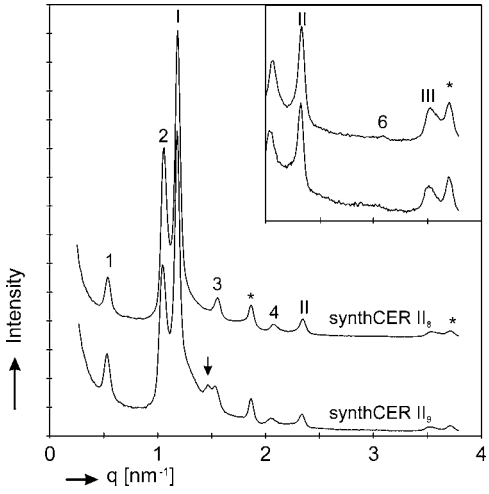

Figure 4 - No substantial change in LPP formation in equimolar CHOL:synthCER II:FFA mixtures in which CER4 and CER6 are absent or the amount of CER2 is decreased. The inset shows a magnification of the reflections in the q-range between 2 and 4 nm^{-1}. The Arabic and Roman numbers indicate the diffraction orders of the LPP and SPP, respectively. The asterisk (*) indicates the reflections of crystalline cholesterol located at 1.87 and 3.74 nm^{-1}, whereas the arrow indicates the reflection attributed to phase-separated CER3(C24) (q = 1.45 nm^{-1}). The various orders of the LPP are located at q = 0.52 nm^{-1} (1) , 1.03 nm^{-1} (2), 1.56 nm^{-1} (3) , 2.08 nm^{-1} (4) and 3.09 nm^{-1} (6). The various orders of the SPP are located at q = 1.17 nm^{-1} (I), 2.34 nm^{-1} (II) and 3.51 nm^{-1} (III).

3.4 Phase behaviour as a function of temperature

The lipid phase behaviour of the equimolar CHOL:synthCER II$_1$:FFA mixture has been examined in the temperature range from 25 to 95°C (see Fig. 5A). Each curve represents the mean of the lipid phases, which are present during a temperature shift of 2°C. The diffraction pattern at 25°C reveals a number of reflections that can be ascribed to the presence of a LPP and SPP with periodicities of 12.2 and 5.4 nm, respectively (similarly as described in Fig. 2). Between 25 and 55°C, no significant changes are observed in positions or intensities of the LPP and SPP reflections. However, a further rise in temperature gradually decreases the peak intensities of the SPP, which eventually disappear at around 61°C. The reflections of the LPP disappear at around 65°C, whereas the two reflections attributed to crystalline cholesterol disappear at approximately 53°C.

At around 45°C a new phase is formed, of which only one reflection can be detected that gradually shifts to q = 1.37 nm^{-1} (repeat distance 4.6 nm) at 63°C. As its intensity drastically increases, it is the most prominent reflection in the diffraction pattern at elevated temperatures. Between 91°C and 93°C, however, the reflection disappears.

3.5 Lateral packing of the lipids

A hexagonal lateral packing is characterised by a strong 0.41 nm reflection in the wide-angle X-ray diffraction pattern, whereas the diffraction pattern of an orthorhombic packing is characterised by two strong 0.41 and 0.37 nm reflections, located at q = 15.40 and 17.12 nm^{-1}, respectively. The diffraction pattern of the equimolar CHOL:

synthCER II_1:FFA mixture monitored as a function of temperature is plotted in Figure 5B. The 0.408 and 0.367 nm peaks indicate an orthorhombic lateral packing. Between 33 and 35°C, the 0.367 nm reflection disappears, indicative for an orthorhombic to a hexagonal phase transition. The 0.408 nm reflection initially decreases in intensity. However, a further rise in temperature slightly increases the intensity of the 0.408 nm reflection, indicating a metastable to stable phase change. Similar results were obtained with isolated stratum corneum [Bouwstra J.A. and Gooris G.S., unpublished results]. A disappearance of this peak is observed at 65°C, which is at the same temperature at which the LPP disappears in the small-angle X-ray diffraction pattern. In addition, two reflections of crystalline cholesterol can be detected (q = 10.98 and 16.58 nm^{-1}), which both disappear at around 53°C.

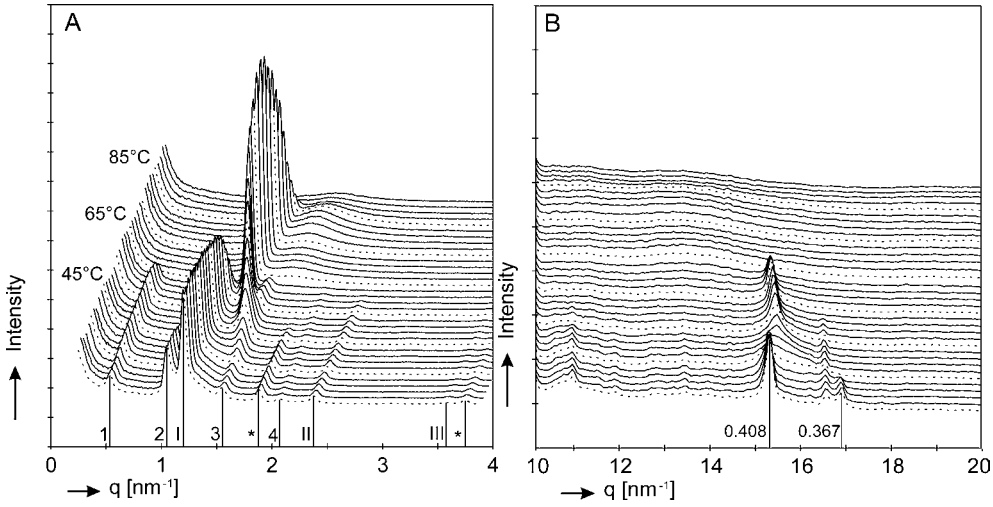

Figure 5 - Changes in the lipid phase behaviour as a function of temperature. (A) The lamellar organisation of equimolar CHOL:synthCER II_1:FFA. (B) The lateral packing of CHOL:synthCER II_1:FFA mixtures. The Arabic numbers indicate the diffraction orders of the LPP, whereas the Roman numbers indicate the diffraction orders of the SPP. The asterisk (*) indicates the reflections of crystalline cholesterol. The dashed lines represent the diffraction curves at 25, 35, 45, 55, 65, 75 and 85°C.

3.6 Relative intensities of the LPP reflections

The relative intensities of the various LPP reflections in six equimolar CHOL: synthCER II_1:FFA mixtures were determined in order to obtain information on the relative electron density distribution in the characteristic 12 nm lamellar phase. The results provided in Table 2 show that the relative intensities of the peaks attributed to the LPP show the same trend in equimolar CHOL:CER:FFA mixtures prepared with

either synthCER I, synthCER II_1 or pig ceramides (pigCER). The values obtained with synthCER II_1 mixtures resemble more closely those of pig ceramide mixtures than the synthCER I mixture (CER1:CER3:ΣCERIV in a 1:7:2 molar ratio).

Table 2 - Relative intensities of the diffraction peaks of the LPP in equimolar CHOL:synthCER II_1:FFA mixtures, equimolar CHOL:synthCER I:FFA mixtures [13] and equimolar CHOL:pigCER mixtures [13].

order	LPP CHOL:synthCER II_1:FFA	LPP CHOL:synthCER I:FFA	LPP CHOL:pigCER:FFA
1	1.0	1.0	1.0
2	2.53 ± 0.15	2.94 ± 0.36	2.55 ± 0.28
3	0.50 ± 0.03	0.37 ± 0.06	0.81 ± 0.10
4	0.13 ± 0.02	0.15 ± 0.02	0.09 ± 0.01
6	0.02 ± 0.01	-	0.03 ± 001
7	-	0.04 ± 0.03	0.08 ± 0.03

For scaling, the intensity of the first order diffraction peak of all phases was set equal to 1. The values are presented as the average (n=6) ± the standard deviation. Due to (partial) overlap with more prominent peaks in the diffraction pattern, the 6^{th} and 7^{th} order of the LPP could not always be determined in the synthCER I and synthCER II mixture, respectively.

4. DISCUSSION

4.1 Lipid organisation in mixtures prepared with well-defined synthetic ceramides

The results of the present study convincingly show that the lipid organisation in mixtures prepared with cholesterol, synthCER II and free fatty acids closely resembles that of natCER mixtures, as both the LPP and SPP are present and a small fraction of cholesterol phase separates into crystalline domains [10-12, 21]. Also at elevated temperatures many similarities can be observed in lipid phase behaviour between equimolar CHOL:CER:FFA mixtures containing synthCER II_1 or natCER [10, 11]: (i) Between 33 and 35°C a phase transition from an orthorhombic to a hexagonal lateral packing occurs. (ii) The LPP and SPP disappear at around 65 and 61°C, respectively. (iii) At elevated temperatures, an additional phase is formed with a repeat distance of 4.6 nm (synthCERII_1) or 4.3 nm (natCER). (iv) The hexagonal lateral packing disappears at 65°C, which is the same temperature at which the LPP disappears. This suggests that either an orthorhombic or a hexagonal lateral packing is a prerequisite for LPP formation, which confirms the findings with natCER: when the fraction of lipids in a liquid phase is too high, the formation of the SPP is increased at the expense of the LPP [21].

4.2 Influence of gradual substitution of CER1 with CER9 on LPP formation

CER1 promotes the formation of the LPP more efficiently than CER9, indicating that the additional hydroxyl group of CER9 and simultaneous loss of the 4,5 double bond (see Fig. 1) inhibits the formation of the LPP. When the diffraction patterns of the lipid mixtures containing either synthCER II or synthCER I [15] are compared, two important differences are noticed, namely (i) CER9 promotes the formation of the LPP more efficiently in the synthCER II mixtures than in the synthCER I mixtures. (ii) In the synthCER II mixtures the maximum solubility of CER9 in the lamellar phases is increased as compared to the synthCER I mixtures, as in the latter mixture CER9 partially phase separates. Both observations illustrate that the lipid organisation in synthCER II mixtures, in which the overall head group variability is increased, is less sensitive to variations in the acylceramide head group architecture. Interestingly, in both synthCER mixtures partial substitution of CER1 with CER9 does not significantly affect the lipid organisation.

4.3 Effect of diminishing the number of synthetic ceramides on phase behaviour

Exclusion of CER4 and CER6 from the synthCER II mixture (synthCER II_8) changes the relative amounts of CER1, CER2, CER3(C24) and CER3(C16) to a 15:57:18:10 molar ratio. The composition of the synthCER I fraction prepared with 15% CER1 is CER1, CER3(C24) and ΣCERIV in a 15:66:19 molar ratio. The ratio between the two most abundantly present acyl chain lengths in ΣCERIV is C24:C18 2:1. Therefore, the molar ratios of the various synthetic ceramides in synthCER II_8 and synthCER I are very similar, with CER2 or CER3(C24) as the most abundantly present. Whereas extensive phase separation of CER3(C24) is observed in mixtures prepared with synthCER I, no additional phases attributed to CER2 can be detected in mixtures prepared with synthCER II. The difference between CER2 and CER3 is the presence of an additional hydroxyl group in CER3 and the simultaneous loss of the 4,5 double bond (see Fig. 1). The additional hydroxyl group enables strong intermolecular head group hydrogen bonding, which is most likely the driving force for molecular organisation of CER3 in separate domains [22]. Striking is that in the synthCER II_9 mixture, prepared with a relative CER2 content of 25%, a small reflection indicates the presence of a additional 4.3 nm phase. This phase can be ascribed to crystalline CER3(C24) in a V-shaped structure [20, 23, 24] and its formation is caused by the increased relative amount of CER3(C24) in synthCER II_9. In a previous study, in which the optimal CER3 to ΣCERIV

ratio for the formation of the LPP was established, phase separation of CER3 was also observed when the relative amount of CER3 increased [14].

4.4 Phase behaviour of natCER mixtures versus synthCER II mixtures

In spite of many similarities, also two differences in phase behaviour are observed between natCER mixtures and synthCER II mixtures. The first difference is the slightly reduced repeat distance of the LPP in mixtures prepared with synthCER II_1 as compared to mixtures prepared with natCER. The periodicity of the LPP in equimolar CHOL:natCER mixtures prepared with isolated human or pig ceramides is very similar, being 12.8 and 12.2 nm, respectively [10, 11]. Addition of free fatty acids to those mixtures slightly increases the LPP periodicity from 12.8 and 12.2 nm to 13.0 and 13.3 nm, respectively. However, the repeat distance of the LPP in synthCER II or synthCER I mixtures is always approximately 12 nm, irrespective from the presence of free fatty acids. Although we may speculate this is related to differences in crystallinity or acyl chain length of the ceramides, further studies are required to unravel this phenomenon.

Secondly, the results of the present study reveal that free fatty acids are required for proper lipid organisation in synthCER II mixtures, as in the equimolar CHOL:synthCER II_1 mixture a marked reduction in the formation of the LPP is observed and an additional phase with a repeat distance of 7.1 nm is formed. This strongly suggests that free fatty acids with varying acyl chain lengths facilitate incorporation of the synthetic ceramides into the lamellar phases. The major difference between natCER and synthCER II is great variation in acyl chain length in natCER versus well-defined chain length in synthCER II. The importance of chain length variation for proper LPP formation was already demonstrated in synthCER I mixtures by systematically increasing the relative amount of free fatty acids or by increasing the amount of ΣCERIV (chain length variation) at the expense of CER3 (uniform chain length). An increased relative amount of free fatty acids or ΣCERIV initially enhances the formation of the LPP. However, when the amount exceeds a certain optimal amount, the formation of the LPP is reduced and the SPP dominates. This suggests that for proper lipid organisation a certain optimal chain length variation should be present in the mixture, present in either the free fatty acids or the synthetic ceramides. However, additional studies should be performed to further elucidate this.

In conclusion, the results of the present study demonstrate that one can generate lipid mixtures with well-defined synthetic ceramides that closely mimic the lamellar and lateral organisation in native stratum corneum. As their composition can be accurately

chosen and modified, synthetic ceramide mixtures provide insight in the importance of molecular structure of individual ceramides in relation to the lipid organisation. Skin disorders are frequently characterised by a defective permeability barrier and an aberrant lipid profile as compared to healthy skin. Synthetic ceramide mixtures are therefore an attractive tool to study in detail the effects of altered lipid composition on the lamellar and lateral lipid organisation.

Acknowledgements

This work was supported by a grant from the Technology Foundation STW (LGN4654). The Netherlands Organisation for Scientific Research (NWO) is acknowledged for the provision of the beamtime. The authors wish to express their gratitude to I.P. Dolbnya and W. Bras for their valuable contribution at the ESRF and the company Cosmoferm B.V. for the provision of the synthetic ceramides.

REFERENCES

1. Wertz P.W., Miethke M.C., Long S.A., Strauss J.S., Downing D.T. The composition of the ceramides from human stratum corneum and from comedones. *J. Invest. Dermatol.* **84** (1985) 410-412.

2. Robson K.J., Stewart M.E., Michelsen S., Lazo N.D., Downing D.T. 6-Hydroxy-4-sphingenine in human epidermal ceramides. *J. Lipid Res.* **35** (1994) 2060-2068.

3. Stewart M.E., Downing D.T. A new 6-hydroxy-4-sphingenine-containing ceramide in human skin. J. Lipid Res. **4** (1999) 1434-1439.

4. Ponec M., Weerheim A., Lankhorst P., Wertz P. New acylceramide in native and reconstructed epidermis. *J. Invest. Dermatol.* **120** (2003) 581-588.

5. Madison K.C., Schwartzendruber D.C., Wertz P.W., Downing D.T. Presence of intact intercellular lipid lamellae in the upper layers of the stratum corneum. *J. Invest. Dermatol.* **88** (1987) 714-718.

6. Swartzendruber D.C., Wertz P.W., Kitko D.J., Madison K.C., Downing D.T. Molecular models of intercellular lipid lamellae in mammalian stratum corneum. *J. Invest. Dermatol.* **92** (1989) 251-257.

7. Bouwstra J.A., Gooris G.S., van der Spek J.A., Bras W. The structure of human stratum corneum as determined by small angle X-ray scattering. *J. Invest. Dermatol.* **96** (1991) 1006-1014.

8. Bouwstra J.A., Gooris G.S., van der Spek J.A., Bras W. Structural investigations of human stratum corneum by small angle X-ray scattering. *J. Invest. Dermatol.* **97** (1991) 1005-1012.

9. Bouwstra J.A., Gooris G.S., Bras W., Downing D.T. Lipid organization in pig stratum corneum. *J. Lipid Res.* **36** (1995) 685-695.

10. Bouwstra J.A., Gooris G.S., Cheng K., Weerheim A., Bras W., Ponec M. Phase behavior of isolated skin lipids. *J. Lipid Res*. **37** (1996) 999-1011.

11. Bouwstra J.A., Gooris G.S., Dubbelaar F.E.R., Ponec M. Phase behaviour of lipid mixtures based on human ceramides. *J. Lipid Res.* **42** (2001) 1759-1770.

12. McIntosh T.J., Stewart M.E., Downing D.T. X-ray diffraction analysis of isolated skin lipids: reconstruction of intercellular lipid domains. *Biochemistry* **35** (1996) 3649-3653.

13. de Jager M.W., Gooris G.S., Dolbnya I.P., Bras W., Ponec M., Bouwstra J.A. Novel lipid mixtures based on synthetic ceramides reproduce the unique stratum corneum lipid organization. *J. Lipid Res.* **45** (2004) 923-932.

14. de Jager M.W., Gooris G.S., Dolbnya I.P., Ponec M., Bouwstra J.A. Modelling the stratum corneum lipid organisation with synthetic lipid mixtures: The importance of ceramide composition. *Biochim. Biophysic. Acta* **1684** (2004) 132-140.

15. de Jager M., Gooris G., Ponec M., Bouwstra J. Acylceramide head group architecture affects lipid organization in synthetic ceramide mixtures. *J. Invest. Dermatol.* **123** (2004) 911-916.

16. Wertz P.W., Downing D.T. Ceramides of pig epidermis: structure determination. *J. Lipid Res.* **24** (1983) 759-765.

17. Wertz P.W., Downing D.T. Epidermal lipids, in: L.A. Goldsmith (Eds.), Physiology, Biochemistry and Molecular Biology of the Skin, 2nd edition, Oxford University Press, Oxford, 1991, pp 205-235.

18. Bras W. A SAXS/WAXS beamline at the ESRF and future experiments. *J. Macromol. Sci. Phys. B* **37** (1998) 557-566.

19. Dolbnya, I.P., Alberda, H., Hartjes, F.G., Udo, F., Bakker, R.E., Konijnenburg, M., Homan, E., Cerjak, I., Goedtkindt, P., Bras, W. A fast position sensitive MSGC detector at high count rate operation. *Rev. Sci. Instrum.* **73** (2002) 3754-3758.

20. de Jager, M.W., Gooris G.S., Dolbnya I.P., Bras W., Ponec M., Bouwstra J.A. The phase behaviour of lipid mixtures based on synthetic ceramides. *Chem. Phys. Lipids* **124** (2003) 123-134.

21. Bouwstra J.A., Gooris G.S., Dubbelaar F.E.R., Ponec M. Phase behavior of stratum corneum lipid mixtures based on human ceramides: the role of natural and synthetic ceramide 1. *J. Invest. Dermatol.* **118** (2002) 606-617.

22. Moore, D.J., Rerek, M.E. Insights into the molecular organisation of lipids in the skin barrier from infrared spectroscopy studies of stratum corneum lipid models. *Acta Derm. Venereol. Suppl. (Stockh.)* **208** (2000) 16-22.

23. Raudenkolb S., Hubner W., Rettig W., Wartewig S., Neubert R.H. Polymorphism of ceramide 3. Part 1: an investigation focused on the head group of N-octadecanoylphytosphingosine. *Chem. Phys. Lipids* **123** (2003) 9-17.

24. Dahlen B., Pascher I. Molecular arrangements in sphingolipids. Thermotropic phase behaviour of tetracosanoylphytosphingosine. *Chem. Phys. Lipids* **24** (1979) 119-133.

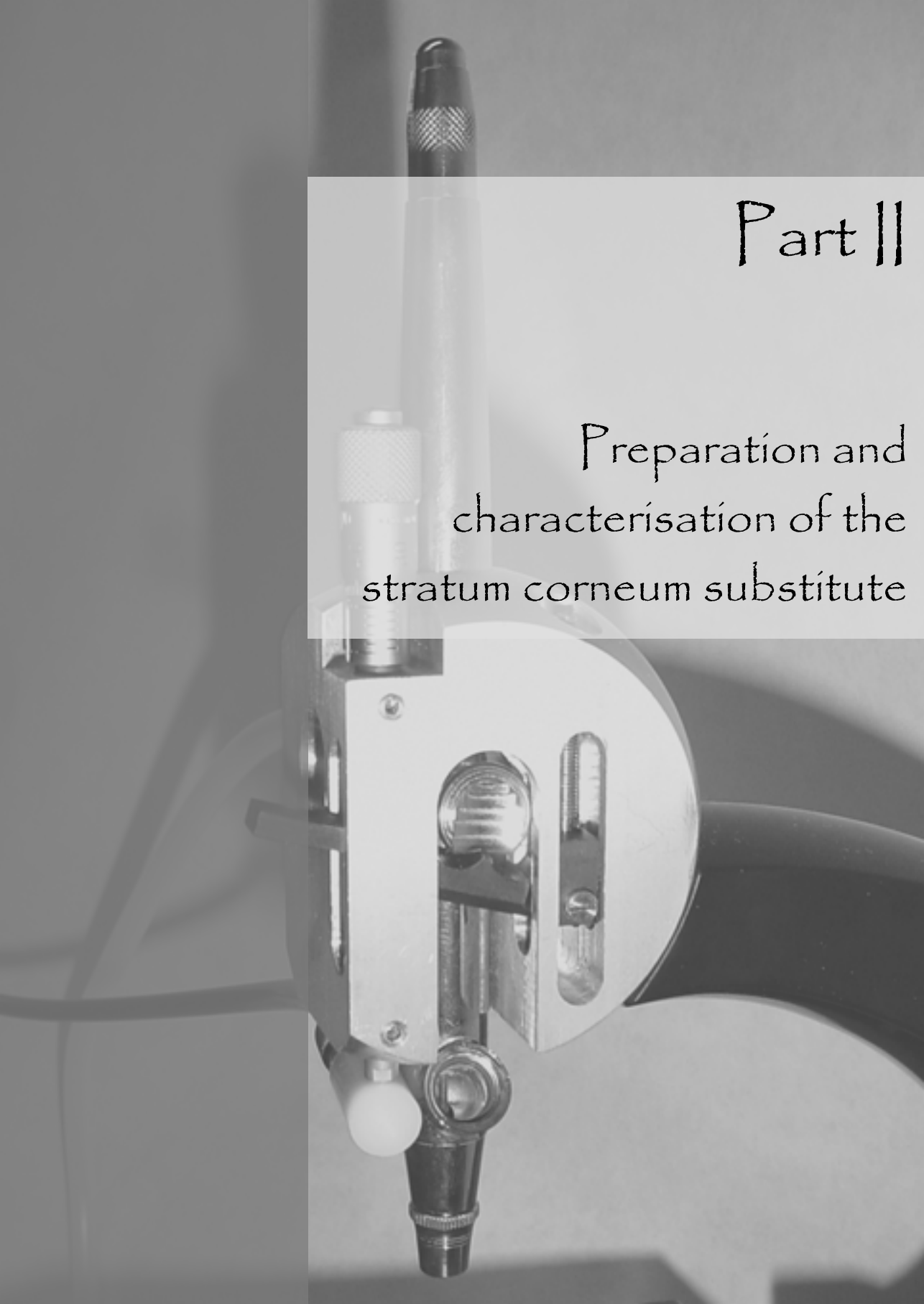

Part II

Preparation and characterisation of the stratum corneum substitute

Chapter 7

Preparation and characterisation of a stratum corneum substitute for in vitro percutaneous penetration studies

M.W. de Jager,* H.W.W. Groenink,* J.A. van der Spek,[#] J.H.G. Janmaat,[§] G.S. Gooris,* M. Ponec,[$] and J.A. Bouwstra*

*Leiden/Amsterdam Center for Drug Research, Department of Drug Delivery Technology, University of Leiden, P.O. Box 9502, 2300 RA Leiden, The Netherlands.
[#]Fine Mechanical Department, Leiden University, Leiden, The Netherlands.
[§]Electronic Department, Leiden University, Leiden, The Netherlands.
[$]Department of Dermatology, Leiden University Medical Center, Leiden, The Netherlands.

(adapted from *Biochim. Biophys. Acta*, in press)

ABSTRACT

The intercellular stratum corneum (SC) lipids form the main barrier for diffusion of substances through the skin. A porous substrate covered with synthetic SC lipids would be an attractive model to study percutaneous penetration, thereby replacing native human SC. Prerequisite is that this stratum corneum substitute (SCS) is prepared with a uniform lipid composition and layer thickness. Furthermore, the lipid organisation and orientation should resemble that in SC. The objective of this study was to investigate the utility of an airbrush spraying device to prepare a SCS composed of cholesterol, ceramides and free fatty acids on a polycarbonate filter. The results demonstrate that a proper choice of solvent mixture and lipid concentration is crucial to achieve a uniform distribution of the lipids over the filter surface. A smooth and tightly packed lipid layer is only obtained when the equilibration conditions are appropriately chosen. The SCS possesses two crystalline lamellar phases with periodicities similar to those present in native SC. The orientation of these lamellae is mainly parallel to the surface of the polycarbonate filter, which resembles the orientation of the intercellular SC lipids. In conclusion, the airbrush technique enables generation of a homogeneous SCS, which ultimately may function as a predictive in vitro percutaneous penetration model.

1. INTRODUCTION

The nonviable outermost layer of the skin, the stratum corneum (SC), serves as a penetration, dehydration and protection barrier against various environmental hazards. The SC consists of several layers of overlapping corneocytes, embedded in a lipid matrix of ordered lamellae. Despite their overall small percentage, the lipids in the SC represent the main barrier to diffusion of substances. These barrier properties are based on the unique composition and organisation of the intercellular lipid lamellae. Ceramides (CER), cholesterol (CHOL) and long-chain free fatty acids (FFA) are the major constituents of the intercellular lamellae [1-4], which are oriented approximately parallel to the surface of the corneocytes [5, 6]. These lipids are organised in two coexisting lamellar phases with periodicities of 6 nm (short periodicity phase: SPP) and 13 nm (long periodicity phase: LPP) [7-9]. In particular the LPP and the crystalline lateral packing are considered to play a crucial role for the skin barrier function.

Recently, there has been an increased interest in drug administration via the skin for both local treatment of the diseased state (dermal delivery) as well as for systemic delivery (transdermal delivery). For this reason, the choice of predictive in vitro test models is important. The use of isolated epidermis or SC sheets from human or animal origin has a number of disadvantages, like high intra- and inter-individual variations and scarcity of the tissue, in particular diseased skin for which numerous topical drug products are designed. In addition, after 2009 there will be an EU-wide ban on the use of animal skin in the testing of cosmetic products. Our ultimate goal is to develop a novel skin barrier model, which can substitute for SC in diffusion studies. The stratum corneum substitute (SCS) consists of a porous substrate covered with specific synthetic SC lipids of uniform composition and layer thickness, mimicking the lipid organisation and orientation in SC. Such SCS may function as a standardised and predictive percutaneous penetration model and will therefore circumvent problems related to SC sheets isolated from human or animal skin. Another major advantage of the SCS is that the composition of the synthetic SC lipid mixtures can easily be modified. This allows studying the relation between lipid composition, lipid organisation and barrier function in one single model. As a result, important insights may be provided into the defective barrier function and altered SC lipid composition and organisation underlying various skin diseases [10-13]. Ultimately, a SCS may be prepared that mimics not only healthy, but also diseased and dry skin, for which there is currently no alternative screening system available.

To mimic the SC barrier function, the SCS should meet the following requirements: (i) The lipids should spread homogeneously over the entire substrate surface. This is important for the formation of the characteristic LPP and the crystalline lateral packing [14-16]. (ii) The lipid layer should have a uniform thickness. Furthermore, cracks or holes should be absent, as these defects will disrupt the barrier properties. (iii) The orientation of the lamellae should be parallel to the substrate surface, which mimics the situation in native SC. (iv) The lipids should be organised in the LPP and SPP with an orthorhombic lateral packing, similarly as observed in SC.

In previous studies we have already demonstrated that the unique SC lipid organisation, including the 13 nm lamellar phase, can be reproduced in vitro with mixtures based on cholesterol, free fatty acids and synthetic ceramides (synthCER), provided that the lipid composition and equilibration temperature are appropriately chosen [17-19]. The objective of the present study was to explore the possibility of preparing a SCS with an airbrush. This was performed by spraying equimolar mixtures of cholesterol, synthetic ceramides and free fatty acids onto a polycarbonate filter. The SCS was subsequently characterised in terms of distribution of the lipid classes over the substrate surface, homogeneity of the lipid layer and orientation and organisation of the lipid lamellae. For these purposes, high performance thin layer chromatography, cryo-scanning electron microscopy, small-angle and wide-angle X-ray diffraction were used.

2. MATERIALS AND METHODS

2.1 Materials

CER1(C30)-linoleate, CER2(C24), CER3(C24), CER3(C16), CER4(C24) and CER6(C24) were generously provided by Cosmoferm B.V. (Delft, the Netherlands). Palmitic acid, stearic acid, arachidic acid, behenic acid, tricosanoic acid, lignoceric acid, cerotic acid and cholesterol were purchased from Sigma-Aldrich Chemie GmbH (Schnelldorf, Germany). Nuclepore polycarbonate filter disks (pore size 50 nm) were purchased from Whatman (Kent, UK). All organic solvents used were of analytical grade and manufactured by Labscan Ltd (Dublin, Ireland). All other chemicals were of analytical grade and the water used was of Millipore quality.

2.2. Preparation of the SCS

For the preparation of the synthCER mixture, CER1, CER2, CER3(C24), CER4, CER3(C16) and CER6 were mixed in a 15:51:16:4:9:5 molar ratio, which resembles the composition of the ceramides in pig SC [14, 20]. For the preparation of the free fatty acids mixtures, the following fatty acid mixture was used: C16:0, C18:0, C20:0, C22:0, C23:0, C24:0 and C26:0 at molar ratios of 1.3, 3.3, 6.7, 41.7, 5.4, 36.8 and 4.7, respectively. This is similar to the free fatty acids composition in SC [21]. Appropriate amounts of individual lipids dissolved in chloroform:methanol (2:1) were combined to yield lipid mixtures at the desired equimolar CHOL:synthCER:FFA composition. After evaporation of the organic solvent under a stream of nitrogen, the lipid mixtures were re-dissolved in either hexane:isopropanol (3:2), methanol:ethylacetate (2:1), or hexane:ethanol (2:1) at a total lipid concentration of 2 or 4.5 mg/ml.

An evolution solo airbrush (Airbrush Service Almere, The Netherlands) connected to gaseous nitrogen was used to spray the lipid mixtures onto a polycarbonate filter disk with a pore size of 50 nm. A schematic representation of the application set-up is illustrated in Figure 1.

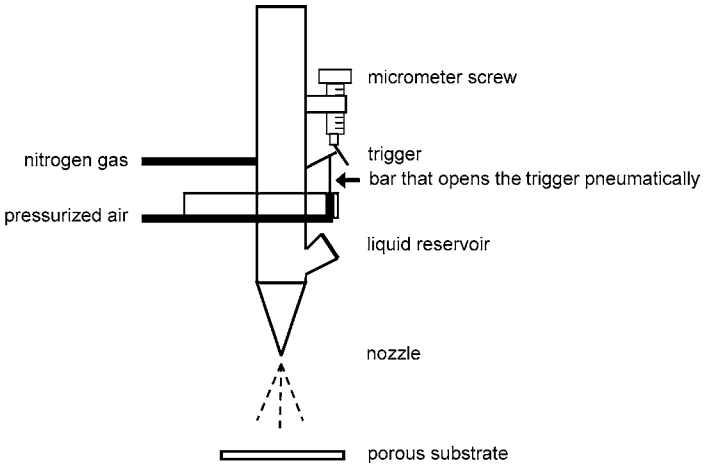

Figure 1 - A schematic representation of the airbrush. During the spraying period, the trigger of the airbrush is opened pneumatically by a bar (indicated with an arrow). After the spraying period, the air pressure drops, the bar goes down, the trigger is closed and the liquid supply immediately stops.

Briefly, the porous substrate was mounted in a holder and fixed under the airbrush, which was constructed vertically with the nozzle facing downwards. The reservoir of the airbrush was subsequently filled with the lipid solution. The device enables us to control: (i) The spraying period. During the spraying period, the trigger is opened

pneumatically for a certain adjustable time period, during which a small fraction of the lipid solution passes the nozzle. Due to this nitrogen pressure, the lipid solution is sprayed in very small droplets onto the porous substrate. The distance over which the trigger is opened can be adjusted accurately with a micrometer screw. (ii) The drying period, which follows the spraying period. During the drying stage, the trigger is closed, the organic solvent evaporates by the nitrogen flow and the lipids attach to the substrate. To ensure proper spreading of the lipids, the nitrogen pressure during the spraying and the drying stage can be regulated independently. This has been achieved by making use of an air valve, which assures a high pressure during spraying and a low pressure during drying. (iii) Multiple application. The number of spraying and drying cycles is adjustable to obtain the required layer thickness. Prior to the spraying stage, the nitrogen pressure is increased to levels required for appropriate spraying. The used equipment settings are listed in Table 1. After preparation, the lipid-loaded filters were equilibrated at 70°C, for a period of 10 minutes. If required, hydration of the lipid membranes was performed by applying an excess of an acetate buffer of pH 5.0 after the equilibration step.

Table 1 - Equipment settings used for spraying of the SCS.

parameter	setting
pressure during spraying (above atmospheric pressure)	1.16 bar
time trigger open	1 sec
distance over which the trigger is opened	5.5 mm
pressure during drying (above atmospheric pressure)	160 mbar
time trigger closed	15 sec
distance between the nozzle and the filter	4.5 cm

2.3 Lipid distribution

One dimensional high performance thin layer chromatography was used to establish the distribution of the various lipid classes over the filter surface. Briefly, the lipid-loaded filters were cut into two circular parts: the centre (diameter 4 mm; area 12.6 mm^2) and the periphery (diameter 9 mm; area 51.0 mm^2). The lipids were extracted in 0.5 ml chloroform:methanol (2:1) by extensive vortexing and were subsequently re-dissolved in ratios according to the surface area. Aliquots were applied on a silica plate (Merck, Darmstad, Germany) under a flow of nitrogen using a Camag Linomat IV (CAMAG, Muttenz, Switzerland). After eluting with different organic solvent mixtures [22], the silica plate was sprayed with copper sulphate. After charring, the intensities of the lipid bands were determined using a photodensiometer with automatic peak

integration (Biorad GS 710, Hercules, USA).

2.4 Homogeneity of lipid layer

Cryo-scanning electron microscopy was used to establish the compactness of the lipid layer of lipid membranes that were (i) equilibrated and hydrated, (ii) not equilibrated and not hydrated, (iii) equilibrated but not hydrated, or (iv) equilibrated and cooled to room temperature prior to hydration. Prior to processing the specimens for cryo-scanning electron microscopy, hydrated lipid membranes were all exposed to the buffer solution for at least 24 hours. Subsequently, the lipid-loaded filters were cut into sheets of 1.5 x 2 mm^2, folded and fixed in a small copper "shoe-nail" using Tissue-Tek O.C.T. Compound (Miles Inc. Elkhart, IN USA). The samples were then quickly frozen by plunge-freezing (Reichert Jung-KF80, Vienna, Austria) into liquid propane at –180°C. The frozen specimens were kept in liquid nitrogen until they were mounted into a sample holder. The cryo-fixed samples were planed in a cryo ultramicrotome (Leica Ultracut UCT/Leica EM FCS, Wetzlar, Germany), using a specimen temperature of –90°C and a knife temperature of –100°C [23]. Subsequently, the samples were vacuum dried for 3 min at –90°C at 0.1 Pa to obtain contrast and sputtered with a layer of platinum (CT 1500 HF, Oxford Instruments, UK). After transferring the specimens into the field emission scanning electron microscope (Jeol 6400F, Tokyo, Japan), the samples were analysed at -190°C. At least 5 electron micrographs were taken from each lipid-loaded filter and at least 2 lipid-loaded filters were prepared and visualised per condition.

2.5 Correlation between the layer thickness and quantity of lipid material

To establish the correlation between the quantity of lipid material and the resulting layer thickness, filters were covered with approximately 0.5, 0.8, 1.2 and 1.5 mg/cm^2 of lipid material and were subsequently equilibrated. Three lipid-loaded filters were prepared and examined per experimental condition. Briefly, circular lipid-loaded filter pieces (diameter 6 mm; area 12.6 mm^2) were cut into two equally sized parts. One part was dissolved in 100 µl chloroform/methanol (2:1) and the lipids were extracted by extensive vortexing. After evaporation of the organic solvent, the amount of lipids was determined by weighing. The other part was used for cryo-scanning electron microscopy to establish the thickness and compactness of the lipid layer. At least 4 microscopic images were taken from each lipid-loaded filter. At equal distances of 20 µm along the cutting plane, the thickness of the cross section of each lipid layer was

determined by establishing the pixel position of the top and bottom of the lipid layer in proportion to that of the magnification bar that is present in each micrograph.

2.6 Orientation and organisation of lipid lamellae

Small-angle X-ray diffraction was used to acquire information about the lamellar organisation (i.e. the repeat distance of a lamellar phase) and the orientation of the lamellae. The scattering intensity I (in arbitrary units) was measured as a function of the scattering vector q (in reciprocal nm). The latter is defined as $q=(4\pi\sin\theta)/\lambda$, in which θ is the scattering angle and λ is the wavelength. From the positions of a series of equidistant peaks (q_n), the periodicity, or d-spacing, of a lamellar phase was calculated using the equation $q_n=2n\pi/d$, n being the order number of the diffraction peak. A preferred orientation of the lamellae parallel to the substrate surface is indicated by small arcs on the detection plane with a maximum intensity at the meridian, whereas disoriented lamellae result in full rings of equal intensity.

All measurements were performed at the European Synchrotron Radiation Facility (ESRF, Grenoble), using station BM26B [24]. The X-ray wavelength and the sample-to-detector distance were 1.24Å and 1.7m, respectively. Diffraction data were collected on a two-dimensional multiwire gas-filled area detector. The spatial calibration of this detector was performed using silver behenate. A filter with lipid layers was mounted parallel to the primary beam in a temperature-controlled sample holder with mica windows. Static diffraction patterns were obtained at room temperature for a period of 5 minutes. The temperature-induced phase changes were investigated by collecting diffraction patterns, while the temperature of the sample was raised to 75°C at a rate of 2°/min. Each successive diffraction curve was collected for a period of one minute.

Wide-angle X-ray diffraction provides information about the lateral packing of the lipids within the lamellae. Data were collected on a microstrip gas chamber detector with an opening angle of 60° [25]. The sample-to-detector distance was 36 cm and the X-ray wavelength was 1.24Å. The spatial calibration of the detector was performed with a mixture of silicium and cholesterol.

3. RESULTS

3.1 Lipid distribution

Polycarbonate filters are not resistant towards chloroform. Therefore, three alternative organic solvent mixtures were selected to dissolve the lipids, namely

methanol:ethylacetate (M:EA), hexane:isopropanol (H:IPA) and hexane:ethanol (H:Et). Filters were covered with approximately 0.25 mg/cm^2 and 0.5 mg/cm^2 of lipid material. Whereas the total amount of lipids applied on the filter does not have an effect on the distribution (data not shown), the solvent mixture and total lipid concentration markedly affect the lipid distribution, in particular that of cholesterol. Figure 2 shows the lipid distribution of the lipid subclasses between the filter centre and periphery, making use of the three organic solvent mixtures at a total lipid concentration of 4.5 mg/ml. From the intensities of the bands it is obvious that an even distribution of cholesterol is only obtained when the lipids are dissolved in H:Et or M:EA. When H:IPA is used as a solvent, the amount of cholesterol present at the filter periphery is nearly 6 to 8-fold higher than the amount present in the central part. With 2 mg/ml solutions an inhomogeneous distribution of the lipid classes is observed for all three solvent mixtures (data not shown), similarly as the distribution obtained with H:IPA at 4.5 mg/ml solution.

Although the distribution of the lipids from H:Et and M:EA solutions is comparable, a considerable improvement of the spraying process is obtained when the lipids are dissolved in H:Et. Moreover, the lipid loss during application is slightly lower, which can most likely be ascribed to the lower solubility of the lipids in M:EA in comparison to that in H:Et. For this reason, all further experiments were performed with lipid solutions in H:Et at a total lipid concentration of 4.5 mg/ml.

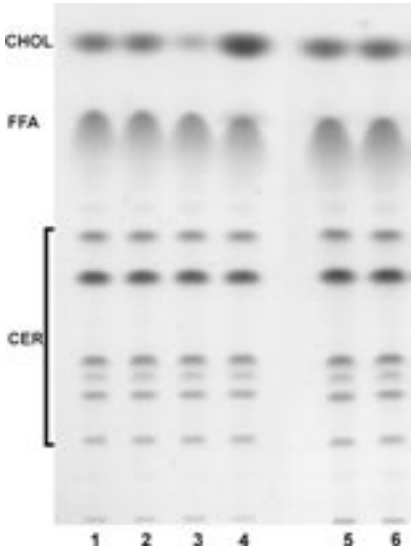

Figure 2 - Lipid distribution from three solvent mixtures at a total lipid concentration of 4.5 mg/ml. 1 = centre M/EA; 2 = periphery M/EA; 3 = centre H/IPA; 4 = periphery H/IPA; 5 = centre H/Et; 6 = periphery H/Et.

3.2 Compactness of the lipid layer

Figure 3A shows an electron micrograph of a cross-section of a lipid membrane and the underlying polycarbonate filter, equilibrated at 70°C and subsequently hydrated with an acetate buffer. It can be clearly observed that this procedure, which is routinely used to obtain proper lipid organisation in synthetic lipid mixtures for X-ray diffraction measurements, results in the formation of large holes in the lipid layer. To elucidate whether the holes are caused by the elevated temperature during equilibration or by the successive addition of the acetate buffer, filters were covered with approximately 0.5 mg/cm^2 of lipid material and the lipid membranes were either i) not equilibrated and not hydrated (Fig. 3B), ii) equilibrated but not hydrated (Fig. 3C), or iii) equilibrated and cooled to room temperature prior to hydration (Fig. 3D).

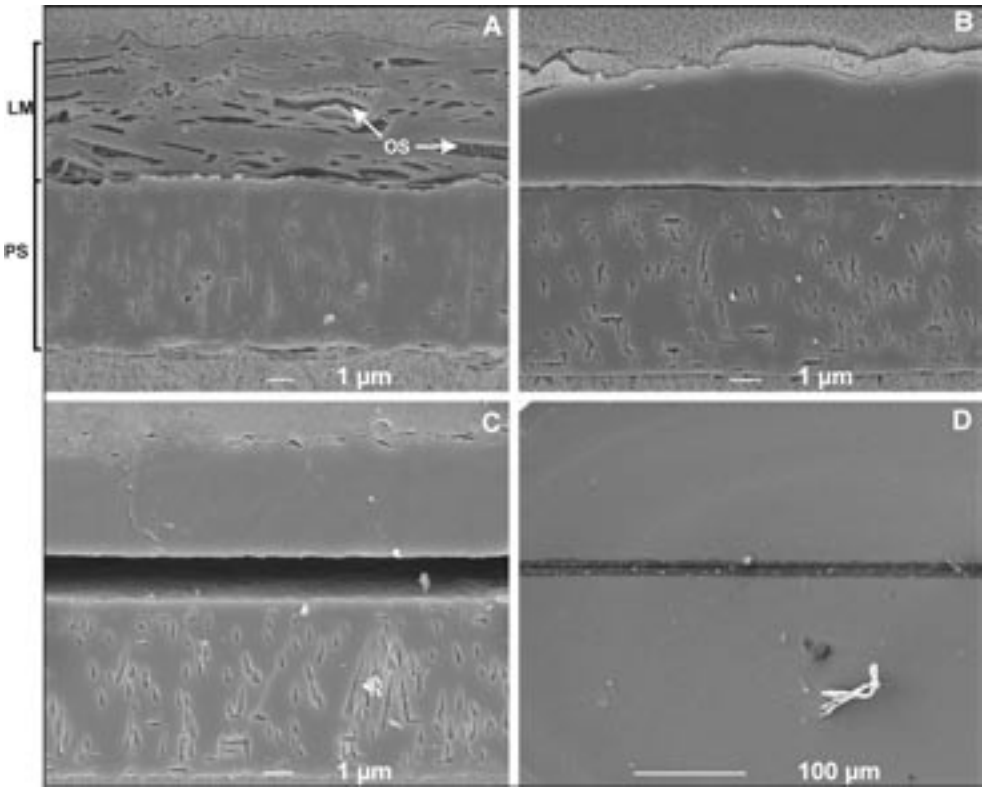

Figure 3 - Cryo-scanning electron microscopy photographs of cross-sections of lipid membranes (LM) and underlying porous substrates (PS). (A) lipid membrane that was equilibrated and hydrated (large open structures (OS) can be observed in the lipid layer). (B) lipid membrane that was not equilibrated and not hydrated. (C) lipid membrane that was equilibrated, but not hydrated. The detachment of the lipid layer from the polycarbonate filter is most likely an artefact, which arose during the preparation of this specimen for electron microscopy. (D) lipid membrane that was equilibrated and cooled to room temperature prior to hydration (lower magnification).

The results indicate that when the buffer is applied directly after the equilibration step, it is able to penetrate the lipid membrane, where it phase separates to form water-rich domains. Because the samples were vacuum dried for a short period prior to visualisation, the water-rich domains are consequently visible as holes in the lipid layer.

No significant differences can be observed between the lipid membranes presented in Figure 3B-3D. All preparation methods result in the formation of a tightly packed lipid layer in the absence of large open structures. In addition, no lipid material is present inside the pores or at the bottom side of the filter. From Figure 3D, in which a lower magnification of the lipid membrane and the underlying filter is presented, it can further be deduced that also over a larger surface area the lipid membranes have a uniform layer thickness.

3.3 Correlation between layer thickness and quantity of lipid material

Figure 4A demonstrates that an almost linear relationship exists between the layer thickness and the quantity of lipid material of individual lipid membranes (correlation coefficient = 0.98). The layer thickness of each individual lipid membrane as well as the quantity of lipid material applied per filter is highly reproducible and only slightly fluctuates with steady relative standard deviations of 10% and 5%, respectively.

From the slope of the line in Figure 4B, in which the average layer thickness is plotted against the number of sprays required to obtain that particular layer thickness, it can be observed that approximately 0.14 µm of lipid material is applied onto the filter per spray.

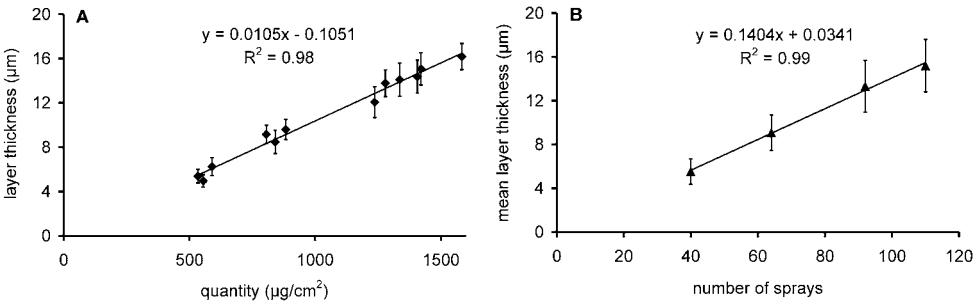

Figure 4 - The correlation between the layer thickness and quantity of lipid material (A) and the correlation between the average layer thickness and the number of sprays (B).

3.4 Orientation and organisation

Figure 5A shows a typical two-dimensional X-ray diffraction pattern of a non-hydrated lipid membrane. The arcs on the detection plane, having a maximum intensity at the meridian, indicate a preferred orientation of the lamellae parallel to the polycarbonate filter. Sector integration (angle 60°) resulted in Figure 5B, in which the intensity of the arcs is plotted versus the scattering vector q. The LPP with a repeat distance of 12.2 nm is indicated by the presence of five reflections (q = 0.52, 1.03, 1.54, 2.06 and 3.08 nm^{-1}). The reflections at q = 1.18, 2.36 and 3.53 nm^{-1} correspond to the first, second and third order diffraction peaks of a lamellar phase with a periodicity of 5.4 nm (SPP). The presence of crystalline cholesterol in separate domains can be deduced from the peaks at 1.86 and 3.72 nm^{-1}. No significant differences in the orientation or lamellar organisation could be observed between hydrated and non-hydrated lipid membranes.

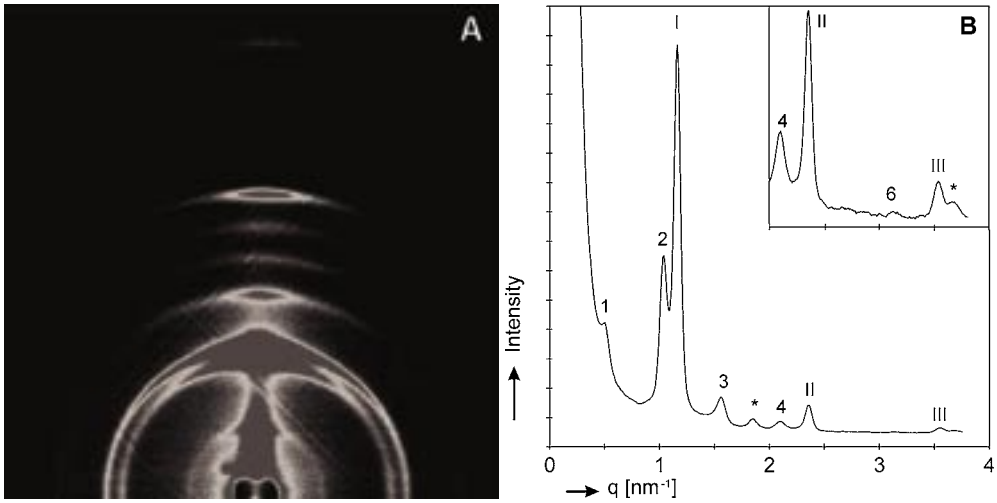

Figure 5 - The orientation (A) and lamellar organisation (A and B) of a non-hydrated lipid membrane. The inset shows a magnification of the reflections in the q-range between 2 and 4 nm^{-1}. The Arabic and Roman numbers indicate the diffraction orders of the LPP and SPP, respectively. The asterisk (*) indicates the reflections of crystalline cholesterol located at 1.87 and 3.74 nm^{-1}. The various orders of the LPP are located at q = 0.52 nm^{-1} (1) , 1.03 nm^{-1} (2), 1.54 nm^{-1} (3) , 2.06 nm^{-1} (4) and 3.08 nm^{-1} (6). The various orders of the SPP are located at q = 1.18 nm^{-1} (I) and 2.36 nm^{-1} (II) and 3.53 nm^{-1} (III).

The lamellar and lateral lipid phase behaviour of the non-hydrated and hydrated lipid membranes was also studied as a function of temperature (Fig. 6A-D). Each curve represents the mean of the lipid phases present during a temperature shift of 2°C. The

diffraction patterns illustrated in Figure 6A (non-hydrated lipid membranes) and Figure 6B (hydrated lipid membranes) reveal a number of reflections that can be ascribed to the presence of the LPP (12.2 nm) and SPP (5.4 nm), similarly as described in Figure 5. In addition, crystalline cholesterol is present in separate domains. No significant changes are observed in the intensities or positions of the reflections of the phases between 25 and 51°C. However, the reflections of the LPP disappear at around 65°C. Despite these similarities, two differences in the lamellar organisation are observed between non-hydrated and hydrated lipid membranes. Firstly, in hydrated lipid membranes the two reflections attributed to crystalline cholesterol disappear at around 57°C, whereas in non-hydrated lipid membranes it is reproducibly observed that the cholesterol reflections disappear only at approximately 73°C. Secondly, in hydrated lipid membranes the reflections of the SPP disappear at around 51°C. In the same temperature range, a new phase is formed, of which only one reflection can be detected that gradually shifts to $q = 1.37\ nm^{-1}$ (repeat distance 4.6 nm). In non-hydrated lipid membranes, however, the reflections of the SPP do not disappear at elevated temperatures and in addition no additional phase with a repeat distance of 4.6 nm is formed. Previous studies performed with mixtures based on isolated ceramides have shown that the formation of the additional phase at elevated temperatures is strongly related to the amount of cholesterol that is available for the formation of this phase [26]. For hydrated lipid membranes it can be observed that the formation of the additional 4.6 nm phase is in the same temperature region in which the reflections of phase-separated cholesterol disappear. The cholesterol reflections in non-hydrated lipid mixtures disappear at a much higher temperature than in hydrated lipid membranes. Hence the amount of available cholesterol is most likely insufficient for the formation of the 4.6 nm phase. In isolated human SC the formation of this additional phase at elevated temperatures is also hardly ever observed [26], which once again demonstrates the high similarity in lipid phase behaviour between SC and the SCS.

A hexagonal lateral packing is characterised by a strong 0.41 nm reflection in the wide-angle X-ray diffraction pattern, whereas the diffraction pattern of an orthorhombic packing is characterised by two strong 0.41 and 0.37 nm reflections. The diffraction patterns of non-hydrated and hydrated lipid membranes monitored as a function of temperature are plotted in Figure 6C and Figure 6D, respectively. Figure 6E, in which the diffraction pattern of isolated human SC as a function of temperature is illustrated, serves as a control. Both non-hydrated and hydrated lipid membranes show similar behaviour as isolated human SC. The 0.408 and 0.367 nm peaks indicate an

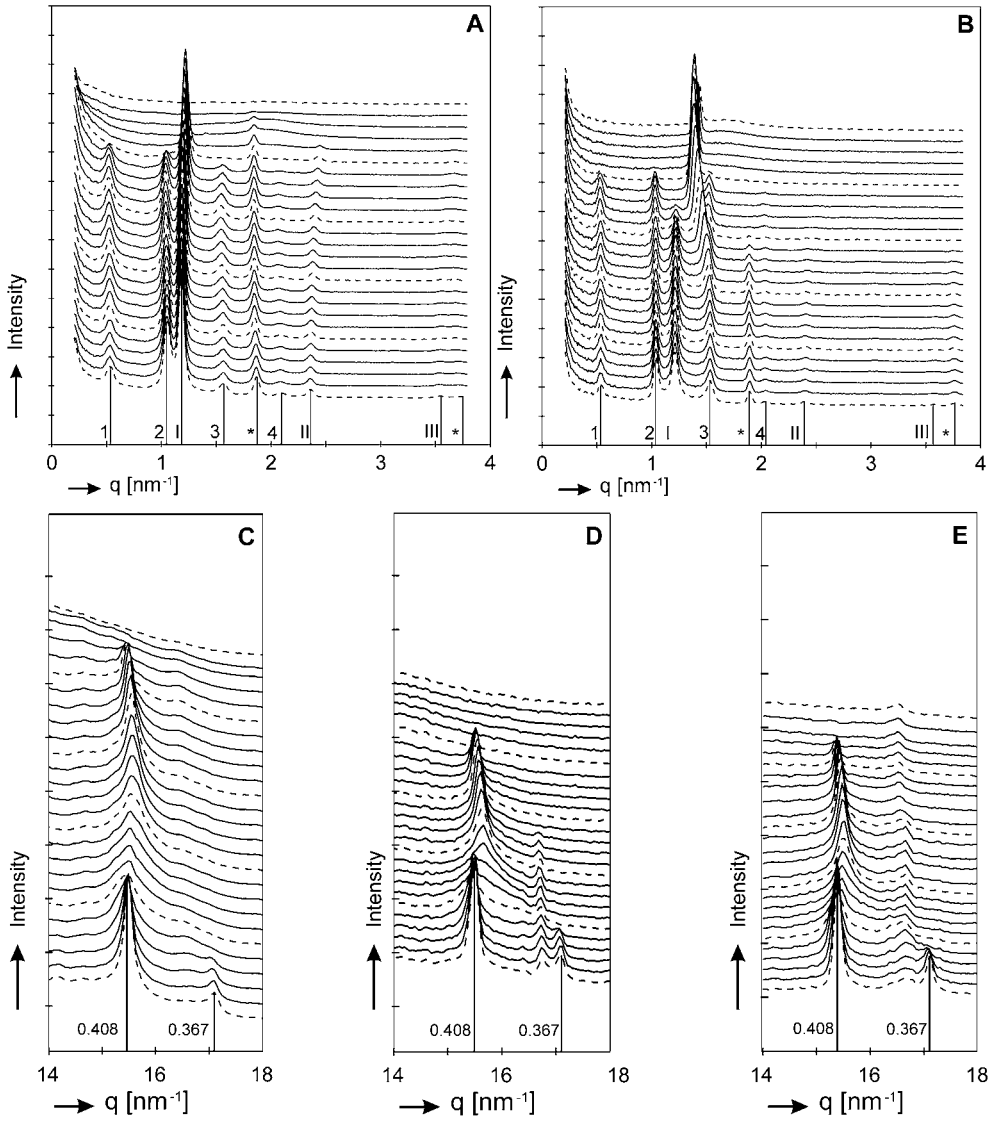

Figure 6 - Temperature-induced changes in (A) the lamellar lipid organisation of a non-hydrated lipid membrane, (B) the lamellar lipid organisation of a hydrated lipid membrane, (C) the lateral lipid organisation of a non-hydrated lipid membrane, (D) the lateral lipid organisation of a hydrated lipid membrane, and (E) the lateral lipid organisation of isolated human SC. The Arabic and Roman numbers indicate the diffraction orders of the LPP and SPP, respectively. The asterisk (*) indicates the reflections of crystalline cholesterol. The dashed lines represent the diffraction curves at 25, 35, 45, 55, 65, and 75°C.

orthorhombic lateral packing. At around 33°C, the 0.367 nm reflection disappears, indicating an orthorhombic to a hexagonal phase transition. The 0.408 nm reflection initially decreases in intensity. However, a further rise in temperature slightly increases the intensity of the 0.408 nm reflection, indicating a metastable to stable phase change. This phenomenon is also observed in the diffraction patterns of SC (see Fig. 6E). A disappearance of this peak is observed at 65°C, which is in the same temperature range at which the LPP disappears in the small-angle X-ray diffraction patterns.

4. DISCUSSION

The objective of the present study was to evaluate the possibility of preparing a SCS, which closely resembles the composition, organisation and orientation of the intercellular lipids in SC. As the resulting SCS may ultimately function as a percutaneous penetration model, it is further important that the lipids of the SCS are tightly packed and have a uniform layer thickness. These various aspects are discussed below.

4.1 Uniform lipid distribution

The results of the present study show that both the organic solvent mixture and the total lipid concentration are important determinants for successful preparation of a SCS of uniform lipid composition. It should be stressed, however, that the equipment settings used for the preparation of the SCS are at least as important as the two aforementioned factors. The most critical parameters in this respect are the distance between the nozzle of the airbrush and the filter, the nitrogen pressure during the spraying and drying stage and the quantity of lipid solution that passes the nozzle per spray. One can state that the evaporation rate during the drying stage should balance the quantity of lipid solution that reaches the polycarbonate filter during the preceding spraying stage.

When the process conditions were not optimally chosen, the evaporation process of the organic solvent occurred from the inside to the periphery and sometimes the lipid solution itself was even blown to the filter periphery. The latter phenomenon was specifically observed when the nitrogen pressure during the drying stage was set too high or when the evaporation velocity was too slow for the supply of lipid solution (e.g. by preparing lipid solutions at a total lipid concentration of 2 mg/ml). In either case, cholesterol was mainly present at the periphery of the lipid membrane, whereas the central part hardly contained any cholesterol (see also Fig. 2).

The solubility of cholesterol in the organic solvent mixtures is higher than that of the synthetic ceramides and free fatty acids. During the evaporation process of the organic solvent, the concentration of the lipids increases and the lipids crystallise according to their solubility. Cholesterol therefore remains in solution up to the edges of the lipid membrane. Interestingly, this could sometimes even be visually observed by a small band of crystals. On the other hand, when the supply of lipid solution was set too low, most of the organic solvent already evaporated before the lipid solution reached the filter. Due to substantial lipid loss, only a small area of the filter could be covered with lipid material.

4.2 Compactness of the lipid layer

The airbrush spraying technique results in the formation of smooth and tightly packed lipid membranes, provided that the hydration step, which immediately follows the equilibration step, is omitted. As demonstrated by the X-ray diffraction data, omission of the hydration step does not affect the lamellar or lateral lipid organisation. It has to be kept in mind, however, that during a diffusion experiment, non-hydrated lipid membranes will be exposed to a donor and an acceptor solution. In order to guarantee proper barrier function, it is necessary that the SCS remains intact under those conditions. Preliminary studies indicate that the SCS remains intact for several hours during diffusion experiments.

The results of the present study demonstrate that lipid membranes that are first cooled to room temperature prior to hydration do not possess large holes, indicating that no water pools are formed in the lipid membranes at room temperature. This finding is crucial, as these defects would disrupt the barrier properties of the SCS.

For preparation of a homogeneous SCS it is further important that the lipid layer is only present on top of the filter and not inside the pores of the filter. Filled or partially filled pores are easily recognisable by the fact that pores are not at all visible over the entire length of the filter, up to a certain depth. However, electron microscopy studies on lipid membranes prepared at the optimal equipment settings evidently demonstrate that the lipids are able to span the pores of the supporting membrane, as no lipid material is present inside the pores or at the bottom side of the filter. The results further demonstrate that a uniform layer thickness and penetration pathway for substances can be obtained and established. This will considerably facilitate the interpretation of future diffusion results.

4.3 Orientation of the lipid lamellae

The orientation of the lipid lamellae in the lipid membranes is parallel to the surface of the hydrophilic polycarbonate filter. From the width of the arcs, however, it cannot be excluded that some disorientation exists. Previous X-ray diffraction measurements on isolated human SC reveal that the orientation of the intercellular lamellae is also not exactly parallel to the skin surface [Bouwstra J.A., Gooris, G.S, unpublished data]. The width of the arcs of the SCS approximates that of SC rather closely, indicating that the synthetic lipids in the SCS resemble the orientation of the intercellular lipids in the SC. In vivo, the monolayer of covalently bound lipids surrounding each corneocyte is often suggested to serve as a template in the assembly of the multilamellar structures parallel to the corneocyte surface [27]. The SCS is solely composed of synthetic SC lipids and does not contain any corneocytes. Nonetheless, the orientation of the lipid lamellae is found to be mainly parallel to the filter surface, which suggests that one lipid layer forms a template for the next layer. Inspection of literature reveals that the airbrush has also been used successfully for the preparation of aligned samples of phospholipids [28, 29].

4.4 Lipid composition and organisation

Although the method of lipid analysis used in the present study did not allow the investigation of the lipid distribution as a function of depth, previous studies have shown that the lipid organisation is not extremely sensitive towards changes in the total CHOL:synthCER:FFA molar ratio [9, 30]. For this reason, small variations in the lipid composition will presumably not affect the lipid organisation to a high extent.

The results of the present study reveal that the LPP (12.2 nm) and SPP (5.4 nm) are both present in non-hydrated and hydrated lipid membranes. Moreover, an orthorhombic lateral packing of the lipids is observed in both non-hydrated and hydrated lipid membranes. This indicates that only the equilibration temperature and no hydration is important for proper lamellar and lateral lipid organisation. This finding is of crucial importance, as only in non-hydrated lipid membranes the lipid layer is tightly packed. The periodicities of the lamellar phases in hydrated and non-hydrated lipid membranes are exactly the same. This is in good agreement with previous X-ray diffraction measurements on hydrated SC [7, 8] and lipid mixtures prepared with isolated ceramides [31] in which an increased hydration level did not result in significant lamellar swelling. However, McIntosh et al. found that mixtures of isolated ceramides prepared in the absence of water are more sensitive to phase separation of cholesterol

than hydrated lipid mixtures of the same composition [31]. This may explain the small differences in the lamellar lipid organisation of non-hydrated and hydrated lipid membranes at elevated temperatures. Studies performed in our group revealed that only in the presence of a buffer the phase behaviour of mixtures prepared with isolated ceramides is similar to that in SC [de Jager, M.W., Gooris, G.S., Ponec, M. and Bouwstra J.A., unpublished data].

In conclusion, the present study has shown that the airbrush is an elegant apparatus to homogeneously spray reconstituted synthetic SC lipids onto a porous polycarbonate filter, provided that the experimental conditions used for spraying as well as for equilibration are appropriately chosen. As the SCS prepared in the present study has a uniform lipid layer thickness and further closely resemble the composition, organisation and orientation of the intercellular lipids in SC, they may have a great potential to ultimately serve as a novel skin barrier diffusion model. The barrier properties of the SCS will therefore be investigated in a future study.

Acknowledgements

This work was supported by a grant from the Technology Foundation STW (LGN4654). The Netherlands Organisation for Scientific Research (NWO) is acknowledged for the provision of the beamtime. The authors wish to express their gratitude to I.P. Dolbnya and W. Bras for their contribution at the ESRF. We would like to thank the company Cosmoferm B.V. for the provision of the synthetic ceramides and Raphaël Zwier (Fine Mechanical Department, Leiden University) for manufacturing the filter holders.

REFERENCES

1. Wertz P.W., Miethke M.C., Long S.A., Strauss J.S., Downing D.T. The composition of the ceramides from human stratum corneum and from comedones. *J. Invest. Dermatol.* **84** (1985) 410-412.

2. Robson K.J., Stewart M.E., Michelsen S., Lazo N.D., Downing D.T. 6-Hydroxy-4-sphingenine in human epidermal ceramides. *J. Lipid Res.* **35** (1994) 2060-2068.

3. Stewart M.E., Downing D.T. A new 6-hydroxy-4-sphingenine-containing ceramide in human skin. J. Lipid Res. **4** (1999) 1434-1439.

4. Ponec M., Weerheim A., Lankhorst P., Wertz P. New acylceramide in native and reconstructed epidermis. *J. Invest. Dermatol.* **120** (2003) 581-588.

5. Madison K.C., Schwartzendruber D.C., Wertz P.W., Downing D.T. Presence of intact intercellular lipid lamellae in the upper layers of the stratum corneum. *J. Invest. Dermatol.* **88** (1987) 714-718.

6. Swartzendruber D.C., Wertz P.W., Kitko D.J., Madison K.C., Downing D.T. Molecular models of intercellular lipid lamellae in mammalian stratum corneum. *J. Invest. Dermatol.* **92** (1989) 251-257.

7. Bouwstra J.A., Gooris G.S., van der Spek J.A., Bras W. The structure of human stratum corneum as determined by small angle X-ray scattering. *J. Invest. Dermatol.* **96** (1991) 1006-1014.

8. Bouwstra J.A., Gooris G.S., van der Spek J.A., Bras W. Structural investigations of human stratum corneum by small angle X-ray scattering. *J. Invest. Dermatol.* **97** (1991) 1005-1012.

9. Bouwstra J.A., Gooris G.S., Bras W., Downing D.T. Lipid organization in pig stratum corneum. *J. Lipid Res.* **36** (1995) 685-695.

10. Di Nardo A., Wertz P., Giannetti A., Seidenari S. Ceramide and cholesterol composition in the skin in patients with atopic dermatitis. *Acta Derm. Venereol. (Stockh.)* **78** (1998) 27-30.

11. Motta S.M., Monti M., Sesana S., Caputo R., Carelli S., Ghidoni R. Ceramide composition of psoriatic scale. *Biochim. Biophysic. Acta* **1182** (1993) 147-151.

12. Yamamoto A., Serizaka S., Ito M., Sato Y. Stratum corneum lipid abnormalities in atopic dermatitis. *Arch. Dermatol. Res.* **283** (1991) 219-223.

13. Lavrijsen A.P.M., Bouwstra J.A., Gooris G.S., Boddé H.E., Ponec M. Reduced skin barrier function parallels abnormal stratum corneum lipid organisation in patients with lamellar ichthyosis. *J. Invest. Dermatol.* **105** (1995) 619-624.

14. Bouwstra J.A., Gooris G.S., Cheng K., Weerheim A., Bras W., Ponec M. Phase behavior of isolated skin lipids. *J. Lipid Res*. **37** (1996) 999-1011.

15. Bouwstra J.A., Gooris G.S., Dubbelaar F.E.R., Ponec M. Phase behaviour of lipid mixtures based on human ceramides. *J. Lipid Res.* **42** (2001) 1759-1770.

16. Bouwstra J.A., Gooris G.S., Dubbelaar F.E.R., Ponec M. Phase behavior of stratum corneum lipid mixtures based on human ceramides: the role of natural and synthetic ceramide 1. *J. Invest. Dermatol.* **118** (2002) 606-617.

17. de Jager M.W., Gooris G.S., Dolbnya I.P., Bras W., Ponec M., Bouwstra J.A. Novel lipid mixtures based on synthetic ceramides reproduce the unique stratum corneum lipid organization. *J. Lipid Res.* **45** (2004) 923-932.

18. de Jager M., Gooris G., Ponec M., Bouwstra J. Acylceramide head group architecture affects lipid organization in synthetic ceramide mixtures. *J. Invest. Dermatol.* **123** (2004) 911-916.

19. de Jager M.W., Gooris G.S., Ponec M., Bouwstra J.A. Lipid mixtures prepared with well-defined synthetic ceramides closely mimic the unique stratum corneum lipid phase behaviour. *J. Lipid Res.* **46** (2005) 2649-2656.

20. Wertz P.W., Downing D.T. Ceramides of pig epidermis: structure determination. *J. Lipid Res.* **24** (1983) 759-765.

21. Wertz P.W., Downing D.T. Epidermal lipids, in: L.A. Goldsmith (Eds.), Physiology, Biochemistry and Molecular Biology of the Skin, 2nd edition, Oxford University Press, Oxford, 1991, pp 205-235.

22. Weerheim A., Ponec M. Determination of stratum corneum lipid profile by tape stripping in combination with high-performance thin-layer chromatography. *Arch. Dermatol. Res.* **293** (2001) 191-199.

23. Nijsse J., van Aelst A.C. Cryo-planing for cryo-scanning electron microscopy. *Scanning* **21** (1999) 372-378.

24. Bras W. A SAXS/WAXS beamline at the ESRF and future experiments. *J. Macromol. Sci. Phys. B* **37** (1998) 557-566.

25. Dolbnya, I.P., Alberda, H., Hartjes, F.G., Udo, F., Bakker, R.E., Konijnenburg, M., Homan, E., Cerjak, I., Goedtkindt, P., Bras, W. A fast position sensitive MSGC detector at high count rate operation. *Rev. Sci. Instrum.* **73** (2002) 3754-3758.

26. Bouwstra J.A., Gooris G.S., Dubbelaar F.E.R., Ponec M. Cholesterol sulfate and calcium affect stratum corneum lipid organization over a wide temperature range. *J. Lipid Res.* **40** (1999) 2303-2312.

27. Wertz P.W., Downing D.T. Stratum corneum: biological and biochemical considerations, in: J. Hadgraft, R.H. Guy (Eds.), Transdermal drug delivery: developmental issues and research initiatives, Marcel Dekker Inc., New York, 1989, pp. 1-22.

28. Bradshaw J.P., Davies S.M.A., Hauss T. Interaction of substance p with phospholipid bilayers: a neutron diffraction study. *Biophys. J.* **75** (1998) 889-895.

29. Katsaras J., Tristram-Nagle S., Liu Y., Headrick R.L., Fontes E., Mason P.C., Nagle J.F. Clarification of the ripple phase of lecithin bilayers using fully hydrated, aligned samples. *Phys. Rev. E Stat. Phys. Plasmas Fluids Relat. Interdiscip. Topics* **61** (2000) 5668-5677.

30. de Jager M.W., Gooris G.S., Dolbnya I.P., Ponec M., Bouwstra J.A. Modelling the stratum corneum lipid organisation with synthetic lipid mixtures: The importance of ceramide composition. *Biochim. Biophysic. Acta* **1684** (2004) 132-140.

31. McIntosh T.J., Stewart M.E., Downing D.T. X-ray diffraction analysis of isolated skin lipids: reconstruction of intercellular lipid domains. *Biochemistry* **35** (1996) 3649-3653.

Chapter 8

A novel in vitro percutaneous penetration model: evaluation of barrier properties with p-aminobenzoic acid and two of its derivatives

M.W. de Jager,* H.W.W. Groenink,* R. Bielsa i Guivernau,[#] E.M. Andersson,[$] N.S. Angelova,* M. Ponec[§] and J.A. Bouwstra*

*Department of Drug Delivery Technology, Leiden/Amsterdam Center for Drug Research, University of Leiden, Leiden, The Netherlands.
[#]Department of Physico-Chemistry, Faculty of Pharmacy, University of Barcelona, Barcelona, Spain.
[$]Department of Pharmacy, University of Uppsala, Uppsala, Sweden.
[§]Department of Dermatology, Leiden University Medical Center, Leiden, The Netherlands.

(adapted from *Pharm. Res.*, in press)

ABSTRACT

The objective of this study was to evaluate the utility of a stratum corneum substitute (SCS) as a novel in vitro percutaneous penetration model. The SCS consists of synthetic stratum corneum (SC) lipids (cholesterol, free fatty acids, and specific ceramides) applied onto a porous substrate. The composition, organisation and orientation of lipids in the SCS bear high resemblance to that of the intercellular barrier lipids in SC. The barrier integrity of the SCS was evaluated by means of passive diffusion studies, using three model compounds with different lipophilicities. The effects of lipid layer thickness, permeant lipophilicity and altered lipid composition on the barrier properties were investigated, using isolated human SC as a control. For all three model compounds the permeability characteristics of the SCS having a 12 μm thick lipid layer closely resemble those of human SC. Modification of the lipid composition, generating a SCS that lacks the characteristic long periodicity phase as present in SC, was accompanied by a two-fold increased permeability. The SCS offers an attractive tool to predict solute permeation through human skin. Moreover, as its lipid composition can be modified, they may also serve as a suitable screening model for diseased skin.

1. INTRODUCTION

For many years, the delivery of drugs into and through the skin has been an important area for research. Due to the natural function of the skin, however, only a limited number of drugs are capable to cross the outer layer of the skin, the stratum corneum (SC). The SC consists of several layers of partially overlapping corneocytes, which are surrounded by a cell envelope and are embedded in a lipid matrix. Because of the highly impermeable character of the cornified envelope, substances that penetrate the SC bypass the corneocytes and follow the tortuous intercellular pathway [1-3]. As a result, the SC lipids provide the actual barrier to the diffusion of substances through the skin. The lipid lamellae, which are oriented approximately parallel to the surface of the corneocytes [4, 5], are predominantly composed of ceramides, cholesterol and free fatty acids. It has been demonstrated that these stacks of crystalline lipid layers have repeating patterns of approximately 13 nm (long periodicity phase: LPP) and 6 nm (short periodicity phase: SPP), respectively [6-8]. In particular the LPP is considered to play a crucial role for proper skin barrier function.

At present, the most common means to screen transdermal and dermal drug delivery systems is the use of epidermis or SC, isolated from excised human or animal skin. However, those studies are hampered by the scarcity of human tissue and high intra- and inter-individual variability of human and animal skin. Although animal skin is frequently used for permeation studies, its anatomical properties differ greatly from those of human skin. Due to the presence of numerous hair follicles and sebaceous glands, deviating composition and organisation of the intercellular SC lipids and SC thickness, skin permeability cannot always be predicted adequately when using animal skin [9-11]. Moreover, there will be an EU-wide ban on the use of animal skin in the testing of cosmetic products from 2009.

The quest to circumvent these problems has prompted an extensive search for novel reliable in vitro penetration models. A few studies described the formation of model membranes by using lipids extracted from pig SC on a porous substrate [12, 13]. However, such an approach does not obviate the variability of native tissue and the laborious and time-consuming isolation and separation of the SC lipids. Accordingly, membranes prepared with isolated ceramides cannot be used for large-scale screening studies. Model membranes have also been prepared with the commercially available bovine brain ceramide type III or IV [14-19]. Although the available information in literature about their use as a percutaneous penetration model is somewhat limited,

the transport of water and some permeants across those model membranes appear to be similar to that across SC [16-18]. However, it has been demonstrated that the lipid organisation in those lipid membranes does not resemble that of SC [19-21]. Moreover, no data on the orientation of the lamellae have been reported.

Obviously, the skin lipid membranes reported in literature do not meet all requirements for a reliable in vitro screening system to substitute for SC in diffusion studies. In a previous study, we developed a method to reproducibly produce a stratum corneum substitute (SCS) composed of cholesterol, long-chain free fatty acids and specific synthetic ceramides on a porous substrate [22]. The SCS was characterised in terms of uniformity of the lipid layer, distribution of the various lipid classes over the substrate surface and the orientation and organisation of the lipid lamellae [22]. To the best of our knowledge, that was the first study in which a SCS was prepared that resembles the composition, organisation and orientation of the intercellular lipid lamellae in SC.

The aim of the present study was to evaluate the barrier properties of this SCS and to explore the possibility of using it as a novel predictive in vitro skin barrier model. This was accomplished by means of passive diffusion studies, using flow-through diffusion chambers, with p-aminobenzoic acid (PABA), ethyl-PABA and butyl-PABA as model compounds and isolated human SC as a control sample. PABA is the most hydrophilic compound and its lipophilicity increases with increasing ester chain length (see Table 1). We aimed to answer the following questions:

(i) What is the effect of layer thickness on the diffusion profile?

(ii) What is the effect of permeant lipophilicity on the diffusion profile?

(iii) Is the presence of the LPP crucial for a proper permeability barrier?

2. MATERIALS AND METHODS

2.1 Materials

CER(EOS)C30, CER(NS)C24, CER(NP)C24, CER(NP)C16, CER(AS)C24 and CER(AP)C24 were generously provided by Cosmoferm B.V. (Delft, the Netherlands). The ceramides are composed of a long-chain sphingosine (S) or phytosphingosine (P) base with variations in the position and number of hydroxyl groups and double bonds. Through amide bonding, long-chain nonhydroxy (N) or α-hydroxy fatty acids (A) with a uniform acyl chain length (24 or 16 hydrocarbon atoms) are linked to the sphingoid bases. The exception is CER(EOS), which contains an ω-hydroxy fatty acid with a chain

length of 30–32 carbon atoms to which linoleic acid is linked (EO) [23].

Para-aminobenzoic acid (PABA), ethyl-PABA and butyl-PABA, trypsin (type III, from bovine pancreas) and trypsin inhibitor (Type II-S from soybean) were purchased from Sigma-Aldrich (Zwijndrecht, The Netherlands). Dialysis membrane disks (cut off value of 5000 Da) were purchased from Diachema (Munich, Germany). Nuclepore polycarbonate filter disks (pore size 50 nm) were purchased from Whatman (Kent, UK). All organic solvents used were of analytical grade and manufactured by Labscan Ltd (Dublin, Ireland). All other chemicals were of analytical grade. All aqueous solutions were prepared with Millipore water (Billerica, MA, USA).

2.2 Isolation of SC from human skin

SC was isolated from abdominal or mammary skin, which was obtained within 24 hours after cosmetic surgery. After removal of the subcutaneous fat tissue, the skin was dermatomed to a thickness of approximately 250 µm using a Padgett Electro Dermatome Model B (Kansas City, KS, USA). The SC was separated from the epidermis by trypsin digestion (0.1% in phosphate buffered saline pH 7.4), after overnight incubation at 4°C and subsequently at 37°C for 1 h. The SC was then placed in a 0.1 % solution of trypsin inhibitor and rinsed twice with Millipore water. Until use, the SC was stored in a silica containing box under gaseous nitrogen in the dark to prevent oxidation of the intercellular SC lipids.

2.3 Preparation of SCS

The components for the synthetic ceramide mixtures were CER(EOS), CER(NS)C24, CER(NP)C24, CER(AS)C24, CER(NP)C16 and CER(AP)C24 in a molar ratio 15:51:16:4:9:5 [22, 24]. This lipid composition resembles the ceramide composition in pig SC [25]. For the preparation of the free fatty acids mixtures, the following fatty acids were used: C16:0, C18:0, C20:0, C22:0, C23:0, C24:0 and C26:0 at molar ratios of 1.3, 3.3, 6.7, 41.7, 5.4, 36.8 and 4.7, respectively. This is similar to the composition of the free fatty acids in SC [26]. Appropriate amounts of individual lipids dissolved in chloroform:methanol (2:1) were combined to yield lipid mixtures at the desired equimolar composition of cholesterol, synthetic ceramides and free fatty acids. After evaporation of the organic solvent under a stream of nitrogen, the lipid mixtures were re-dissolved in hexane:ethanol (2:1) at a total lipid concentration of 4.5 mg/ml. An evolution solo airbrush (Airbrush Service Almere, The Netherlands) was used to spray the lipid mixtures onto a polycarbonate filter disk with a pore size of 50 nm.

Briefly, the substrate was mounted in a holder and fixed under the airbrush, which was constructed vertically with the nozzle facing downwards. The reservoir of the airbrush was subsequently filled with lipid solution. During the spraying period, the trigger of the airbrush was opened pneumatically for a certain adjustable time period, during which a small fraction of the lipid solution passed the nozzle. Due to this nitrogen pressure, the lipid solution was sprayed in very small droplets onto the porous substrate. During the drying stage, the trigger was closed, the organic solvent evaporated by the nitrogen flow and the lipids attached to the substrate. The number of spraying and drying cycles was adjustable to obtain the required layer thickness. The lipid-loaded filters were held at 70°C for 10 minutes and subsequently cooled to room temperature, after which the lipid organisation closely resembles that in human SC [22].

2.4 Diffusion studies

In vitro permeation studies were performed using Permegear in-line diffusion cells (Bethlehem, PA, USA) with a diffusion area of 0.28 cm^2. SC on a dialysis supporting membrane (apical side facing the donor chamber) or the SCS was mounted in the diffusion cell and was hydrated for 1h in phosphate buffered saline pH 7.4 prior to the experiment. The donor compartment was filled with 1280 µl of the drug solution in acetate buffer pH 5.0 at saturated concentrations to obtain equal thermodynamic activities. The acceptor compartment consisted of phosphate buffered saline pH 7.4, which was perfused at a flow rate of about 2 ml/h. The exact volume per collected fraction was determined by weighing. Each experiment was performed under occlusive conditions, by closing the opening of the donor compartment with adhesive tape. The temperature of the SC or SCS was maintained at 32°C during the total length of the experiment, using a thermostated water bath. Fractions were collected for 20 hours at a 1-hour interval. At the end of each experiment, the recovery was determined according to the following equation:

$$\text{Recovery} = \frac{(\text{amount penetrated} + \text{amount remaining in donor compartment})}{\text{initial amount in donor compartment}} \text{x}100\%$$

Table 1 - Compounds used in the present study

	PABA	ethyl-PABA	butyl-PABA
MW (g/mol)	137.1	165.2	193.2
$LogP_{oct/H2O}$	0.58	1.44	2.61
C_d (mg/ml)	6.16	0.65	0.05

2.4.1 Influence of compound lipophilicity on the diffusion profile across SC

Transport studies were performed across isolated human SC from 4 different donors. PABA, ethyl-PABA and butyl-PABA were used as model compounds (see Table 1). Each experiment was performed with SC originating from 1 donor, using 6 diffusion cells (i.e. 2 cells were used per test compound).

2.4.2 Influence of layer thickness on the diffusion profile across SC

To assess the effect of the SC thickness on the diffusion profile of ethyl-PABA, the diffusion was measured across i) a single SC sheet, ii) two SC sheets laid on top of each other or iii) three SC sheets placed on top of each other. Each experiment was performed with SC originating from 1 donor, using 6 diffusion cells (i.e. 2 cells were used per layer thickness). SC derived from 4 different donors was used per experimental condition.

2.4.3 Influence of lipid layer thickness on the diffusion profile across the SCS

Diffusion profiles of ethyl-PABA were measured across the SCS, that was prepared with 160, 230, 350 and 420 µg of lipid material in the diffusion area. Six lipid-loaded filters were prepared and used per condition.

2.4.4 Influence of compound lipophilicity on the diffusion profile across the SCS

Transport studies were performed across lipid-loaded filters, covered with approximately 350 µg of lipid in the diffusion area. PABA, ethyl-PABA and butyl-PABA were used as model compounds. Each experiment was performed with 6 diffusion cells (i.e. 2 cells were used per compound). The experiment was performed in triplicate.

2.4.5 Influence of altered lipid composition on the diffusion profile across the SCS

Diffusion profiles of ethyl-PABA were measured across the SCS, prepared with two ceramide mixtures, either containing or not containing CER(EOS). Each experiment was performed with 6 diffusion cells. In 3 diffusion cells, the SCS that was prepared with ceramide mixtures lacking CER(EOS) was mounted, whereas the other 3 cells served as a control and contained the SCS prepared with ceramide mixtures containing CER(EOS). The experiment was performed in duplicate.

2.5 HPLC analysis

The samples were analysed using a reverse-phase HPLC assay. The HPLC system consisted of a SP8810 LC pump (Spectra-Physics, California, USA) equipped with a Gilson 234 auto injector and UV-detector (Spectra-Physics UV150). A microparticulated C-18 column (Varian, Chromosper C-18, 100 x 3.0 mm) was used as stationary phase. The mobile phase for ethyl-PABA and butyl-PABA consisted of acetonitrile and water in a ratio of 40:60. Acetonitrile, water and acetic acid in a ratio of 20:78:2 was used as a mobile phase for PABA. The flow rate and the detection wavelength were set to 1.0 ml/min and 286 nm, respectively. A series of standards was run with each series of samples.

2.6 Data analysis

The flux and cumulative amount of the model compounds were plotted as a function of time. Steady state flux values (J_{ss}) were determined from the linear portions of the individual cumulative amount versus time plot. The lag time (t_{lag}) was determined by extrapolation of this curve to the intercept with the time axis. Permeability coefficients (P) were calculated according to the equation $P = J_{ss} / C_d$, in which C_d is the concentration of the solute in the donor solution (mg/cm^3). Diffusion coefficients (D) were calculated from the slopes of the linear portions of the permeability coefficients versus path length plots, according to the equation $P = (K*D)/h$, in which K represents the partition coefficient of the permeant between the SC or SCS and the donor solution, D the diffusion coefficient of the permeant in the SC or SCS (cm^2/s) and h the length of the pathway through the SC or SCS (cm).

All results are expressed as mean values ± standard deviations. Statistical analyses were performed using one-way ANOVA at a significance level set at $p<0.05$. When a statistical analysis was performed for only 2 groups, an unpaired two-tailed t-test was used.

2.7 Determination of the amount and thickness of the lipid layer on the filter

After each diffusion experiment, the quantity of lipid material that was present in the diffusion area was determined. Briefly, the SCS was cut into two equally sized parts. One part was dissolved in 100 µl chloroform/methanol (2:1) and the lipids were extracted by extensive vortexing. After evaporation of the organic solvent, the amount of lipids was subsequently determined by weighing. The other part was used for cryo-scanning electron microscopy to establish the thickness of the lipid layer and

to establish whether the SCS remains intact under the aqueous solutions used in the transport studies [22]. Briefly, the lipid-loaded filters were cut into sheets of 1.5 x 2 mm^2, folded and fixed in a small copper "shoe-nail" using Tissue-Tek O.C.T. Compound (Miles Inc. Elkhart, IN USA). The samples were then quickly frozen by plunge-freezing (Reichert Jung-KF80, Vienna, Austria) into liquid propane at –180°C. The frozen specimens were kept in liquid nitrogen until they were mounted into a sample holder. The cryo-fixed samples were planed in a cryo ultramicrotome (Leica Ultracut UCT/ Leica EM FCS, Wetzlar, Germany), using a specimen temperature of –90°C and a knife temperature of –100°C. Subsequently, the samples were vacuum dried for 3 min at –90°C at 0.1 Pa to obtain contrast and sputtered with a layer of platinum (CT 1500 HF, Oxford Instruments, UK). After transferring the specimens into the field emission scanning electron microscope (Jeol 6400F, Tokyo, Japan), the samples were analysed at -190°C. At least 4 microscopic images were taken from each SCS and 3 SCSs were examined per experimental condition. At equal distances of 20 µm along the cutting plane, the thickness of the cross section of each lipid layer was determined by establishing the pixel position of the top and bottom of the lipid layer in proportion to that of the magnification bar that is present in each micrograph.

3. RESULTS

3.1 The effect of layer thickness on the diffusion profile

To assure that the polycarbonate filter used for the generation of the SCS does not form an additional diffusion barrier, experiments were first carried out with lipid-free polycarbonate filters. The measured flux values of ethyl-PABA were approximately 15-fold higher (data not shown) than those measured across the SCS prepared with a 12 µm thick lipid layer or isolated human SC, indicating that the polycarbonate filter does not act as an additional barrier. In addition, the flux values of ethyl-PABA across the supporting dialysis membranes were investigated. These appeared to be approximately 10-fold higher (data not shown) than those across SC.

Figure 1 shows the flux profiles of ethyl-PABA across SC and the SCS as a function of time. The average steady-state flux (J_{ss}) and lag time (t_{lag}) values obtained from the individual cumulative amount versus time plots, together with the calculated permeability coefficient (P) are presented in Table 2. The t_{lag} values obtained in these permeation experiments are quite variable, which is reflected by large standard deviations. An increase in the SC thickness by increasing the number of SC layers from

one to three is accompanied by an almost 3-fold decrease in the J_{ss} and an almost 4-fold increase in the t_{lag}. For the SCS it can also be observed that the flux is highly affected by the layer thickness. Plots of P versus the reciprocal quantity of lipid material in the diffusion area (Fig. 2A) or P versus the reciprocal layer thickness of the SCS (Fig. 2B) both have positive linear slopes and a correlation coefficient of 0.96, indicating that the steady state diffusion across the SCS is in accordance with Fick's Law.

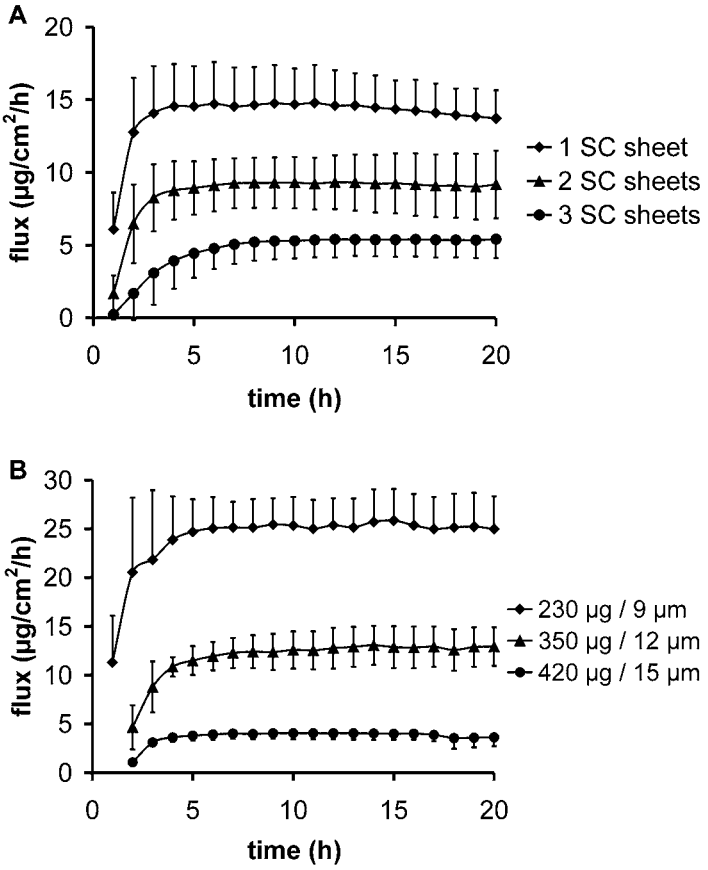

Figure 1 - The effect of layer thickness on the flux profiles of ethyl-PABA across isolated human SC (A) and the SCS (B). An increased layer thickness is accompanied by a decrease in the steady state flux. Data are presented as average ± sd (n=8 for SC and n=6 for the SCS).

In contrast to the J_{ss}, no relationship is found between the lipid layer thickness of the SCS and the t_{lag}. Independent of the lipid layer thickness, an average t_{lag} of approximately 1 h is observed. It should be stressed, however, that very short t_{lag} values cannot be appropriately determined with the diffusion set up used in the present

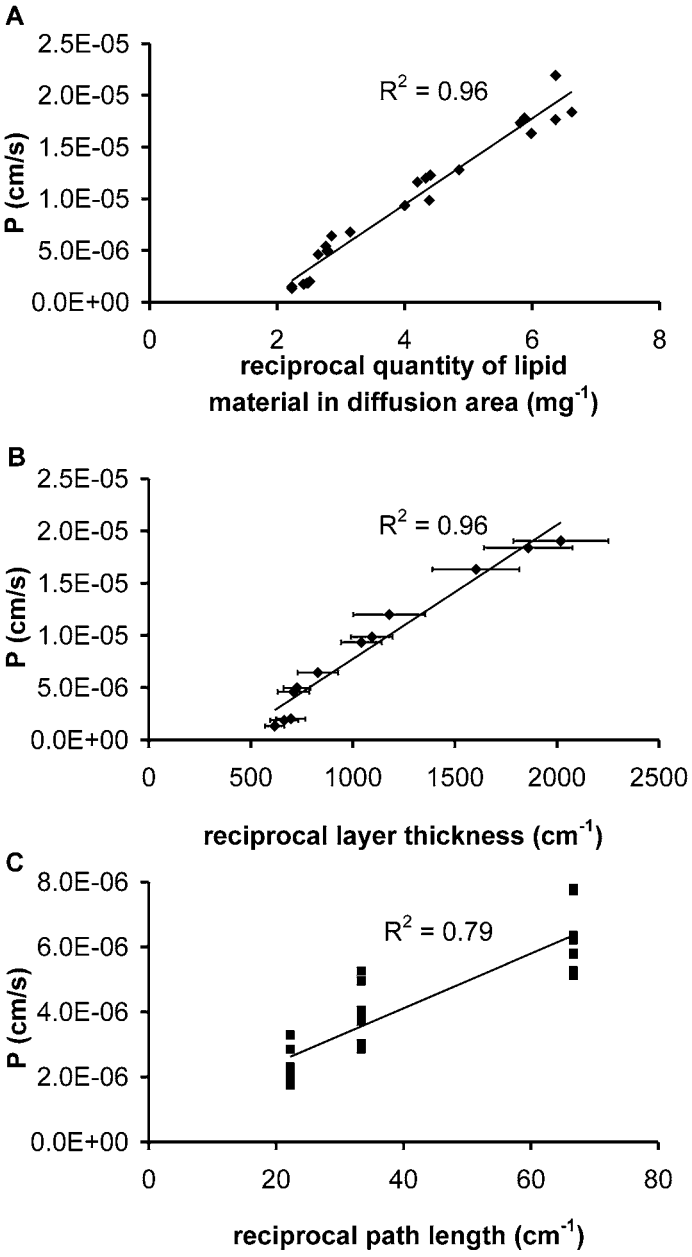

Figure 2 - The relationship between the partition coefficient and the reciprocal quantity of lipid material in the diffusion area (A), the relationship between the partition coefficient and the reciprocal layer thickness of the SCS (B), and the relationship between the partition coefficient and the reciprocal path length in SC (C). In accordance with Fick's first law of diffusion, the linear slope represents the diffusion coefficient multiplied with the partition coefficient. The reciprocal layer thickness values are presented as average ± sd. All lipid-loaded filters examined were still intact after the permeation studies and did not reveal the presence of any defects (open structures).

study. At a flow rate of 2 ml/hr it takes about 1 hour to replace the acceptor fluid in the acceptor compartment and the connecting tubings to the fraction collector. As a result, the obtained t_{lag} values of ethyl-PABA across the SCS may not reflect the real situation.

The results of these experiments convincingly show that the diffusion profile of ethyl-PABA across the SCS can be regulated by means of its layer thickness. Diffusion profiles of ethyl-PABA across a single SC sheet bear high resemblance to the SCS prepared with approximately 350 µg of lipid material in the diffusion area. This quantity corresponds to a lipid layer thickness of approximately 12 µm (see also Fig. 2B and 5B).

Table 2 - Influence of the layer thickness on the diffusion characteristics of ethyl-PABA. The numbers provided with the SCS are the amount of lipid in the diffusion area and the lipid membrane thickness, respectively.

parameter	1 SC sheet	2 SC sheets	3 SC sheets	SCS 160 µg/6 µm	SCS 230 µg/9 µm	SCS 350 µg/12 µm	SCS 420 µg/15 µm
J_{ss} (µg/cm²/h)	14.6 ± 2.4	9.2 ± 1.9	5.4 ± 1.2	42.6 ± 4.5	26.4 ± 3.3	12.9 ± 2.1	4.0 ± 0.6
t_{lag} (h)	0.8 ± 0.4	1.3 ± 0.4	3.0 ± 1.4	0.8 ± 0.6	1.3 ± 1.0	1.4 ± 0.3	1.0 ± 0.3
P (cm/s)	$6.3x10^{-6}$ ± $1.0x10^{-6}$	$4.0x10^{-6}$ ± $8.3x10^{-7}$	$2.3x10^{-6}$ ± $5.2x10^{-7}$	$1.8x10^{-5}$ ± $1.9x10^{-6}$	$1.1x10^{-5}$ ± $1.4x10^{-6}$	$5.5x10^{-6}$ ± $8.9x10^{-7}$	$1.7x10^{-6}$ ± $2.5x10^{-6}$
recovery (%)	101.3 ± 7.0	100.7 ± 6.5	99.2 ± 7.4	95.6 ± 3.9	100.2 ± 8.1	97.6 ± 5.6	95.2 ± 3.1

3.2 The effect of permeant lipophilicity on the diffusion profile

Figure 3A and 3B show the flux versus time profiles of the three model compounds across a single layer of SC and across the SCS prepared with approximately 350 µg of lipid material, respectively. In case of the SCS, a slight decrease in the J_{ss} of butyl-PABA can be observed after approximately 10 hours, which is due to depletion of the compound from the donor phase (Fig. 3B).

The average J_{ss} and t_{lag} values obtained from the individual cumulative amount versus time plots, together with P are presented in Table 3. The diffusion profiles of the three compounds across the SCS and SC are very similar. For both SCS and SC it can be observed that the t_{lag} of PABA is significantly longer than for the more lipophilic compounds ethyl-PABA and butyl-PABA. Furthermore, the t_{lag} of PABA across the SCS was found to be longer than that across SC. With respect to the t_{lag} of other two model compounds, however, no significant differences are observed between the SCS and SC.

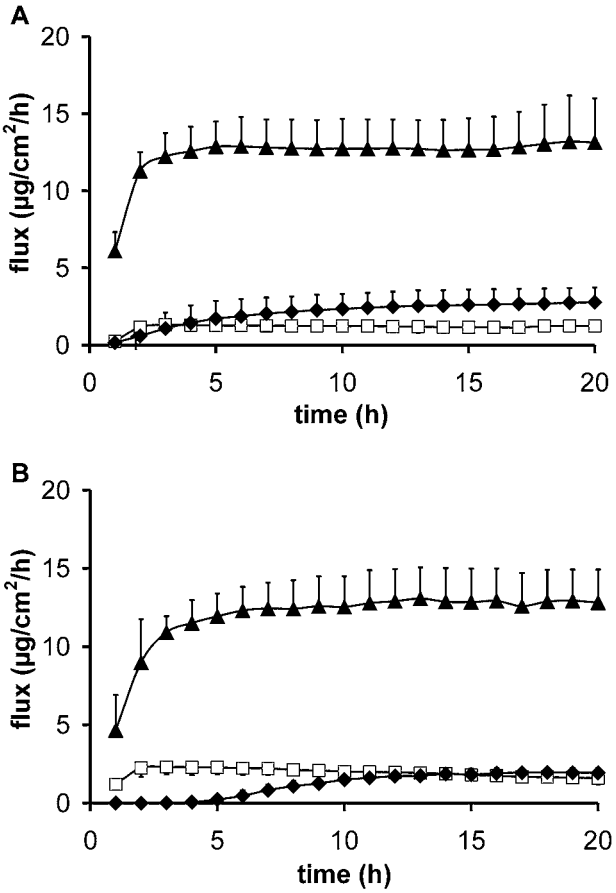

Figure 3 - The effect of permeant lipophilicity on the diffusion profile. Flux versus time profiles of PABA (-♦-), ethyl-PABA (-▲-) and butyl-PABA (-□-) across SC (A) and the SCS prepared with approximately 350 µg lipid material in the diffusion area (B).

The results further reveal that the highest fluxes are obtained with the intermediate lipophilic ethyl-PABA. Increasing (butyl-PABA) or decreasing (PABA) the compound lipophilicity results in a significant decrease in the J_{ss}. The calculated P values indicate that the permeability of both SC and SCS increases with increasing compound lipophilicity. For PABA and ethyl-PABA no significant differences in P (or J_{ss}) are observed between the SCS and SC. Compared to SC, however, the SCS appears to be slightly more permeable to butyl-PABA, as can be derived from the nearly 2-fold higher P (and J_{ss}).

Table 3 - Influence of the permeant lipophilicity on the diffusion characteristics across SC and the SCS

parameter	PABA SC	Ethyl-PABA SC	Butyl-PABA SC	PABA SCS	Ethyl-PABA SCS	Butyl-PABA SCS
J_{ss} (µg/cm²/h)	2.7 ± 1.0	12.5 ± 2.0	1.2 ± 0.3	2.0 ± 0.3	12.9 ± 2.1	2.2 ± 0.5
t_{lag} (h)	4.7 ± 1.7	0.7 ± 0.3	0.8 ± 0.6	7.4 ± 0.8	1.4 ± 0.3	0.7 ± 0.4
P (cm/s)	$1.2x10^{-7}$ ± $4.5x10^{-8}$	$5.4x10^{-6}$ ± $8.5x10^{-7}$	$7.2x10^{-6}$ ± $2.0x10^{-6}$	$8.8x10^{-8}$ ± $1.2x10^{-8}$	$5.5x10^{-6}$ ± $8.9x10^{-7}$	$1.3x10^{-5}$ ± $2.6x10^{-6}$
recovery (%)	n.d.	n.d.	n.d.	101.0 ± 1.1	97.6 ± 5.6	98.9 ± 3.4

3.3 Effect of altered lipid composition on the diffusion profile across the SCS

To investigate the effect of altered lipid composition on the permeability barrier, the SCS was also prepared with ceramide mixtures lacking CER(EOS). From previous X-ray diffraction studies it became evident that synthetic SC lipid mixtures prepared lacking CER(EOS) do not form the characteristic LPP [24, 27]. Figure 4 and Table 4 show that the SCS prepared with mixtures lacking CER(EOS) show almost two-fold higher J_{ss} values ($p<0.01$) than the SCS prepared with CER(EOS). This indicates that the 13 nm lamellar phase, at least partially, contributes to the barrier integrity of the SCS.

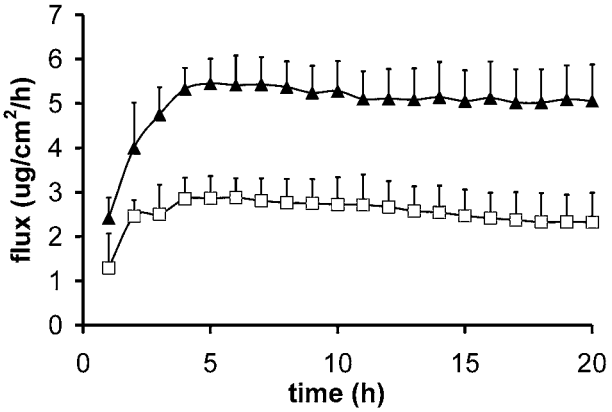

Figure 4 - The effect of altered lipid composition on the flux profiles of ethyl-PABA across the SCS, prepared with approximately 440 µg of lipid material in the diffusion area. The SCS prepared in the absence of CER(EOS) (-▲-) do not reveal the long periodicity phase. The reduced barrier efficacy of this SCS is reflected by a 2-fold increase in the steady state flux as compared to the SCS prepared in the presence of CER(EOS) (-□-). Data are presented as average ± sd (n=6).

Table 4 - Influence altered lipid composition of SCS on diffusion characteristics of ethyl-PABA

parameter	SCS prepared in the presence of CER(EOS)	SCS prepared in the absence of CER(EOS)
J_{ss} (µg/cm²/h)	2.7 ± 0.4	5.2 ± 0.7
t_{lag} (h)	0.6 ± 0.4	0.8 ± 0.6
P (cm/s)	$1.2x10^{-6}$ ± $1.8x10^{-7}$	$2.2x10^{-6}$ ± $3.2x10^{-7}$
recovery (%)	97.8 ± 9.1	94.9 ± 3.0

4. DISCUSSION

Our overall goal is to develop a skin barrier model (consisting of a porous substrate covered with synthetic SC lipids), which mimics the lipid composition, lipid organisation, lipid orientation and permeability barrier of human SC. This SCS may ultimately function as an in vitro screening system pertaining transdermal drug delivery. The main advantages of such a percutaneous penetration model are that i) it is a well-defined system, ii) it circumvents problems related to human or animal skin, iii) it is easy to handle and can be mounted in a commercially available Permegear diffusion cell, and iv) the composition of the synthetic SC lipids can be manipulated, which offers the opportunity to mimic the lipid organisation in healthy as well as diseased skin.

In a previous study, we have already demonstrated that an airbrush is an elegant apparatus to apply smooth and tightly packed lipid membranes of uniform thickness onto a polycarbonate filter [22]. Lipid analysis revealed that all lipids within the SCS are homogeneously distributed over the filter surface. The SCS further possesses two crystalline lamellar phases with periodicities of 12.2 and 5.4 nm, which are oriented parallel to the filter surface. Those results indicate that it is possible to prepare a SCS that closely resemble the lipid composition, organisation and orientation of the intercellular lipids in SC.

The present study investigated the permeability barrier of this SCS. The results convincingly show that the barrier properties of the SCS prepared with a 12 µm thick lipid layer are very similar to those of isolated human SC. However, some items need to be discussed to evaluate the full potential of the SCS as a novel in vitro percutaneous penetration model, namely i) differences in the penetration route between the SCS and SC, ii) the effect of permeant lipophilicity on the penetration profile, and iii) the effect of altered membrane composition on the permeability barrier of lipid membranes. Each of these items is discussed below.

4.1 Differences in penetration route between SCS and SC

Diffusion profiles of ethyl-PABA across the SCS prepared with a 12 µm thick lipid layer show high similarity to those obtained with isolated human SC. An increased layer thickness is accompanied by an increased barrier efficacy, which is reflected by a decrease in J_{ss}. However, an increased layer thickness does not result in an increased t_{lag}, which is different from the observations made with SC. It is therefore of interest to compare the organisation of the synthetic lipids in the SCS with the intercellular lipids in SC.

4.1.1 Difference in number of lipid lamellae

SC consists of approximately 15 layers of partially overlapping corneocytes (28). When the assumptions are made that (i) 6 lamellae are present between two adjacent corneocytes and (ii) the repeat distance of these lamellae is 13 nm, it can be calculated that the total thickness of the intercellular lipid lamellae in SC is approximately 1.2 µm [3]. This is 10-fold smaller than the thickness of the lipid layer in the SCS, being approximately 12 µm. When the quantity of lipid material present per unit area in SC and the SCS is compared, again a nearly 10-fold difference is observed. Whereas the SCS is composed of approximately 350 µg lipid material in the diffusion area, SC only contains approximately 30 µg lipids. This latter calculation is based on the assumptions that (i) ceramides, cholesterol and free fatty acids account for 10% of the SC dry weight (3), (ii) the density of SC is 1 g/cm^3, and (iii) the thickness of dry SC is 10 µm [29].

4.1.2 Difference in penetration path length

Another difference between SC and the SCS is the penetration path length, h. Figure 5A shows a cryo-scanning electron microscopy picture of isolated human SC, hydrated in phosphate buffered saline. SC contains corneocytes, which are all surrounded by a very impermeable cornified envelope. As a result, compounds that penetrate the SC do not traverse the interior of the corneocytes, but follow the tortuous path along the corneocytes [1-3]. Based on this principle, Talreja et al. [29] calculated the tortuous lipid path length in alkali-expanded human SC from arbitrary points on the SC surface to the viable epidermis. Based on their results, average path lengths of 180 and 130 µm are reported for alkali-expanded and dry SC, respectively. As the alkaline expansion technique produces swelling of the SC comparable to that obtained with full hydration [29], 150 µm has been advocated as a realistic penetration path length in

PBS hydrated SC, used in the present study.

In contrast to SC, the SCS is solely composed of synthetic lipids and does not contain corneocytes. We hypothesise that the path length in the SCS is perpendicular to the lipid membrane surface, rather than tortuous, and therefore equal to the thickness of the lipid layer, being approximately 12 µm. As compounds may not only diffuse perpendicularly to the lipid lamellae, but also parallel to the lipid lamellae, the actual path length in both the SCS and SC might be considerably longer than the proposed 150 and 12 µm. In fact, to bypass the corneocytes in the SC, a compound already needs to diffuse laterally to some extent. For instance, through mathematical modeling, Johnson et al. [3] calculated that the effective tortuosity in SC (i.e. taking into account parallel diffusion) is approximately 3.6 cm.

4.1.3 Difference in diffusion coefficient

Figure 2C shows the relationship between the calculated permeability coefficient in SC and the reciprocal penetration path length, assuming an intercellular path length of 150, 300 and 450 µm in 1, 2 and 3 SC sheets, respectively. From the slope of the linear portions of Figure 2B and 2C, the diffusion coefficient D was calculated. For these calculations, the partition coefficient of ethyl-PABA between the SC or lipid membranes and the donor solution is assumed to be equal to the octanol to water partition coefficient of ethyl-PABA. The diffusion coefficient in the SCS ($D = 4.7 \times 10^{-10}$ cm^2/s) is nearly 6-fold smaller than in SC ($D = 2.7 \times 10^{-9}$ cm^2/s). This indicates that, despite the shorter path length in the SCS, the mobility of ethyl-PABA is lower than in SC, assuming that the estimated penetration path lengths in SC and SCS are correct. A possible explanation for the lower diffusion coefficient in the SCS is that ethyl-PABA has to cross 10-fold more lamellae, as the total thickness of the SCS is 10-fold larger than in SC. Moreover, the corneocytes and adjacent lamellae in SC are not exactly running parallel to the skin surface. As a result, the penetration into the SC is not only affected by diffusion perpendicular to the lipid lamellae but also by diffusion parallel to the lipid lamellae (illustrated in Fig. 5C). We would like to stress that the diffusion rate parallel to the lipid lamellae may be higher than the diffusion rate perpendicular to the lipid lamellae, as in the latter a compound has to pass alternately lipophilic and hydrophilic domains.

In contrast to the SCS, native SC contains appendages, such as sweat glands and hair follicles with their associated sebaceous glands. As the appendages only represent approximately 0.1% of the total skin area [30], for passive diffusion

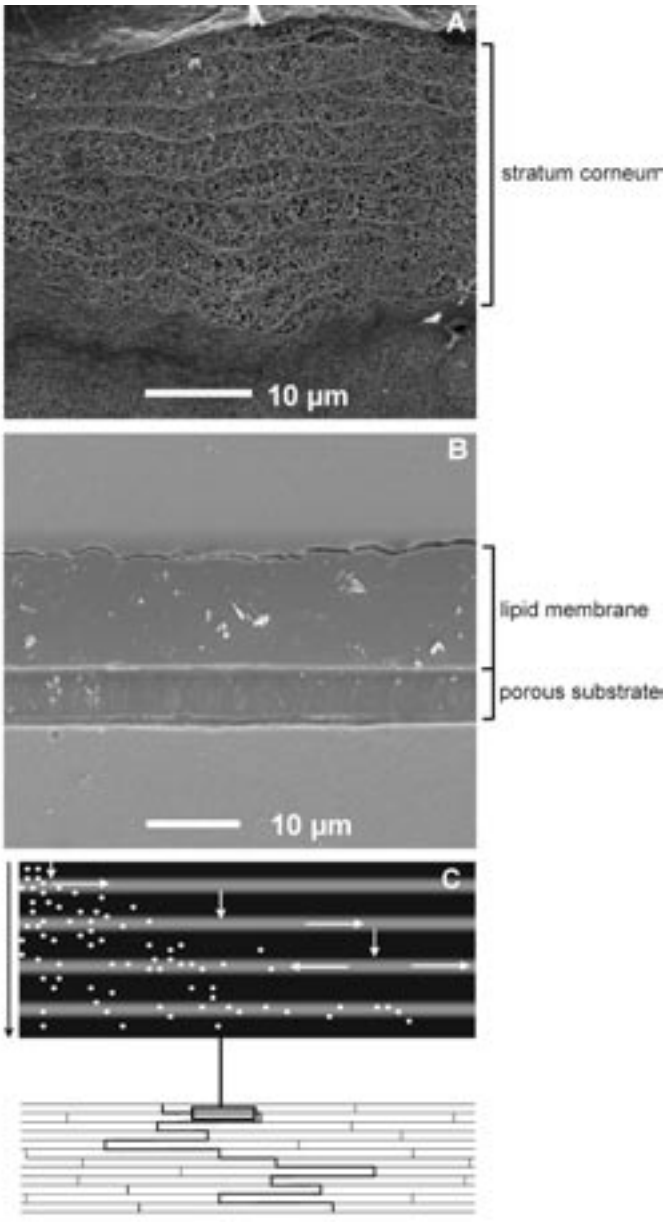

Figure 5 - Cryo-scanning electron microscopy photos of isolated human SC, hydrated in phosphate buffered saline (A). and the SCS after a permeation experiment (B). Schematic representation of SC and parallel diffusion (C). The wall-like structure represents the partially overlapping corneocytes (bricks) and the surrounding lipids (mortar). The thick line illustrates a possible penetration route, which a substance may take to travel from the SC surface to the viable epidermis. However, as parallel diffusion of molecules within the stacks of lamellae is possible (see magnification), the actual path length may be considerably increased. The black vertical arrow indicates the concentration gradient.

the transappendageal route is frequently considered to be less important than the transepidermal route. The results of the present study reveal that pores as remnants of the transappendageal route, which may be present in the diffusion area of the isolated SC pieces, do not contribute significantly to the transport of ethyl-PABA. Pores that might be present in the SC pieces are blocked when two or more SC sheets are placed on top of each other. When pores would play a significant role in the diffusion of ethyl-PABA across SC, a non-linear decrease in the permeability coefficient is expected [31]. However, as a linear relationship is obtained between the permeability coefficient and the reciprocal path length (see Fig. 2C), pores are not considered to contribute significantly to the transport of ethyl-PABA through SC. Moreover, constant relative standard deviations are found for J_{ss} and t_{lag} of ethyl-PABA across one, two or three SC sheets.

4.2 The effect of permeant lipophilicity on the permeability coefficient in SCS is similar to that in SC

The results of the present study show that the permeability coefficients of PABA, ethyl-PABA and butyl-PABA in the SCS prepared with a 12 µm thick lipid layer closely resemble those in SC. This means that the SCS has very similar permeability characteristics as human SC. It has further been demonstrated that the permeability coefficient increases in the order PABA<ethyl-PABA<butyl-PABA (see Table 3). This is consistent with literature data obtained with human or hairless mouse skin, in which a linear relationship between the permeability and the lipophilicity of homologous *n*-alkanols or hydrocortisone-21 esters is reported until a plateau is reached [32, 33].

The SCS appears to be slightly more permeable to the most lipophilic compound butyl-PABA. However, the observed differences in P and J_{ss} are maximal 2-fold, which are much smaller than reported for other compounds when using animal or in vitro reconstructed skin to replace human SC [10, 11, 34-36]. Differences in the permeability between SC and the SCS may be explained by differences in the lipid composition. The SCS is composed solely of synthetic ceramides, cholesterol and free fatty acids, whereas SC also contains more hydrophilic lipids, in particular in the deepest layers. This may also explain the slightly increased t_{lag} of PABA through the SCS as compared with SC. The barrier properties of the SCS to extremely lipophilic and hydrophilic compounds, including water, remain to be elucidated.

4.3 Alteration of lipid composition of SCS affects solute permeation

The LPP is always considered to play an important role in the skin barrier function. To date, however, no direct evidence is available from permeability studies that this is indeed the case. One of the major advantages of the SCS is that the composition of the lipid mixtures can be accurately chosen and modified. This offers excellent opportunities to systemically investigate the role of each lipid subclass for proper lipid organisation and barrier function. The results of the present study show that the SCS prepared with a ceramide mixture lacking CER(EOS) is more permeable to solute permeation than the SCS prepared in the presence of CER(EOS). In previous studies it has been established that lipid mixtures lacking CER(EOS) do not form the LPP [24, 27]. These results demonstrate that the LPP contributes to the barrier integrity of the SCS. In certain skin disorders, such as psoriasis and atopic dermatitis, a marked reduction of CER(EOS) in the lesion parts of the SC is observed [23, 37-40]. Extrapolation of the present results to the in vivo situation suggests that the observed barrier malfunction in these skin diseases can at least in part be explained by a reduced formation of the LPP.

Ultimately, a SCS may be generated that imitates the lipid composition and organisation as observed in various skin diseases. Such studies are of crucial importance to elucidate the relationship between lipid composition, organisation and barrier function. Moreover, this may provide unique possibilities to more adequately predict the permeation of drug substances through diseased skin, for which there is currently no alternative.

5. CONCLUSION

The results of the present study convincingly show that the SCS prepared with cholesterol, free fatty acids and specific synthetic ceramides can successfully be used to predict solute permeation through the skin. The barrier properties of the SCS can easily be adjusted by applying different amounts of lipids or by modifying its lipid composition, mimicking that of diseased skin. This demonstrates that this novel SCS has a great potential to be used in screening studies. However, further studies are required in order to investigate the barrier properties of the SCS to other compounds and different formulations, including those with penetration enhancers.

Acknowledgements

This work was supported by a grant from the Technology Foundation STW (LGN4654). The authors would like to thank the Center for Electron Microscopy (Leiden University Medical Center) and the Department of Plant Sciences (Wageningen University) for the use of their electron microscopy facilities.

REFERENCES

1. Boddé H.E., van den Brink I., Koerten H.K., de Haan F.H.N. Visualization of in vitro percutaneous penetration of mercuric chloride transport through intercellular space versus cellular uptake through desmosomes. *J. Control. Release* **15** (1991) 227-236.

2. Meuwissen M.E.M.J., Janssen J., Cullander C., Junginger H.E., Bouwstra J.A. A cross-section device to improve visualization of fluorescent probe penetration into the skin by confocal laser scanning microscopy. *Pharm. Res.* **15** (1998) 352-356.

3. Johnson M.E., Blankschtein D., Langer R. Evaluation of solute permeation through the stratum corneum: lateral bilayer diffusion as the primary transport mechanism. J. *Pharm. Sci.* **86** (1997)1162-1172.

4. Madison K.C., Schwartzendruber D.C., Wertz P.W., Downing D.T. Presence of intact intercellular lipid lamellae in the upper layers of the stratum corneum. *J. Invest. Dermatol.* **88** (1987) 714-718.

5. Schwartzendruber D.C., Wertz P.W., Kitko D.J., Madison K.C., Downing D.T. Molecular models of intercellular lipid lamellae in mammalian stratum corneum. *J. Invest. Dermatol*. **92** (1989) 251-257.

6. Bouwstra J.A., Gooris G.S., van der Spek J.A., Bras W. The structure of human stratum corneum as determined by small angle X-ray scattering. *J. Invest. Dermatol.* **96** (1991) 1006-1014.

7. Bouwstra J.A., Gooris G.S., van der Spek J.A., Bras W. Structural investigations of human stratum corneum by small angle X-ray scattering. *J. Invest. Dermatol.* **97** (1991) 1005-1012.

8. Bouwstra J.A., Gooris G.S., Bras W., Downing D.T. Lipid organization in pig stratum corneum. *J. Lipid Res.* **36** (1995) 685-695.

9. Behl C.R., Flynn G.L., Kurihara T., Smith W., Higuchi W.I., Ho N.F.W., Pierson C.L. Hydration and percutaneous absorption: I. Influence of hydration on alcohol permeation through hairless mouse skin. *J. Invest. Dermatol.* **75** (1980) 346-352.

10. Catz P., Friend D.R. Transdermal delivery of levonorgestrel. VII. Effect of enhancers on rat skin, hairless mouse skin, hairless guinea pig skin, and human skin. *Int. J. Pharm.* **58** (1990) 93-102.

11. Schmook F.P., Meingassner J.G., Billich A. Comparison of human skin or epidermis models with human and animal skin in in-vitro percutaneous absorption. *Int. J. Pharm.* **215** (2001) 51-56.

12. Friberg S.E., Kayali I., Beckerman W., Rhein L.D., Simion A. Water permeation of reaggregated stratum corneum with model lipids. *J. Invest. Dermatol.* **94** (1990) 377-380.

13. Kuempel D., Swartzendruber D.C., Squier C.A., Wertz P.W. In vitro reconstitution of stratum corneum lipid lamellae. *Biochim. Biophys. Acta* **1372** (1998) 135-140.

14. Abraham W., Downing D.T. Preparation of model membranes for skin permeability studies using stratum corneum lipids. *J. Invest. Dermatol.* **93** (1989) 809-813.

15. Friberg S.E., Kayali I. Water evaporation rates from a model of stratum corneum lipids. *J. Pharm. Sci.* **78** (1989) 639-643.

16. Kittayanond D., Dowton S.M., Ramachandran C., Flynn G.L., Weiner N. Development of a model of the lipid constituent phase of the stratum corneum: II. Preparation of artificial membranes from synthetic lipids and assessment of permeability properties using in vitro diffusion experiments. *J. Soc. Cosmet. Chem.* **43** (1992) 237-249.

17. Matsuzaki K., Imaoka T., Asano M., Miyajima K. Development of a model membrane system using stratum corneum lipids for estimation of drug skin permeability. *Chem. Pharm. Bull.* **41** (1993) 575-579.

18. Miyajima K., Tanikawa S., Asano M., Matsuzaki K. Effects of absorption enhancers and lipid composition on drug permeability through the model membrane using stratum corneum lipids. *Chem. Pharm. Bull.* **42** (1994) 1345-1347.

19. Lieckfeldt R., Villalain J., Gomez-Fernandez J.C., Lee G. Diffusivity and structural polymorphism in some model stratum corneum lipid systems. *Biochim. Biophys. Acta* **1151** (1993) 182-188.

20. Bouwstra J.A., Thewalt J., Gooris G.S., Kitson N. A model membrane approach to the epidermal permeability barrier: an X-ray diffraction study. *Biochemistry* **36** (1997) 7717-7725.

21. de Jager, M.W., Gooris G.S., Dolbnya I.P., Bras W., Ponec M., Bouwstra J.A.. The phase behaviour of lipid mixtures based on synthetic ceramides. *Chem. Phys. Lipids* **124** (2003) 123-134.

22. de Jager M.W., Gooris G.S., Ponec M., and Bouwstra J.A.. Preparation and characterization of a stratum corneum substitute for in vitro percutaneous penetration studies. *Biochim. Biophys. Acta*, in press.

23. Motta S., Monti M., Sesana S., Caputo R., Carelli S., Ghidoni R. Ceramide composition of the psoriatic scale. *Biochim. Biophys. Acta* **8** (1993) 147-151.

24. de Jager M.W., Gooris G.S., Ponec M., Bouwstra J.A. Lipid mixtures prepared with well-defined synthetic ceramides closely mimic the unique stratum corneum lipid phase behaviour. *J. Lipid Res.* **46** (2005) 2649-2656.

25. Bouwstra J.A., Gooris G.S., Cheng K., Weerheim A., Bras W., Ponec M. Phase behavior of isolated skin lipids. *J. Lipid Res*. **37** (1996) 999-1011.

26. Wertz P.W., Downing D.T. Epidermal lipids, in: L.A. Goldsmith (Eds.), Physiology, Biochemistry and Molecular Biology of the Skin, 2nd edition, Oxford University Press, Oxford, 1991, pp 205-235.

27. de Jager M., Gooris G., Ponec M., Bouwstra J. Acylceramide head group architecture affects lipid organization in synthetic ceramide mixtures. *J. Invest. Dermatol.* **123** (2004) 911-916.

28. Ya-Xian Z., Suetake T., Tagami H. Number of cell layers of the stratum corneum in normal skin - relationship to the anatomical location on the body, age, sex and physical parameters. *Arch. Dermatol. Res.* **291** (1999) 555-559.

29. Talreja P.S., Kasting G.B., Kleene N.K., Pickens W.L., Wang T.F. Visualization of the lipid barrier and measurement of lipid pathlength in human stratum corneum. *AAPS Pharm. Sci.* **3** (2001) Article 13:1-9.

30. Barry B.W. Structure, function, diseases, and topical treatment of human skin. In Dermatological Formulations: Percutaneous absorption, Marcel Dekker Inc., New York, 1983, pp 1-48.

31. Essa E.A., Bonner M.C., Barry B.W. Human skin sandwich for assessing shunt route penetration during passive and iontophoretic drug and liposome delivery. *J. Pharm. Pharmacol.* **54** (2002) 1481-1490.

32. Cross S.E., Magnusson B.M., Winckle G., Anissimov Y., Roberts M.S. Determination of the effect of lipophilicity on the in vitro permeability and tissue reservoir characteristics of topically applied solutes in human skin layers. *J. Invest. Dermatol.* **120** (2003) 759-764.

33. Schaefer H., Redelmeier T.E. Skin barrier. Principles of percutaneous absorption. Karger, Basel, 1996.

34. Garcia N., Doucet O., Bayer M., Fouchard D., Zastrow L., Marty J.P. Characterization of the barrier function in a reconstituted human epidermis cultivated in chemically defined medium. *Int. J. Cosm. Sci.* **24** (2002) 25-34.

35. Roy S.D., Fujiki J., Fleitman J.S. Permeabilities of alkyl p-aminobenzoates through living skin equivalents and cadaver skin. *J. Pharm. Sci.* **82** (1993) 1266-1269.

36. Wagner H., Kosta K.H., Lehr K.M., Schaefer U.F. Interrelation of permeation and penetration parameters obtained from in vitro experiments with human skin and skin equivalents *J. Control. Release* **75** (2001) 283-295.

37. Di Nardo A., Wertz P., Giannetti A., Seidenari S. Ceramide and cholesterol composition in the skin in patients with atopic dermatitis. *Acta Derm. Venereol. (Stockh.)* **78** (1998) 27-30.

38. Ghadially R., Reed J.T., Elias P.M. Stratum corneum structure and function correlates with phenotype in psoriasis. *J. Invest. Dermatol.* **107** (1996) 558-564.

39. Yamamoto A., Serizaka S., Ito M., Sato Y. Stratum corneum lipid abnormalities in atopic dermatitis. A*rch. Dermatol. Res.* **283** (1991) 219-223.

40. Lavrijsen A.P.M., Bouwstra J.A., Gooris G.S., Boddé H.E., Ponec M. Reduced skin barrier function parallels abnormal stratum corneum lipid organisation in patients with lamellar ichthyosis. *J. Invest. Dermatol.* **105** (1995) 619-624.

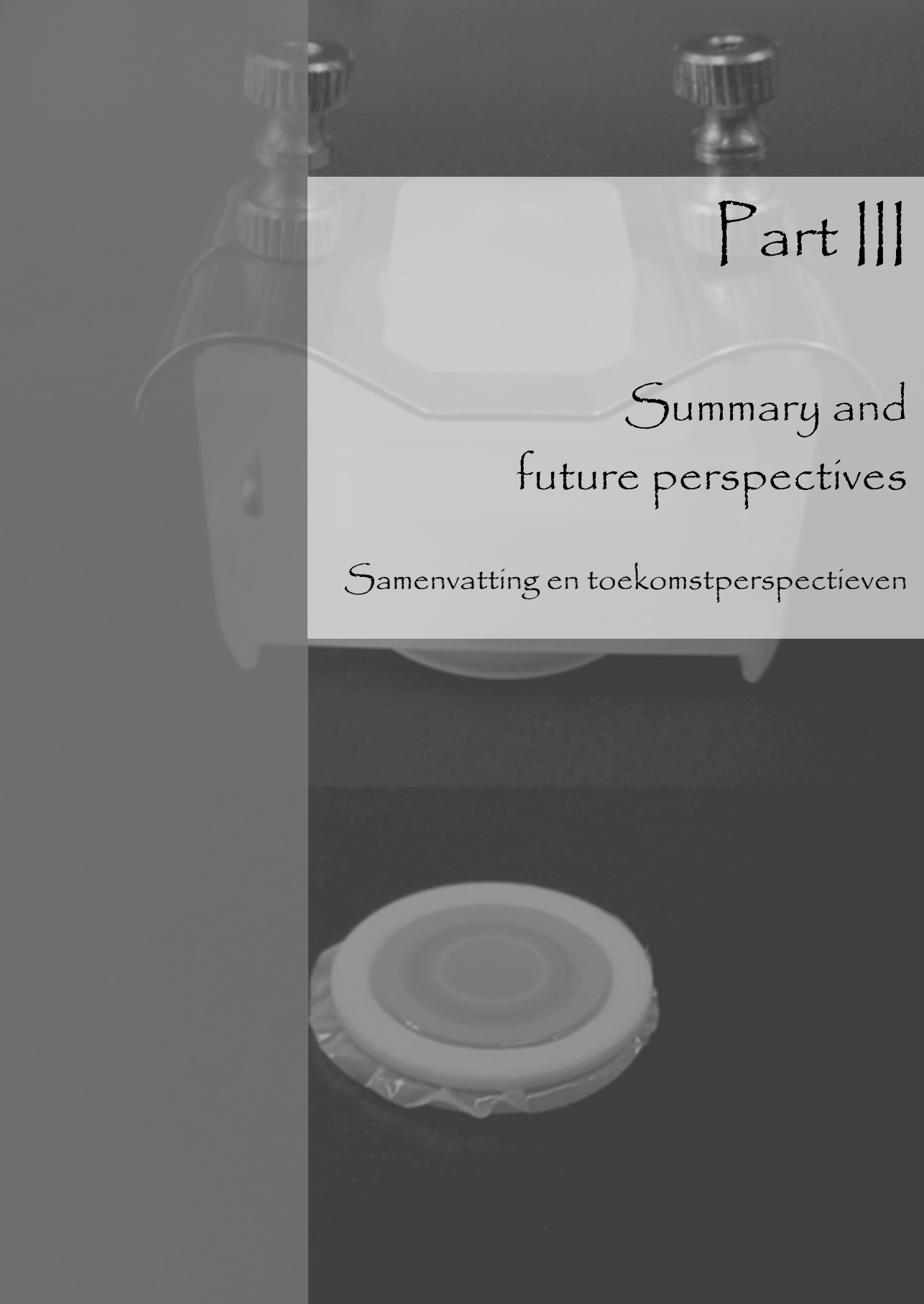

Part III

Summary and future perspectives

Samenvatting en toekomstperspectieven

Chapter 9

Summary and future perspectives

INTRODUCTION

The outer layer of the skin, the stratum corneum (SC), forms an effective barrier to retain water within the body and keep exogenous compounds out of the body. It consists of several layers of overlapping corneocytes, which are surrounded by a cell envelope and embedded in a matrix of lipid lamellae. Because of the highly impermeable character of the cornified envelope, substances that penetrate the SC bypass the corneocytes and follow the tortuous intercellular pathway. As a result, the SC lipids provide the actual barrier to the permeation of substances through the skin. The lipid lamellae, which are oriented approximately parallel to the surface of the corneocytes, are predominantly composed of cholesterol, free fatty acids and various classes of ceramides. It has been demonstrated that these stacks of lamellar lipid layers have repeating patterns of approximately 13 nm (long periodicity phase: LPP) and 6 nm (short periodicity phase: SPP), respectively [1]. In particular the LPP and the crystalline packing are believed to be critical for the skin barrier function.

SC, isolated from excised animal or human skin, is often used to study the transport of compounds from cosmetic formulations or drug delivery systems into or through the skin. However, human and animal skin are notorious for the high intra- and inter-individual variability. In addition, there is a scarcity of human tissue, in particular diseased and dry skin, whereas numerous topical products are especially designed for these skin types. Diseased and dry skin often show a defective barrier function, which is at least in part attributable to alterations in the SC lipid profile [2-4]. Animal skin, on the other hand, is usually more permeable to solute permeation than human skin. It can therefore be questioned whether animal skin is a representative model for human skin [5-6]. Moreover, due to regulations of the European Union, the use of animal skin for cosmetic purposes will be prohibited from 2009 [7]. Ultimately, there is an urgent demand for novel reproducible screening systems to predict the penetration of drug candidates through the skin.

The research outlined in this thesis is focused on the development of a skin barrier

model, which can substitute for SC in diffusion studies. This so-called stratum corneum substitute (SCS) consists of reconstituted synthetic SC lipids (cholesterol, ceramides and free fatty acids), applied onto a porous substrate. To mimic the barrier properties of human skin, the SCS should mimic the composition, organisation and orientation of the intercellular lipids in the SC.

The objectives of this thesis are:

(i) Selection of a synthetic ceramide mixture that mimics the phase behaviour of the intercellular lipids in human SC.

(ii) Preparation of a homogeneous SCS in terms of lipid composition, organisation, orientation and membrane layer thickness.

(iii) Evaluation of the permeability barrier of the SCS.

PART I – Selection of a synthetic SC lipid mixture

Ceramides are structurally heterogeneous and consist of two long saturated hydrocarbon chains and a small polar head group with several functional groups. Each of the 9 ceramides (CER1-CER9) identified in human SC [8] contains a sphingoid base and a fatty acid, which are linked by an amide bond between the carboxyl group of the fatty acid and the amino group of the base. The sphingoid moiety can be sphingosine, phytosphingosine or 6-hydroxysphingosine, whereas the fatty acid moiety is non-hydroxylated or α-hydroxylated with chain lengths of predominantly 24 to 26 hydrocarbon atoms. The most remarkable ceramides are the acylceramides (CER1, CER4 and CER9). These ceramides consist of an unusual long ω-hydroxy fatty acid of 30 to 34 hydrocarbon atoms to which unsaturated linoleic acid is ester-linked.

In previous studies it has been demonstrated that mixtures of cholesterol, free fatty acids and ceramides isolated from human or pig SC closely resemble the lamellar and lateral organisation in native SC, provided that CER1 is present in the mixture [9, 10]. In addition, mixtures based on commercially available ceramides have been developed to elucidate the unique SC lipid organisation. The most widely studied mixture consists of equimolar amounts of cholesterol, palmitic acid and bovine brain ceramide type III (structurally similar to CER2, but with shorter fatty acid chain lengths [11]). Although some features of the SC lateral organisation appeared to be similar, the characteristic long periodicity phase was not formed in mixtures based on bovine brain ceramide type III [12, 13].

Chapter 2 serves as a first link between the lipid organisation in well-defined synthetic ceramide mixtures and the more complex ceramide mixtures isolated from native SC. Therefore, the phase behaviour of synthetic ceramides, either single or mixed with cholesterol or cholesterol and free fatty acids, was investigated with small-angle and wide-angle X-ray diffraction. Four commercially available ceramides were selected for that study, namely CER3 with a chain length of 24 carbon atoms (CER3(C24)), CER3 with a chain length of 16 carbon atoms (CER3(C16)), bovine brain ceramide type III (ΣCERIII) and bovine brain ceramide type IV (ΣCERIV). Whereas CER3 contains a phytosphingoid backbone to which fatty acids of a single chain length are bound, ΣCERIII and ΣCERIV contain a sphingosine backbone to which fatty acids with varying chain lengths are linked. The effects of compositional changes, including the addition of synthetic CER1(C30), on the phase behaviour of synthetic ceramide mixtures were systematically examined.

In contrast to the observations made with single ΣCERIII or ΣCERIV, two coexisting crystalline phases can be detected in CER3(C16) or CER3(C24). This kind of polymorphism has previously been reported by Dahlen and Pascher [14]. Due to strong intermolecular head group hydrogen bonding, CER3 forms a V-shaped structure (the phytosphingosine and fatty acid chain form separate matrices). The difference in periodicities between the two phases depends on the tilt angles of the two hydrocarbon chains.

It was further demonstrated that both the presence of synthetic CER1 as well as a proper composition of the other ceramides in the mixture are crucial for the formation of a phase with a long periodicity. Lipid mixtures prepared with a ceramide fraction of CER1 and ΣCERIII or CER1 and ΣCERIV do not form the LPP. Only a mixture containing synthetic CER1, CER3(C24), cholesterol and free fatty acids shows the formation of a lamellar phase with a long periodicity. However, the number and intensities of the reflections attributed to this phase are rather small, which indicates that only a small fraction of lipids participates in the formation of this phase. Moreover, the periodicity of 11.6 nm differs from that observed in SC or in lipid mixtures prepared with isolated ceramides.

To increase the repeat distance and the fraction of lipids forming the LPP, both the preparation method and the composition of the lipid mixtures were optimised. Firstly, the influence of the equilibration temperature during sample preparation and the fraction of free fatty acids in the lipid mixture on the phase behaviour was investigated (chapter 3). All variations in that study were performed with a fixed composition of

synthetic ceramides, namely CER1, CER3(C24) and ΣCERIV in a 1:7:2 molar ratio (further referred to as synthCER I). ΣCERIV was incorporated into the mixture to introduce some variation in acyl chain length and in head group architecture.

Equimolar mixtures of cholesterol and synthCER I were equilibrated at temperatures ranging from 60 to 100°C. The results demonstrate that an increased equilibration temperature promotes the formation of the LPP. Whereas no LPP is present in lipid mixtures equilibrated at 60°C, a dominant formation of the LPP with a periodicity of 12.2 nm is observed in lipid mixtures that were equilibrated at 95 or 100°C. Besides, an increased equilibration temperature enhances the formation of a phase with a periodicity of 4.3 nm at the expense of a phase with a periodicity of 3.7 nm. Both phases are attributed to phase-separated CER3 in a V-shaped structure (see chapter 2) and are not present in native SC.

The influence of the relative content of free fatty acids on the lipid phase behaviour was subsequently investigated by preparing mixtures of cholesterol, synthCER I and free fatty acids ranging from a molar ratio of 1:1:0 to 1:1:1.8. Addition of free fatty acids to equimolar mixtures of cholesterol and synthCER I obviously increased the fluidity of the lipids, as equilibration at 95°C resulted in melting of the lipids. For this reason, a lower equilibration temperature was chosen, namely 80°C. Up to an equimolar content, systematic increase in the free fatty acids content promotes the formation of both LPP (12.2 nm) and SPP (5.5 nm). However, when the relative free fatty acids content is further raised, the formation of the LPP is reduced and the SPP dominates. Other observations made in the presence of free fatty acids are: (i) The lamellar phases are more ordered, as diffraction peaks up to a higher order can be observed for both LPP and SPP. (ii) The intensities of the reflections attributed to crystalline cholesterol and CER3 are reduced. This indicates that free fatty acids increase the solubility of cholesterol and CER3 into the lamellar phases. (iii) Only in the presence of free fatty acids the lipids are organised in an orthorhombic lateral packing, which is similar to the observations made with lipid mixtures prepared with isolated ceramides [15].

The main difference between mixtures prepared with synthetic and isolated ceramides or SC is the presence of either one or two additional phases in the former. These additional phases with repeat distances of approximately 4.3 and 3.7 nm can be ascribed to phase-separated CER3 in crystalline domains. In a follow-up study (chapter 4), the main focus was to establish the optimal CER3 to ΣCERIV molar ratio to minimise the formation of these additional phases and to maximise the fraction of lipids forming the LPP. All lipid mixtures in that study were prepared with a fixed

CER1 level (10%), whereas the molar ratio between CER3 (uniform chain length) and ΣCERIV (chain length variation) ranged from 1:8 to 8:1. In the absence of free fatty acids, the optimal CER3 to ΣCERIV ratio is 5:4. A further reduction in the CER3 content in favour of the ΣCERIV level reduces the formation of the additional phases. However, it also considerably inhibits the formation of the LPP. Identical observations are made with lipid mixtures prepared in the presence of free fatty acids. However, in those mixtures the optimal CER3 to ΣCERIV molar ratio is found to be 7:2. This shift towards an increased CER3 content is most likely due to the chain length variation of the free fatty acids (ranging from C16 to C26).

The results of chapter 3 and chapter 4 demonstrate that the unique SC lipid organisation can be reproduced in vitro with mixtures based on cholesterol, free fatty acids and a limited number of synthetic ceramides, provided that both the equilibration temperature and the acyl chain length variation in the mixture (present in either the free fatty acids or the synthetic ceramides) are optimal. The results further reveal that the formation of the LPP is rather insensitive towards changes in the total composition of cholesterol, synthCER I and free fatty acids over a wide range of molar ratios. This is in excellent agreement with the in vivo situation, in which a high inter-individual variability in SC lipid composition does usually not lead to substantial changes in the lipid organisation.

To assess the effect of acylceramide type and relative content on the lipid phase behaviour, synthetic ceramide mixtures were prepared with various amounts of sphingosine based CER1, phytosphingosine based CER9 or combinations of CER1 and CER9, thereby maintaining a constant CER3 to ΣCERIV molar ratio (chapter 5). The difference between CER1 and CER9 is the presence of an additional hydroxyl group at the sphingosine base in the latter. The results reveal that CER9 less efficiently enhances the formation of the LPP than CER1. This was specially observed in lipid mixtures prepared in the absence of free fatty acids, in which CER9 is not able to induce the formation of the LPP. Instead, strong reflections in the diffraction pattern reveal the presence of crystalline CER9 in separate domains. Presumably, the larger and more hydrophilic head group of CER9 impedes the formation of the LPP.

Free fatty acids promote incorporation of CER9 into the lamellar phases. The effect of the relative acylceramide content on the lipid organisation was therefore only assessed in lipid mixtures prepared in the presence of free fatty acids. The results demonstrate that even in the presence of free fatty acids the maximum solubility of CER9 in the lamellar phases is lower than that of CER1. Whereas a rise in CER1 content from 0 to

20% leads to a consistent enhancement of the LPP formation, a more complex ordering is observed in mixtures prepared with CER9. There, a rise in CER9 content up to 10% promotes the formation of the LPP. However, a further rise in CER9 content inhibits the formation of the LPP and increases the intensities of the reflections attributed to phase-separated CER9. Interestingly, partial replacement of CER1 by CER9 does not affect the lipid organisation. This indicates that in addition to free fatty acids, CER1 promotes intercalation of CER9 into the lamellar phases.

In contrast to the previous chapters, in which solely mixtures prepared with a limited number of synthetic ceramides were studied, chapter 6 focused on the lipid organisation in mixtures prepared with various synthetic ceramides (referred to as synthCER II). The initial composition of synthCER II was 15% CER1(C30), 51% CER2(C24), 16% CER3(C24), 4% CER4(C24), 9% CER3(C16) and 5% CER6(C24), which resembles the composition of the ceramides in pig SC. To elucidate the role of the various synthetic ceramides in the formation of the LPP, the synthCER II fraction was gradually modified. As the synthetic counterpart of CER5 is not available, all synthCER II mixtures were prepared with CER3(C16).

The lipid organisation in equimolar mixtures of cholesterol, synthCER II and free fatty acids closely resembles that in SC, as both LPP (12.2. nm) and SPP (5.4 nm) are present, the lateral packing of the lipids is orthorhombic, a minor fraction of cholesterol phase separates into crystalline domains, and no additional phases are detected. Interestingly, free fatty acids are required for proper lipid organisation in synthCER II mixtures, as only in their presence the LPP is dominantly present. This might be related to the limited acyl chain length distribution present in the synthCER II fraction.

Similarly as observed for synthCER I mixtures (CER1, CER3 and ΣCERIV), no LPP is present in mixtures prepared in the absence of any acylceramide. Whereas partial substitution of CER1 with CER9 does not affect the lipid organisation, complete substitution of CER1 with CER9 slightly reduces the formation of the LPP in synthCER II mixtures. Furthermore, exclusion of CER4, CER6, or both CER4 and CER6 from the synthCER II fraction or reduction in the CER2 content does not significantly affect the lipid organisation.

The results of chapter 2 to chapter 6 unequivocally demonstrate that lipid mixtures prepared with synthCER I or synthCER II offer an attractive tool to unravel the importance of individual ceramides for proper SC lipid organisation. Such studies are crucial to increase our insight in the impaired barrier function as observed in diseased and dry skin. SynthCER II mixtures most closely mimic the lipid composition and

organisation of the intercellular lipids in human SC, as no additional crystalline phases are present. For this reason, equimolar mixtures of cholesterol, synthCER II and free fatty acids were selected for preparation of the SCS. The lipid organisation in mixtures prepared with synthCER I and synthCER II is schematically represented in Figure 1.

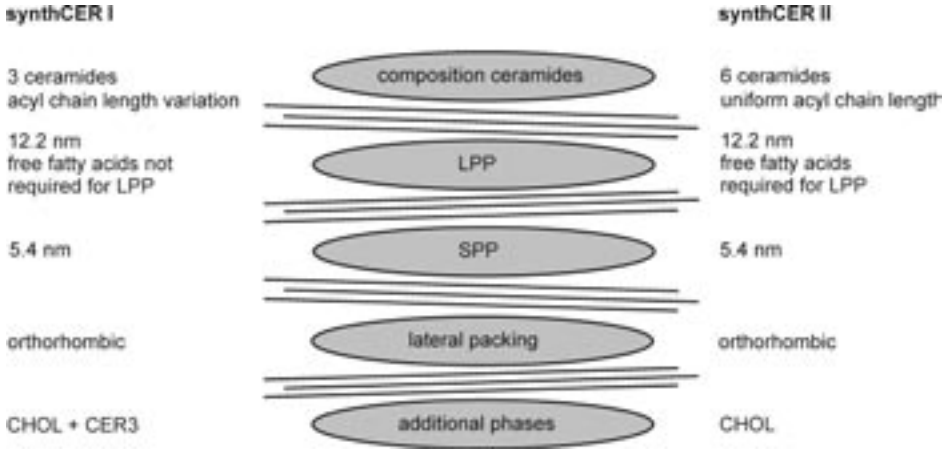

Figure 1 – Schematic representation of the lipid organisation in synthCER I and synthCER II mixtures.

PART II – Preparation and characterisation of the SCS

Chapter 7 focused on the preparation and characterisation of circular skin lipid membranes on a porous substrate, which can substitute SC in diffusion studies. Firstly, an application method was developed, making use of an airbrush spraying device. The airbrush, which is connected to gaseous nitrogen, consists of a reservoir, a nozzle, and a trigger. Briefly, a polycarbonate filter, which serves as a porous substrate, is mounted in a holder and fixed under the airbrush. The reservoir is subsequently filled with lipid solution. During the spraying period, the trigger is opened pneumatically for a certain time period, during which a small fraction of the lipid solution passes the nozzle. Due to this nitrogen pressure, the lipid solution is sprayed in very small droplets onto the polycarbonate filter. During the drying stage, the trigger is closed, the organic solvent evaporates by the nitrogen flow and the lipids attach to the substrate. This procedure can be repeated until the required layer thickness has been obtained. As polycarbonate filters are not resistant towards chloroform, hexane:isopropanol (3:2), methanol:ethylacetate (2:1) and hexane:ethanol (2:1) were selected as alternative

solvents for chloroform:methanol (2:1). One dimensional high performance thin layer chromatography was used to establish the distribution of the various lipid classes over the filter surface. It was demonstrated that the solvent mixture as well as the total lipid concentration considerably affect the lipid distribution, in particular that of cholesterol. The best results were obtained with hexane:ethanol (2:1) at a total lipid concentration of 4.5 mg/ml.

Cryo-scanning electron microscopy studies on cross-sections of the SCS reveal that buffer application immediately after the equilibration step, which is the normal procedure to obtain the LPP and SPP in mixtures prepared with synthetic or isolated ceramides, results in large open structures in the lipid layer. Smooth and tightly packed lipid layers in the absence of holes are only obtained when the SCS is equilibrated and subsequently cooled to room temperature in the absence of acetate buffer. X-ray diffraction studies on this SCS reveal that even in the absence of acetate buffer two crystalline lamellar phases are present with periodicities of 12.2 nm (LPP) and 5.4 nm (SPP), respectively. In addition, the lipid lamellae are predominantly oriented parallel to the filter surface, which resembles the orientation of the intercellular lipids in the SC. The results of that study demonstrate that the airbrush is a suitable method to prepare a homogeneous SCS in terms of lipid composition, organisation, orientation and lipid layer thickness.

The final objective of this thesis was to evaluate the diffusional resistance of the SCS (chapter 8). The barrier function of the skin lipid membrane system was studied in a series in vitro passive diffusion studies (see Fig. 2). Human SC isolated from various donors was used as a control sample. The effects of compound lipophilicity on the diffusion profile were investigated, using three structurally related compounds, namely p-aminobenzoic acid (PABA), ethyl-PABA and butyl-PABA. PABA is the most hydrophilic compound and its lipophilicity increases with increasing ester chain length. The effects of lipid layer thickness and altered lipid composition of the SCS on the diffusion profile were investigated with the model compound ethyl-PABA.

An increased SCS layer thickness is accompanied by an increased barrier efficacy, which is reflected by a decrease in the steady state flux of ethyl-PABA. However, an increased lipid layer thickness does not result in an increased lag time, which is different from the observations made with SC. It should be stressed, however, that very short lag time values cannot be appropriately determined with the diffusion set up used in these studies. As a result, the obtained lag time values of ethyl-PABA across the SCS may not reflect the real situation.

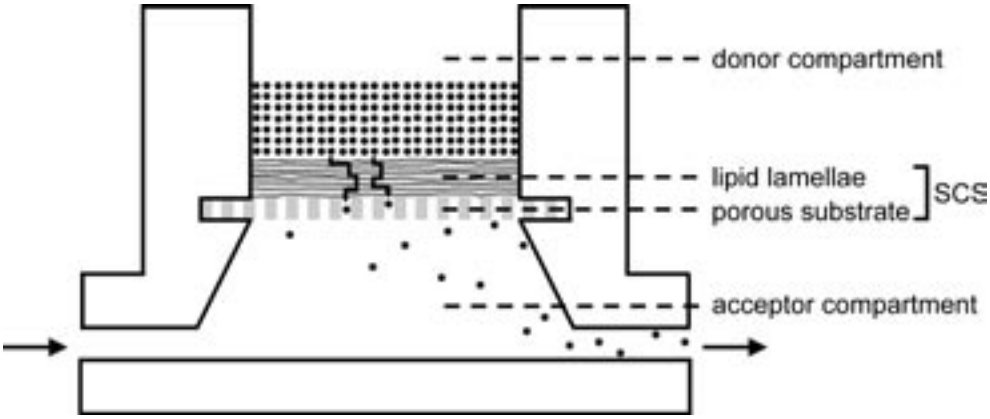

Figure 2 – Schematic representation of a diffusion cell. A diffusion cell consists of a donor and an acceptor compartment, separated by the SCS (or SC). In order to travel from the donor compartment to the acceptor compartment, a drug needs to diffuse through the SCS (or SC). Analysis of the collected fractions of the acceptor compartment enables calculation of the relevant diffusion characteristics.

The diffusion profiles of all three model compounds across the SCS prepared with a 12 µm thick lipid layer closely resemble those obtained with human SC. The observed differences in steady state flux and lag time values between the SCS and human SC are much smaller than reported for other compounds when using animal or reconstructed human skin [5, 6, 16]. Omission of CER1 from the synthCER II fraction, generating a SCS lacking the characteristic LPP, is accompanied by a nearly 2-fold increase in the steady state flux of ethyl-PABA. This demonstrates the importance of the LPP for the barrier integrity of the SCS.

CONCLUSION

The results presented in this thesis demonstrate that the SCS offers an attractive tool to predict solute permeation through the skin. Moreover, it offers excellent possibilities to investigate the role of each lipid subclass for proper membrane organisation and barrier function. Such studies are crucial to increase our insight in the impaired barrier function as observed in diseased and dry skin. To the best of our knowledge, this is the first study in which a SCS was prepared that mimics the lipid organisation, lipid orientation and the barrier function of SC.

FUTURE PERSPECTIVES

The first series of permeation studies performed with the model compounds PABA, ethyl-PABA and butyl-PABA reveal that the permeability barrier of the SCS closely mimics that of isolated human SC. However, despite these very encouraging results, more studies are required in order to conclusively prove its utility as a skin barrier model. Future diffusion studies should therefore be performed with model compounds that cover a broad range of molecular weights, charges and polarities. In addition, vehicle and dosing effects should be investigated, as in the studies described in this thesis solute permeation was only investigated from an acetate buffer at an infinite dose.

An important advantage of the SCS is that the composition of the lipid mixtures can be accurately chosen and modified. This offers excellent possibilities to systematically investigate the role of each lipid subclass for proper membrane organisation and barrier function. It has already been demonstrated that the presence of the LPP is important for the barrier function of the SCS and that the formation of this phase depends on the presence of CER1. Future research should not only focus on the importance of the lamellar organisation, but also on the contribution of the lateral lipid packing on the permeability barrier of the SCS. This can be accomplished by preparing the SCS with lipid mixtures in which long-chain free fatty acids have been substituted with short-chain free fatty acids. Previous X-ray diffraction studies on lipid mixtures prepared with isolated SC lipids have demonstrated that lipid mixtures prepared with long-chain free fatty acids, as observed in healthy SC, predominantly form an orthorhombic packing, whereas lipid mixtures prepared with short-chain free fatty acids, as observed in atopic dermatitis [3], organise in a hexagonal phase. Another compositional change of interest would be the addition of high levels of cholesterol sulphate, as observed in recessive X-linked ichthyosis [2], as cholesterol sulphate induces the formation of a fluid phase.

As described above, it is possible to prepare a SCS that mimics the lipid composition and organisation of diseased skin. This may provide unique possibilities to more adequately predict the permeability of these skin types to a variety of drugs. However, it should be kept in mind that in various skin disorders not only the composition and organisation of the intercellular lipids is affected, but also the formation of the cornified envelope [3]. Abnormalities in the formation and composition of the monolayer of covalently bound lipids may decrease the structural and functional integrity of the cornified envelope. As a result, substances that penetrate diseased skin may not

only bypass, but also travel through the corneocytes (intracellular route). It would be very interesting, although experimentally complicated, to incorporate corneocytes in the skin lipid membranes. In this way, the permeability in healthy and diseased SC may be even more closely mimicked. Furthermore, it would be interesting to investigate the effects of increased temperature or different agents (e.g. penetration enhancers, iontophoresis, and moisturisers) on the skin lipid membrane organisation and permeability of the SCS.

With respect to the application method, future optimisation should be aimed to produce the SCS at larger scale under controlled environmental conditions (temperature and relative humidity). At present, one lipid membrane is prepared at a time. A challenge for the future would therefore be to adapt the application method in order to spray a large filter surface with lipid material in one batch. Firstly, such an adaptation will increase the flexibility of the system, as potential users of the SCS are not restricted to one particular diffusion area. Secondly, a further increase in reproducibility is desirably to minimise the number of replicates required per diffusion experiment. This is especially important in screening studies. Hence, an increased flexibility and reproducibility will markedly improve the commercial attractiveness of the system.

REFERENCES

1. Bouwstra J.A., Gooris G.S., van der Spek J.A., Bras W. The structure of human stratum corneum as determined by small angle X-ray scattering. *J. Invest. Dermatol.* **96** (1991) 1006-1014.

2. Zettersten E., Man M.Q., Sato J., Denda M., Farrell A., Ghadially R., Williams M.L., Feingold K.R., Elias P.M. Recessive x-linked ichthyosis: role of cholesterol-sulfate accumulation in the barrier abnormality. *J Invest. Dermatol.* **111** (1998) 784-790.

3. Macheleidt O., Kaiser H.W., Sandhoff K. Deficiency of epidermal protein-bound omega-hydroxyceramides in atopic dermatitis. *J. Invest. Dermatol*. **119** (2002) 166-173.

4. Lavrijsen A.P.M., Bouwstra J.A., Gooris G.S., Weerheim A., Bodde H.E., Ponec M. Reduced skin barrier function parallels abnormal stratum corneum lipid organization in patients with lamellar ichthyosis. *J. Invest. Dermatol.* **105** (1995) 619-624.

5. Schmook F.P., Meingassner J.G., Billich A. Comparison of human skin or epidermis models with human and animal skin in in-vitro percutaneous absorption. *Int. J. Pharm.* **215** (2001) 51-56.

6. Catz P., Friend D.R. Transdermal delivery of levonorgestrel. VII. Effect of enhancers on rat skin, hairless mouse skin, hairless guinea pig skin, and human skin. *Int. J. Pharm.* **58** (1990) 93-102.

7. Council Directive 2003/15/EEC of 27 February 2003 (amending for the seventh time Directive 76/6/768/EEC), Official Journal L 66, 11.3.2003, pp 26-35.

8. Ponec M., Weerheim A., Lankhorst P., Wertz P. New acylceramide in native and reconstructed epidermis. *J. Invest. Dermatol.* **120** (2003) 581-588.

9. Bouwstra J.A., Gooris G.S., Dubbelaar F.E.R., Weerheim A.M., IJzerman A.P., Ponec M. Role of ceramide 1 in the molecular organization of the stratum corneum lipids. *J. Lipid Res.* **39** (1998) 186-196.

10. McIntosh T.J., Stewart M.E., Downing D.T., 1996. X-ray diffraction analysis of isolated skin lipids: reconstitution of intercellular lipid domains. *Biochemistry* **35** (1996) 3649-3653.

11. ten Grotenhuis E., Demel R.A., Ponec M., Boer D.R., van Miltenburg J.C., Bouwstra J.A. Phase-behavior of stratum corneum lipids in mixed langmuir-blodgett monolayers. *Biophys. J.* **71** (1996) 1389-1399.

12. Bouwstra J.A., Thewalt J., Gooris G.S., Kitson N. A model membrane approach to the epidermal permeability barrier: an X-ray diffraction study. *Biochemistry* **36** (1997) 7717-7725.

13. Lieckfeldt R., Villalain J., Gomez-Fernandez J.C., Lee G. Diffusivity and structural polymorphism in some model stratum corneum lipid systems. *Biochim. Biophys. Acta* **1151** (1993) 182-188.

14. Dahlen B., and Pascher I. Molecular arrangements in sphingolipids. Thermotropic phase behaviour of tetracosanoylphytosphingos ine. *Chem. Phys. Lipids* **24** (1979) 119-133.

15. Bouwstra, J.A., Gooris G.S., Cheng K., Weerheim A., Bras W., Ponec M. Phase behavior of isolated skin lipids. *J. Lipid Res.* **37** (1996) 999-1011.

16. Wagner H., Kosta K.H., Lehr K.M., Schaefer U.F. Interrelation of permeation and penetration parameters obtained from in vitro experiments with human skin and skin equivalents *J. Control. Release* **75** (2001) 283-295.

Chapter 10

Samenvatting en toekomstperspectieven

INLEIDING

De huid beschermt het lichaam tegen uitdrogen en het binnendringen van ongewenste stoffen. De belangrijkste barrière wordt gevormd door de buitenste huidlaag, het stratum corneum (SC). Het SC is opgebouwd uit verhoornde cellen (corneocyten), welke zijn ingebed in een matrix van gestapelde lipidenlagen (lamellen). Aangezien de wand van de corneocyten een nogal ondoordringbare structuur heeft, passeren de meeste stoffen het SC via de ruimte tussen de cellen. Dit betekent dat de lipiden, die zowel qua samenstelling als qua structuur uniek zijn voor biologische membranen, uitermate belangrijk zijn voor de barrièrefunctie van de huid. De lamellen zijn voornamelijk opgebouwd uit cholesterol, diverse soorten ceramiden en vrije vetzuren met lange ketens. Verder is aangetoond dat de lipiden gerangschikt zijn in twee lamellaire structuren met repeterende afstanden van respectievelijk 13 nm (lange periodiciteitsfase: LPP) en 6 nm (korte periodiciteitsfase: SPP) [1]. Algemeen wordt aangenomen dat met name de aanwezigheid van de LPP en de kristallijne laterale ordening van de lipiden zeer belangrijk zijn voor de barrièrefunctie van de huid.

Om het transport van stoffen vanuit farmaceutische of cosmetische producten door de huid te voorspellen, wordt veelvuldig gebruik gemaakt van SC, geïsoleerd van humane of dierlijke huid. Er kleven echter nogal wat nadelen aan deze aanpak, zoals grote intra- en interindividuele variatie en de zeer beperkte beschikbaarheid van humane huid. Tevens bestaan er geen in vitro modellen voor zieke en droge huid, terwijl veel producten juist voor deze huidtypen ontwikkeld worden. In zieke en droge huid is de barrièrefunctie vaak verstoord, d.w.z. dat de huid beter doorlaatbaar is voor stoffen. Dit kan grotendeels worden toegeschreven aan veranderingen in de samenstelling en structuur van de lipiden in het SC [2-4]. Een bijkomend nadeel van het gebruik van dierlijke huid is dat dit vaak beter doorlaatbaar is voor stoffen dan humane huid [5, 6]. Het is dus de vraag of dierlijke huid daadwerkelijk als geschikt model voor humane huid kan worden beschouwd. Bovendien wordt vanaf 2009 binnen de EU een verbod van kracht op het gebruik van proefdieren voor het testen van cosmetische

producten [7]. Uit bovengenoemde punten blijkt dat er een dringende behoefte bestaat aan reproduceerbare testsystemen om het transport van geneesmiddelen door de huid te voorspellen.

Het onderzoek beschreven in dit proefschrift betreft de ontwikkeling van een huidbarrièremodel, welke gebruikt kan worden om het transport van geneesmiddelen door de huid te voorspellen. Deze zogenaamde SC vervanger (SCS) bestaat uit synthetische SC lipiden (cholesterol, ceramiden en vrije vetzuren) op een poreuze drager. Om de barrière-eigenschappen van humane huid na te bootsen, moeten de samenstelling, de organisatie en de oriëntatie van de synthetische lipiden die van de intercellulaire SC lipiden zo dicht mogelijk benaderen.

De doelstellingen van dit proefschrift zijn:

(i) Selecteren van synthetische lipidenmengsels, welke de lipidenorganisatie in humaan SC nabootsen.

(ii) Vervaardigen van een homogeen SCS wat betreft samenstelling, organisatie, oriëntatie en laagdikte van het lipidenmembraan.

(iii) Evalueren van de barrièrefunctie van het ontwikkelde huidbarrièremodel.

DEEL I - Selectie van een synthetisch SC lipidenmengsel

Ceramiden bestaan uit twee lange verzadigde koolwaterstofketens en een kleine polaire kopgroep. In humaan stratum corneum zijn tenminste 9 verschillende ceramiden (CER1-CER9) geïdentificeerd [8]. De structuren van deze ceramiden zijn o.a. te zien op pagina 17 van dit proefschrift. Een ceramide bestaat uit een sphingosine, phytosphingosine of 6-hydroxysphingosine, waaraan een niet-gehydroxyleerd of α-gehydroxyleerd vetzuur (met een ketenlengte van hoofdzakelijk 24 tot 26 koolwaterstofatomen) chemisch is gebonden. De acylceramiden (CER1, CER4 en CER9) zijn uniek, omdat ze bestaan uit een ongebruikelijk lang ω-hydroxyvetzuur van 30 tot 34 koolwaterstofatomen, waaraan het onverzadigde linolzuur is gebonden.

Recentelijk is aangetoond dat de lipidenorganisatie in SC kan worden nagebootst met een mengsel van cholesterol, vrije vetzuren met lange ketens en uit SC geïsoleerde ceramiden. In deze mengsels blijkt de aanwezigheid van CER1 een vereiste te zijn voor de vorming van de unieke 13 nm structuur. De lipidenorganisatie is tevens veelvuldig onderzocht in mengsels bestaande uit commercieel beschikbare ceramiden. Hoewel bepaalde aspecten van de lipidenorganisatie in humaan SC kunnen worden nagebootst

met lipidenmengsels gemaakt met cholesterol, palmitinezuur en ceramide type III (een gemodificeerd ceramide geïsoleerd uit koeienhersenen welke qua structuur overeenkomt met CER2, maar met kortere vetzuurketens [11]), wordt de karakteristieke LPP echter niet gevormd [12, 13].

In hoofdstuk 2 wordt voor het eerst een verband gelegd tussen de lipidenorganisatie in goed gedefinieerde lipidenmengsels (gemaakt met synthetische ceramiden) en de complexere lipidenmengsels (gemaakt met geïsoleerde ceramiden). Het fasegedrag van enkelvoudige synthetische ceramiden, ceramiden gemengd met cholesterol of gemengd met cholesterol en vrije vetzuren, werd onderzocht met kleine hoek en grote hoek röntgendiffractie. Voor deze studie werden vier commercieel verkrijgbare ceramiden geselecteerd, namelijk CER3 met een acylketenlengte van 24 atomen (CER3(C24)), CER3 met een acylketenlengte van 16 koolstofatomen (CER3(C16)), ceramide type III (ΣCERIII) en ceramide type IV (ΣCERIV). CER3 bestaat uit een phytosphingosine, waaraan een vetzuur met slechts één ketenlengte is gebonden. ΣCERIII en ΣCERIV zijn daarentegen opgebouwd uit een sphingosine, waaraan een vetzuur met een variabele ketenlengte is gebonden. Er werd systematische onderzocht wat de invloed is van de lipidensamenstelling, met inbegrip van toevoeging van synthetisch CER1(C30), op de lipidenorganisatie.

In tegenstelling tot de bevindingen met ΣCERIII en ΣCERIV zijn in CER3(C16) en CER3(C24) twee fasen aanwezig met verschillende repeterende afstanden. Voor CER3(C24) werd dergelijk polymorfisme al eerder beschreven door Dahlen en Pascher [14]. Door de vorming van waterstofbruggen tussen de kopgroepen van naast elkaar gelegen CER3 moleculen vormt CER3 een V-vormige structuur, waarbij de phytosphingosineketen en de acylketen zich in afzonderlijke lagen bevinden. Het verschil in repeterende afstand tussen beide fasen wordt veroorzaakt door een verschil in de kantelhoek tussen de twee koolwaterstofketens.

In hoofdstuk 2 wordt verder voor het eerst aangetoond dat de LPP kan worden gevormd in mengsels die zijn bereid met synthetische ceramiden. Een lamellaire structuur met een lange periodiciteit werd echter slechts in één mengsel waargenomen, bestaande uit synthetisch CER1, CER3 (C24), cholesterol en vrije vetzuren. De lage intensiteit van de LPP-reflecties duiden er echter op dat slechts een klein deel van de lipiden daadwerkelijk de LPP vormt. Verder verschilt de repeterende afstand van 11.6 nm aanzienlijk van die waargenomen in SC of in lipidenmengsels bereid met geïsoleerde ceramiden.

Om de vorming van de LPP te bevorderen en de repeterende afstand te vergroten,

werden zowel de bereidingsmethode als de samenstelling van de lipidenmengsels geoptimaliseerd. Eerst werd de invloed van de equilibratietemperatuur tijdens de monstervoorbereiding onderzocht. Vervolgens werd de invloed van de hoeveelheid vrije vetzuren in het lipidenmengsel op het fasegedrag onderzocht (hoofdstuk 3). Alle variaties werden uitgevoerd met een ceramidenmengsel bestaande uit CER1, CER3 (C24) en ΣCERIV in een molverhouding 1:7:2 (verder aangeduid als synthCER I). ΣCERIV werd in het ceramidenmengsel opgenomen om meer variatie in de acylketenlengte en kopgroepstructuur te introduceren.

Mengsels gemaakt met cholesterol en synthCER I in een gelijke molverhouding werden geëquilibreerd bij een temperatuur variërend tussen 60 en 100°C. Uit de resultaten blijkt dat een verhoogde equilibratietemperatuur de vorming van de LPP bevordert. De LPP is niet aanwezig in lipidenmengsels die geëquilibreerd zijn bij 60°C. Wanneer echter een equilibratietemperatuur van 95 of 100°C wordt gekozen, is de LPP met een repeterende afstand van 12.2 nm dominant aanwezig. Tevens blijkt een verhoogde equilibratietemperatuur de vorming van een fase met een repeterende afstand van 4.3 nm te bevorderen ten koste van een fase met repeterende afstand van 3.7 nm. Beide structuren zijn niet aanwezig in SC en kunnen worden toegeschreven aan CER3 dat is uitgekristalliseerd in een V-vormige structuur (zie hoofdstuk 2).

Vervolgens werd de invloed van de relatieve hoeveelheid vrije vetzuren in het lipidenmengsel op de lipidenorganisatie onderzocht. Hiervoor werden mengsels gemaakt met cholesterol, synthCER I en vrije vetzuren in een molverhouding variërend van 1:1:0 tot 1:1:1.8. Door de toevoeging van vrije vetzuren smolten de lipiden bij een equilibratietemperatuur van 95°C. Daarom werden de lipidenmengsels bij een iets lagere temperatuur geëquilibreerd, namelijk 80°C. Door de hoeveelheid vrije vetzuren systematisch te verhogen, tot een mengsel van cholesterol, synthCER I en vrije vetzuren in een 1:1:1 molverhouding, wordt de vorming van zowel de LPP (12.2 nm) als de SPP (5.5 nm) bevorderd. Een verdere toename van de fractie vrije vetzuren remt de vorming van de LPP en als gevolg daarvan overheerst de SPP. Uit de resultaten blijkt verder dat in aanwezigheid van vrije verzuren de lamellaire fasen meer zijn geordend, de oplosbaarheid van cholesterol en CER3 in de lamellaire fasen wordt verhoogd en dat de lipiden alleen in aanwezigheid van vrije vetzuren een orthorhombische structuur vormen. Dit laatste is ook waargenomen voor mengsels gemaakt met geïsoleerde ceramiden [15].

Het voornaamste verschil tussen lipidenmengsels gemaakt met synthetische ceramiden enerzijds en SC of mengsels gemaakt met geïsoleerde ceramiden anderzijds

is de aanwezigheid van of één of twee additionele fasen in de eerstgenoemde mengsels. Deze additionele fasen met repeterende afstanden van ongeveer 4.3 en 3.7 nm kunnen worden toegeschreven aan CER3 dat is uitgekristalliseerd in aparte domeinen. Om de vorming van deze additionele fasen te minimaliseren en de vorming van de LPP te bevorderen, werd in een vervolgstudie (hoofdstuk 4) de molverhouding tussen CER3 en ΣCERIV onderzocht. Alle lipidenmengsels in die studie werden bereid met een vaste hoeveelheid CER1 (10%), terwijl de molverhouding tussen CER3 (vaste ketenlengte) en ΣCERIV (variatie in ketenlengte) varieerde van 1:8 tot 8:1. In lipidenmengsels bereid zonder vrije vetzuren blijkt een CER3:ΣCERIV verhouding van 5:4 optimaal te zijn. Een verdere verlaging van de hoeveelheid CER3 ten gunste van ΣCERIV vermindert de vorming van de additionele fasen, maar leidt tevens tot een aanzienlijke afname in de vorming van de LPP. Vergelijkbare waarnemingen werden gedaan met lipidenmengsels gemaakt in aanwezigheid van vrije vetzuren. Echter, in die mengsels werd een optimale CER3:ΣCERIV verhouding gevonden van 7:2. Deze verschuiving naar een grotere hoeveelheid CER3 wordt waarschijnlijk veroorzaakt door de variatie in ketenlengten van de vrije vetzuren (variërend van C16 tot C26).

Uit hoofdstuk 3 en hoofdstuk 4 blijkt dat de unieke SC lipidenorganisatie in vitro kan worden nagebootst met mengsels bestaande uit cholesterol, vrije vetzuren en een beperkt aantal synthetische ceramiden. Voorwaarde hiervoor is dat zowel de equilibratietemperatuur als de variatie in acylketenlengte in het mengsel (aanwezig in òf de fractie vrije vetzuren òf de synthetische ceramiden) optimaal zijn. Verder blijkt dat de vorming van de LPP redelijk ongevoelig is voor veranderingen in de molverhouding tussen cholesterol, synthCER I en vrije vetzuren. Laatstgenoemde komt zeer goed overeen met de in vivo situatie, waarin een grote interindividuele variatie in de samenstelling van de SC lipiden normaliter niet leidt tot een aanzienlijke verandering in de lipidenorganisatie.

In hoofdstuk 5 werd de invloed van het type en de relatieve hoeveelheid acylceramide op de lipidenorganisatie in synthetische lipidenmengsels onderzocht. Hiertoe werden synthetische lipidenmengsels gemaakt met verschillende hoeveelheden CER1 (sphingosine), CER9 (phytosphingosine; met een extra hydroxylgroep aan de kopgroep) of combinaties van CER1 en CER9. In al deze mengsels werd de molverhouding tussen CER3 en ΣCERIV constant gehouden. De resultaten laten zien dat CER1 beter in staat is om de vorming van de LPP te bevorderen dan CER9. In mengsels zonder vrije vetzuren kristalliseert CER9 uit in afzonderlijke domeinen en is het niet mogelijk om de LPP te vormen. Vermoedelijk belemmert de grotere en meer hydrofiele kopgroep van CER9

de vorming van de LPP.

Aangezien vrije vetzuren de integratie van CER9 in de lamellaire fasen bevorderen, werd de invloed van de relatieve hoeveelheid acylceramide op de lipidenorganisatie alleen onderzocht in lipidenmengsels die bereid waren in aanwezigheid van vrije vetzuren. Uit de resultaten blijkt dat ook in aanwezigheid van vrije vetzuren de maximale oplosbaarheid van CER9 in de lamellaire fasen lager is dan die van CER1. Een toename van 0 tot 20% CER1 bevordert de vorming van de LPP aanzienlijk. Een dergelijk verband werd niet waargenomen voor mengsels die gemaakt waren met CER9. Bij een CER9 gehalte hoger dan 10% wordt de vorming van de LPP namelijk geremd en kristalliseert CER9 gedeeltelijk apart uit. Opmerkelijk is dat de lipidenorganisatie niet verandert indien CER1 slechts gedeeltelijk door CER9 vervangen werd. Dit duidt erop dat zowel vrije vetzuren als CER1 de inbouw van CER9 in de lamellaire fasen bevorderen.

In tegenstelling tot de voorgaande studies, waarin alleen mengsels zijn onderzocht die werden gemaakt met een beperkt aantal synthetische ceramiden, werd het onderzoek beschreven in hoofdstuk 6 uitgevoerd met een mengsel bestaande uit 15% CER1(C30), 51% CER2(C24), 16% CER3(C24), 4% CER4(C24), 9% CER3(C16) en 5% CER6(C24). Deze samenstelling (verder aangeduid als synthCER II) is vergelijkbaar met die van de ceramiden in varkenshuid. Aangezien de synthetische tegenhanger van CER5 niet voorhanden is, werden alle synthCER II mengsels bereid met CER3(C16). Om de invloed van diverse synthetische ceramiden op de vorming van de LPP te onderzoeken, werd de fractie synthCER II systematisch gewijzigd.

De lipidenorganisatie in mengsels gemaakt met cholesterol, synthCER II en vrije vetzuren lijkt sterk op die in het SC: (i) zowel de LPP (12.2 nm) als SPP (5.4 nm) zijn aanwezig, (ii) de laterale ordening van de lipiden is orthorhombisch, (iii) een klein deel van de cholesterol is in aparte domeinen uitgekristalliseerd en iv) er zijn geen additionele fasen aanwezig. Opmerkelijk is dat vrije vetzuren noodzakelijk zijn om de lipidenorganisatie in het SC na te bootsen. Dit wordt waarschijnlijk veroorzaakt door de geringe variatie in de acylketenlengten in het synthCER II mengsel.

In lipidenmengsels die zijn gemaakt zonder acylceramide wordt de LPP niet gevormd. Dit is in overeenstemming met de mengsels gemaakt met het synthCER I (CER1, CER3 en ΣCERIV) mengsel. Ook blijkt het mogelijk om CER1 gedeeltelijk door CER9 te vervangen. Een volledige vervanging van CER1 door CER9 leidt echter wel tot een lichte afname in de vorming van de LPP in de synthCER II mengsels. Uitsluiting van CER4, CER6 of beide ceramiden van het synthCER II mengsel beïnvloedt

de lipidenorganisatie niet. De lipidenorganisatie wordt evenmin beïnvloed door het CER2 gehalte in het synthCER II mengsel te verlagen.

Uit de resultaten beschreven in hoofdstuk 2 tot en met hoofdstuk 6 blijkt dat lipidenmengsels gemaakt met synthCER I of synthCER II uitstekend gebruikt kunnen worden om de rol van individuele ceramiden in de lipidenorganisatie te onderzoeken. Dergelijke studies zijn essentieel om een beter inzicht te krijgen in de verstoorde barrièrefunctie zoals aanwezig in zieke en droge huid. Omdat het mengsel gemaakt met cholesterol, synthCER II en vrije vetzuren de lipidenorganisatie in humaan SC het dichtst benaderen, werd dit mengsel geselecteerd voor de ontwikkeling van het SCS. De lipidenorganisatie in mengsels gemaakt met synthCER I en synthCER II is schematisch weergegeven in Figuur 1.

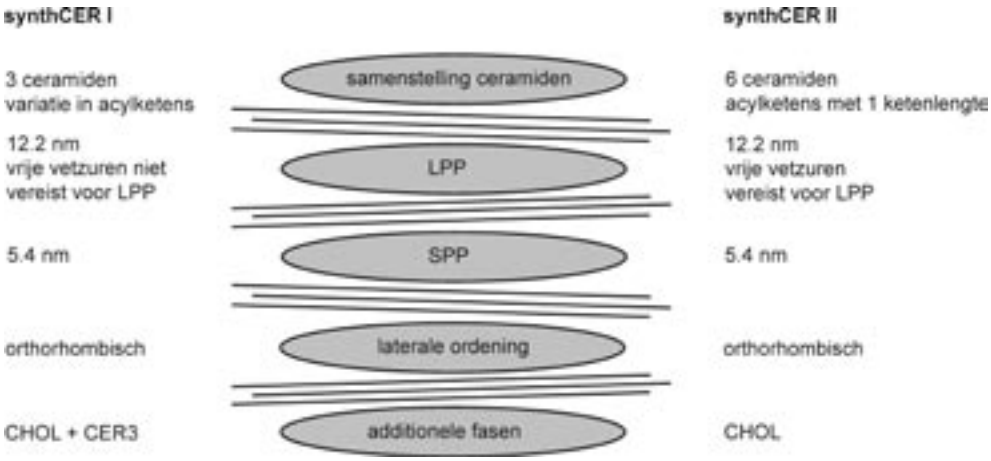

Figuur 1 – Schematische weergave van de lipidenorganisatie in synthCER I en synthCER II mengsels.

DEEL II – Ontwikkeling van het SCS met synthetische lipidenmengsels

Hoofdstuk 7 beschrijft de vervaardiging en karakterisering van het SCS. Allereerst werd een methode ontwikkeld, gebruikmakend van een airbrush, om de lipiden op een poreuze drager aan te brengen. De airbrush, die aangesloten is op stikstofgas, bestaat uit een vloeistofreservoir, een mondstuk en een trekker. Een polycarbonaatfilter, dat dient als poreuze drager, wordt ingeklemd in een houder en recht onder de airbrush gefixeerd. Het vloeistofreservoir wordt vervolgens gevuld met een lipidenoplossing. Gedurende het spraystadium wordt de trekker pneumatisch geopend voor een bepaalde tijdsduur, waardoor een kleine fractie van de lipidenoplossing het mondstuk

passeert. Door de stikstofdruk wordt de lipidenoplossing verneveld en hierdoor wordt de lipidenoplossing in zeer kleine druppeltjes op het polycarbonaatfilter gesproeid. Tijdens het droogstadium is de trekker gesloten, verdampt het organisch oplosmiddel door de stikstofstroom en hechten de lipiden aan het filter. Deze procedure kan worden herhaald tot de vereiste laagdikte is verkregen. Aangezien de polycarbonaatfilters niet bestand zijn tegen chloroform, werden hexaan:isopropanol (3:2), methanol:ethylacetaat (2:1) en hexaan:ethanol (2:1) geselecteerd als alternatieve oplosmiddelen voor chloroform: methanol (2:1). Laatstgenoemde mengsel werd in alle voorgaande studies gebruikt voor de bereiding van de lipidenmengsels. Dunnelaagchromatografie werd gebruikt om de verdeling van de diverse lipidenklassen over het filteroppervlak vast te stellen. Uit de resultaten blijkt dat de lipidenverdeling, met name die van cholesterol, sterk wordt beïnvloed door het gebruikte oplosmiddel en de totale lipidenconcentratie. De beste resultaten werden verkregen met hexaan:ethanol (2:1) en een lipidenconcentratie van 4.5 mg/ml.

Dwarsdoorsneden van lipidenmembranen werden onderzocht met cryo-scanning elektronenmicroscopie. Een egale lipidenlaag zonder gaten wordt alleen verkregen wanneer het SCS in afwezigheid van een buffer wordt gemaakt. Uit röntgendiffractiestudies blijkt dat in het SCS gemaakt zonder buffer twee kristallijne lamellaire fasen aanwezig zijn met repeterende afstanden van respectievelijk 12.2 (LPP) en 5.4 nm (SPP). Tevens zijn de lamellen parallel aan het filteroppervlak georiënteerd, wat de oriëntatie van de intercellulaire lipiden in het SC zeer dicht benadert. Uit de resultaten van hoofdstuk 7 blijkt dat de ontwikkelde spraymethode zeer geschikt is om een homogeen SCS te maken.

De laatste doelstelling van het onderzoek beschreven in dit proefschrift was het evalueren van de barrièrefunctie van het ontwikkelde huidbarrièremodel (hoofdstuk 8). De doorlaatbaarheid van het SCS werd onderzocht in een serie in vitro passieve diffusiestudies (zie Fig. 2), waarbij geïsoleerd humaan SC werd gebruikt als controle. De invloed van de lipofiliteit van de modelstof op het diffusieprofiel werd onderzocht met behulp van drie structureel verwante modelstoffen, namelijk p-aminobenzoëzuur (PABA), ethyl-PABA en butyl-PABA. PABA is de meest hydrofiele verbinding en de lipofiliteit neemt toe met de ketenlengte van de ester. De invloed van de dikte van de lipidenlaag en de lipidensamenstelling van het SCS op het diffusieprofiel werd alleen onderzocht met de modelstof ethyl-PABA.

Een dikkere lipidenlaag resulteert in een verhoogde barrièrefunctie van het SCS, welke wordt weerspiegeld in een afname van het transport van ethyl-PABA tijdens

de stationaire toestand. De diffusieprofielen van de drie modelstoffen door het SCS gemaakt met een 12 µm dikke lipidenlaag lijken sterk op die door geïsoleerd humaan SC. De waargenomen verschillen tussen het SCS en humaan SC voor wat betreft het transport tijdens stationaire toestand en de vertragingstijd zijn veel kleiner dan die gerapporteerd in studies waarbij gebruik werd gemaakt van dierlijke huid of humane kweekhuid [5, 6, 16]. Het transport tijdens stationaire toestand van ethyl-PABA door het SCS gemaakt zonder CER1, waarin de karakteristieke LPP dus ontbreekt, is bijna een factor twee hoger dan door het normale SCS. Hieruit blijkt overtuigend het belang van de LPP voor een goede barrièrefunctie.

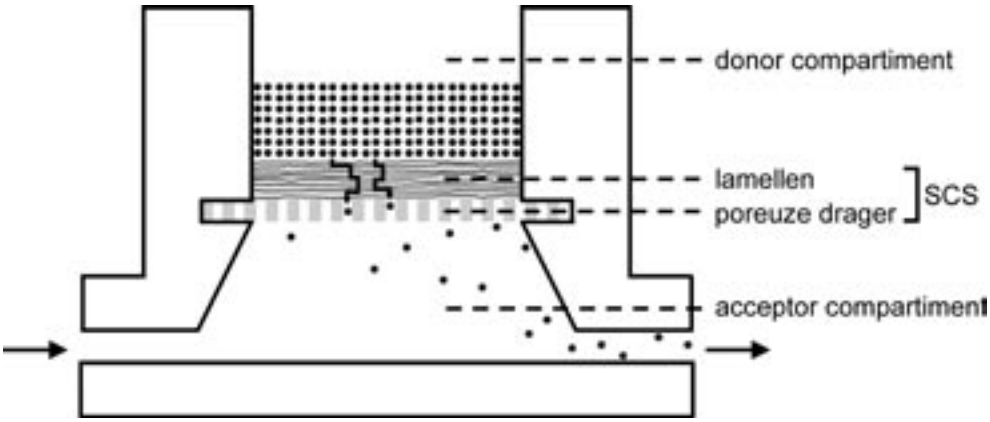

Figuur 2 – Schematische weergave van een diffusiestudie. Een diffusiecel bestaat uit een donor en een acceptor compartiment, waartussen het SCS (of SC) is ingeklemd. Vervolgens wordt de te onderzoeken stof in het donor compartiment gebracht. Om van het donor compartiment in het acceptor compartiment te komen, moet de stof door het SCS (of SC) diffunderen. Door fracties van het acceptor compartiment op te vangen en te analyseren kan uitgerekend worden hoeveel stof het SCS (of SC) in stationaire toestand passeert.

CONCLUSIE

Uit de resultaten gepresenteerd in dit proefschrift blijkt dat het SCS een aantrekkelijk hulpmiddel is om het transport van stoffen door de huid te voorspellen. Bovendien biedt het uitstekende mogelijkheden om de rol van de afzonderlijke lipiden in zowel de lipidenorganisatie als de barrièrefunctie in één model te onderzoeken. Dergelijke studies zijn cruciaal om onze kennis over de verstoorde barrièrefunctie, zoals in zieke en droge huid, te vergroten. Voor zover bij ons bekend, is dit de eerste studie waarin een SCS werd ontwikkeld dat zowel de lipidenorganisatie, de lipidenoriëntatie als de barrièrefunctie van SC nabootst.

TOEKOMSTPERSPECTIEVEN

Uit de eerste serie diffusiestudies die zijn uitgevoerd met de modelstoffen PABA, ethyl-PABA en butyl-PABA blijkt dat de barrière-eigenschappen van het SCS die van geïsoleerd humaan SC zeer dicht benaderen. Ondanks deze zeer veelbelovende resultaten, zijn er echter meer studies nodig om de bruikbaarheid van het SCS als huidbarrièremodel vast te stellen. Toekomstige diffusiestudies zouden daarom moeten worden uitgevoerd met modelstoffen die een breed scala aan molecuulgewichten, ladingen en polariteiten omvatten. Verder zou de invloed van de formulering en de dosering onderzocht moeten worden, aangezien tot op heden alleen de diffusie van modelstoffen opgelost in een acetaatbuffer bij een oneindige dosering is onderzocht.

Een belangrijk voordeel van het SCS is dat de samenstelling van de lipidenmengsels nauwkeurig kan worden gekozen en gewijzigd. Dit biedt uitstekende mogelijkheden om de rol van afzonderlijke lipiden voor een juiste membraanorganisatie en barrièrefunctie systematisch te onderzoeken. Er is reeds aangetoond dat de aanwezigheid van de LPP belangrijk is voor de barrièrefunctie van het SCS en dat de vorming van deze fase afhangt van de aanwezigheid van CER1. In vervolgonderzoek zou niet alleen de rol van de lamellaire organisatie op de barrièrefunctie van het SCS onderzocht moeten worden, maar ook de bijdrage van de laterale lipidenstructuur. Dit zou kunnen worden onderzocht door de vrije vetzuren met lange ketens te vervangen door vrije vetzuren met korte ketens. Uit eerdere studies met lipidenmengsels gebaseerd op geïsoleerde SC ceramiden is namelijk gebleken dat in mengsels gemaakt met vrije vetzuren met lange ketens, zoals in gezond SC, hoofdzakelijk een orthorhombische fase wordt gevormd, terwijl in mengsels gemaakt met vrije vetzuren met korte ketens, zoals in atopisch dermatitis [3], een hexagonale fase wordt gevormd. Een andere interessante samenstellingsverandering is de toevoeging van verhoogde hoeveelheden cholesterolsulfaat, zoals in recessieve x-gebonden ichthyosis [2], aangezien cholesterolsulfaat de vorming van een vloeibare fase induceert.

Zoals hierboven beschreven, is het mogelijk om een SCS te produceren die de lipidensamenstelling en de organisatie van zieke huid nabootst. Dit kan unieke mogelijkheden bieden om de doorlaatbaarheid van deze huidtypen voor diverse geneesmiddelen beter te voorspellen. Er dient echter opgemerkt te worden dat in diverse huidziekten niet alleen de samenstelling en de organisatie van de intercellulaire lipiden is verstoord, maar ook de structuur van de corneocyten [3]. Als gevolg hiervan zou het transport van stoffen door SC van zieke huid niet alleen via de

ruimte tússen de corneocyten (intercellulaire route), maar ook dóór de corneocyten (transcellulaire route) kunnen plaatsvinden. Het zou daarom zeer interessant zijn, hoewel experimenteel gecompliceerd, om corneocyten in de lipidenlaag van het SCS in te sluiten. Op die manier zou de barrièrefunctie van zowel gezonde als zieke huid wellicht nog beter kunnen worden nagebootst en hiermee zal de voorspellende waarde van het SCS nog verder toenemen. Voorts zou het zeer interessant zijn om de invloed van de temperatuur of verschillende andere aspecten (bijv. penetratiebevorderaars, iontoforese, en moisturisers) op de lipidenorganisatie en de doorlaatbaarheid van het SCS te onderzoeken.

Met het oog op de applicatiemethode zou in de toekomst getracht moeten worden om het SCS op grotere schaal en onder gecontroleerde klimaatomstandigheden (temperatuur en relatieve vochtigheid) te produceren. Momenteel worden de filters één voor één bedekt met een lipidenlaag. Een uitdaging voor de toekomst zou daarom zijn om de applicatiemethode zodanig aan te passen dat in één keer een groot filteroppervlak met lipidenmateriaal kan worden bedekt. Allereerst zal een dergelijke aanpassing de flexibiliteit van het systeem vergroten, aangezien potentiële gebruikers van het SCS niet meer gebonden zijn aan een bepaald diffusieoppervlak. Ten tweede is een verdere verhoging van de reproduceerbaarheid wenselijk om het vereiste aantal replica's per diffusie-experiment te minimaliseren, wat met name belangrijk is voor screening-studies. Derhalve zal een verhoogde flexibiliteit en reproduceerbaarheid de commerciële aantrekkelijkheid van het SCS aanzienlijk verhogen.

REFERENTIES

1. Bouwstra J.A., Gooris G.S., van der Spek J.A., Bras W. The structure of human stratum corneum as determined by small angle X-ray scattering. *J. Invest. Dermatol.* **96** (1991) 1006-1014.

2. Zettersten E., Man M.Q., Sato J., Denda M., Farrell A., Ghadially R., Williams M.L., Feingold K.R., Elias P.M. Recessive x-linked ichthyosis: role of cholesterol-sulfate accumulation in the barrier abnormality. *J Invest. Dermatol.* **111** (1998) 784-790.

3. Macheleidt O., Kaiser H.W., Sandhoff K. Deficiency of epidermal protein-bound omega-hydroxyceramides in atopic dermatitis. *J. Invest. Dermatol*. **119** (2002) 166-173.

4. Lavrijsen A.P.M., Bouwstra J.A., Gooris G.S., Weerheim A., Bodde H.E., Ponec M. Reduced skin barrier function parallels abnormal stratum corneum lipid organization in patients with lamellar ichthyosis. *J. Invest. Dermatol.* **105** (1995) 619-624.

5. Schmook F.P., Meingassner J.G., Billich A. Comparison of human skin or epidermis models with human and animal skin in in-vitro percutaneous absorption. *Int. J. Pharm.* **215** (2001) 51-56.

6. Catz P., Friend D.R. Transdermal delivery of levonorgestrel. VII. Effect of enhancers on rat skin, hairless mouse skin, hairless guinea pig skin, and human skin. *Int. J. Pharm.* **58** (1990) 93-102.

7. Council Directive 2003/15/EEC of 27 February 2003 (amending for the seventh time Directive 76/6/768/EEC), Official Journal L 66, 11.3.2003, pp 26-35.

8. Ponec M., Weerheim A., Lankhorst P., Wertz P. New acylceramide in native and reconstructed epidermis. *J. Invest. Dermatol.* **120** (2003) 581-588.

9. Bouwstra J.A., Gooris G.S., Dubbelaar F.E.R., Weerheim A.M., IJzerman A.P., Ponec M. Role of ceramide 1 in the molecular organization of the stratum corneum lipids. *J. Lipid Res.* **39** (1998) 186-196.

10. McIntosh T.J., Stewart M.E., Downing D.T., 1996. X-ray diffraction analysis of isolated skin lipids: reconstitution of intercellular lipid domains. *Biochemistry* **35** (1996) 3649-3653.

11. ten Grotenhuis E., Demel R.A., Ponec M., Boer D.R., van Miltenburg J.C., Bouwstra J.A. Phase-behavior of stratum corneum lipids in mixed langmuir-blodgett monolayers. *Biophys. J.* **71** (1996) 1389-1399.

12. Bouwstra J.A., Thewalt J., Gooris G.S., Kitson N. A model membrane approach to the epidermal permeability barrier: an X-ray diffraction study. *Biochemistry* **36** (1997) 7717-7725.

13. Lieckfeldt R., Villalain J., Gomez-Fernandez J.C., Lee G. Diffusivity and structural polymorphism in some model stratum corneum lipid systems. *Biochim. Biophys. Acta* **1151** (1993) 182-188.

14. Dahlen B., and Pascher I. Molecular arrangements in sphingolipids. Thermotropic phase behaviour of tetracosanoylphytosphingos ine. *Chem. Phys. Lipids* **24** (1979) 119-133.

15. Bouwstra, J.A., Gooris G.S., Cheng K., Weerheim A., Bras W., Ponec M. Phase behavior of isolated skin lipids. *J. Lipid Res.* **37** (1996) 999-1011.

16. Wagner H., Kosta K.H., Lehr K.M., Schaefer U.F. Interrelation of permeation and penetration parameters obtained from in vitro experiments with human skin and skin equivalents *J. Control. Release* **75** (2001) 283-295.

List of publications

Published papers

M.W. de Jager, G.S. Gooris, I.P. Dolbnya, W. Bras, M. Ponec, J.A. Bouwstra. The phase behaviour of skin lipid mixtures based on synthetic ceramides. *Chem. Phys. Lipids* **124** (2003) 123-134.

M.W. de Jager, G.S. Gooris, I.P. Dolbnya, W. Bras, M. Ponec, J.A. Bouwstra. Novel lipid mixtures based on synthetic ceramides reproduce the unique stratum corneum lipid organization. *J. Lipid Res.* **45** (2004) 923-932.

M.W. de Jager, G.S. Gooris, I.P Dolbnya, M. Ponec, J.A. Bouwstra. Modelling the stratum corneum lipid organisation with synthetic lipid mixtures: the importance of synthetic ceramide composition. *Biochim. Biophys. Acta* **1664** (2004) 132-140.

M. de Jager, G. Gooris, M. Ponec, J. Bouwstra. Acylceramide head group architecture affects lipid organization in synthetic ceramide mixtures. *J. Invest. Dermatol.* **123** (2004) 911-916.

M.W. de Jager, G.S. Gooris, M. Ponec, J.A. Bouwstra. Lipid mixtures prepared with well-defined synthetic ceramides closely mimic the unique stratum corneum lipid phase behavior. *J. Lipid Res.* **46** (2005) 2649-2656.

M. de Jager, W. Groenink, J. van der Spek, C. Janmaat, G.Gooris, M. Ponec, J. Bouwstra. Preparation and characterization of a stratum corneum substitute for in vitro percutaneous penetration studies. *Biochim. Biophys. Acta*, in press.

M. de Jager, W. Groenink, R. Bielsa i Guivernau, E. Andersson, N. Angelova, M. Ponec, J. Bouwstra. A novel in vitro percutaneous penetration model: evaluation of barrier properties with p-aminobenzoic acid and two of its derivatives. *Pharm. Res.*, in press.

Patent application

M.W. de Jager, J.A. Bouwstra, M. Ponec. NL1027178 (2004).

Acknowledgements

Chapter 2 has been reprinted from Chemistry and Physics of Lipids, Vol. 124, M.W. de Jager, G.S. Gooris, I.P. Dolbnya, W. Bras, M. Ponec, J.A. Bouwstra, The phase behaviour of skin lipid mixtures based on synthetic ceramides, 123-134, Copyright (2003), with permission from Elsevier.

Chapter 3 has been reprinted from Journal of Lipid Research, M.W. de Jager, G.S. Gooris, I.P. Dolbnya, W. Bras, M. Ponec, J.A. Bouwstra, Novel lipid mixtures based on synthetic ceramides reproduce the unique stratum corneum lipid organization, 923-932, Copyright (2004), with permission from The American Society for Biochemistry and Molecular Biology.

Chapter 4 has been reprinted from Biochimica et Biophysica Acta, M.W. de Jager, G.S. Gooris, I.P Dolbnya, M. Ponec, J.A. Bouwstra, Modelling the stratum corneum lipid organisation with synthetic lipid mixtures: the importance of synthetic ceramide composition, 132-140, Copyright (2004), with permission from Elsevier.

Chapter 5 has been reprinted from Journal of Investigative Dermatology, M. de Jager, G. Gooris, M. Ponec, J. Bouwstra. Acylceramide head group architecture affects lipid organization in synthetic ceramide mixtures, 911-916, Copyright (2004), Nature Publishing Group.

Chapter 6 has been reprinted from Journal of Lipid Research, M.W. de Jager, G.S. Gooris, M. Ponec, J.A. Bouwstra, Lipid mixtures prepared with well-defined synthetic ceramides closely mimic the unique stratum corneum lipid phase behavior, 2649-2656, Copyright (2005), with permission from The American Society for Biochemistry and Molecular Biology.

Chapter 7 is in press at Biochimica et Biophysica Acta, M. de Jager, W. Groenink, J. van der Spek, C. Janmaat, G.Gooris, M. Ponec, J. Bouwstra, Preparation and characterization of a stratum corneum substitute for in vitro percutaneous penetration studies, with permission from Elsevier.

Chapter 8 is in press at Pharmaceutical Research, M. de Jager, W. Groenink, R. Bielsa i Guivernau, E. Andersson, N. Angelova, M. Ponec, J. Bouwstra, A novel in vitro percutaneous penetration model: evaluation of barrier properties with p-aminobenzoic acid and two of its derivatives. with kind permission from Springer Science and Business Media.

Stellingen

behorende bij het proefschrift

Development of a stratum corneum substitute for in vitro percutaneous penetration studies

a skin barrier model comprising synthetic stratum corneum lipids

1. Cholesterol, synthetische ceramiden en vrije vetzuren, aangebracht op een poreuze drager, vormen een aantrekkelijk hulpmiddel om het geneesmiddelentransport door de huid te onderzoeken.

   Dit proefschrift

2. De doorlaatbaarheid van het ontwikkelde huidbarrièremodel kan worden aangepast door de hoeveelheid òf de samenstelling van het lipidenmateriaal op de poreuze drager te veranderen.

   Dit proefschrift

3. De lamellaire en laterale lipidenorganisatie in synthetische lipidenmengsels, bestaande uit cholesterol, ceramiden en vrije vetzuren, worden niet beïnvloed door het achterwege laten van de hydratatiestap direct na equilibratie.

   Dit proefschrift

4. De diffusieweglengte in stratum corneum is ongeveer 10 maal groter dan in het ontwikkelde huidbarrièremodel.

   Dit proefschrift

5. Naast de kristallijne laterale structuur is de aanwezigheid van een vloeibare laterale fase een voorwaarde voor de vorming van de unieke lamellaire structuur met lange periodiciteit aanwezig in stratum corneum.

   Bouwstra J.A., et al. J. Invest. Dermatol. 118 (2002) 606-617

6. De impact die huidaandoeningen hebben op de kwaliteit van leven wordt vaak onderschat.

   Finlay A.Y. Indian J. Dermatol. Venereol. Leprol. 70 (2004) 143-148

7. "Although, by definition, the stratum corneum cannot be considered a viable tissue, it is nevertheless a dynamic structure in which many enzymatic reactions are carefully regulated to ensure full functionality."

   Harding C.R., Watkinson A., Rawlings A.V. Int. J. Cosm. Sci. 22 (2000) 21-52

8. Hoewel de huid ons voortreffelijk beschermt tegen allerlei schadelijke invloeden van buitenaf, vormt zij een slechte barrière tegen kwetsende uitspraken van anderen.

9. Onderzoek doen is vergelijkbaar met transdermaal geneesmiddelentransport: resultaten worden vaak pas zichtbaar na een lange "lag time".

10. (Mogelijke) patentaanvragen vormen een niet te onderschatten belemmering voor de ontwikkeling van jonge onderzoekers.

11. Happiness always looks small while you hold it in your hands, but let it go, and you learn at once how big and precious it is.

    Maxim Gorky

12. Iemand die altijd alles zwart op wit wil hebben, leeft een kleurloos bestaan.

Miranda de Jager
Leiden, 27 april 2006